ISSN 0370—8691

NATIONAL ACADEMY OF SCIENCES OF THE REPUBLIC OF ARMENIA

Communications of the Byurakan Astrophysical Observatory

1

Erevan 2021

Communications of BAO, Vol. 68, Issue 1, 2021, pp. 1-11

Byurakan Astrophysical Observatory: 75 years of outstanding achievements

A. M. Mickaelian*

NAS RA V. Ambartsumian Byurakan Astrophysical Observatory (BAO)

Abstract

The Byurakan Astrophysical Observatory (BAO) is one of the most famous observatories of the Soviet Union and may be of the world. It was founded in 1946 by the outstanding scientist Viktor Ambartsumian (1908-1996) and became the leader of studies on instability phenomena in the Universe. Many discoveries have been carried out at BAO related to stars, star clusters and other systems, nebulae, galaxies and systems of galaxies. BAO has two major instruments; 1m Schmidt and 2.6m classical telescopes. Together with V. Ambartsumian, outstanding scientists Beniamin Markarian, Grigor Gurzadyan, Marat Arakelian and others have worked at BAO. Many important international meetings and schools for young astronomers have been held. Many important people, including State authorities, Nobel Prize Winners and others have visited BAO. BAO has statuses of RA National Value, Regional Astronomical Centre, it has UNESCO Documentary Heritage item, its garden is recognized as Dendrarium, and there is RA National Hero Viktor Ambartsumian's house-museum.

Keywords: *Viktor Ambartsumian, Byurakan Astrophysical Observatory, history of science, instability phenomena*

This year the National Academy of Sciences of the Republic of Armenia (NAS RA) V. Ambartsumian Byurakan Astrophysical Observatory (BAO) celebrates 75^{th} anniversary of its foundation. It is notable that it was founded just after the Second World War in 1946; this emphasizes the importance of the development of astronomy in Armenia by our great scientist Viktor Ambartsumian (1908-1996) who moved from the Leningrad (present Saint Petersburg) State University (LSU) to Armenia to establish the Armenian SSR Academy of Sciences together with Hovsep Orbeli (1887-1961) and other famous scientists. Orbeli was elected the President and Ambartsumian, the first Vice-President of the Academy of Sciences. However, very soon in 1947, Ambartsumian was elected the President and stayed at this position till 1993.

Though the decision at the Academy of Sciences to found an observatory and the selection of the location were made in late 1946, the construction works and first observations (with small telescopes without any building or dome) started in spring of 1947. Samvel Safaryan was appointed as the chief architect and a beautiful ensemble was designed near Byurakan village, at an average altitude of 1405m, including administrative buildings, laboratories, telescope towers with domes, Viktor Ambartsumian house and some auxiliary buildings. The first observations were carried out under the leadership of two experienced astronomers; Hayk Badalian (1908-1972) and Beniamin Markarian (1913-1985). The first scientific staff members were 8 researchers: Viktor Ambartsumian (Director), Hayk Badalian (Deputy Director), Beniamin Markarian, Pargev Gevorgyan, Levon Vatyan, Ruben Sahakian, Vagharshak Sanamian and Nina Ivanova. Very soon, Lyudwik Mirzoyan joined in 1947 and Grigor Gurzadian in 1948 (he was Ambartsumian's PhD student since 1944), who were not even astronomers. The Chair of Astrophysics was formally established in Yerevan State University (YSU)

*aregmick@yahoo.com

doi: https://doi.org/10.52526/25792776-2021.68.1-1

Physics Faculty in 1944, and the first graduates (as astronomy specialists) to work at BAO appeared in 1951 (Marat Arakelian, Carlos Grigorian and Edward Khachikian). In a few years, Hrant Tovmassian, Romela Shahbazian, Arsen Kalloghlian, Elma Parsamian, Vigen Malumian and many others joined the Observatory research staff.

In 1946, the Communications of the Byurakan Astrophysical Observatory (ComBAO) were founded as the main journal for Byurakan astronomers. Ambartsumian became its first Editor-in-Chief.

It is notable that the first scientific results came immediately after the foundation of BAO. In 1947 stellar systems of new type, Stellar Associations, groups of hot (OB) giants and T Tauri stars, were discovered by V. A. Ambartsumian (Ambartsumian, 1948, 1949). It was shown for the first time that the star formation process continues at all stages of the evolution of our Galaxy, including the present one and that the star formation is a permanent process (the maximum ages of stellar associations were estimated at 10^7 yr compared to 10^{10} yr of the age of the Galaxy). A conclusion was drawn that stars are formed not individually, but in groups, in stellar associations, together with gas and dust but not from them.

In November 1951, the first scientific meeting was held in BAO. *Stellar Associations* were the subject of the conference. The Observatory was not entirely built yet, but the investigations of Byurakan astronomers became well-known to the international astronomical community. On September 19, 1956, the official opening of BAO was celebrated by holding a conference on *Non-stable stars*. J. Greenstein, G. Herbig, G. Haro, E. Schatzman, P. L. Kapitsa, B. V. Kukarkin, V. V. Sobolev and other prominent scientists were among the guests.

Figure 1. The Principal administrative building of BAO built in 1951.

In the mid-1950s Ambartsumian gave a new explanation for radiogalaxies radiation and proposed a new conception on the activity of galactic nuclei (Ambartsumian, 1956a,b). By the time, it was accepted by all the astronomers, and at present most of the astrophysical observatories have the sub-

doi: https://doi.org/10.52526/25792776-2021.68.1-1

ject of Active Galactic Nuclei (AGN) as one of their main research areas. The discovery of stellar associations and Ambartsumian's idea on activity of galactic nuclei, as well as investigations on radiation transfer theory, based on Ambartsumian's Principle of Invariance (Ambartsumian, 1941, 1942), elucidated the further development of the research activities in BAO.

V. A. Ambartsumian and R. K. Shahbazian found in nearby galaxies concentrations of young stars, which they called superassociations, as well as blue companions around some galaxies, which might be thrown out from them. Later on, Shahbazian found compact groups of compact galaxies (named after Shahbazian); objects that are subject for detailed studies up to present days (Baier et al., 1974 and references therein). In early 1960s, V. A. Ambartsumian and G. S. Sahakian (from Yerevan State University, YSU) studied possible states of superdense matter and proved the possibility of existence of baryonic and hyperionic configurations with nuclear-like densities and of several Solar masses (Ambartsumian & Saakyan, 1960, 1962a,b).

In 1960, a new Schmidt telescope with 40" (102 cm) correcting lens and 52" (132 cm) mirror was installed in Byurakan. Soon, in 1965, B. E. Markarian (Markarian, 1967) started a survey with a goal of revealing UV-excess galaxies (First Byurakan Survey – FBS, co-authors V. A. Lipovetski and J. A. Stepanian; Markarian et al., 1989). It was continued for 15 years and became one of the most famous surveys in modern astronomy. As a result, 1515 galaxies with UV-excess, named Markarian galaxies, were discovered. Up to now, Byurakan Schmidt is one of the largest and one of the most efficient Schmidt telescopes in the world. Markarian survey was the first systematic survey for AGN and is the largest spectroscopic survey in the world.

Observations of Markarian galaxies in Byurakan and other observatories revealed a lot of new interesting objects. E. Ye. Khachikian, together with D. Weedman (USA), discovered many new Seyfert-type galaxies and for the first time made a classification of these AGN (Weedman & Khachikyan, 1968). H. M. Tovmassian and colleagues discovered and studied the radio emission of many Markarian galaxies. More active galaxies were discovered from the lists compiled by M. A. Arakelian, who selected and published 621 galaxies with high surface brightness (Arakelian, 1975). Later on, Markarian galaxies have been studied by K. A. Sahakian, A. R. Petrosian, et al.

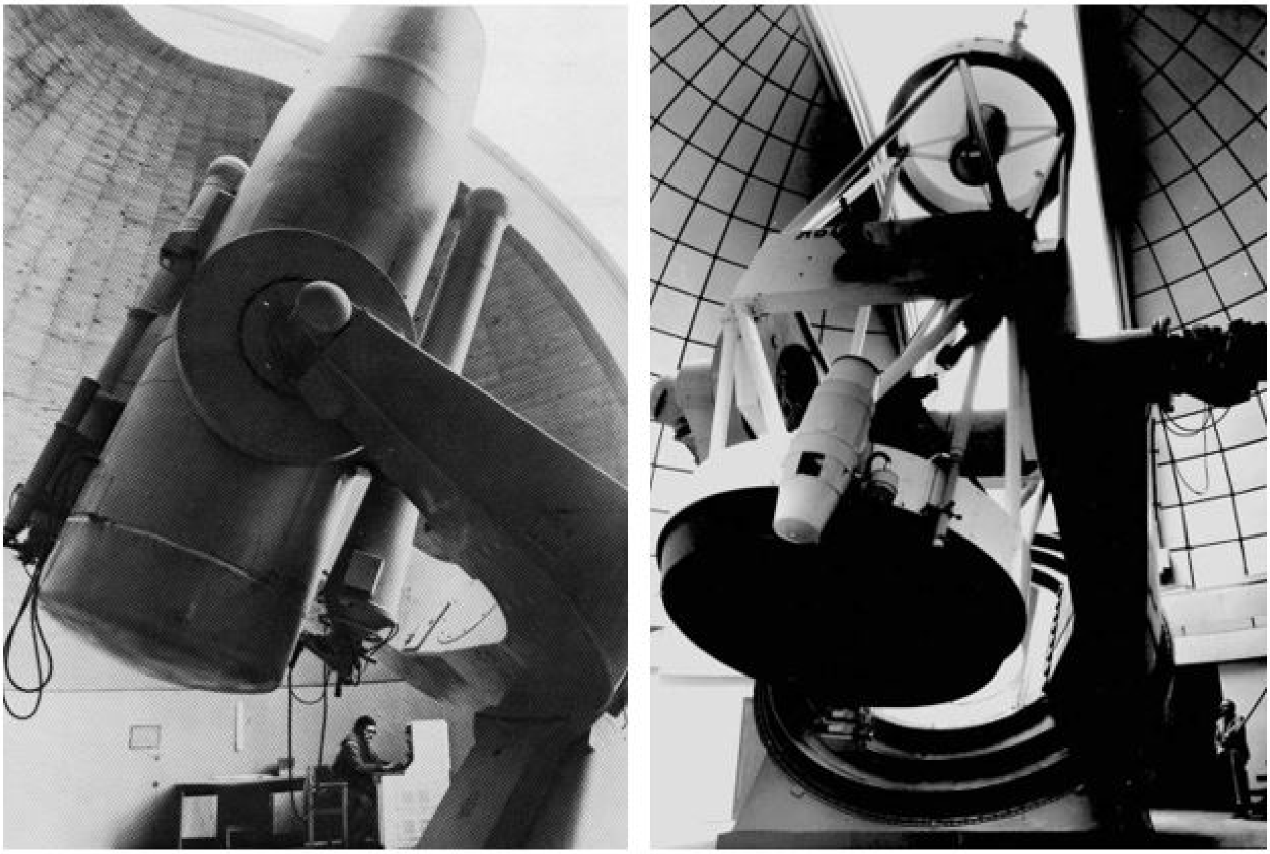

Figure 2. BAO main instruments; 1m Schmidt telescope and 2.6m classical reflector.

doi: https://doi.org/10.52526/25792776-2021.68.1-1

In 1964 and 1971 conferences on *Extraterrestrial Civilizations* were held. The meeting of 1971 was the first international symposium on the problem of Extraterrestrial Civilizations and Communication with Them. Many prominent scientists, including astronomers, physicists, chemists, biologists, philosophers, and specialists of other related fields participated in the symposium.

In 1965 an all-Union astrophysical journal, *Astrofizika* (English translation: *Astrophysics*) was founded, and Byurakan astronomers began to publish their papers mainly in it. The *Astrofizika* became the main astrophysical journal of the Soviet Union as well.

IAU Symposium #29 in May 1966 on Non-Stable Phenomena in Galaxies will remain as one of the most interesting events during the history of the observatory. J. Oort, F. Zwicky, G. Burbidge, E. Burbidge, M. Schmidt, and many other well-known scientists were present.

In 1960, H. S. Badalian carried out classification of cometary nebulae. E. S. Parsamian discovered many new cometary nebulae and published their catalogs (Parsamian, 1965, Parsamian & Petrosian, 1979). Later on, A. L. Gyulbudaghian and T. Yu. Magakian found and studied the variability of some cometary nebulae (Giulbudagian et al., 1977). Together with colleagues, later on they discovered and studied many other young stellar objects and stellar jets.

In 1968, for its great merit to the development of science, BAO was awarded the highest prize of the Soviet Union, Lenin Order. A conference was held, devoted to V. A. Ambartsumian's 60-years anniversary. He presented a new work on statistical investigation of flare stars, estimating the real number of these objects, and predicted that all dwarf stars pass through the stage of flare activity (Ambartsumian, 1969). Beginning with the late 1960s, the investigation of flare stars became one of the main subjects of BAO. Hundreds of flare stars in star clusters and associations (Pleiades, Orion, Hyades, Praesepe, Cygnus, Coma, etc.) were discovered by L. V. Mirzoyan, E. S. Parsamian, H. S. Chavushian, L. K. Erastova, et al. Early stages of evolution of dwarf non-stable stars were investigated (Mirzoyan et al., 1981).

A project on Space Astronomy studied in Byurakan in late 1960s. Under the supervision of G. A. Gurzadyan, Byurakan scientists designed and built 2 ultraviolet "Orion" space observatories that operated onboard Soviet spacecrafts in 1971 and 1973. Later on, H. M. Tovmassian designed and built "Glazar" space observatory, which operated in 1987 onboard Soviet space station "Mir" (Tovmassian et al., 1988).

A. G. Nikoghossian, M. A. Mnatsakanian, and N. B. Yengibarian in late 1960s and 1970s obtained new solutions in Radiation Transfer Theory (RTT) with application of principle of invariance for finite thickness layers and plain-parallel medium (e.g. Nikoghossian, 1995, 2016). They also obtained new results in various fields of mathematical physics. Important contributions in theoretical astrophysics (RTT and other fields) were also made by E. Kh. Danielian, H. A. Harutyunian, G. T. Ter-Kazarian, H. V. Pikichian, R. R. Andreasyan and others.

The installation of the 2.6 m telescope (one of the largest telescopes in the world at that time) was rather important event in the Observatory's life. The opening of the telescope in October 1976 was accompanied by a symposium on *Flare Stars*. Scientific meetings on these and related objects were held in 1979 and 1984, too. The 2.6m telescope is the largest at BAO; its operations were stopped in 1991-1996 and it is again operational since 1996, when a new digital equipment was installed due to French-Armenian collaboration.

Since 1977, a specialized council for theses defenses functions. Ambartsumian was its chairman in 1977-96. The council accepts theses on astronomy, astrophysics and theoretical physics. More than 50 scientists have defended Ph.D. (Candidate) and Doctoral theses during these years.

In 1978 the Second Byurakan Survey (SBS) was conducted by B. E. Markarian, J. A. Stepanian, et al. The main goal was to obtain a homogeneous sample of quasars, emission-line and UV-excess galaxies for further cosmological investigations. More than 600 deep-limit plates were obtained during 15 years and some 3600 interesting objects were discovered (Markarian et al., 1983, Stepanian, 2005).

In October 1981, a Symposium on *Principle of Invariance and its Applications* was held. It was devoted to the 40th anniversary of the Principle of Invariance, Ambartsumian's theory, which found many applications in various fields of science. In 1980s two IAU symposia were organized in Byurakan. IAU Symposium #121 on *Observational Evidences of Activity in Galaxies* (June 1986) gathered many outstanding astrophysicists from 17 countries. Many aspects of Ambartsumian's hypothesis and the

doi: https://doi.org/10.52526/25792776-2021.68.1-1

classical theory of AGN were discussed. IAU Symposium #137 on *Flare Stars in Star Clusters, Associations and Solar Vicinity* was held in October 1989 and gathered specialists of the corresponding field. BAO was recognized as one of the world main centres of investigations on flare stars.

In 1987 the Second Part of the First Byurakan Survey (FBS) was conducted, search and studies of the FBS stellar objects; both blue (UV excess) stellar objects (BSOs) and red (late-type) stars. It was carried out by H. V. Abrahamian, A. M. Mickaelian, and K. S. Gigoyan and resulted in discovery of 1103 BSOs (including bright QSOs, Seyferts, white dwarfs, cataclysmic variables, etc.; Mickaelian, 2008) and 1471 red stars (late M-type and C stars; Gigoyan et al., 2019). Later on, A. M. Mickaelian started a project of optical identifications based on the FBS low-dispersion spectra and revealed many galaxies and stars named Byurakan-IRAS Galaxies (BIG; Mickaelian, 1995) and Byurakan-IRAS Stars (BIS; Mickaelian & Gigoyan, 2006).

In 1986 the Research Departments were abolished and small research groups were formed for more efficient scientific work. The Departments were re-established in 2017; at present 9 Research Departments exist like small groups, each involving a few scientists. In 1988 V. A. Ambartsumian retired from the position of the director of the observatory, and E. Ye. Khachikian occupied it. Ambartsumian remained the honorary director of BAO until his death in 1996. In 1993-1994 H. A. Harutyunian was the acting director, in 1994-1999, the director was A. R. Petrosian, and in 1999-2003, E. Ye. Khachikian became the director for the second term, then H. A. Harutyunian was the director in 2004-2017. Since 2017, A. M. Mickaelian is the director of BAO.

After the disintegration of the Soviet Union, the Byurakan astronomers underwent difficult situation in economy and science, however, in a few years a new activity began in mid-1990s with some re-organizational process and new international collaborations. Due to French astronomers, the 2.6m telescope was equipped with new instrumentation and started to give in 1996 new interesting results.

Two meetings (French-Armenian Astronomical Colloquium in 1995 and an International Symposium, devoted to the 50th anniversary of BAO in October 1996) showed that astronomers of the Observatory continue to develop Ambartsumian's ideas and have achieved new interesting results. In August 1998, the IAU Symposium #194 on *Activity in Galaxies and Related Phenomena*, dedicated to Ambartsumian's 90th anniversary, was held in Byurakan. More than 100 astronomers – the most known specialists of the field from 24 countries, presented and discussed their results and prospects in this area. A new important meeting, IAU Colloquium #184 on AGN Surveys was organized in Byurakan in June 2001. 95 scientists from 20 countries took part. The meeting was devoted to B. E. Markarian, the scientist who carried out the first systematic survey for active galaxies and opened a new era of investigations.

One of the important activities in Byurakan is the organization of Summer Schools and astronomical Olympiads (competitions for pupils and students). A number of such events were organized in 1995-2020, and the first Byurakan International Summer School (BISS) was held in August-September 2006, where 8 foreign lecturers and some 30 students participated. The next school was organized in September 2008. The 3rd one was combined with the IAU International School for Young Astronomers (ISYA) in 2010, where 18 lecturers from 7 countries and 49 students from 19 countries participated. Four more schools were organized in 2012, 2016, 2018 and 2020. BISS are being held regularly once in each two years. 7BISS was the last one.

In 2002-2007, in collaboration with Università di Roma "La Sapienza" (Italy) and Cornell University (USA) teams, the Markarian survey (First Byurakan Survey) plates were digitized and the Digitized First Byurakan Survey (DFBS; Mickaelian et al., 2007) database was created under the supervision of A. M. Mickaelian. It is one of the largest spectroscopic databases in the world and the largest astronomical database in Armenia. DFBS was the first digitization project in Armenia in all spheres. Since 2011, Markarian Survey and its Digitized version (DFBS) have been included in UNESCO "Memory of the World" International Register. Based on the DFBS and other related projects, Armenian Virtual Observatory (ArVO) was created in 2005 and was involved in International Virtual Observatories Alliance (IVOA).

In August 2007, BAO, together with the European and Armenian astronomical societies and Yerevan State Univ. (YSU), was one of the organizers of the Joint European and National Astronomy Meeting (JENAM-2007) in Yerevan. It was the largest scientific event ever organized in Armenia;

doi: https://doi.org/10.52526/25792776-2021.68.1-1

8 parallel EAS symposia and 5 special sessions were organized. 248 scientists from 31 countries participated, and 358 plenary, invited, oral, and poster contributions were presented.

In October 2013, IAU Symposium #304 on Multiwavelength AGN Surveys and Studies, dedicated to B. E. Markarian's 100th anniversary was held at NAS RA in Yerevan. It was the largest astronomical symposium by the number of participants (141) and represented countries (28) held in Armenia. Another large meeting, International Conference on Astronomical Heritage of the Middle East sponsored by UNESCO, was organized in Nov 2017 at NAS RA in Yerevan. This was a unique meeting representing archaeoastronomical and cultural astronomy research and results from the regional countries.

A Russian-Armenian space safety project on the monitoring of space debris was started in 2014 between BAO and Astronomical Scientific Centre related to Roskosmos, the Russian space agency. Three small telescopes were installed in Saravand (former Radioastronomy and Applied Astronomy departments location) and BAO astronomers are engaged to carry out observations led by Haik Harutyunian.

Due to obtained results the Byurakan Astrophysical Observatory is recognized by the scientific community as one of the main centres for astrophysical research. In 2013 it was recognized by the Armenian Government as National Value. The conceptions and ideas proposed in Byurakan have found their further elaboration in many observatories, a few thousands of new objects discovered in Byurakan are observed worldwide by famous astrophysicists. In 2015, BAO was recognized by IAU as one of its regional centres of astronomy for development, namely for the South-West and Central Asia.

Byurakan astronomers have participated in all large international astronomical meetings: International Astronomical Union (IAU) General Assemblies, Symposia, and Colloquia. Many of them are members of various IAU Commissions. V. A. Ambartsumian was the IAU President in 1961-64 and Vice-President in 1948-55, B. E. Markarian and E. Ye. Khachikian have been the Presidents of the IAU Commission No. 28 (Galaxies), each for 3 years. Since 2002, A. M. Mickaelian was a member of the Council of the Euro-Asian Astronomical Society (EAAS), and since 2015, he is its Vice-Chair.

In 2001, on the initiative of BAO astronomers, the Armenian Astronomical Society (ArAS) was founded, which unifies many Armenian astronomers in the world. At present 100 scientists are its members, including Armenian and other famous scientists representing 20 countries. ArAS organizes annual meetings, 12 times per year releases ArAS electronic newsletters, awards annual prize (Yervant Terzian Prize) to young astronomers, actively participates in all events organized in Byurakan, as well as maintains webpage with rich information about Armenian astronomy (including the online database of all Armenian astronomers in the world).

During the recent years, on the initiative of BAO, collaboration has started on archaeoastronomical matters with NAS RA Institute of History, NAS RA Institute of Archaeology and Ethnography, and Matenadaran. In 2012, Armenian medieval great scientist Anania Shirakatsi's 1400^{th} jubilee was celebrated and an archaeoastronomical meeting was organized. BAO and ArAS jointly organized in October 2014 a meeting "Relation of Astronomy to other Sciences, Culture and Society" and together with Archaeoastronomy and Astronomy in Culture, many other interdisciplinary and multidisciplinary fields related to astronomy were discussed, including Astrochemistry, Astrobiology, Astroinformatics, etc.

BAO started another activity for collaboration between astronomers and computer scientists based on the collaboration of BAO and the NAS RA Institute of Informatics and Automation Problems (IIAP), as well as collaboration between ArVO and IVOA. BAO organized in 2015 and 2020 two international symposia on *Astronomical Surveys and Big Data* (ASBD and ASBD-2) related to astronomy, Big Data, computer science, Astroinformatics, etc.

The prestige of BAO was enhanced by the many-years fruitful research work and is on high level during its 75-years history. Many international scientific meetings have been held in Byurakan and dozens of astronomical institutions all over the world collaborate with BAO, including observatories and astronomical institutes of Australia, Chile, China, France, Georgia, Germany, Greece, India, Iran, Italy, Japan, Kazakhstan, Latvia, Mexico, Poland, Portugal, Russia, South Africa, Spain, UK, USA, Uzbekistan, etc. Nobel Prize winners Pablo Neruda, Subrahmanyan Chandrasekhar, Charles

doi: https://doi.org/10.52526/25792776-2021.68.1-1

Towns, Francis Crick, Freeman Dyson, Sin-Itiro Tomonaga, Vitaly Ginzburg, John Mather and Michel Mayor, outstanding scientists J. Oort, F. Zwicky, J. Greenstein, G. Herbig, G. Haro, H. Arp, B. Bok, E. Burbidge, G. Burbidge, M. Schmidt, P. L. Kapitza, V. M. Keldish, Y. B. Zeldovich, J. Narlikar and many others and other honorary guests have visited BAO to make an acquaintance of famous astronomical centre, study its scientific program, discuss different scientific problems with Byurakan astronomers and to take part in joint investigations. State authorities, including the Soviet leaders (Nikita Khrushchov in 1961 and others), all Armenian Presidents and some Prime-Ministers, many ministers, Ambassadors of foreign countries in Armenia and others have visited BAO.

Since 1998 BAO bears the name of V. A. Ambartsumian – its founder and scientific leader. It is 75 years that BAO is among the world astronomical centers and successfully continues its new discoveries and high-level research.

Figure 3. BAO Conference Hall, where many important international meetings were held.

Here we give the lists of most important scientific meetings held in BAO or organized by BAO (including all IAU meetings) (Table 1) and the list of the Byurakan International Summer Schools and other events for young scientists (Table 2).

Table 1: Most important scientific meetings held in BAO or organized by BAO.

Dates	**Meeting**	**Title / subject / description**
1956 Sep 20-22	BAO-1956	***Non-Stable Stars***, a Symposium Devoted to the Official Inauguration of the Byurakan Astrophysical Observatory
1966 May 4-12	IAU S029	***Non-Stable Phenomena in Galaxies***
1971 Sep 6-11	CETI-1971	***Communication with Extraterrestrial Intelligence***, First International Symposium on the Problem of Extraterrestrial Civilizations and Communication with them
1976 Oct 5-8	ZTA-2.6	***Flare Stars***, an International Symposium Devoted to the Official Opening of the 2.6m telescope

doi: https://doi.org/10.52526/25792776-2021.68.1-1

1981 Oct 26-30	InvPrinciple-40	***Principle of Invariance and its Applications***, an All-Union Symposium Devoted to the 40^{th} Anniversary of the Principle of Invariance Introduction to the Radiation Transfer Theory
1986 June 3-7	IAU S121	***Observational Evidence of Activity in Galaxies***
1989 Oct 23-27	IAU S137	***Flare Stars in Star Clusters, Associations and Solar Vicinity***
1998 Aug 17-21	IAU S194	***Activity in Galaxies and Related Phenomena***
2001 June 18-22	IAU C184	***AGN surveys***
2008 Sep 15-18	VA-100	***Evolution of Cosmic Objects through their Physical Activity***, International Conference devoted to the 100^{th} Anniversary of V. A. Ambartsumian
2013 Oct 7-11	IAU S304	***Multiwavelength AGN Surveys and Studies***
2014 Oct 7-10	RASCS	***Relation of Astronomy to Other Sciences, Culture and Society***, Inter- and Multi-disciplinary Conference
2015 Oct 5-8	ASBD	***Astronomical Surveys and Big Data***, International Symposium dedicated to 50^{th} anniversary of Markarian Survey and 10^{th} anniversary of Armenian Virtual Observatory (ArVO)
2017 Nov 13-17	UNESCO	***Astronomical Heritage of the Middle East***, International Conference supported by UNESCO
2020 Sep 14-18	ASBD-2	***Astronomical Surveys and Big Data 2***, International Symposium
2021 Sep 20-24	BAO-75	***Astronomy in the Crossroads of Interdisciplinary and Multidisciplinary Sciences***, International Conference Dedicated to 75^{th} Anniversary of Byurakan Astrophysical Observatory

Table 2: International schools and conferences for young astronomers held in BAO or organized by BAO.

Dates	**School / Conf.**	**Title / subject / description**
1987 Sep 22-28	ESO-BAO	***Observations with Large Telescopes***, an International School for Young Astronomers, organized jointly by ESO and BAO
1988 Sep 27-30	VA-80 Conf.	***Observational Evidences of Instability Phenomena and their Interpretation***, a Conference of Young Astrophysicists Devoted to the 80^{th} Anniversary of V. A. Ambartsumian
2006 Aug 26 – Sep 3	1BISS	***Observational Astrophysics***, 1^{st} Byurakan International Summer School (1BISS) for Young Astronomers

doi: https://doi.org/10.52526/25792776-2021.68.1-1

2008 Sep 20-30	2BISS	***Practical Astrophysics***, 2^{nd} Byurakan International Summer School for Young Astronomers
2010 Sep 12 – Oct 2	3BISS/ISYA	3^{rd} Byurakan International Summer School for Young Astronomers combined with IAU 32^{nd} International School for Young Astronomers
2011 Nov 21-25	Gagarin-50	***50 Years of Cosmic Era: Real and Virtual Studies of the Sky***, Conference for Young Astronomers
2012 Sep 15-23	4BISS	4^{th} Byurakan International Summer School for Young Astronomers
2016 Sep 12-23	5BISS	5^{th} Byurakan International Summer School for Young Astronomers
2018 Sep 10-15	6BISS	6^{th} Byurakan International Summer School for Young Astronomers
2019 Sep 2-6	1RASS	***Space Sciences and Technologies***, 1^{st} Regional Astronomical Summer School
2020 Sep 7-11	7BISS	***Astronomy and Data Science***, 7^{th} Byurakan International Summer School for Young Astronomers
2021 Sep 13-17	2RASS	2^{nd} Regional Astronomical Summer School

In Figure 4, we give the world map with collaborating with BAO countries highlighted. There are many forms of collaboration, including collaborative research projects, observing programs, organization of and participation in meetings, training of students and young researchers, etc.

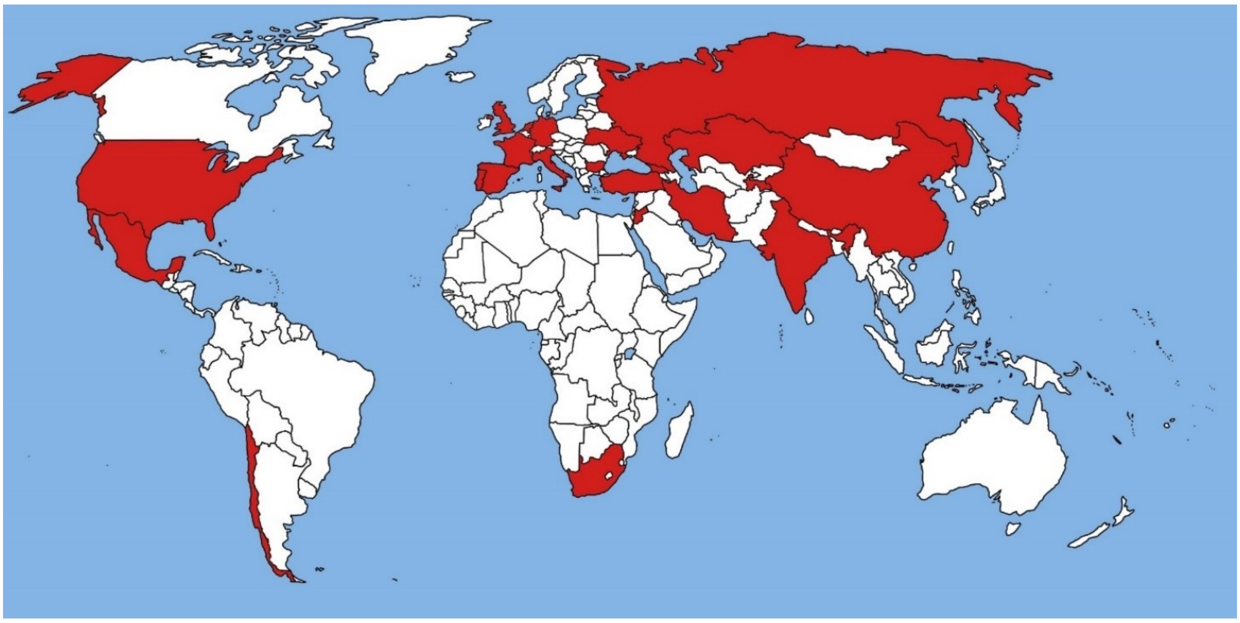

Figure 4. World map with countries collaborating with BAO.

BAO has several official statuses. We list them in Table 3. As it is obvious, most of these statuses BAO has been awarded during the last 20 years, in 2000s-2010s, which indicates about the research, educational and public activities in these years.

doi: https://doi.org/10.52526/25792776-2021.68.1-1

Table 3. Official statuses of BAO.

BAO official statuses	**Awarded / established**	
	Organization / body	Year
BAO as **NAS RA research institute**	National Academy of Sciences of the Republic of Armenia	1946
BAO as **RA National Value**	RA Government	2013
Armenia as **IAU Regional Astronomical Centre** hosted by BAO	International Astronomical Union (IAU)	2015
BAO 2.6m telescope as one of the 10 biggest telescopes in Europe/Asia/Africa/Australia and in the list of biggest scientific instruments in USSR	USSR Academy of Sciences	1975
BAO 1m Schmidt telescope as one of the world 10 biggest Schmidt telescopes	World Astronomy	1960
Markarian Survey as UNESCO “Memory of the World” Documentary Heritage	UNESCO	2011
BAO among top-10 cities most often organized IAU symposia and colloquia	IAU (announced at IAU GA XXX in 2018)	2018
Byurakan International Summer Schools (BISS) among top-3 astronomical schools in the world	IAU (announced at IAU GA XXX in 2018)	2018
BAO was awarded Lenin Order, highest Soviet award, the first among all Soviet observatories	USSR Government	1968
BAO was awarded NAS RA medal, the only among all academic research institutes	NAS RA Presidium	2021
Armenian Astronomical Society (ArAS) based in BAO	European Astronomical Society (EAS) affiliated society	2001
BAO project **Armenian Virtual Observatory (ArVO)**	International Virtual Observatory Alliance (IVOA) member	2005
RA National Hero **Viktor Ambartsumian’s house-museum**	RA Government	1998
BAO garden as Dendrarium	RA Ministry of Ecology	2017
BAO Architectural Ensemble in Armenian monuments list	RA Ministry of Culture	1992
BAO as Scientific Tourism initiator and centre	IAU Office of Astronomy for Development (OAD), Armenian Institute of Tourism (AIT)	2016
BAO Pantheon (Cemetery) as a monument of local significance	RA Ministry of Education, Science, Culture and Sports	2021

Thousands of celestial objects bear Armenian names: Armenian astronomers, Byurakan, Armenia, etc. There are Markarian, Arakelian and Kazarian galaxies, Shahbazian compact groups of compact galaxies, Parsamian cometary nebulae, Gyulbudaghian-Magakian objects, First and Second Byurakan Survey objects (stars, galaxies and quasars), Byurakan-IRAS Stars (BIS) and Byurakan-IRAS Galaxies

doi: https://doi.org/10.52526/25792776-2021.68.1-1

(BIG), Byurakan-Hamburg X-ray (ROSAT) Catalogue sources (BHRC), etc.

For more information, please see Mickaelian (2016) and visit BAO webpage at https://www.bao.am/index.php.

References

Ambartsumian V. A., 1941, Journal of Phisycs, 5, 1, 93

Ambartsumian V. A., 1942, Izvestiya Acad. Sci. USSR, Ser. Geograph. and Geophys. Sci., 3, 97

Ambartsumian V. A., 1948, Evolution of Stars and Astrophysics. Acad. Sci. ArmSSR, 39p., Yerevan

Ambartsumian V. A., 1949, Doklady USSR Acad. Sci., 68, 1, 21

Ambartsumian V. A., 1956a, Proc. Fifth conf. on Problems of Cosmogony: "Radioastronomy", held on 9-12 Mar 1955. Acad. Sci. USSR, pp 413–416

Ambartsumian V. A., 1956b, Izvestiya Acad. Sci. ArmSSR, Ser. Phys.-Math., Nat. and Tech. Sci., 9, 1, 23

Ambartsumian V. A., 1969, Proc. symp. "Stars, Nebulae, Galaxies", devoted to the 60th anniversary of academician V. A. Ambartsumian, held in Byurakan, 16-19 Sep 1968. Acad. Sci. ArmSSR, pp 283–292

Ambartsumian V. A., Saakyan G. S., 1960, Soviet Astronomy, 4, 2, 187

Ambartsumian V. A., Saakyan G. S., 1962a, Soviet Astronomy, 5, 5, 601

Ambartsumian V. A., Saakyan G. S., 1962b, Soviet Astronomy, 5, 6, 779

Arakelian M. A., 1975, Commun. BAO, 47, 3

Baier F. W., Petrosyan M. B., Tiersch H., Shakhbazian R. K., 1974, Astrofizika, 10, 327

Gigoyan K. S., Mickaelian A. M., Kostandyan G. R., 2019, MNRAS, 489, 2030

Giulbudagian A. L., Magakian T. Y., Amirkhanian A. S., 1977, Astronomy Letters, 3, 84

Markarian B. E., 1967, Astrophysics, 3, 55

Markarian B. E., Lipovetski V. A., Stepanian J. A., 1983, Astrophysics, 19, 29

Markarian B. E., Lipovetski V. A., Stepanian J. A., Erastova L. K., Shapovalova A. I., 1989, Communications of SAO, 62, 1

Mickaelian A. M., 1995, Astrophysics, 38, 4, 349

Mickaelian A. M., 2008, AJ, 136, 3, 946

Mickaelian A. M., 2016, Byurakan Astrophysical Observatory. Yerevan, Edit Print Publ. House, 64p.

Mickaelian A. M., Gigoyan K. S., 2006, Astron. Astrophys., 455, 765

Mickaelian A. M., Nesci R., Rossi C., et al. 2007, Astron. Astrophys., 464, 3, 1177

Mirzoyan L. V., Chavushyan O. S., Oganyan G. B., Ambaryan V. V., Garibdzhanyan A. T., Melikyan N. D., Natsvlishvili R. S., 1981, Astrophysics, 17, 1, 38

Nikoghossian A. G., 1995, Astrophysics, 38, 577

Nikoghossian A. G., 2016, J. Quantit. Spectrosc. Radiat. Transfer, 183, 90

Parsamian E. S., 1965, Izv. Akad. Nauk Arm. SSR., Ser. Fiz.-Math, 18, 146

Parsamian E. S., Petrosian V. M., 1979, Commun. BAO, 51, 3

Stepanian J. A., 2005, Rev. Mex. Astron. Astrofis., 41, 155

Tovmassian H. M., Khodzhayants Y. M., Krmoyan M. N., et al. 1988, Astron Letters, 14, 2, 123

Weedman D. W., Khachikyan E. E., 1968, Astrophysics, 4, 4, 243

doi: https://doi.org/10.52526/25792776-2021.68.1-1

On the kinematic interpretation of cosmological redshifts

G.Ter-Kazarian*

Byurakan Astrophysical Observatory, 378433, Aragatsotn District, Armenia

Abstract

We describe what is essentially a correct solution to the kinematic interpretation of cosmological redshifts in standard cosmological model. In the framework of `stretching of space´ point of view of standard cosmological model, we study the `lookforward´ history of expanding universe, subject to certain rules, in order to define the *kinetic* recession velocity of luminous source along the observer's line-of-sight in unique way, straightforwardly in terms of cosmological redshift. In doing this, we use an alternative way of separating the spectral shifts into infinitesimally displaced `relative´ spectral bins between adjacent emitter and absorber consequent on expansion of the universe, measured at infinitesimally separated space-time points, and sum over them to overcome the ambiguity which presents the parallel transport of four-velocity of source to an observer in the Robertson-Walker curved space-time. The crux of our solution - the *kinetic* recession velocity of comoving astronomical object, is always subluminal even for large redshifts of order one or more, so that it does not violate the fundamental physical principle of *causality.* Our analysis establishes the ubiquitous relationship of overall cosmological redshift and *kinetic* recession velocity, which is utterly distinct from a familiar global Doppler shift formula. A difference of global Doppler velocity and *kinetic* recession velocity, for redshifts $0.9 \leq z \leq 800$, is $\geq 0.072c$, where a maximum value, $0.187c$, is reached at redshifts $z = 4.5 - 5.1$. In particular case of such an implementation along the null geodesic, we show that the *kinetic* recession velocity is reduced to a well known global Doppler velocity. We discuss the implications for the case of a zero-density cosmological model of Milne universe, whereas a correspondence to the more usual special relativity notion of relative speed retains. In Table 1, we are summing up *kinetic* recession velocities of some typical distant astronomical objects with spectroscopic redshift determinations collected from the literature.

Keywords: *galaxies: high-redshift—galaxies: distances and redshifts—cosmology: theory*

1. Introduction

A complex study of more distant astronomical objects raises several disturbing questions of the physical interpretation of cosmological dynamics, see e.g. (Bolós & Klein, 2012, Bunn & Hogg, 2009, Chodorowski, 2011, Davis & Lineweaver, 2004, Emtsova & Toporensky, 2019, Grøn & Elgarøy, 2007, Harrison, 1993, 1995, 2000, Kaya, 2011, Klein & Collas, 2010, Klein & Randles, 2011, Liebscher, 2007, Murdoch, 1977, Narlikar, 1994, Peacock, 1999, 2008, Peebles, 1993, Peebles et al., 1991, Pössel, 2019, Silverman, 1986, Stuckey, 1992, Whiting, 2004).

The astronomers for decades routinely do not distinguish between the Hubble's empirical linear `redshift-distance´ law, $cz = HL$ and the linear `velocity-distance´ law, $\dot{L} = HL$, derived later on theoretical basis, where and throughout the overdot represents differentiation with respect to epoch synchronous time, t, z is the redshift, L is the proper distance from a galaxy to an observer at epoch t, and H is the Hubble's parameter. They express redshifts as if they were radial velocities to convert cosmological redshifts into velocity. But aside from the observations for relatively nearby galaxies, for later measurements of more distant objects, with redshifts of order one or more, a special relativity (SR) Doppler interpretation is neither useful nor adequate. One should, therefore, drop this interpretation in favor of the `stretching of space´ point of view of general relativity (GR) description with a

*gago_50@yahoo.com

doi: https://doi.org/10.52526/25792776-2021.68.1-12

dynamical space. Such a concept of `stretching of space´ has by itself no physical content, but it is merely the choice for analysing phenomena. In accord to it, the peculiar velocity of the object with respect to the Hubble flow declines in magnitude as the universe expands $\delta v \propto 1/R(t)$, where $R(t)$ is the scale factor, and thus, at $t \to \infty$, the peculiar velocity tends to zero leaving the object moving with the Hubble flow. This immediately has fostered a startling view to think of present day values of the rate of expansion $\dot{L}(t, z)$ as the so-called `proper´ recession velocity of comoving galaxy of redshift $z$ away from an observer. We should look very sceptically at any argument which uses or implies the concept of superluminal `proper´ recession velocity as a real physical velocity, as if the meaning of that were clear and obvious. Although it is extremely hard to envisage a consistent theory having such a logical impossibility of superluminal `proper´ recession velocity, this problem stood open for nearly a century as a startling preoccupation of wide community of astronomers, see e.g. (Davis & Lineweaver, 2004, Lineweaver & Davis, 2005). There is an important reason to question the validity of such a description of apparent superluminal growth of the universe, because we inevitably encounter with a crucial question of "what is a practical measure of being swept up of galaxy in expanding universe?"

Our primary interest in this article is rather to focus on the principle issue of how to reconcile the cosmological interpretation of redshifts with the most natural kinematic interpretation. We try to impart some knowledge about the physical nature of the kinetic velocity of luminous source along the observer's line-of-sight in unique way, straightforwardly in terms of cosmological redshift, in a mostly non-technical, nevertheless hopefully precise and consistent language. The solutions given in present article demonstrate its advantage over the specific extant definitions in the cited literature.

- We solve startling difficulties of superluminal `proper´ recession velocities in standard cosmological model, which is the principle issue for the physics. This peculiarity deserves careful study, because it furnishes valuable theoretical clues about the interpretation of kinetic velocity of luminous object relative to observer in GR, a systematic analysis of properties of which happens to be surprisingly difficult by conventional methods. Avoiding from any mistakes, therefore, we preferred to work in an infinitesimal domain. The problem of subjecting the four-velocity vector of the luminous source to parallel transport will not be broached in this paper, though it is hoped that the present formulation of the theory will facilitate the task. We advocate with so-called `lookforward´ history of expanding universe, to achieve an unique definition of the *kinetic* recession velocity of astronomical object in terms of redshift. At any rate, it is remarkable that these definitions above completely determine this velocity to always be subluminal even for large redshifts of order one or more, and thus, it does not violate the fundamental physical principle of *causality*. This will help astronomers to derive measurable quantities for further study of the problems of fundamental physics of early universe.

- We discuss the implications of this approach for two instructive cases: (i) We show that a derived general solution is reduced to global Doppler shift along null geodesic. (ii) For the limit of a zero-density cosmological model of Milne universe, a correspondence to the more usual special relativity notion of relative speed retains.

- We give (App.A) a reappraisal in a deep way of the preliminary attempts of `standard´ kinematic interpretation of redshifts as accumulated Doppler-shifts consequent on recession, widely discussed in literature. Its study is valuable as affording insight into the whole subject. In doing this, we are not suggesting any doubt about the principle statement. Rather, we doubt the method of calculations, which as we have shown are in error. Moreover, this statement is a crux of our derivation of an essentially correct solution to a kinematic interpretation of cosmological redshifts.

Regarding a generalization, in the original sense of the term, of relative velocity of luminous source in a general Riemannian space-time, indeed this problem is the most important for GR. It will be separate topic for an investigation elsewhere.

doi: https://doi.org/10.52526/25792776-2021.68.1-12

With this perspective in sight, we will proceed according to the following structure. To start with, Section 2 deals with a startling challenge of the superluminal recession velocities. Deriving in Section 3 the *kinetic* recession velocity of a distant astronomical object, we reconcile the cosmological interpretation of redshift with the correct solution to a kinematic interpretation of redshifts as accumulated Doppler-shifts. In Subsection 3.1, we show that a general solution is reduced to a global Doppler shift along the null geodesic. In Section 4, we give a brief outline of a cosmological toy model of the Friedmann-Robertson-Walker (FRW)-universe for zero-density in the RW coordinates. Concluding remarks are given in Section 5. A few more technical details in use are deferred to appendices. Appendix A provides a brief critical discussion of some key objectives with the analysis aimed at clarifying the current situation of the often met preliminary attempts of kinematic interpretation of redshifts as accumulated Doppler-shifts. This illustrates the problems and also hint at a possible solution. It was used as a backdrop to explore in Section 3 the *kinetic* recession velocity. Since many of the issues discussed in this contribution are conceptual, the observational status of these concepts is important. In Appendix B, therefore, we calculate the *kinetic* recession velocities of some typical distant astronomical objects with spectroscopic redshift determinations collected from the literature, which are listed in Table 1.

2. The concerns of the superluminal recession velocities

In past decades, the debate about superluminal `proper´ recession velocities was less fettered by observational evidence for large redshifts, but it gathers support from a breakthrough made in recent observational efforts, and at present it would require a good deal more ingenuity, which is of immense significance for the foundation of GR. Today there is no known feasible alternative way to account for credible explanation of the principle problem of superluminally receding galaxies. Such claims cannot be accepted as a convincing ones. This belief is suspect, and should be critically re-examined. A healthy degree of scepticism based on at least three objections is in order:

- The conclusions derived from assertion that the object is moving with the `relative´ velocity, $\dot{L}(t, z)$, to an observer must be treated with caution. Indeed, the incredibility of such an inference has been greatly enhanced by the recall that GR provides no *a priori* definition of `relative´ velocity, because their velocities are vectors at different events. This inability to compare vectors at widely separated space-time events was the fundamental feature of a curved space-time. Different coordinate reference frames and notions of `relative´ velocity yield different results for the motion of distant test particles relative to a particular observer. Bolós (2006, 2007), Bolós & Klein (2012), Bolós et al. (2002), Klein & Collas (2010), Klein & Randles (2011) address the question of relative velocities in GR. Consequently, three distinct coordinate charts, each with different notions of simultaneity, are employed by Bolós & Klein (2012) in the calculations of the four geometrically defined inequivalent concepts of relative velocity: Fermi, kinematic, astrometric, and the spectroscopic relative velocities. These definitions of relative velocities depend on two different notions of simultaneity: `spacelike simultaneity´ (or `Fermi simultaneity´) (Klein & Randles, 2011, Walker, 1935) as defined by Fermi coordinates of an observer, and `lightlike simultaneity´ as defined by optical (or observational) coordinates of an observer (Ellis, 1985). The Fermi and kinematic relative velocities can be described in terms of the `Fermi simultaneity´, according to which events are simultaneous if they lie on the same space slice determined by Fermi coordinates. Thereby, for an observer following a timelike worldline in Riemannian space-time, Fermi-Walker coordinates provide a system of locally inertial coordinates. If the worldline is geodesic, the coordinates are commonly referred to as Fermi or Fermi normal coordinates. Useful feature of Fermi coordinates was that the metric tensor expressed in these coordinates is Minkowskian to first order near the path of the Fermi observer, with second order corrections involving only the curvature tensor (Manasse & Misner, 1963). Klein & Randles (2011) find explicit expressions for the Fermi coordinates for Robertson-Walker (RW) space-times and show that the Fermi chart for the Fermi observer in non-inflationary RW space-times is global. However, rigorous results for the radius of a tubular neighborhood of a timelike path for the domain of Fermi coordinates are not available. The spectroscopic (or barycentric) and

doi: https://doi.org/10.52526/25792776-2021.68.1-12

astrometric relative velocities, which can be derived from spectroscopic and astronomical observations, mathematically, both rely on the notion of light cone simultaneity. According to the latter, two events are simultaneous if they both lie on the same past light cone of the central observer. It is shown that the astrometric relative velocity of a radially receding test particle cannot be superluminal in any expanding RW space-time. Necessary and sufficient conditions are given for the existence of superluminal Fermi speeds. Note that for the Hubble velocity, the proper distance is measured along non geodesic paths, while for the Fermi velocity, the proper distance is measured along spacelike geodesics. In this respect the Fermi velocity seems to be more natural, but the Hubble velocity is defined at all space-time points, whereas the Fermi velocity makes sense only on the Fermi chart of the central observer. Although alluded four definitions of relative velocities have own physical justifications, all they are subject to many uncertainties, and the ambiguity still remains.

- What is more, the `proper´ recession velocity, $\dot{L}(t, z)$, referred to in this claim is an unnatural quantity, because specifically it is the rate of change of the proper distance to the object with respect to the cosmic time coordinate, as measured at the present cosmic time. It has nothing to do with the object at all existed in the past. This coordinate velocity is a mere artifact to discuss, because it refers to events far outside of an observer's light cone.

- The picture of expanding universe is fully consistent with SR locally and GR globally (Robertson, 1935, Walker, 1936). One may, therefore, consider the large enough distance characteristic of the universe as a whole only within a theoretical framework capable of dealing with velocities approaching that of light. Any correctly defined relative velocity should be less than the speed of light, independent of any distance or time lag. The important reason to question the validity of a prediction of superluminal recession velocities, which became untenable, is the fact that it violates the fundamental principle of *causality* within these frameworks. As Hu et al. (1993) assert, "Superluminal expansion might be most naturally defined as that where any two comoving points eventually lose causal contact." Let us put aside subtleties of RW-metric of expansion (or whatever) of curved space, and focus on a clear academic question whether it is allowed for particle to attain superluminal velocity in this space with the given metric (g), where the particle always resides on the mass shell:

$$p^2 = g_{\mu\nu} p^\mu p^\nu = m_0^2 c^4, \tag{1}$$

provided, $p^\mu(E, c\overrightarrow{p})$ are the components of 4-momentum. But the truth is the contrariwise: situating on the mass shell, the particles cannot attain the velocities exceeding the speed of light even after making due allowances for bringing one back in time to an epoch when the universe was very young. A reliable way to see that the prediction of superluminal velocities (recession or whatever) is in error is the `monad´ formulation of metric theory of GR. The latter is the mathematical apparatus of physically observable quantities (Cattaneo, 1958, Eckart, 1940, Leaf, 1951, Pirani, 1962, Zelmanov, 1944, 1976). Monad formalism in the terms of Cartan's external calculus is worked out by Massa (1974). In this framework, one chooses a suitable family of observers based on the definition of `congruence´ of time-like world lines in given region. Whereas the tangent unit vector $\tau^\mu$ (`monad´) of `congruence´ time-like world line is $\tau^\mu \equiv u^\mu = dx^\mu/ds$, incorporated with the normalization condition $\tau^\mu \tau_\mu = \tau^\mu \tau^\nu g_{\mu\nu} = 1$. The metric tensor can be written in the form $g_{\mu\nu} = \tau_\mu \tau_\nu - h_{\mu\nu}$, where $h_{\mu\nu}$ is the metric tensor of local 3D spatial section of an observer orthogonal to unit vector τ^μ: $\tau^\mu h_{\mu\nu} = \tau^\mu h^\nu_\mu = \tau_\mu h^\mu_\nu = \tau_\mu h^\mu_\nu = \tau_\mu h^{\mu\nu} = \tau_\mu(\tau^\mu \tau^\nu - g^{\mu\nu}) = 0$. Then, instead of an arbitrary unobservable local displacement dx^μ, usually, the observable standards of spatial, $\widetilde{dx}^\nu = -h^\nu_\mu dx^\mu$, and time, $d\tau = \tau_\mu dx^\mu$, intervals can be introduced for whatever metric, so that the temporal and spatial components of tensors are clearly separated. Going to a new time coordinate, τ, one sets the potentials to zero at the world-point one is considering. The line element should be $ds = cd\tau\sqrt{1 - v^2/c^2}$, where $v^2 = h_{\mu\nu} v^\mu v^\nu$, and $v^\mu = -h^\mu_\nu (dx^\nu/d\tau)$ are the spacial components of particle velocity, so that the 4-dimensional speeds can be expressed through 3-dimensional, $u^\mu = (\tau^\mu + v^\mu/c)/\sqrt{1 - v^2/c^2}$. The `congruence´ of time-like world lines of the reference frame are characterized by four scalars,

doi: https://doi.org/10.52526/25792776-2021.68.1-12

subject to certain rules (Vladimirov, 1982), respectively: (i) the `first curvature´, $R_1$, defined by relation $R_1^2 = -F_\mu F^\mu$, where $F_\mu$ is the chr.inv.-vector of the `acceleration of the instrument of reference frame´ (`gravitational inertial force´), (ii) `stretching´, ε, defined as $\varepsilon = -(1/2)D$, where $D_{\mu\nu}$ is the chr.inv.-tensor of the `velocities of deformation of space´, (iii) the `rotation´, Ω, defined by relation $\Omega^2 = (1/2)A_{\mu\nu}A^{\mu\nu}$, where $A_{\mu\nu}$ is the chr.inv.-tensor of the `angular velocity of the rotation of space´ due to its non-holonomity (the non-orthogonality of the time lines to the spatial section), and (iiii) `shear´, σ, of congruence defined as $\sigma^2 = (1/2)(D_{\mu\nu}D^{\mu\nu} - \varepsilon^2/2)$. The `monad´ method is most effective in special systems of coordinates, so-called `chronometric´ ($\tau^i = dx^i/ds) = 0$, chosen so that the congruence of coordinate lines x^0 ($x^i = const$) coincides with the congruence of time-like world lines of the reference system τ. Solving the normalization condition $\tau^\mu\tau^\nu g_{\mu\nu} = 1$ the `monad´ is calibrated $\tau^\mu = g_0^\mu/\sqrt{g_{00}}$. The condition of coincidence of the congruence $\tau$ and $x^i = const$ defines a whole class of `chronometric´ coordinate systems linked to each other by special "chronometric" coordinate transformations, which are found from condition $\tau^i = 0$ in all chronometric coordinate systems. The physically observable (projected) quantities are invariant under "chronometric" coordinate transformations, and called 3-tensors or "chronometric invariants" (chr.inv.), which are invariant in the spatial section of the observer. So that the dispersion relation (1) can be recast into the form

$$p^2 = E^2 - c^2\overrightarrow{p}^2 = E^2 - c^2 h_{\mu\nu}\overline{p}^\mu\overline{p}^\nu = m_0^2c^4, \tag{2}$$

provided, $\overline{p}^\mu = -m_0 c h_\alpha^\mu(dx^\alpha/ds) = mv^\mu$ are the components of chr.inv.-vector of 3-momentum, and $m = m_0 c\tau_\alpha dx^\alpha/ds = m_0/\sqrt{1 - v^2/c^2}$ is the chr.inv.-invariant of moving (relativistic) particle dynamical mass. In no sense, therefore, can GR be said to allow for particle to attain superluminal velocity, and hence the vacuum value of a velocity of light is the universal maximum attainable velocity of a material body found in this space regardless of coordinate reference frame. Thus, the `monad´ formulation of GR ruptures once and for all the claim of separation between two more distant objects to increase faster than the speed of light as it has insufficient dimensions. The above said appears to provide a new perspective to have met the challenge of superluminal recession velocities, which the conventional scenario of expanding universe of standard cosmological model presents. In some instances, the distant astronomical objects are observed to exhibit redshifts in excess of unity (earlier epochs), thus, only a consistent theory would fill the void to tackle the key problems of a dynamics of such objects.

3. The *kinetic* recession velocity of comoving astronomical object in RW space-time

In the framework of standard cosmological model, one assumes that the universe is populated with comoving observers. In the homogeneous, isotropic universe comoving observers are in freefall, and obey Wayl's postulate: their all worldlines form a 3-bundle of non-intersecting geodesics orthogonal to a series of spacelike hypersurfaces, called comoving hypersurfaces. In case of expansion, all worldlines are intersecting only at one singular point. The clocks of comoving observers, therefore, can be synchronized once and for all. Let the proper time, t, of comoving observers be the temporal measure. Suppose $R(t)$ is the scale factor in expanding homogenous and isotropic universe. One considers in the so-called cosmological rest frame a light that travels from a galaxy to a distant observer, both of whom are at rest in comoving coordinates. As the universe expands, the wavelengths of light rays are stretched out in proportion to the distance $L(t)$ between co-moving points ($t > t_1$), which in turn increase proportionally to $R(t)$ (Harrison, 1993, 1995):

$$\tfrac{\lambda(t)}{\lambda(t_1)} = \tfrac{dt}{dt_1} = \tfrac{R(t)}{R(t_1)} = \tfrac{L(t)}{L(t_1)}. \tag{3}$$

Reviewing notations, $L_1 \equiv L(t_1)$ is the proper distance to the source at the time when it emits light, $L(t)$ is the same distance to the same source at light reception. Thus, the photons are seen as permanently loosing energy due to being cosmologically redshifted, because of which in modern cosmology

doi: https://doi.org/10.52526/25792776-2021.68.1-12

the photons are usually taken as negligibly influencing the present-day expansion dynamics. Such confidence is somehow based on the undoubted successes of GR in our immediate cosmic surroundings, with or without a L-term which has been termed `dark energy´ when it has the sign opposite to that of energy, whose necessity is still debated.

In what follows, we are going to define a more rigorous viable concept of *kinetic* recession velocity of a comoving distant galaxy of redshift z, which crossed past light cone at time t_1, at point (A_1) away from comoving observer (O) at the present time t. This is rather technical topic, and it requires care to do correctly. To clarify the issues further, it should help a few noteworthy points of Fig. 1, which illustrates the *lookforward* history of expanding homogenous and isotropic universe. The principle

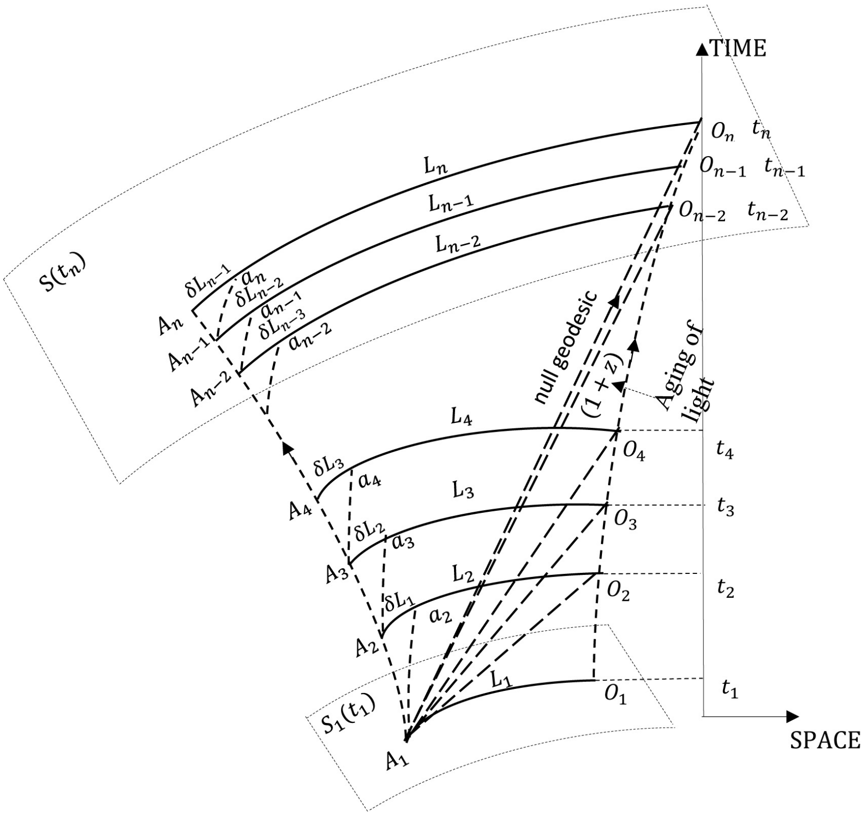

Figure 1. "Lookforward" history of expanding homogenous and isotropic universe: The increase of the proper distance L_i between a galaxy (A_i) and observer (O_i) (at epoch t_i) is viewed over different epochs $(i = 1, 2, ..., n)$, with the infinitesimal time difference $((t_i - t_{i-1}) \to 0)$. Whereas $t_n \equiv t$ and $L_n \equiv L(t)$. An observer (O_i) in its rest frame of reference measures the frequency of light rays emitted by a galaxy (A_i) viewed over different epochs $(1, ..., i)$ of expansion. Each proper distance $L_{A_{i-1}O_{i-1}}(t_{i-1})$ (at epoch t_{i-1}) is identically mapped on the line segment $L_{a_iO_i}(t_i)$ of proper distance (at infinitesimally close epoch t_i), such that $L_{a_iO_i}(t_i) \equiv L_{A_{i-1}O_{i-1}}(t_{i-1})$. Proper distance is the spatial geodesic measured along a comoving hypersurface $S(t_i)$ of constant cosmic time, into which a natural foliation of the space-time is defined by the RW metric. Null geodesic of a light signal from a galaxy (A_1) to the observers O_i $(O_n \equiv O)$ is also plotted.

foundation of our approach comprises the following steps. Let $L_i \equiv L(t_i)$ be the `proper distance´ between a galaxy (A_i) and observer (O_i), at given epoch (t_i), while the increment of the L_i is viewed over different epochs $(i = 1, 2, ..., n)$, with the infinitesimal time difference $((t_i - t_{i-1}) \to 0,\ n \to \infty)$. Whereas $t_n \equiv t$ and $L_n \equiv L(t)$. We assume that an observer (O_i) in its rest frame of reference measures the frequency of light rays emitted by a galaxy (A_i), viewed over different epochs $(1, ..., i)$ of expansion. Each proper distance $L_{A_{i-1}O_{i-1}}(t_{i-1})$ (at epoch t_{i-1}) is identically mapped on the line segment $L_{a_iO_i}(t_i)$ of proper distance (at infinitesimally close epoch t_i), such that $L_{a_iO_i}(t_i) \equiv L_{A_{i-1}O_{i-1}}(t_{i-1})$. Null geodesic of a light signal travelling from a galaxy (A_1) to the observer O_i $(O_n \equiv O)$ is also plotted. This picture, of course, wholly agrees with the Cosmological Principle. The requirement for spacial

doi: https://doi.org/10.52526/25792776-2021.68.1-12

homogeneity and isotropy is implemented by this principle in order to avoid a privileged observer. In accord to modern cosmology, the universe does not expand in space, but consists of expanding space. It does not say anything about the point of origin of the universe, either it does not mean that every pair of galaxy (A_i) and observer (O_i) is in any specially favoured or unfavoured position in the universe: the universe is isotropic about this pair, which moving apart as universe expands. Now let us explore the definition of Hubble's parameter to write

$$H = \frac{d}{dt}\log\left(\frac{R(t)}{R_1}\right) = \frac{d}{dt}\ln(1+z) = \frac{1}{1+z}\frac{dz}{dt}. \tag{4}$$

According to (3), the redshift, z must be expressed in terms of the increment $z = \frac{L-L_1}{L_1} \equiv \frac{L(t_n)-L(t_1)}{L(t_1)}$, which incorporated with the relations $dt/dt_1 = 1+z$ and (4) yield

$$\frac{dL_1}{dt_1} = \dot{L} - HL = 0. \tag{5}$$

It is then mere question of convenience to think of an observer $(O_{(1)})$ having observed in its rest frame of reference that any point of curve $L_1 (= L_{A_1 O_{(1)}})$ is not receding:

$$v_{A_1 O_{(1)}}(t_1)(\text{recession velocity}) = 0 \quad (\text{redshift} = 0). \tag{6}$$

Thus the relation $\lambda_{A_1} = \lambda_{O_{(1)}}$ holds for the wavelengths, which is of course consistent with (3). Imagine a family of comoving adjacent observers situated at the points a_i $(i = 2, ..., n)$ on the infinitesimal distances from the galaxies (A_i), who measure the frequency of light rays emitted by (A_i) as it goes by. After making due allowances for (3), particularly, the `relative´ infinitesimal increment δz_j $(j = 1, ..., n-1)$ of redshift reads

$$\delta z_j = \frac{\delta\lambda_j}{\lambda_j} = \frac{\lambda_{j+1}-\lambda_j}{\lambda_j} = \frac{\delta L_j}{L_j} = \frac{L_{j+1}-L_j}{L_j} = \frac{\tilde{\delta} z_j}{1+z_j} \equiv \frac{z_{j+1}-z_j}{1+z_j}, \quad 1+z_j = \frac{\delta\lambda_j}{\lambda_1}. \tag{7}$$

Consequently, an observers should observe the successive increments of `relative´ redshifts, $\delta z_1, \delta z_2, \delta z_3, ..., \delta z_{n-1}$, of the light when passing across the infinitesimal distances $(A_2, a_2), (A_3, a_3), ..., (A_n, a_n)$. Thus, the wavelength of light emitted at A_i is infinitesimally stretched out relative to the wavelength of light emitted at the adjacent point a_i. While weak, such effects considered cumulatively over a great number of successive increments of redshifts could become significant. The resulting redshift is the accumulation of a series of infinitesimal `relative´ redshifts. This interpretation holds rigorously even for large redshifts of order one or more.

If this view would prove to be true, it would lead to the chain rule for the wavelengths:

$$\frac{\lambda_{A_n}}{\lambda_1} \equiv \frac{\lambda_n}{\lambda_1} = \frac{\lambda_n}{\lambda_{n-1}} \cdot \frac{\lambda_{n-1}}{\lambda_{n-2}} \cdots \frac{\lambda_3}{\lambda_2} \cdot \frac{\lambda_2}{\lambda_1} = \prod_{i=1}^{n-1}(1+\delta z_i), \tag{8}$$

where $\lambda_1 \equiv \lambda_{A_1} (= \lambda_{O_1} = \lambda_{O_n})$, which readily yields

$$1 + z = \frac{\lambda_{A_n}}{\lambda_{O_n}} = \prod_{i=1}^{n-1}(1+\delta z_i). \tag{9}$$

With no loss of generality, we may of course apply (9) all the way to $n \to \infty$. Let us view the increment of the proper distance, $L_i = L(t_i)$, between a galaxy (A_i) and observer (O_i) over epochs $t_i \quad (i = 2, ..., n)$ as follows: $L_i = L_1 + (i-1)\varepsilon$, where ε can be made arbitrarily small by increasing n. In the limit $n \to \infty$, all the emitters (A_i) and respective adjacent observers (a_i) are arbitrarily close to each other, the physical separations (A_i, a_i) are approaching to zero, so that $\delta z_i = \delta L_i / L_i \simeq \varepsilon / L_1 \to 0$. This allows us to write the following relation for the infinitesimal `relative´ redshifts:

$$\begin{gathered}(\delta z_{n-1} = \delta z_{n-2} = \cdots = \delta z_1 = \varepsilon/L_1)_{n\to\infty} = \delta z^{(a)} = \\ \lim_{n\to\infty} \delta z^{(a)}_{(n-1)} \equiv \lim_{n\to\infty}\left(\frac{1}{n-1}\sum_{i=1}^{n-1}\delta z_i\right),\end{gathered} \tag{10}$$

where $\delta z^{(a)}$ is the average infinitesimal increment of `relative´ redshift. The relation (9) then becomes

$$1 + z = \lim_{n\to\infty}\prod_{i=1}^{n-1}(1+\delta z_i) = \lim_{n\to\infty}\left(1+\delta z^{(a)}_{(n-1)}\right)^{n-1}. \tag{11}$$

doi: https://doi.org/10.52526/25792776-2021.68.1-12

There does not seem to be any reason to doubt a validity of the relation (10). Certainly, the identification adopted here can be readily proved as follows. According to (7), in curved space of expanding universe, in general, the infinitesimal `relative´ redshifts arise at a series of infinitesimal stretching of the proper distance, so that the relation (11), by virtue of (10), can be recast into the form

$$1+z=\lim_{n\to\infty}\left(1+\frac{1}{n-1}\sum_{i=1}^{n-1}\frac{\delta L_i}{L_i}\right)^{n-1}=\lim_{n\to\infty}\left(1+\frac{1}{n}\ln\frac{L_n}{L_1}\right)^{n}=\lim_{n\to\infty}\frac{L_n}{L_1}, \tag{12}$$

which agrees with (3). Hence the overall cosmological redshift is a new physical phenomenon consequent on expansion of the universe, which induces the wave stretching of the traveling light via the Lemaître's important relationship:

$$z=\frac{L(t)}{L(t_1)}-1=\frac{R(t)}{R(t_1)}-1, \tag{13}$$

provided, $(1+z)$ is the factor by which the universe has expanded while the light was travelling towards an observer.

It is worth emphasizing that the general equation (11) is the result of a series of infinitesimal stretching of the proper distance in RW space-time, whereas the path of a light appears nowhere, thus this equation does not relate to the special choice of any transport path. Therefore, to overcome the ambiguity of parallel transport of four-velocities, particularly, in RW space-time, in what follows we advocate exclusively with this proposal. To obtain some feeling about this statement, below we give more detailed explanation.

According to well-known generalization of the spectral shift rule in a Riemannian space-time (Synge, 1960), the infinitesimal increments of `relative´ spectral shifts $(\delta z_1, \delta z_2, \delta z_3, ..., \delta z_{n-1})$ can be derived from Doppler effect between adjacent emitter and absorber in relative motion measured in the respective tangent local inertial rest frames at infinitesimally separated space-time points. Let $v_{A_i a_i}(t_i)$ be the relative infinitesimal velocity consequent on recession of a galaxy (A_i) to adjacent observer at the point a_i, separated by the infinitesimal distance $\delta L_i \equiv L_{A_i a_i}(t_i)$. Since each proper distance $L_{A_{i-1}O_{i-1}}(t_{i-1})$ (at epoch t_{i-1}) is identically mapped on the line segment $L_{a_i O_i}(t_i)$ of proper distance (at infinitesimally close epoch t_i), the relative velocity $v_{A_i a_i}(t_i)$ is the same as it is relative to a galaxy (A_{i-1}): $v_{A_i A_{i-1}}(t_i) \equiv v_{A_i a_i}(t_i)$. Continuing along this line, we may commit ourselves in the series of `relative´ spectral shifts a certain substitution of increments of relative velocities. Taking into account that such infinitesimal relative velocities arise at a series of infinitesimal stretching of the proper distance $L_{A_2 a_2}(t_2), ..., L_{A_n a_n}(t_n)$ as it is seen from the Fig. 1, we may at equal footing fill out now the whole pattern of monotonic increments of `relative´ spectral shifts $(\delta z_1, \delta z_2, \delta z_3, ..., \delta z_{n-1})$ by replacing the respective pairs $(A_2, A_1), ..., (A_n, A_{n-1})$ with new ones $(A_2, a_2), ..., (A_n, a_n)$, which attribute to the successive increments of recession (relative) velocities $v_{A_2 A_1}(t_2), ..., v_{A_n A_{n-1}}(t_n)$ of a galaxy (A_n) away from observer (O_n) in the rest frame of (O_n), viewed over different epochs $(t_2, ..., t_n)$. Thereby the principle of time-invariant homogeneity requires that if a galaxy (A_i) recedes from an adjacent observer (a_i) with velocity $v_{A_i a_i}(t_i)(= v_{A_i A_{i-1}}(t_i))$, then a galaxy (A_{i-1}) simultaneously recedes from an equally spaced observer (a_{i-1}) with the same velocity $v_{A_{i-1}a_{i-1}}(t_{i-1})(= v_{A_{i-1}A_{i-2}}(t_{i-1}))$: $v_{A_i a_i}(t_i) = v_{A_{i-1}a_{i-1}}(t_{i-1})$. This framework furnishes justification for the recession velocity $v_n \equiv v_{A_n A_1}$, to be now referred to as the *kinetic* recession velocity, of galaxy (A_n) away from observer (O_n), in its rest frame, at epoch (t_n). According to relation (10), at the limit $n \to \infty$, the infinitesimal recession velocities tend to zero: $v_{A_i a_i}(t_i) = c\delta\beta_i = c\delta z_i = c\delta L_i/L_i \simeq c\varepsilon/L_1 \to 0$, such that

$$\begin{gathered}\lim_{n\to\infty}\delta\beta_1=\lim_{n\to\infty}\delta\beta_2=\cdots=\lim_{n\to\infty}\delta\beta_{n-1}=\\ \delta\beta^{(a)}\left(\equiv\lim_{n\to\infty}\frac{1}{n-1}\sum_{i=1}^{n-1}\delta\beta_i\right)=\lim_{n\to\infty}\frac{1}{n}\beta_n.\end{gathered} \tag{14}$$

Remark: Although we are free to deal with any infinitesimal `relative´ spectral shift δz_i of emitter (A_i) in local tangent inertial rest frame of adjacent absorber (a_i) (where we may approximate away the curvature of space in the infinitesimally small neighborhood), we should take into account that the infinitesimal relative velocities arise in RW space-time at a series of infinitesimal stretching of the proper distance, and that the *SR law of composition of velocities cannot be implemented globally along*

doi: https://doi.org/10.52526/25792776-2021.68.1-12

the non-null geodesic, because these velocities are velocities at the different events, which should be in a different physical frames, and cannot be added together.

Facilitating further the calculations of recession velocity (β_n) in quest, we may address a galaxy (A_n) and an adjacent observer at (a_n). Suppose $V^{\mu}_{(A_n)}$ and $V^{\mu}_{(a_n)}$ ($\mu = 0, 1, 2, 3$) are the unit tangent four-velocity vectors to their respective world-lines, thus in their respective rest frame we have $V^0_{(A_n)} = 1$ and $V^0_{(a_n)} = 1$, as the only nonzero components of velocity. Employing a generalization of the spectral shift rule in a Riemannian space-time (Synge, 1960), the infinitesimal increment δz_{n-1} of spectral shift can be written

$$\delta z_{n-1} = \frac{U_{\mu(A_n)}V^{\mu}_{(A_n)}}{U_{\nu(a_n)}V^{\nu}_{(a_n)}} - 1, \tag{15}$$

where $U_{\mu(A_n)}$ and $U_{\mu(a_n)}$ are the tangent vector to null geodesic $\Gamma_{A_n a_n}$ at end points. The frequency shift δz_{n-1} is expressed by the metric tensor, the direction of the velocity of light and the velocities of source and observer. Since all the paths between infinitesimally separated space-time points (A_n) and (a_n) coincide at $n \to \infty$, there is no need to worry about specific choice of the path of parallel transport of four-vector. Therefore, let us further subject the unit tangent four-velocity vector $V^{\mu}_{(A_n)}$ to parallel transport along the null geodesic joining (A_n) and (a_n). This yields at (a_n) the vector $\beta_{\mu(a_n)} = \mathrm{g}_{\mu\nu'}(a_n, A_n)V^{\nu'}_{(A_n)}$, where the two point tensor $\mathrm{g}_{\mu\nu'}(a_n, A_n)$ is the parallel propagator, which is determined by the points A_n and a_n. At $(A_n) \to (a_n)$, we have the coincidence limit $[\mathrm{g}_{\mu\nu}](a_n) = g_{\mu\nu}(a_n)$. As we have at point ($a_n$) two velocities $V^{\mu}_{(a_n)}$ and $\beta^{\mu}_{(a_n)}$, following Synge, (see also Narlikar (1994), we can associate Doppler shift δz_{n-1} to a galaxy (A_n) with four-velocity $\beta^{\mu}_{(a_n)}$ observed by an adjacent observer (a_n) with four-velocity $V^{\mu}_{(a_n)}$ as measured by the latter:

$$\delta z_{n-1} = \frac{U_{\mu(a_n)}\beta^{\mu}_{(a_n)}}{U_{\nu(a_n)}V^{\nu}_{(a_n)}} - 1 = 1 - \frac{1}{(1+\beta^2_{(a_n)})^{\frac{1}{2}} + \beta_{R(a_n)}}, \tag{16}$$

where $c\beta^{\mu}_{(a_n)} = v^{\mu}_{(a_n)}$, $c\beta_{(a_n)} = v_{(a_n)}$, $c\beta_{R(a_n)} = v_{R(a_n)}$, and

$$v^2_{(a_n)} = v_{(\alpha)(a_n)}v^{(\alpha)}_{(a_n)}, \quad v_{(\alpha)(a_n)} = v_{\mu(a_n)}\xi^{\mu}_{(\alpha)(a_n)}, \quad v_{R(a_n)} = v_{\mu(a_n)}r^{\mu}_{(a_n)} = v_{(\alpha)(a_n)}v^{(\alpha)}_{(a_n)}. \tag{17}$$

Reviewing notations the three-velocity of (A_n) relative to (a_n) are defined by the tree invariant components $v_{(\alpha)(a_n)}$, the relative speed is $v_{(a_n)}$, and $v_{R(a_n)}$ is the speed of recession of (A_n). The frame of reference $\xi^{\mu}_{(\alpha)(a_n)}$ defined at (a_n) implies $\xi^{\mu}_{0(a_n)} = V^{\mu}_{(a_n)}$, the unit vector $r^{\mu(a_n)}$ at (a_n) is orthogonal to world-line of (a_n) ($r_{\mu(a_n)}V^{\mu}_{(a_n)} = 0$) and lying in the 2-element which contains the tangent at (a_n) to world-line of an observer (a_n) and (A_n, a_n).

In the local inertial rest frame $\xi^{\mu}_{(\alpha)(a_n)}$ of an observer (a_n), the velocity vector $\beta^{\mu}_{(a_n)}$ takes the form $(\gamma, \gamma\delta\beta_{(a_n)}, 00)$, where a galaxy ($A_n$) is moving away from an observer (a_n) with the relative infinitesimal three-velocity $c\delta\beta_{(a_n)}$ in a direction making an angel $\theta_{(a_n)}$ with the outward radial direction from (a_n) to (A_n), and $\gamma = (1 - \delta\beta^2_{(a_n)})^{-1/2}$. Hence, the equation (16) is reduced to

$$\begin{aligned} \delta z_{n-1} = \frac{1+\delta\beta_{(a_n)}\cos\theta}{\sqrt{1-\delta\beta^2}} - 1 = \beta_{R(a_n)} - \beta^2_{R(a_n)} + \tfrac{1}{2}\beta^2_{(a_n)} + \cdots \simeq \beta_{R(a_n)} = \\ \frac{p_{(\alpha)(a_n)}v^{(\alpha)}_{(a_n)}}{E_{(a_n)}} = \delta\beta_{(a_n)}\cos\theta_{(a_n)}, \end{aligned} \tag{18}$$

where $p_{(\alpha)(a_n)}$ and $E_{(a_n)}$ are, respectively, the momentum and energy of light ray as measured locally by an observer (a_n). Thus, at $n \to \infty$, the wavelength of emitted by a galaxy (A_n) radiation is increased by the first-order Doppler shift caused unambiguously by the infinitesimal recession velocity $\delta\beta_{(a_n)} \equiv \delta\beta^{(r)}_{n-1}$ in radial direction ($\cos\theta_{(a_n)} \to 1$):

$$\delta z_{n-1} = \frac{\delta L_{n-1}}{L_{n-1}} = \delta\beta^{(r)}_{n-1}. \tag{19}$$

doi: https://doi.org/10.52526/25792776-2021.68.1-12

In the local tangent inertial rest frame of an observer (a_n), the latter reads (see subsect. 3.1):

$$\delta\beta^{(r)}_{n-1} = \frac{\beta_n-\beta_{n-1}}{1-\beta_n\beta_{n-1}} \simeq \frac{\delta\beta_{n-1}}{1-\beta^2_{n-1}}, \tag{20}$$

where $v_n = c\beta_n \equiv cV_{(A_n)}$ and $v_{n-1} = c\beta_{n-1} \equiv cV_{(a_n)}$ are, respectively, the three-velocities of a galaxy (A_n) and an observer (a_n) along the radial direction from (a_n) to (A_n). A resulting infinitesimal increment δz_{n-1} of spectral shift, at $n \to \infty$ then reads

$$\lim_{n\to\infty} \delta z_{n-1} = \lim_{n\to\infty} \frac{\delta\beta_{n-1}}{1-\beta^2_{n-1}} = \lim_{n\to\infty} \frac{\beta_n}{n(1-\beta^2_n)}, \tag{21}$$

For our goal, the most straightforward guess at the convenient form of (13), by virtue of (10), is written

$$1+z = \frac{R(t)}{R(t_1)} = \lim_{n\to\infty}(1+\delta z_{n-1})^n. \tag{22}$$

Certainly, it is merely the choice to be rewarding to go ahead with a finite spectral shift

$$1+z = \frac{R(t)}{R(t_1)} = \lim_{n\to\infty}\left[1+\frac{1}{n}\left(\frac{\beta_n}{(1-\beta^2_n)}\right)\right]^n. \tag{23}$$

This straightforwardly yields the general kinematic relationship of the overall cosmological redshift, z, and *kinetic* recession velocity β_{rec} (in units of the speed of light) of the comoving distant galaxy (A_1) of redshift z, which crossed past light cone at time t_1 away from comoving observer (O):

$$1+z = \frac{R(t)}{R(t_1)} = \exp\left(\frac{\beta_{rec}}{1-\beta^2_{rec}}\right), \tag{24}$$

where, hereinafter, the *kinetic* recession velocity β_n is marked with subscript $()_{rec}$. This interpretation so achieved has physical significance as it agrees with a view that the light waves will be stretched by travelling through the expanding universe, and in the same time the *kinetic* recession velocity of a distant astronomical object is always subluminal even for large redshifts of order one or more. It, therefore, does not violate the fundamental physical principle of *causality*.

The *kinetic* recession radial velocity of a galaxy is plotted on the Fig. 2 (*Top panel(a):* for redshifts $0 \le z \le 10$; and *Bottom panel(b):* for redshifts $0 \le z \le 800$), where the global Doppler velocity, and their difference are also presented to guide the eye. As it can be seen from the Figure 2, the difference of global Doppler velocity and *kinetic* recession velocity, for redshifts $0.9 \le z \le 800$, is $(\beta_{Dop} - \beta_{rec}) \ge 0.072c$, where a maximum value, $(\beta_{Dop} - \beta_{rec})_{max} = 0.187c$, is reached at redshifts $= 4.5 - 5.1$.

If, and only if, for the distances at which the Hubble empirical linear `redshift-distance´ law $(cz = HL)$ is valid, the relationship between the *physical* recession velocity, v_{rec}, and the expansion rate, $\dot{L}$ $(= HL)$, reads

$$\beta_{rec} = \frac{\sqrt{1+4\ln^2(1+\dot{L}/c)}-1}{2\ln(1+\dot{L}/c)}. \tag{25}$$

Once we are equipped with the general solution, it is worth emphasizing the importance of the parameter $\zeta(z)$ of practical measure of being swept up of galaxy in expanding universe:

$$\zeta(z) = \frac{v_{rec}}{\dot{L}} = \frac{\beta_{rec}}{z}. \tag{26}$$

Next we will study a particular case of establishing a global Doppler shift from a general solution (24).

3.1. A global Doppler shift along the null geodesic

Once we are equipped with the general solution (24), it is worth to show that this solution is reduced to a global Doppler shift along the null geodesic, previously studied by Synge (1960) (see also Bunn & Hogg (2009), Narlikar (1994)) who used the parallel transport of source four-velocity along the null geodesic to an observer. Certainly, suppose a dense family of adjacent comoving observers being in free fall populated along the path of light ray from a galaxy (A_1) to an observer (O_n) (Fig. 1). The (i)-th

doi: https://doi.org/10.52526/25792776-2021.68.1-12

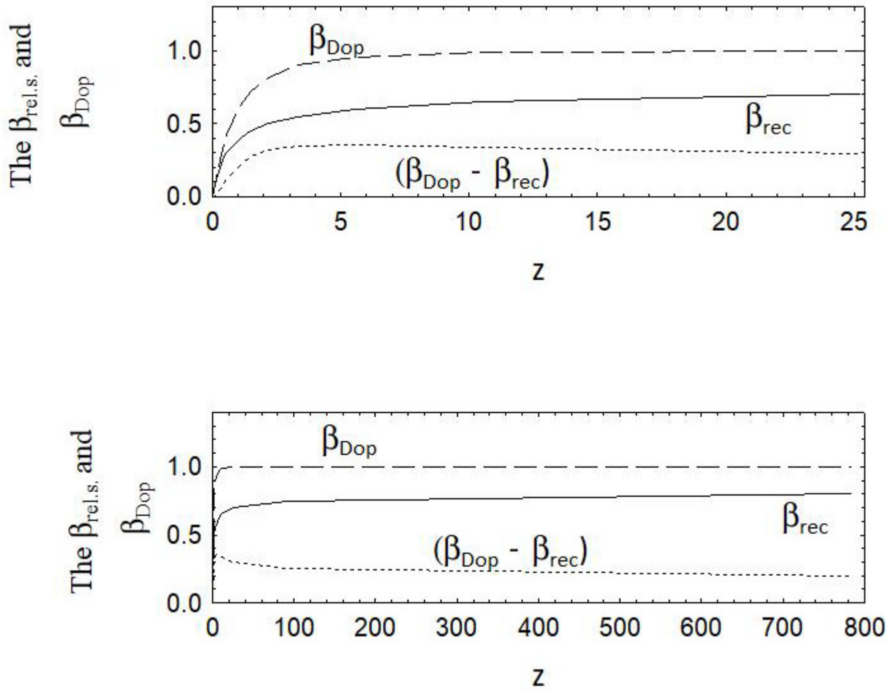

Figure 2. The recession velocity along the line of sight (β_{rec}) of luminous source (S) with redshift z away from the observer (O), the global Doppler velocity (β_{Dop}), and their difference (in units of the speed of light). *Top panel:* $0 \leq z \leq 25$; *Bottom panel:* $0 \leq z \leq 800$.

observer situated at the point (i) of intersection of the ray's trajectory with a comoving hypersurface $S(t_i)$ of constant cosmic time. Then, the end points of infinitesimal distance $\delta l_i = c\delta t_i$ between the adjacent observers $(i+1)$ and (i) will respectively be the points of intersection of the ray's trajectory with the comoving hypersurfaces $S(t_{i+1})$ and $S(t_i)$. Thus the infinitesimal increment of the frequency shift on the distance $\delta l_i = c\delta t_i$, caused by expansion of the universe during the infinitesimal epoch time interval $\delta t_i = t_{i+1} - t_i$, according to (7), should be $\delta z_i = \delta\lambda_i/\lambda_i = \delta L_i/L_i$. Due to the equivalence principle, we may approximate away the curvature of space in the infinitesimally small neighborhood of two adjacent observers. Thereby, approximating away the curvature of spacetime in the infinitesimally small neighborhood does not mean approximating away the expansion altogether. That is, it must be stated emphatically that if we approximate an infinitesimally small neighborhood of the size δL_i of an expanding spacetime as flat, the resulting errors are of order $(\delta L_i/L_H)^2$ in the metric. If we regard such errors as negligible, then we can legitimately approximate spacetime as flat. The increment of redshift δz_i is not approximated away in this limit because it is in that neighborhood of leading order $(\delta L_i/L_i)$. Imagine a thin world tube around the null geodesic within which the space-time is flat to arbitrary precision. In particular, this implies the vacuum value of a velocity of light to be universal maximum attainable velocity of a material body found in this space. This statement is true for any thin neighborhood around a null geodesic. Therefore, each observer has a local reference frame in which SR can be taken to apply, and an observers are close enough together that each one $(i+1)$ lies within the local frame of his neighbor (i). Only in this particular case of null geodesic, the relative velocity of observers can be calculated by the SR law of composition of velocities globally along this path. Within each local inertial frame, there are no gravitational effects, and hence the infinitesimal frequency shift from each observer to the next is a Doppler shift. Hence, at the limit $n \to \infty$, a resulting infinitesimal frequency shift δz_i, can be unambiguously equated to infinitesimal increment of a fractional SR Doppler shift $\delta\bar{z}_i$ from observer $(i+1)$ to the next (i) caused by infinitesimal relative velocity $\delta\bar{\beta}^r_i$:

$$\left(\delta z_i = \frac{\delta L_i}{L_i}\right)_{n\to\infty} = \left(\delta\bar{z}_i = \delta\bar{\beta}^r_i = \frac{\bar{\beta}_{i+1} - \bar{\beta}_i}{1 - \bar{\beta}_{i+1}\bar{\beta}_i} \simeq \frac{\delta\bar{\beta}_i}{1 - \bar{\beta}^2_i}\right)_{n\to\infty}, \tag{27}$$

doi: https://doi.org/10.52526/25792776-2021.68.1-12

where by $\bar{()}$ we denote the null-geodesic value, as different choice of geodesics yields different results for the motion of galaxy relative to a particular observer. The relation (27), incorporated with the identity (10), yield

$$(\delta z_{n-1} =)_{n\to\infty} = \left(\frac{\delta\beta_{n-1}}{1-\beta_n^2}\right)_{n\to\infty} = \left(\delta\bar{z}^{(a)}_{(n-1)} = \delta\bar{\beta}^{r(a)}_{(n-1)} \equiv \frac{1}{n-1}\sum_{i=1}^{n-1}\frac{\delta\bar{\beta}_i}{1-\bar{\beta}_i^2}\right)_{n\to\infty}, \tag{28}$$

which, by virtue of (14), for sufficiently large but finite n gives

$$\frac{\beta_n}{1-\beta_n^2} = \sum_{i=1}^{n-1}\frac{\delta\bar{\beta}_i}{1-\bar{\beta}_i^2} = \int_0^{\bar{\beta}_n}\frac{d\bar{\beta}}{1-\bar{\beta}^2}, \tag{29}$$

or

$$\bar{\beta}_n = \frac{e^{\varrho_n}-1}{e^{\varrho_n}+1}, \quad \varrho_n \equiv \frac{2\beta_n}{1-\beta_n^2}. \tag{30}$$

Hence the general solution (24), by means of (29), is reduced to a global Doppler shift along the null geodesic:

$$1+z = \exp\left(\frac{\beta_{rec}}{1-\beta_{rec}^2}\right) = \sqrt{\frac{1+\bar{\beta}_{rec}}{1-\bar{\beta}_{rec}}}, \tag{31}$$

where $\bar{\beta}_{rec} = \lim_{n\to\infty}\bar{\beta}_n$. Thus, this procedure in fact is exactly equivalent to performing parallel transport of the source four-velocity in curved space of expanding universe along the null geodesic to an observer. In Minkowski space a parallel transport of vectors is trivial and mostly not mentioned at all. This allows us to apply globally the SR law of composition of velocities to relate the velocities $\bar{\beta}_{i+1}$ to the $\bar{\beta}_i$ of adjacent observers along the path of light ray, measured in the i-th adjacent observer's frame. Then, according to (27)-(31), a global Doppler shift of light ray emitted by luminous source as it appears to observer at rest in flat Minkowski space can be derived by summing up the infinitesimal Doppler shifts caused by infinitesimal relative velocities of adjacent observers.

4. A cosmological toy model of FRW-universe for zero-density in the RW coordinates

In our actual universe space-time is not exactly flat, but a sufficiently large region of the transparent universe, say on length scales of one to ten or so billion light years, usually can be well approximated by a zero-density spatially flat homogeneous isotropic cosmological model having ($k = 0$) FRW metric (Page 2009):

$$ds^2 = c^2dt^2 - R^2(t)d\chi^2, \tag{32}$$

where $d\chi = \sqrt{dx^2+dy^2+dz^2}$ is the (constant) comoving coordinate distance between the comoving two particles, with (dx, dy, dz) being the differences between their comoving coordinates. The particles in this idealized model each stay at fixed comoving coordinates (x, y, z) as their proper time t increases. The physical distance between two particles, as measured along a geodesic of a comoving hypersurface of constant t, grows at the Hubble expansion rate of the universe at the time t. For the spatially flat model (32), there is no upper limit to the comoving coordinate distance χ, and that also to the proper distance $L(t) = R(t)\chi$, at any fixed t. The metric (32) can be rewritten as an expanding open RW-metric ($k = -1$) with $R(t) \propto t$ (Gron 2007; Page 2009), i.e. the Milne model (Milne 1934). The Milne universe is the Minkowski space-time described from an expanding reference frame. Although in the RW coordinates the 3D comoving hypersurface of constant t (constant proper time) does have an extrinsically non-zero curvature, nevertheless the 4D curvature is zero. Therefore, simple coordinate transformations transform the metric to the standard Minkowski form with the Minkowski coordinates. The Minkowski coordinates (T, X, Y, Z) are the coordinates of a rigid inertial reference frame of an arbitrarily chosen reference particle P in the expanding cloud of particles defining the Milne universe model. The time T is the private time of P. The time t is measured on clocks following all of the reference particles. The Milne universe can be identified as the forward light cone in Minkowski space-time, foliated by negatively curved hyperboloids orthogonal to the time axis. In the inertial and rigid Minkowski coordinate system the velocity of a reference particle with comoving coordinate χ is less than the speed of light for all values of χ. The components of a parallel transported four-vector in

doi: https://doi.org/10.52526/25792776-2021.68.1-12

inertial coordinates are constant and, thus, a parallel transport is trivial and mostly not mentioned at all. As mentioned in Subsection 3.1, the general equation (11) of redshift is unambiguously reduced in this limit to a conventional global Doppler shift formula with SR-relative speed, because the SR law of composition of velocities can be implemented globally in the whole Minkowski space. Thus, in this limit a correspondence to the more usual notion of SR-relative speed retains.

But this is no longer true for non-inertial coordinates RW of expanding cosmic frame. In this frame, the reference particles with Milne coordinates (t, χ) define the expanding public space of the universe model. The Hubble's expansion refers to the GR space defined by simultaneity on the clocks following the reference particles. It is valid in the public space of the universe model, not the private space of a particular observer. It has infinite extension. Hence the reference particles have superluminal velocity at sufficiently great distances from an observer. Moreover, in the extrinsically curved 3D comoving hypersurface $t = const$ (public space) a parallel transport is not trivial and needs consideration (Page 2009). A geodesic between two events on such hypersurface passes through the future, and a transport along this geodesic will yield a different result. Using the length of geodesics of a particular spatial hypersurface worsens the problem of superluminal expansion. The infinitesimal relative velocities arise at a series of infinitesimal stretching of the proper distance, and that the SR law of composition of velocities cannot be implemented globally in the curved 3D hypersurface. In this case, the relation (11) leads to the general solution (24) of the overall cosmological redshift, with a *kinetic* recession velocity, which is always subluminal even for large redshifts of order one or more.

5. Concluding remarks

The conceptual and technical problems involved in this contribution provide scope for the arguments discussed, aiming to reconcile the cosmological interpretation of redshift with the most natural kinematic interpretation. Below we briefly reflect upon a few relevant points. The solutions given in present report demonstrate its advantage over the specific extant definitions in the cited literature:

- Section 3 presents what is essentially a correct solution to a kinematic interpretation. In the framework of "stretching of space" point of view of the spatially homogeneous and isotropic RW space-time of standard cosmological model, we overcome an ambiguity of the procedure of parallel transport of source four-velocity along the null geodesic to an observer by an alternative study of a "lookforward" history of expanding universe. We use a way of separating the cosmological redshifts into infinitesimal `relative´ redshift bins and sum over them to achieve an unique definition of the *kinetic* recession velocity of comoving astronomical object. The latter is always subluminal even for large redshifts of order one or more, so that it does not violate the fundamental physical principle of *causality*. The difference of global Doppler velocity and *kinetic* recession velocity, for redshifts $0.9 \leq z \leq 800$ is $\geq 0.072c$, where a maximum value, $0.187c$, is reached at redshifts $z = 4.5 - 5.1$. We calculate a practical measure parameter $\zeta(z)$ of being swept up of galaxy in expanding universe. We show that the derived general solution is unambiguously reduced to global Doppler shift along null geodesic.

- We discuss the obtained results in the limit of a zero-density cosmological model of Milne universe. Whereas, in the inertial and rigid Minkowski coordinate system the components of a transported four-vector in inertial coordinates are constant and, thus, a parallel transport is trivial and mostly not mentioned at all. The general solution (24) of redshift is unambiguously reduced in this limit to a conventional global Doppler shift with SR-relative speed, because the SR law of composition of velocities can be implemented globally in the whole Minkowski space. Thus, in this limit a correspondence to the more usual notion of SR-relative speed retains. But this is no longer true for non-inertial RW coordinates of expanding cosmic frame. In this frame, the reference particles with Milne coordinates define the expanding public space of the universe model. In the extrinsically curved 3D hypersurface (public space) a parallel transport is not trivial and needs consideration. The infinitesimal relative velocities arise at a series of infinitesimal stretching of the proper distance so that the SR law of composition of velocities cannot

doi: https://doi.org/10.52526/25792776-2021.68.1-12

be implemented globally in the curved 3D hypersurface. In this case, the overall cosmological redshift is described by the formula (24) with a *kinetic* recession velocity.

- In Appendix A, we give a reappraisal in a deep way of the preliminary attempts of `standard´ kinematic interpretation of redshifts as accumulated Doppler-shifts consequent on recession, widely discussed in literature. Its study is valuable as affording insight into the whole subject. In doing this, we are not suggesting any doubt about the principle statement. Rather, we doubt the method of calculations, which as we have shown are in error. Moreover, the principle statement is a crux of our derivation of an essentially correct solution to a kinematic interpretation of cosmological redshifts. In appendix B, we calculate the *kinetic* recession velocities of some typical distant astronomical objects with spectroscopic redshift determinations collected from the literature, which are listed in Table 1.

References

Bahcall J. N., Oke J. B., 1971, ApJ, 163, 235

Bañados E., Venemans B., Morganson E. e. a., 2014, AJ, 148, 14

Bañados E., Venemans B. P., Mazzucchelli C. e. a., 2018, Nature, 553, 473

Bolós V. J., 2006, J. Geom. Phys., 56, 813

Bolós V. J., 2007, Commun. Math. Phys., 273, 217

Bolós V. J., Klein D., 2012, Gen Relativ Gravit., 44, 1361

Bolós V. J., Liern V., Olivert J., 2002, Int. J. Theor. Phys., 41, 1007

Bunn E. F., Hogg D. W., 2009, Am. J. Phys., 77, 6888

Cattaneo C., 1958, Nuovo Cimento, 2, 318

Chambers R. H., 2011, BAAS, 43, 217

Chodorowski M. J., 2011, MNRAS, 413, 585

Davis T. M., Lineweaver C. H., 2004, PASAu, 21, 97

Dirac P. A. M., 1979, Proc. R. Soc. London A, 365, 19

Eckart C., 1940, Pys.Rev., 58, 919

Edge A e. a., 2013, Msngr, 154, 32

Ellis G. F. R. e. a., 1985, Phys. Rep., 124, 315

Emtsova E., Toporensky A., 2019, arXiv:[gr-qc], 1901.03602, 1

Fan X., Strauss M. A., Schneider D. P. e. a., 1999, AJ, 118, 1

Fan X., Strauss M. A., Richards G. T. e. a., 2001, AJ, 121, 31

Fan X., Carilli C. L., Keating B., 2006a, ARA&A, 44, 415

Fan X., Strauss M. A., Richards G. T. e. a., 2006b, AJ, 131, 1203

Fan X., Strauss M. A., Becker R. H. e. a., 2006c, AJ, 132, 117

Gautreau R., 1984, Phys. Rev. D, 29, 198

Grøn Ø., Elgarøy Ø., 2007, Am. J. Phys., 75, 151

Grøn Ø., Rippis P. D., 2003, Gen. Re. Grav., 35, 2189

Harrison E. R., 1993, ApJ, 403, 28

Harrison E. R., 1995, ApJ, 446, 63

Harrison E. R., 1981 and 2000, Cosmology: the science of the universe, 1 and 2 edn. Cambridge U. Press, Cambridge

Hashimoto T., Laporte N., Mawatari K. e. a., 2018, Nature, 557, 312

Hu Y., Turner M. S., Weinberg E. J., 1993, Phys. Rev. D, 49, 3830

doi: https://doi.org/10.52526/25792776-2021.68.1-12

Hu E. M., Cowie L. L., McMahon R. G. e. a., 2002, ApJ, 568, L75

Iwamuro F., Motohara K. e. a., 2002, ApJ, 565, 63

Jiang L., Fan X., Vestergaard M. e. a., 2007, AJ, 134, 1150

Jiang L., Fan X., Annis J. e. a., 2008, AJ, 135, 1057

Jiang L., McGreer I. D., Fan X. e. a., 2016, ApJ, 833, 222

Kaiser N., Aussel H., Burke B. E. e. a., 2002, in Society of Photo-Optical Instrumentation Engineers (SPIE) Conference Series. p. 154

Kaiser N., Burgett W., Chambers K. e. a., 2010, in Society of Photo-Optical Instrumentation Engineers (SPIE) Conference Series. p. 77330E

Kashikawa N. e. a., 2015, ApJ, 798, 28

Kaya A., 2011, Am. J. Phys., 79, 1151

Klein D., Collas P., 2010, Phys. Rev. D, 81, 063518

Klein D., Randles E., 2011, Ann. Henri Poincaré, 12, 303

Kurk J. D., Walter F., Fan X. e. a., 2009, ApJ, 702, 833

Laporte N., Ellis R. S., Boone F. e. a., 2017, ApJ, 837, L21

Lawrence A., 2007, MNRAS, 379, 1599

Leaf B., 1951, Pys.Rev., 84, 345

Liebscher D.-E., 2007, Astron. Nachr. / AN, 328, 586

Lilly S. J., Longair M. S., 1984, MNRAS, 211, 833

Lineweaver C. H., Davis T. M., 2005, SciAm, 292, 36

Lynds R., Wills D., 1970, Nature, 226, 532

Manasse F. K., Misner C. W., 1963, J. Math. Phys., 4, 735

Massa E., 1974, Gen.Rel. and Grav., 5, 555, 573, 715

Matsuoka Y. e. a., 2016, ApJ, 828, 26

McConnell N. J., Ma C.-P., Gebhardt K. e. a., 2011, Nature, 480, 215

McVittie C. C., 1933, MNRAS, 93, 325

Milne E. A., 1934, Quarterly J. of Math., 5, 64

Mortlock D. J., Warren S. J., Venemans B. P. e. a., 2011, Nature, 474, 616

Murdoch H. S., 1977, QJRAS, 18, 242

Narlikar J. V., 1994, Am. J. Phys., 62, 903

Oesch P. A., Brammer G., van Dokkum P. G. e. a., 2016, ApJ, 819, 129

Padmanabhan T., 1993, Structure Formation in the Universe. Cambridge Univ. Press, Cambridge

Page D. N., 2009, Class. Quantum Grav., 26, 127001

Pâris I., Petitjean P., Aubourg É. e. a., 2012, A&A, 548A, 66

Pâris I., Petitjean P., Aubourg É. e. a., 2014, A&A, 563A, 54

Peacock J. A., 1999, Cosmological Physics. Cambridge Univ. Press (Ninth printing with corrections 2010), address = Paris

Peacock J. A., 2002, in Modern Cosmology, Proceedings of the Como School 2000, ed. by Bonometto, S and Gorini, V and Moschella U. IOP, Bristol

Peacock J. A., 2008, arXiv:[astro-ph], 0809.4573, 1

Peebles P. J. E., 1993, Principles of Physical Cosmology. Princeton Univ.Press.

Peebles P. J. E., Schramm D., Turner E., Kron R., 1991, Nature, 352, 769

Pirani F., 1962, Le Theories relativistes dee la Gravitation. CNRS, Paris

doi: https://doi.org/10.52526/25792776-2021.68.1-12

Pössel M., 2019, arXiv: [gr-qc], 1912.11677, 1

Postman M., Lauer T. R., Donahue M. e. a., 2012, ApJ, 756, 159

Reed S. L., McMahon R. G., Banerji M. e. a., 2015, MNRAS, 454, 3952

Robertson H. P., 1935, ApJ, 82, 284

Scharẅachter J., Combes F., Salomé P., Sun M., Krips M., 2016, MNRAS, 457, 4272

Schmidt M., Schneider D. P., Gunn J. E., 1987, ApJ, 321, L7

Schneider D. P., Richards G. T., Hall P. B. e. a., 2010, AJ, 139, 2360

Shanks T. e. a., 2015, MNRAS, 451, 4238

Silverman A. N., 1986, Am. J. Phys., 54, 1092

Stern D., Spinrad H., 1999, PASP, 111, 1475

Stern D., Moran E. C., Coil A. L. e. a., 2002, ApJ, 568, 71

Stuckey W. M., 1992, Am. J. Phys., 60, 142

Synge J. L., 1960, Relativity: The General Theory. North-Hollaand, Amsterdam

Tanvir N. R., Fox D. B., Levan A. J. e. a., 2009, Nature, 461, 1254

Thomas J., Ma C.-P., McConnell N. J., Greene J. E., Blakeslee J. P., Janish R., 2016, Nature, 532, 340

Turner E., 2001, AJ, 101, 5

Vanzella E., Pentericci L., Fontana A. e. a., 2011, ApJ Lett., 730, L35

Venemans B. P., Findlay J. R., Sutherland W. J. e. a., 2013, ApJ, 779, 24

Vladimirov I. S., 1982, Reference systems in gravitation theory. Energoizdat, (In Russian), Moscow

Walker A. G., 1935, Proc. Lond. Math. Soc., 4, 170

Walker A. G., 1936, Proc. Lond. Math. Soc., 42, 90

Wang R., Carilli C. L., Beelen A. e. a., 2007, ApJ, 134, 619

Wang F., Wu X. B., Fan X. e. a., 2016, ApJ, 819, 24

Warren S. J., Hewett P. C., 1990, Rep. on Prog. in Phys., 53, 1095

Warren S. J., Hewett P. C., Osmer P. S. e. a., 1987, Nature, 330, 453

Watson D., Christensen L., Knudsen K. K. e. a., 2015, Nature, 519, 327

Whiting A. B., 2004, The Observatory, 124, 174

Willott C. J., Delorme P., Omont A. e. a., 2007, AJ, 134, 2435

Willott C. J., Albert L., Arzoumanian D. e. a., 2010, AJ, 140, 546

Wolf C., Onken C. A., Luvaul L. C. e. a., 2018, PASA, 35, 10

Wu X.-B., Wang F., Fan X. e. a., 2015, Nature, 518, 512

Yang J., Fan X., Wu X.-B. e. a., 2017, AJ, 153, 184

Zelmanov A. L., 1944, Chronometric Invariants. Am. Research Press (Tr. 2006), New Mexico, USA

Zelmanov A. L., 1956, Dokl. Acad. Nauk USSR, 107, 815

Zelmanov A. L., 1976, Dokl. Acad. Nauk USSR, 227, 78

Zitrin A., Labbé I., Belli S. e. a., 2015, ApJ, 810, L12

doi: https://doi.org/10.52526/25792776-2021.68.1-12

Appendices

Appendix A The standard kinematic interpretation of redshifts

One source of the preliminary attempts along this line of alternative understanding of a complex problem is the "standard" kinematic interpretation that cosmological redshift of distant galaxy is the recession effect of the accumulation of a series of infinitesimal Doppler shifts due to infinitesimal relative velocities of the Hubble flow along the line of sight. Following Padmanabhan (1993), Peacock (1999, 2008), Peebles (1993), (see also e.g. Bunn & Hogg (2009), Chodorowski (2011), Grøn & Elgarøy (2007), Whiting (2004)), within the "stretching of space" point of view, assume that an observer at the origin at the present epoch time measures the redshift of a galaxy at some comoving distance. Consider a light ray that travels from a galaxy to this observer, both of whom are at rest in comoving coordinates. Imagine a family of comoving observers along the path of light ray, each of whom measures the frequency of light ray as it goes by. It was assumed that each observer is close enough to his neighbor so that we can accommodate them both in one inertial reference frame and use SR to calculate the change in frequency from one observer to the next. If adjacent observers are separated by the infinitesimal proper distance δL, then their relative velocity in this frame is $\delta v = H\delta L$. This infinitesimal recessional velocity should cause a fractional shift given by the non-relativistic Doppler formula:

$$\frac{\delta\nu}{\nu} = -\frac{\delta v}{c} = -\frac{H\delta L}{c} = -H\delta t. \tag{33}$$

And hence, as it was concluded, the relation (33) for overall redshift, by means of $H = \dot{R}/R$, becomes $\frac{\delta\nu}{\nu} = -\frac{\delta R}{R}$. This integrates to give the main result of expansion scenario that the frequency decreases in inverse proportion to the scale factor, $\nu \propto 1/R$.

It was claimed even more that the cosmological redshifts can be interpreted as a combination of Doppler and gravitational shifts with the difference in gravitational potential between the point of emission and reception of a light ray. It is the purpose of this Section to give a reappraisal of the key aspects of the "standard" interpretation in a deep way. We wish to make clear at the outset that we are not suggesting any doubt about the principle statement that the redshift of distant galaxy is the recession effect of the accumulation of a series of infinitesimal Doppler shifts due to infinitesimal relative velocities along the line of sight, which seemed appealing and attractive. Moreover, this statement has been a crux of our derivation of a correct solution to a kinematic interpretation of cosmological redshifts presented in Section 4. Rather, we doubt the method of calculations. A hard look at the basic relation (33) reveals the following objections, which together constitute a whole against the claim:

- Even this worry is subtle, but here we have called attention to the fact that there is no necessity for integration of (33) to reveal the "stretching-of-wavelength" effect, because the term of assumed expansion dynamics, $H\delta L$, written for the infinitesimal change of expansion rate on the infinitesimal distances, δL, is already steeped in (33), which implies the wave-stretching relation, $\delta\lambda \propto \delta L \propto \delta R$.
- We doubt a validity of a scale-behavior $\nu \propto 1/R$ of the frequency that enters the equation (33). Upon closer examination, the arguments about this are completely futile because they are conducted without any attempt to analyze the meanings of the terms employed in (33). The factor $1+z$ measures the expansion of the universe between emission and absorption of a light. The equation (33) would lead to the relation $\frac{\delta\nu}{\nu} = -\frac{\delta R}{R}$ if, and only if, $\dot{L}(t,z) = c$, i.e. when galaxy situates on the Hubble sphere: $L = L_H \equiv c/H$, where L_H is the Hubble length. But in general case of $\dot{L}(t,z) \neq c$ ($L \neq L_H$), it was in conflict because the infinitesimal time interval $\delta t' = \delta L/c$ does not equal to the infinitesimal epoch time interval $\delta t = \delta L/\dot{L}$ ($\delta t'/\delta t = \dot{L}/c$):

$$\frac{H\delta L}{c} = \frac{1}{R}\left(\frac{dR}{dt}\delta t\right)\frac{\delta L}{c\delta t} = \frac{\dot{L}(t,z)}{c}\frac{\delta R}{R}, \tag{34}$$

  and hence (33) leads to

$$\frac{\delta\nu}{\nu} = -\frac{\dot{L}(t,z)}{c}\frac{\delta R}{R}. \tag{35}$$

doi: https://doi.org/10.52526/25792776-2021.68.1-12

This can readily be transformed into the equation

$$\delta \ln \nu = \delta \left[\ln \left(\frac{1}{R}\right)^{\dot{L}/c} \right] + \frac{\delta \dot{L}}{c} \ln R. \tag{36}$$

As it is evidently seen, the result of integration of (36) will be utterly distinct from the simple behavior of $\nu \propto 1/R$.

- To render our discussion more transparent, it is worthwhile to clarify the ingredient relation $\delta v = H\delta L$ in (33), where δv is the Doppler velocity: $c\delta z = \delta v$. We argue that this relation is in error at the infinitesimal distances. It is necessary to substantiate this principle statement further by the reasoning recast in more physical terms. For the self-contained arguments, it must be stated emphatically that the Hubble's linear 'redshift-distance' law, $cz = HL$, certainly must be classified as an empirical law rather than as a law of pure reason. It must then suffice to expect some objections against its idealization and, thus, it should be a subject of limited validity (an approximate relation). One ought to be cautious about a validity of this law in the vicinity of nearby clusters of galaxies, or on much smaller scales. It seems there is rather no local counterpart for the dynamics from the Hubble law on the much smaller distances, say in the vicinity of a star such as our Sun. In this, the Schwarzschild field will dominate, with the cosmological field perhaps exerting some small perturbative effects (Dirac, 1979, Gautreau, 1984, Grøn & Rippis, 2003, McVittie, 1933). Needless thus to say that the Hubble's linear "redshift-distance" law becomes a dangerously flawed way of thinking and cannot be representative of the global behavior at least on the infinitesimally smaller distances, because if this law could affect local dynamics this should contradict profoundly to principle of "relativity". Our conclusion drawn from the above discussion can be stated as follows:

$$\delta v = c\delta z \neq H\delta L. \tag{37}$$

- We further argue that the cosmological redshift, in general, cannot be interpreted as a combination of the global Doppler and gravitational shifts. Certainly, Narlikar (1994) has presented the proof that as the universe expands, the parallel transported in curved space four-velocity vector of a distant source along the null geodesic to an observer does yield Doppler four-velocity in the rest frame of observer. This result is particular case of a general rule described in comprehensible terms by Synge (1960) (Chap.III). We seem to have attractive proposal of choosing a null geodesics for the parallel transport since it does not require any additional structures, like particular foliation of space-time, which in turn is applicable to any space-time. However, a resulting global Doppler effect is inconclusive, and could not be regarded as a final word, because a definition of relative velocity has disadvantage that in a curved space-time for Levi-Civita connection the result of parallel transport depends on the chosen path along which the vector is transported. This is the defining property of curvature. Hence, there is no relative velocity of distant objects without prior choice of transport paths. If such definition of relative velocity is not accepted, then the statement attributing frequency shifts to relative velocity cannot be accepted either.

- Finally, recall that the gravitational redshift occurs if light travels from a strong to a weak gravitational field and blueshift occurs for the light traveling in the reverse direction. But the cosmological redshift occurs in both these cases as the universe expands. Moreover, the GR interpretation of the expansion interprets cosmological redshift as an indication of velocity since the proper distance between comoving objects increases. Since the Riemann tensor appears nowhere, thus the cosmological redshifts do not relate to gravitational effect.

doi: https://doi.org/10.52526/25792776-2021.68.1-12

Appendix B The *kinetic* recession velocities of some typical distant astronomical objects

A tremendous observational effort has been put in many decades into the programme of detection and characterization of distant galaxies and high redshift bright quasars, which is pivotal for elucidating the physics in time to an epoch when the universe was very young and galaxies in their infancy. The high redshift bright quasars have fundamental implications for the formation and growth history of supermassive black holes ((SMBHs), see e.g. (Mortlock et al., 2011, Wu et al., 2015), and probe the progress of cosmic reionisation (Fan et al., 2006a,b). This ultimately yields the constraints imposed for the metal enrichment and dust production in the early epoch of the universe, (Jiang et al., 2016). The largest SMBH-candidates are a few $10^{10}\,M_{\odot}$ (McConnell et al., 2011, Postman et al., 2012, Scharẅachter et al., 2016, Thomas et al., 2016).

The first $z > 5$ quasars were found in the the large-area Sloan Digital Sky Survey (SDSS, (Fan et al., 1999, 2001, Pâris et al., 2012, 2014, Schneider et al., 2010)). The SDSS quasar surveys provided the largest quasar sample (~ 500 quasars at $z > 4.5$). Quasars at $z > 4.5$ are routinely discovered in varieties of wide-field surveys, including the Canada-France High-Redshift Survey (CFHQS, (Willott et al., 2007)). There are newly identified quasars from the the Panoramic Survey Telescope and Rapid Response System (Pan-STARRS, (Bañados et al., 2018, Kaiser et al., 2002)), the UKIRT Infrared Deep Sky Survey (UKIDSS, (Lawrence, 2007, Yang et al., 2017)), Large Area Survey (ULAS), the VISTA VIKING (Edge, 2013), and VST ATLAS (Shanks, 2015) surveys, the Subaru Suprime Cam surveys (Kashikawa, 2015), and the Hyper Suprime Cam (HSC) survey (Matsuoka, 2016), the Dark Energy Survey (DES, (Reed et al., 2015)), and the Dark Energy Camera Legacy Survey (DECaLS, (Wang et al., 2007)).

However, the SDSS spectroscopic surveys have a lower degree of completeness at high redshift. The SDSS only covers a large portion of the Northern sky, although the Pan-STARRS1 survey (PS1, (Chambers, 2011, Kaiser et al., 2002, 2010)) has extended coverage of 1.5 hemispheres to a declination of -30 deg South. The Sky Mapper Southern Survey is a full hemispheric imaging survey carried out by the Sky Mapper telescope at Siding Spring Observatory in New South Wales, Australia (Wolf et al., 2018). By combining Wide-field Infrared Survey Explorer (WISE) and SDSS photometric data, Wang et al. (2016) have spectroscopically identified 72 new $z \sim 5.0$ quasars. The Table A1 is summing up the *kinetic* recession velocities of some typical distant astronomical objects with spectroscopic redshift determinations collected from the literature.

doi: https://doi.org/10.52526/25792776-2021.68.1-12

Table 1. The *kinetic* recession velocities (β_{rec}) (in units of the speed of light) of some typical distant astronomical objects.

Name	Redshift	Type (Ref.)	β_{rec}
GN-z11	11.09	Galaxy, e.g. (1)	0.819
MACS1149-JD1	9.11	Galaxy, e.g. (2)	0.807
EGSY8p7	8.68	Galaxy, e.g. (3)	0.804
A2744 YD4	8.38	Galaxy, e.g. (4)	0.801
GRB 090423	8.2	Gamma-ray burst, e.g. (5)	0.8
EGS-zs8-1	7.73	Galaxy, e.g. (1)	0.796
ULAS J1342+0928	7.54	Quasar, e.g. (6)	0.794
A1689-zD1	7.5	Galaxy, e.g. (7)	0.793
BDF-3299	7.109	Galaxy, e.g. (8)	0.789
ULAS J0109-3047	6.75	Quasar, e.g. (9)	0.785
ULAS J0305-3150	6.6	Quasar, e.g. (9)	0.783
HCM-6A	6.56	Galaxy, e.g. (10)	0.783
CFHQS J2329-0301	6.417	Quasar, e.g. (11)	0.781
SDSS J010013.02+280225.8	6.3	Quasar, e.g. (12,13)	0.78
SDSSJ1048+4637	6.2	Quasar, e.g. (14,15)	0.778
SDSS J125051.93+313021.9	6.13	Quasar, e.g. (16)	0.777
SDSS J030331.40001912.9	6.07	Quasar, e.g. (17,18)	0.777
CFHQS J1641+3755	6.047	Quasar, e.g. (19)	0.776
SDSS J081827.40+172251.8	6	Quasar, e.g. (15,16)	0.776
PSO J183.2991-12.7676	5.86	Quasar, e.g. (19)	0.774
J104433.04-012502.2	5.8	Quasar, e.g. (20)	0.773
PSO J215.1514-16.0417	5.73	Quasar, e.g. (19)	0.772
PSO J045.1840-22.5408	5.7	Quasar, e.g. (19)	0.771
HDF 4-473.0	5.6	Galaxy, e.g. (20)	0.77
RD300	5.5	Quasar, e.g. (21)	0.768
SDSS J003125.86+071036.92	5.33	Quasar, e.g. (13)	0.765
SDSS J133257.45+220835.91	5.11	Quasar, e.g. (13)	0.761
SDSS J160111.16-182835.08	5.06	Quasar, e.g. (13)	0.76
SDSSp J120441.73-002149.6	5.03	Quasar, e.g. (22,23)	0.76
SDSS J025121.33+033317.42	5	Quasar, e.g. (13)	0.759
PC 1247+3406	4.9	Quasar, e.g. (21)	0.757
SDSS J014741.53-030247.88	4.75	Quasar, e.g. (13)	0.754
BR 1033-0327	4.51	Quasar, e.g. (22)	0.749
Q0046-293	4.01	Quasar,e.g. (23)	0.737
Q1208+1011	3.8	Quasar,e.g. (24)	0.731
OH471	3.408	Quasar, (25)	0.718
4C 05.34	2.877	Quasar,e.g. (26)	0.697
5C 02.56	2.399	Quasar,e.g. (27)	0.672
3C 241	1.617	radio galaxy, e.g. (28)	0.607
3C 252	1.105	radio galaxy, e.g. (29)	0.533

(1) Oesch et al. (2016); (2) Hashimoto et al. (2018); (3) Zitrin et al. (2015); (4) Laporte et al. (2017); (5) Tanvir et al. (2009); (6) Bañados et al. (2018); (7) Watson et al. (2015); (8) Vanzella et al. (2011); (9) Venemans et al. (2013); (10) Hu et al. (2002); (11) Willott et al. (2010); (12) Wu et al. (2015); (13) Wang et al. (2016); (14) Fan et al. (2006b); (15) Fan et al. (2006c); (16) Wang et al. (2007); (17) Jiang et al. (2008); (18) Kurk et al. (2009); (19) Bañados et al. (2014); (20) Jiang et al. (2007); (21) Stern et al. (2002); (22) Iwamuro & Motohara (2002); (23) Warren et al. (1987); (24) Schmidt et al. (1987); (25) Warren & Hewett (1990); (26) Bahcall & Oke (1971); (27) Lynds & Wills (1970); (28) Lilly & Longair (1984); (29) Stern & Spinrad (1999)

doi: https://doi.org/10.52526/25792776-2021.68.1-12

Communications of BAO, Vol. 68, Issue 1, 2021, pp. 32-37

The Time-dependent Problem of the Line Radiation Reflection

A. Nikoghossian*

NAS RA V.Ambartsumian Byurakan Astrophysical Observatory, Byurakan 0213, Aragatsotn Province, Armenia

Abstract

We consider the classical time-dependent problem of diffuse reflection of the line-radiation from a semi-infinite absorbing and scattering atmosphere. By the example of the simplest 1D problem it is shown how its solution is constructed in the general case, when both the photon lifetime in the absorbed state and the time of its travel between two consecutive acts of scattering are taken into account. The numerical values of the coefficients in the expansion of the reflection function in the Neumann series are given. The obtained solution is applied to the problem, in which the scattering in both the spectral line and in the continuous spectrum is taken into account.

1. Introduction

Temporal changes in the spectra of various cosmic objects are an important direction in the study of physical phenomena occurring in them. The problems arising in this case belong to the theory of the time-dependent transfer of radiation, in which the residence time of quanta in the medium is taken into account. The theory has been developed in the works of a number of authors, of which we shall mention here only the works of Ganapol (1979), Ganapol & Matsumoto (1986), Matsumoto (1967, 1974), Minin (1964, 1965, 1967), Sobolev (1963). A number of methods for solving such problems under one or another simplifying assumptions have been proposed. In particular, the first two of the mentioned authors proposed methods based on finding the Laplace transform of any characteristic of the radiation field in time directly from the corresponding characteristic in the stationary case. In this way Minin considered the problem of diffuse reflection from semi-infinite atmosphere for isotropic scattering.

Another way based on expanding the requisite quantities into Neumann series was developed in works of Matsumoto and Ganapol. Central to their theory is the analogy between the forms of time-dependent and time-independent emergent intensity when expressed in Neumann series format. This allows to obtain a factor in each term in the required time-dependent series directly from those in the time-independent problem. In the latter case the corresponding factors are determined via recursion relations.

It is known that the time spent by a quantum during multiple scattering in a medium is due to two processes: the time spent by it in the absorbed state and the time spent on the path between two consecutive acts of scattering. Depending on the particular physical problem, one of them predominates, which simplifies the corresponding theory. For instance, Sobolev (1963) considered the 1D time-dependent transfer problem for two extreme cases $t_1 \gg t_2$ and $t_2 \gg t_1$.

This paper pursue two goals. On the example of the simplest one-dimensional problem of diffuse reflection of radiation from a semi-infinite atmosphere the method of obtaining the required solution is proposed for the general case, when both above mentioned processes are taken into account.The immediate motivation for turning to this problem is our study of the changes in the spectra of giants of the early spectral classes, caused by the scattering of radiation in the continuous spectrum (Nikoghossian, 2020a,b,c).

*nikoghoss@yahoo.com

doi: https://doi.org/10.52526/25792776-2021.68.1-32

2. The problem of the diffuse reflection from a semi-infinite atmosphere.

In this paper, we limit ourselves to considering the simplest 1D problem when the scattering of radiation both in the line and in the continuous spectrum is assumed to be monochromatic. Problems in this approximation have at least two advantages. First, many of the features required for the study can be obtained analytically and, second, by abstracting from the frequency and direction redistribution effects, the investigated features of the spectral line variations are manifested in a pure form.

We start by considering the steady-state problem of diffuse reflection from a semi-infinite atmosphere absorbing and scattering both in the line and continuous spectrum. The atmosphere is assumed to be illuminated by the continuous radiation of unite intensity. Obviously, the reflected radiation is due to scattering in both the line and continuous spectra. If no distinction is made between which of these two processes results in the observed radiation, then, as shown in Nikoghossian (2020a,b), the reflection coefficient is given by the formula

$$\rho\left(x\right) = \frac{1}{\tilde{\lambda}}\left(2-\tilde{\lambda}-2\sqrt{1-\tilde{\lambda}}\right), \tag{1}$$

with

$$\tilde{\lambda}\left(x\right) = \frac{\lambda\alpha\left(x\right)+\gamma}{\alpha\left(x\right)+\beta+\gamma}, \tag{2}$$

where the commonly accepted notations are used: λ is the scattering coefficient in the line (the probability of reradiation of the absorbed photon by the exited atom), $\alpha(x)$ is the line absorption profile in terms of dimensionless frequency measured by displacement from the centre of the line in Doppler-widths, β and γ are correspondingly the ratios of the continuum absorption and continuum scattering coefficients χ_ν and σ to the absorption coefficient in the center of the line (k_0). Assuming that the scattering in the continuous spectrum is due to free electrons, we can write $\sigma = n_e\sigma_0$, where n_e is the electron density and

$$\sigma_0 = \frac{8\pi}{3}\left(\frac{e^2}{mc^2}\right)^2, \tag{3}$$

where m and e are the mass and the charge of electron, and c is the light speed. As it was shown in Israelian & Nikoghossian (1996), Nikoghossian (2020a,b,c), the values of parameters β and γ appeared in Eq. 2 determine whether the line will be observed in absorption, or in emission (the so called Shuster's mechanism (1905)). In the two-level isothermal atmosphere the condition of the emission line reads

$$\left(1-\lambda\right)\gamma > \lambda\beta. \tag{4}$$

The physical meaning of this inequality is not difficult to understand if one pre-tests two mutually opposite elementary processes: a photon is scattered in a continuous spectrum (on free electrons) and then is absorbed and thermalized in the spectral line, and, conversely, a photon scatters in frequencies of the spectral line and is absorbed afterwards in the continuum. The condition particularly implies that the appearance of spectral lines in emission should be expected in the case of weak lines. It should be noted that there is a simple relationship between the profile of the line formed by reflection from a homogeneous semi-infinite atmosphere R_* and that formed in a semi-infinite isothermal atmosphere R_0: $R_* + R_0 = 1$ (Arutyunyan & Nikogosyan, 1978), so the line emission profile in one of these problems corresponds to the absorption profile in the other.

Our interest in this paper is the lines formation resulting in reflection from the semi-infinite medium. The Neumann series for the reflectance $\rho(x)$ has a form

$$\rho\left(x\right) = \sum_{n=1}^{\infty}\rho_n\tilde{\lambda}^n\left(x\right), \tag{5}$$

doi: https://doi.org/10.52526/25792776-2021.68.1-32

where $\rho_1 = 0,25$; $\rho_2 = 0,125$, and the higher order factors being found recursively according to

$$\rho_n = \frac{1}{2}\left(\rho_{n-1} + \frac{1}{2}\sum_{k=1}^{n-2}\rho_k\rho_{n-k-1}\right), \tag{6}$$

Obviously, each summand is the probability of reflection from the medium as a result of a certain number of n scattering events. Below is a brief table of these values

Table 1.

n	ρ_n	n	ρ_n	n	ρ_n	n	ρ_n
1	0.250000	11	0.014015	21	0.005562	31	0,003154
2	0.125000	12	0.012398	22	0.005200	32	0,003011
3	0,078125	13	0,011070	23	0,004875	33	0,002878
4	0,054687	14	0,009963	24	0,004583	34	0,002754
5	0,041015	15	0,009029	25	0,004318	35	0,002640
6	0,032226	16	0,008232	26	0,004078	36	0,002533
7	0,026184	17	0,007546	27	0,003860	37	0,002433
8	0,021820	18	0,006951	28	0,003660	38	0,002340
9	0,018547	19	0,006429	29	0,003477	39	0,002251
10	0,01602	20	0,005970	30	0,003309	40	0,002169

A characteristic feature of the Neumann series, as can also be seen from the table above, is its slow convergence. In this 1D problem of coherent scattering, the required factors are found easily recursively. In a more general formulation of the problem, their computation is fraught with difficulties, to overcome which asymptotic methods have been developed (see, for instance, Uesugi & Irvine, 1970).

3. Temporal picture of the reflected line formation depending on the scattering in continuum.

Turning to the non-stationary problem, we remind that in each act of scattering a photon takes time both to stay in the absorbed state and to travel to the next act of scattering. Both quantities are independent random variables distributed according to the same exponential law with mean values equal to t_1 and t_2, respectively. If the medium is taken to consist of two-level atoms, then, allowing for scattering in the continuum, we can write, $t_2 = 1/[(1+n^+/n_1)n_1k_0c]$, where n_1 is the number of atoms on the ground level, and we also assume that $n_e \approx n^+$. Instead of time t, we introduce dimensionless variables $u = t/t_1$ and $\omega = t/t_2$ correspondingly for each of the mentioned two processes. The total time it takes for a photon to stay in a medium is obviously the sum of two random quantities, each of which, in turn, is the sum of independent random quantities realized in the course of multiple scattering. It is well known that the distribution function of the sum of the number of n such quantities distributed equally according to the exponential law is given by the Erlang-n distribution. Recall that it is a two-parameter function and is a special case of the Gamma distribution,

$$\mathrm{Er}(x,k,\Lambda) = \frac{\Lambda^k x^{k-1}}{(k-1)!}\mathrm{e}^{-\Lambda x}, \tag{7}$$

Parameters k and Λ are known as the shape and rate parameters, respectively. It is important to note that the Erlang distribution is stable so that the sum and the product of such distributions yields again the Erlang distribution with proper parameters.

When applied to our problem, taking into account the dimensionless values for time introduced in it, the parameter Λ takes on the meaning of the value inverse to the mean time for each of the two elementary processes associated with the waste of time mentioned above. Then for the distribution

doi: https://doi.org/10.52526/25792776-2021.68.1-32

function of the probability density function (PDF) of time lost by a photon to stay in the absorbed state during n-fold scattering we will have

$$f_1(u,n) = \frac{u^{n-1}}{(n-1)!}\mathrm{e}^{-u} \tag{8}$$

Similarly, for the second process associated with spending time traveling in the medium, we can write

$$f_2(\omega, n+1) = \frac{\omega^n}{n!}\mathrm{e}^{-\omega} \tag{9}$$

Here we have taken into account that the number of elementary events associated with the travel of photons in the medium exceeds the number of scatterings in the medium by one. This is due to the fact that the path taken by a photon as it falls from the outside onto the medium, and hence the time it takes to travel this path, is not related to the act of scattering.

Distributions Eq. 8 and Eq. 9 specify the PDF for the total duration of each of the two processes under consideration. In turn, the PDF of the total time spent by a photon in the medium, regardless of the type of process, is set, as we know, by the convolution of the above two PDF

$$F_n(z) = \int_0^z f_2(\omega, n+1) f_1(z-\omega, n)\,\mathrm{d}\omega \tag{10}$$

The resulting integral is calculated explicitly to give

$$F_n(z) = \frac{z^{2n-1}}{(2n-1)!}\mathrm{e}^{-z} \tag{11}$$

Introducing a function $\bar{\rho}(x,z)$ into consideration, such that $\bar{\rho}dz$ is the probability of reflection from the medium of quantum of frequency x in the time interval $z, z+dz$. we return to the reflection function in the stationary problem Eq. 5, and represent it in the form of a Neumann series

$$\bar{\rho}(x,z) = \sum_{n=1}^{\infty} \rho_n \tilde{\lambda}^n(x) F_n(z,n), \tag{12}$$

or

$$\bar{\rho}(x,z) = \mathrm{e}^{-z}\sum_{n=1}^{\infty} \rho_n \tilde{\lambda}^n(x) \frac{z^{2n-1}}{(2n-1)!} \tag{13}$$

Eq. 13 shows the time distribution of the probability of quanta of different frequencies leaving the medium within a spectral line. At the same time, the cumulative distribution function (CDF), which demonstrates the evolution of the spectral line profile up to a certain time point z_0, is also of great interest. Denoting it by $\mathrm{P(x, z_0)}$, from Eq. 10 we find

$$\mathrm{P}(x, z_0) = \mathrm{e}^{-z_0}\sum_{n=1}^{\infty} \rho_n \tilde{\lambda}^n \sum_{k=0}^{\infty} \frac{z^{2n+k}}{(2n+k)!} \tag{14}$$

As it follows from the physical meaning of the dimensionless time variables $z = t/\bar{t}$ and $z_0 = t_0/\bar{t}$, the scale factor $\bar{t} = t_1 t_2/(t_1+t_2)$,

As an application of the results obtained, we will limit ourselves here to examining the behavior of the found temporal characteristics and for different frequencies within the spectral line. In Figures 1, 2 we present the PDF and CDF for the same line with a moderate scattering coefficient $\lambda = 0.5$, and different values of the γ parameter, characterizing the role of scattering in the continuous spectrum. Comparing the locations of the curves corresponding to the same frequency value in the above graphs, it is easy to find that they are symmetrically inverted. In one case it corresponds to the absorption line (Figure 1), while the other refer to the emission line (Figure 2). The evolution of the spectral line profiles before the stationary mode was established is also reciprocally reversed. If, in the case of

doi: https://doi.org/10.52526/25792776-2021.68.1-32

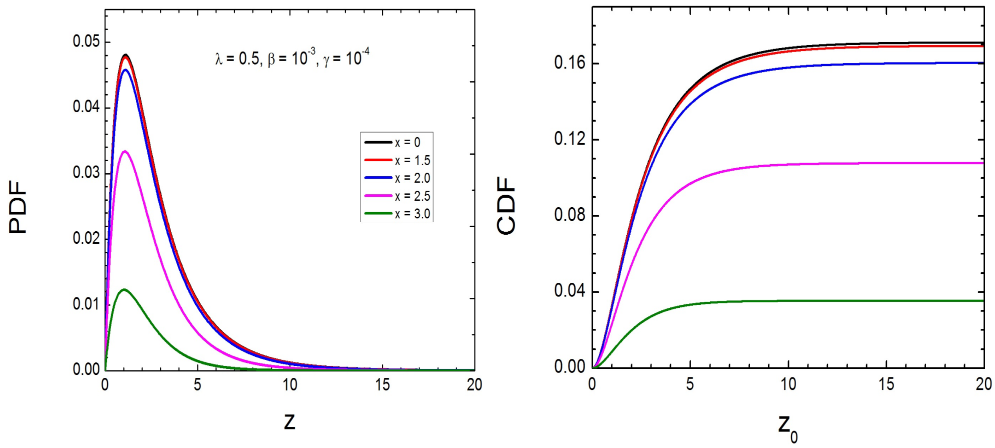

Figure 1. The frequency (center to wings) variation of the mean number of scattering events (left) and the average time the photons spent in diffusing within the atmosphere for $\lambda = 0.5$ and indicated values of γ. In both cases β is 10^{-3}.

.

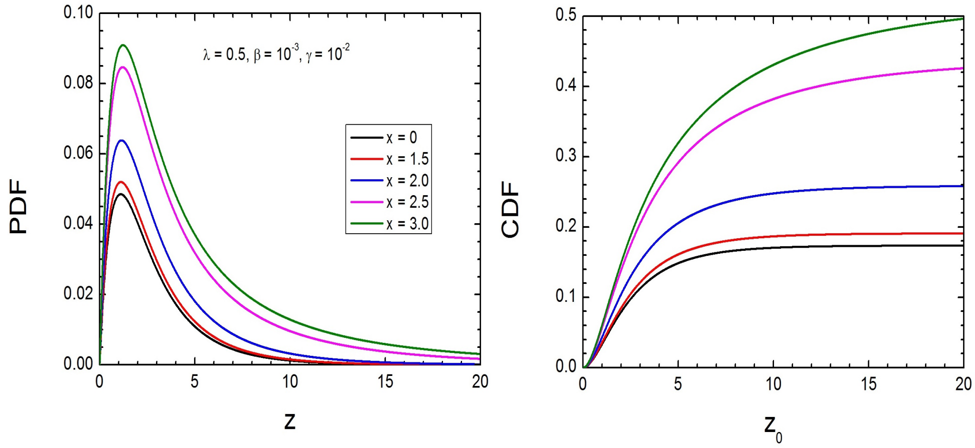

Figure 2. The mean number of scattering events underwent by reflected photons in continuous spectrum for the same as in Fig.1 values of parameters.

the absorption line, the saturation first occurs in the line core, in the case of the emission line, the wings of the lines are established first. The difference between the saturation times of the different parts of the line reaches 10 or more in the scale of units adopted in the paper, which, as we remember, depends significantly on the atmospheric density. Thus, there is a direct correlation between the role of the indicated scattering due to the presence of a certain number of free electrons in our case and the saturation time of the spectral line profiles.

The results presented in the paper show that despite the comparatively small coefficient of electron scattering, under certain physical conditions spectral lines can be observed in the emission. It is also important to note that the temporal variation of PDF obtained in this work, as one would expect, adequately describes the physical picture of the multiple scattering process in a medium, in contrast to the often used approach, which uses a single Erlang distribution over dimensionless time on a scale containing both t_1 and t_2.

doi: https://doi.org/10.52526/25792776-2021.68.1-32

References

Arutyunyan G. A., Nikogosyan A. G., 1978, Akademiia Nauk SSSR Doklady, 242, 66

Ganapol B. D., 1979, J. Quant. Spectrosc. Radiat. Transfer. , 22, 135

Ganapol B. D., Matsumoto M., 1986, J. Quant. Spectrosc. Radiat. Transfer. , 35, 71

Israelian G., Nikoghossian A., 1996, J. Quant. Spectrosc. Radiat. Transfer. , 56, 509

Matsumoto M., 1967, Publ. Astron. Soc. Jpn. , 19, 163

Matsumoto M., 1974, Publ. Astron. Soc. Jpn. , 26, 241

Minin I. N., 1964, Soviet Physics Doklady, 9, 114

Minin I. N., 1965, Astrophysics, 1, 104

Minin I. N., 1967, Astrophysics, 3, 154

Nikoghossian A. G., 2020a, Astrophysics,

Nikoghossian A. G., 2020b, Communications of the Byurakan Astrophysical Observatory, 67, 1

Nikoghossian A. G., 2020c, Communications of the Byurakan Astrophysical Observatory, 67, 21

Schuster A., 1905, Astrophys. J. , 21, 1

Sobolev V. V., 1963, A treatise on radiative transfer.

Uesugi A., Irvine W. M., 1970, Astrophys. J. , 159, 127

doi: https://doi.org/10.52526/25792776-2021.68.1-32

Communications of BAO, Vol. 68, Issue 1, 2021, pp. 38-49

Unique definition of relative velocity of luminous source as measured along the observer's line-of-sight in a pseudo-Riemannian space-time

G.Ter-Kazarian*

Byurakan Astrophysical Observatory, 378433, Aragatsotn District, Armenia

Abstract

Using a way of separating the spectral shifts into infinitesimally displaced `relative´ spectral bins and sum over them, we overcome the ambiguity of the parallel transport of four-velocity, in order to give an unique definition of the so-called *kinetic* relative velocity of luminous source as measured along the observer's line-of-sight in a generic pseudo-Riemannian space-time. The ubiquitous relationship between the spectral shift and the *kinetic* relative velocity is utterly distinct from a familiar global Doppler shift rule (Synge, 1960). Such a performance of having found a *kinetic* relative velocity of luminous source, without subjecting it to a parallel transport, manifests its virtue in particular case when adjacent observers are being in free fall and populated along the null geodesic, so that it is reduced to a global Doppler velocity as studied by Synge. We discuss the implications for the instructive case of spatially homogeneous and isotropic Robertson-Walker space-time, which leads to cosmological consequences that the resulting *kinetic* recession velocity of a galaxy is always subluminal even for large redshifts of order one or more, and thus, it does not violate the fundamental physical principle of *causality*.

Keywords: *Classical general relativity; Riemannian space-time; Relative velocity*

1. Introduction

For test particles and observers there is no unique way to compare four-vectors of the velocities at widely separated space-time events in a curved Riemannian space-time, because general relativity (GR) provides no *a priori* definition of relative velocity. This inability to compare vectors at different points was the fundamental feature of a curved space-time. Different coordinate reference frames and notions of relative velocity yield different results for the motion of distant test particles relative to a particular observer. The three distinct coordinate charts are employed by Bolós (2006, 2007), Bolós & Klein (2012), Bolós et al. (2002), Klein & Collas (2010), Klein & Randles (2011), each with different notions of simultaneity, to calculate the four geometrically defined inequivalent concepts of relative velocity: Fermi, kinematic, astrometric, and the spectroscopic relative velocities. The four definitions of relative velocities depend on two different notions of simultaneity: "spacelike simultaneity" (or "Fermi simultaneity") (Klein & Randles, 2011, Walker, 1935) as defined by Fermi coordinates of the observer, and "lightlike simultaneity" as defined by optical (or observational) coordinates of the observer (Ellis, 1985). The Fermi and kinematic relative velocities can be described in terms of the "Fermi simultaneity", according to which events are simultaneous if they lie on the same space slice determined by Fermi coordinates. Thereby, for an observer following a timelike worldline in Riemannian space-time, Fermi-Walker coordinates provide a system of locally inertial coordinates. If the worldline is geodesic, the coordinates are commonly referred to as Fermi or Fermi normal coordinates. Useful feature of Fermi coordinates was that the metric tensor expressed in these coordinates is Minkowskian to first order near the path of the Fermi observer, with second order corrections involving only the curvature tensor (Manasse & Misner, 1963). In (Klein & Randles, 2011), the authors find explicit expressions

*gago_50@yahoo.com

doi: https://doi.org/10.52526/25792776-2021.68.1-38

for the Fermi coordinates for Robertson-Walker (RW) space-times and show that the Fermi chart for the Fermi observer in non-inflationary RW space-times is global. However, rigorous results for the radius of a tubular neighborhood of a timelike path for the domain of Fermi coordinates are not available. The spectroscopic (or barycentric) and astrometric relative velocities, which can be derived from spectroscopic and astronomical observations, mathematically, both rely on the notion of light cone simultaneity. According to the latter, two events are simultaneous if they both lie on the same past light cone of the central observer. It is shown that the astrometric relative velocity of a radially receding test particle cannot be superluminal in any expanding RW space-time. Necessary and sufficient conditions are given for the existence of superluminal Fermi speeds. Note that for the Hubble velocity, the proper distance is measured along non geodesic paths, while for the Fermi velocity, the proper distance is measured along spacelike geodesics. In this respect the Fermi velocity seems to be more natural, but the Hubble velocity is defined at all space-time points, whereas the Fermi velocity makes sense only on the Fermi chart of the central observer. Although alluded four definitions of relative velocities have own physical justifications, all they are subject to many uncertainties, and the ambiguity still remains.

Keeping in mind aforesaid, below we restrict our analysis to seeking solution for particular case when a test particle is being a luminous object. In this case, the problem of a definition of relative velocity can be significantly simplified because of available spectral shift measured by observer. The hope appears that a relative velocity of luminous source as measured along the observer's line-of-sight (speed) can be defined in unique way straightforwardly from kinematic spectral shift rule, which holds on a generic pseudo-Riemannian manifold (Synge, 1960). In the same time, aforementioned inability to immediately compare the four-velocity vector V^{μ}_{S} of the luminous object S with the four-velocity vector V^{μ}_{O} of the observer O in pseudo-Riemannian space-time necessitates to seek a useful definition of the relative velocity by bringing both vectors to a common event. Historically, Synge has subjected the vector V^{μ}_{S} to parallel transport along the null geodesic to the observer, and deduced a global Doppler effect in terms of energy and frequency. It is well known that null geodesics are peculiar, in a sense that they lie in a metric space wherein they are being only 1D-affine spaces, so that only a parallel displacement, not a metric distance is defined along them. As a corollary, their geometric properties become a rather unexpected mixture of affine and metric properties. At first glance, we seem to have attractive proposal of choosing a null geodesics for the parallel transport since it does not require any additional structures, like particular foliation of space-time, which in turn is applicable to any space-time. However, a resulting Doppler effect is inconclusive, because a definition of relative velocity has disadvantage that there is no unique way to compare four-vectors of the velocities at widely separated space-time events by parallel transport.

Our primary interest, in the present article is rather to extend those geometrical ideas developed by (Synge, 1960), to build a series of infinitesimally displaced shifts and then sum over them in order to achieve an unique definition of the so-called *kinetic* relative velocity of luminous source, without subjecting it to a parallel transport, as measured along the observer's line-of-sight in a generic pseudo-Riemannian space-time. These peculiarities deserve careful study, because they furnish valuable theoretical clues about the interpretation of kinetic velocity of luminous object relative to observer in GR, a systematic analysis of properties of which happens to be surprisingly difficult by conventional methods. The problem of subjecting the four-velocity vector of the luminous source to parallel transport will not be broached in this paper, though it is hoped that the present formulation of the theory will facilitate the task. A resulting general relationship between the spectral shift and the *kinetic* relative velocity is utterly distinct from a familiar global Doppler shift. We discuss the implications for a particular case of a global Doppler shift along the null geodesic, and the spatially homogeneous and isotropic Robertson-Walker space-time of standard cosmological model. The latter leads to important cosmological consequences that the resulting *kinetic* recession velocity of a galaxy is always subluminal even for large redshifts of order one or more, and thus, it does not violate the fundamental physical principle of *causality*. This provides a new perspective to solve startling difficulties of superluminal `proper´ recession velocities, which the conventional scenario of expanding universe of standard cosmological model presents (see e.g. Bolós & Klein, 2012, Bunn & Hogg, 2009, Chodor-

doi: https://doi.org/10.52526/25792776-2021.68.1-38

owski, 2011, Davis & Lineweaver, 2004, Emtsova & Toporensky, 2019, Grøn & Elgarøy, 2007, Harrison, 1993, 1995, Kaya, 2011, Klein & Collas, 2010, Klein & Randles, 2011, Murdoch, 1977, Narlikar, 1994, Peacock, 1999, 2008, Peebles, 1993, Peebles et al., 1991, Silverman, 1986, Whiting, 2004). In some instances (in earlier epochs), the distant astronomical objects are observed to exhibit redshifts in excess of unity, and only a consistent theory could tackle the key problems of a dynamics of such objects.

With this perspective in sight, we will proceed according to the following structure. To start with, Section 2 deals with the relationship of the overall spectral shift, z, and the speed of source (S) relative to observer (O) in its rest frame along the line of sight, in a general Riemannian space-time. On these premises, in Subsection 2.1, we show that a general solution is reduced to global Doppler shift along the null geodesic, as it is studied by Synge (1960). We use a general solution as a backdrop to explore in Subsection 2.2 a new concept of the *kinetic* recession velocity of an astronomical object in other context of RW space-time of standard cosmological model. In these terms we reconcile the cosmological interpretation of redshift with the correct solution to a kinematic interpretation of redshifts as accumulation of a series of infinitesimal spectral shifts. The *kinetic* recession velocity is always subluminal even for large redshifts of order one or more, and thus, it does not violate the fundamental physical principle of *causality*. Concluding remarks are given in Section 3.

2. The relative speed along the observer's line-of-sight in a generic pseudo-Riemannian space-time

Avoiding from any mistakes, we preferred to work in an infinitesimal domain. The principle foundation of our setup comprises the following steps. Let (o) and (s) be two world lines respectively of observer O and source S in the pseudo-Riemannian space-time. Suppose the passage of light signals from S to O is described by a single infinity of null geodesics $\Gamma(v)$ connecting their respective world lines. To clarify the issues further, it should help a few noteworthy points of Fig. 1. Avoiding from any mistakes, we preferred to work in an infinitesimal domain. The $S_{(1)}$ and $S_{(2)}$ are two neighboring world points on (s). The parametric values for these geodesics are $v, v+\triangle v$, respectively, where $v = const$ and $\triangle v$ is infinitesimally small. Accordingly, the world line (s) is mapped pointwise on the (o) by a set of null geodesics $\Gamma(v)$. That is, a set of null geodesics are joining (s) to (o), each representing the history of a wave crest. The totality of these null geodesics forms a 2-space with equation $x^\mu = x^\mu(u, v)$, which is determined once (s) and (o) are given. The u denote the affine parameter on each of these geodesics running between fixed end-values $u = 0$ on (s) and $u = 1$ on (o). The $O_{(1)}$ and $O_{(2)}$ are corresponding world points on (o), where the null geodesics from $S_{(1)}$ and $S_{(2)}$ meet it. Also we will denote by τ_O and τ_S the proper times of the observer and the source, respectively, and $\triangle\tau_O$ and $\triangle\tau_S$ are the elements of proper time corresponding to the segments (the clock measures of) $O_{(1)}O_{(2)}$ and $S_{(1)}S_{(2)}$. Imagine now a dense family of adjacent observers O_j $(j = 1, ..., n-1)$ with the world lines (o_j) populated between the two world lines (o) and (s). Each observer O_j measures the frequency of light rays emitted by the source S as it goes by. The $O_{j(1)}$ and $O_{j(2)}$ are two neighboring world points on (o_j) where the null geodesics from $S_{(1)}$ and $S_{(2)}$ meet it. The u_j denote the values of affine parameter on each of the null geodesics chosen at equal infinitesimally small δu_i, so that $u = u_j$ on (o_j). The τ_{O_j} denotes the proper times of the adjacent observers, i.e. $\triangle\tau_{O_j}$ are the elements of proper time corresponding to the segment $O_{j(1)}O_{j(2)}$. Here and throughout we use the proper space scale factor l_i $(i = 0, 1, 2, ..., n)$ which encapsulates the beginning and evolution of the elements of proper time $\triangle\tau_S$ of source, namely $l_0 = c\triangle\tau_S$, $l_1 = c\triangle\tau_{O_{(1)}}$, $\dots$, $l_{n-1} = c\triangle\tau_{O_{n-1}}$, $l_n = c\triangle\tau_O$. Each line segment l_{i-1} of proper space scale factor (at the affine parameter u_{i-1}) is identically mapped on the line segment $(l_i - \delta l_{i-1})$ of proper space scale factor (at infinitesimally close affine parameter u_i), such that $l_{i-1} \equiv (l_i - \delta l_{i-1})$, where δl_i denotes infinitesimal segment $a_i O_{i(2)}$. If there are N wave crests of the light, the wavelength of light λ_{O_i} at the observers O_i $(i = 1, ..., n$, where $O_n \equiv O)$, who measures the wavelength of light ray as it goes by, satisfies the following condition:

$$N = \frac{l_n}{\lambda_n} = \frac{l_{n-1}}{\lambda_{n-1}} = \cdots = \frac{l_1}{\lambda_1} = \frac{l_0}{\lambda_0}, \tag{1}$$

doi: https://doi.org/10.52526/25792776-2021.68.1-38

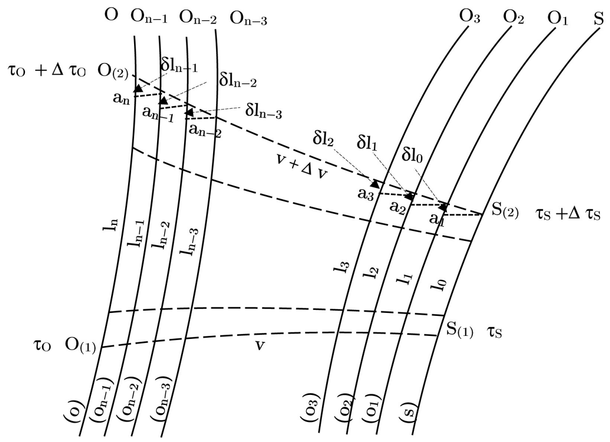

Figure 1. The infinitesimal spectral shifts as measured locally by emitter and adjacent receivers in a generic pseudo-Riemannian space-time. The (o) and (s) are two world lines respectively of observer O and source S. A dense family of adjacent observers O_j $(j = 1, ..., n-1)$ with the world lines (o_j) populated between the two world lines (o) and (s). A set of null geodesics (the dotted lines) is mapping (s) on (o), each representing the history of a wave crest. Each line segment l_{i-1} of proper space scale factor (at the affine parameter u_{i-1}) is identically mapped on the line segment $(l_i - \delta l_{i-1})$ of proper space scale factor (at infinitesimally close affine parameter u_i), such that $l_{i-1} \equiv (l_i - \delta l_{i-1})$, where δl_i denotes infinitesimal segment $a_i O_{i(2)}$.

where $\lambda_i\,(\equiv \lambda_{O_i})$. The wavelength λ_i of light ray is varied on the infinitesimal distance between the observers O_{i+1} and O_i in a general Riemannian space-time in proportion to the proper space scale factor l_i :

$$\frac{\lambda_{i+1}}{\lambda_i} = \frac{\triangle\tau_{O_{i+1}}}{\triangle\tau_{O_i}} = \frac{l_{i+1}}{l_i}, \tag{2}$$

such that the spectral shift z_i reads

$$z_i = \frac{\lambda_i}{\lambda_S} - 1 = \frac{l_i}{l_0} - 1 = \frac{\triangle\tau_{O_i}}{\triangle\tau_S} - 1. \tag{3}$$

The spectral shift z_i, in general, can be evaluated straightforwardly in terms of the world function $\Omega(SO_i)$ for two points $S(x')$ and $O_i(x_{(i)})$ $(i = 1, ..., n)$ through an integral defined along the geodesic $\Gamma_{SO_i}(v)$ joining them (Synge, 1960), taken along any one of the curves $v = const.$ Following Synge, the world function $\Omega(SO_i)$ can be defined for any of the geodesics in the family linking points on (o_i) and (s):

$$\Omega(SO_i) = \Omega(x'x_{(i)}) \equiv \Omega_i(v) = \tfrac{1}{2}(u_{Oi} - u_S)\int_{u_S}^{u_{Oi}} g_{\mu\nu}U^\mu U^\nu du, \tag{4}$$

taken along $\Gamma_{SO_i}(v)$ with $U^\mu = \frac{dx^\mu_{(i)}}{du}$, has a value independent of the particular affine parameter chosen. The holonomic metric $g = g_{\mu\nu}\,\vartheta^\mu \otimes \vartheta^\nu = g(e_\mu, e_\nu)\,\vartheta^\mu \otimes \vartheta^\nu$, is defined in the Riemannian space-time, with the components, $g_{\mu\nu} = g(e_\mu, e_\nu)$ $(\mu = 0, 1, 2, 3)$ in the dual holonomic base $\{\vartheta^\mu \equiv dx^\mu\}$. We have taken $u_S = 0$ and $u_{Oi} \leq 1$ for given world function $\Omega_{(i)}(v)$, which becomes

$$\Omega_{(i)}(v) = \tfrac{1}{2}u_{Oi}\int_0^1 g_{\mu\nu}U^\mu U^\nu du. \tag{5}$$

By virtue of $\delta U^\mu/\delta u = 0$, we have $g_{\mu\nu}U^\mu U^\nu = const$ along $\Gamma_{SO_i}(v)$, therefore, (4) is reduced to

$$\Omega_{(i)}(v) = \tfrac{1}{2}(u_{O_{(i)}} - u_S)^2 g_{\mu\nu}U^\mu U^\nu, \tag{6}$$

with the last part evaluated anywhere on $\Gamma_{SO_i}(v)$. Taking $u_S = 0$ and $u_{Oi} = 1$, and applying conventional methods (Synge, 1960), we then have

$$\Omega_{(i)}(v) = \tfrac{1}{2}g_{\mu\nu}U^\mu U^\nu = \tfrac{1}{2}\varepsilon L_i^2, \quad L_i = \int_S^{O_i} ds, \tag{7}$$

that is, to within the factor $\varepsilon = \pm 1$, the world-function is half the square of the measure, L_i, of geodesic joining S and O_i. Synge has proved that the following relations hold in general:

$$\frac{\partial\Omega_{(i)}(v)}{\partial x^\mu}\Big|_S = -u_{Oi}\, g_{\mu\nu}\frac{\partial x^\nu}{\partial u}\big|_S\,, \quad \frac{\partial\Omega_{(i)}(v)}{\partial x^\mu}\Big|_{O_i} = u_{Oi}\, g_{\mu\nu}\frac{\partial x^\nu}{\partial u}\big|_{O_i}\,. \tag{8}$$

The right hand sides are invariant under transformation of the affine parameter. If the geodesic is not null, one has

$$\frac{\partial\Omega_{(i)}}{\partial x'^\mu} = -L_i\tau_{\mu(S)}, \quad \frac{\partial\Omega_{(i)}}{\partial x^\mu_{(i)}} = L_i\tau_{\mu(O_i)}, \tag{9}$$

where $\tau_{\mu(S)}$ and $\tau_{\mu(O_i)}$ are the unit tangent vectors to the geodesic at S and O_i.

For null geodesics $\Gamma_{S_{(1)}O_{i(1)}}(v)$ and $\Gamma_{S_{(2)}O_{i(2)}}(v+\triangle\, v)$, in particular, the world functions $\Omega_{(i)}(v)$ does not change in the interval v and $v+\triangle\, v$, therefore

$$\frac{\partial\Omega_{(i)}(v)}{\partial x^\mu}\frac{dx^\mu}{dv}\Big|_{O_i} + \frac{\partial\Omega_{(i)}(v)}{\partial x^\mu}\frac{dx^\mu}{dv}\Big|_S = 0, \tag{10}$$

which yields

$$p_{\mu(i)}V^\mu_{(i)}\triangle\,\tau_{O_i} - p_{\mu(S)}V^\mu_{(S)}\triangle\,\tau_S = 0, \tag{11}$$

where $V^\mu_{(i)} = dx^\mu/d\tau_{O_i}|_{O_{i(1)}}$ and $V^\mu_{(S)} = dx^\mu/d\tau_S|_{S_{(1)}}$ are the respective four-velocity vectors of observer O_i and source S (or world lines (o_i) and (s)) at points $O_{i(1)}$ and $S_{(1)}$, $p^\mu_{(i)} = dx^\mu_{(i)}/du_i$ and $p^\mu_{(S)} = dx'^\mu/du_0$ are respective four-momenta of light ray (tangent to null geodesic) at the end points. Then, by virtue of (2), we obtain

$$1+z_i = \frac{l_i}{l_0} = \frac{p_{\mu(S)}V^\mu_{(S)}}{p_{\mu(i)}V^\mu_{(i)}}. \tag{12}$$

For $i=n$, (12) becomes a well-known generalization of the overall spectral shift rule in a Riemannian space-time (Synge, 1960)

$$z = \frac{\triangle\tau_O}{\triangle\tau_S} - 1 = \frac{p_{\mu(S)}V^\mu_{(S)}}{p_{\mu(O)}V^\mu_{(O)}} - 1. \tag{13}$$

Let us subject the vector $V^\mu_{(S)}$ to parallel transport along the null geodesic $\Gamma_{S_{(1)}O_{(1)}}(v)$ to the observer. This yields at $O_{(1)}$ the vector $\beta^\mu_{(S1)} = \mathrm{g}^{\mu\nu'}(O_{(1)}, S_{(1)})V^{\nu'}_{(S1)}$, where the two point tensor $\mathrm{g}^{\mu\nu'}(O_{(1)}, S_{(1)})$ is the parallel propagator. The latter is determined only by the points $S_{(1)}$ and $O_{(1)}$. At $S_{(1)} \to O_{(1)}$, we have the coincidence limit $[\mathrm{g}^{\mu\nu'}](O_{(1)}) = g^{\mu\nu}(O_{(1)})$. Then we obtain a relativistically invariant form of global Doppler shift:

$$z = \frac{p_{\mu(O1)}\beta^\mu_{(S1)}}{p_{\mu(O1)}V^\mu_{(O1)}} - 1, \tag{14}$$

where $V^\mu_{(O1)}$ is the four-velocity vector of the observer O at point $O_{(1)}$, $p_{\mu(S1)}$ and $p_{\mu(O1)}$ are the tangent vectors to the typical null geodesics $\Gamma_{S_{(1)}O_{(1)}}(v)$ at their respective end points. Narlikar (Narlikar, 1994) has proved a rule (14) in other context of standard cosmological model of expanding universe. A Doppler effect (14), having recast in an alternative form by Synge (1960), reads:

$$z = 1 - \frac{1}{(1+\beta^2_{(O_{(1)})})^{\frac{1}{2}} + \beta_{R(O_{(1)})}}, \tag{15}$$

where $c\beta^\mu_{(S1)} = v^\mu_{(S1)}$, $c\beta_{(O_{(1)})} = v_{(O_{(1)})}$, $c\beta_{R(O_{(1)})} = v_{R(O_{(1)})}$, and

$$\begin{aligned} &v^2_{(O_{(1)})} = v_{(\alpha)(O_{(1)})}v^{(\alpha)}_{(O_{(1)})}, \quad v_{(\alpha)(O_{(1)})} = v_{\mu(S1)}\xi^\mu_{(\alpha)(O_{(1)})}, \\ &v_{R(O_{(1)})} = v_{\mu(S1))}r^\mu_{(O_{(1)})} = v_{(\alpha)(O_{(1)})}v^{(\alpha)}_{(O_{(1)})}. \end{aligned} \tag{16}$$

Reviewing notations the three-velocity of (s) relative (o) are defined by the tree invariant components $v_{(\alpha)(O_{(1)})}$, $v_{(S1)}$ is the relative speed, $v_{R(O_{(1)})}$ is the speed of recession of (s). Whereas $\xi^\mu_{(\alpha)(O_{(1)})}$ is the frame of reference on world-line (o) with $\xi^\mu_{0(O_{(1)})} = V^\mu_{(O_{(1)})}$, the unit vector $r^{\mu(O_{(1)})}$ at $O_{(1)}$ is orthogonal

doi: https://doi.org/10.52526/25792776-2021.68.1-38

to world-line (o) $(r_{\mu(O_{(1)})}V^{\mu}_{(O_{(1)})} = 0)$ and lying in the 2-element which contains the tangent at $O_{(1)}$ to (o) and $S_{(1)}O_{(1)}$.

In studying further a set of null geodesics $\Gamma(v)$ with equations $x^{\mu}(u_i, v)$ (where $v = const$), we may deal with the deviation vector $\eta^{\mu}_{(i)}$ drawn from $O_{i(1)}S_{(1)}$ to $O_{i(2)}S_{(2)}$, and that we have along null geodesic

$$\eta_{\mu(i)}\frac{\partial x^{\mu}}{\partial u_i} = const. \tag{17}$$

The equation (17) yields

$$\eta_{\mu(i+1)}p^{\mu}_{(i+1)} = \eta_{\mu(i)}p^{\mu}_{(i)}. \tag{18}$$

Then

$$\begin{aligned} &\eta_{\mu(i+1)} = V^{\mu}_{(i+1)}l_{i+1}, \quad \eta_{\mu(i)} = V^{\mu}_{(i)}l_i, \\ &\eta_{\mu(i+1)}p^{\mu}_{(i+1)} = E_{i+1}l_{i+1}, \quad \eta_{\mu(i)}p^{\mu}_{(i)} = E_i l_i, \end{aligned} \tag{19}$$

where $E_i = p_{\mu(i)}V^{\mu}_{(i)}$ is the energy of light ray relative to an observer O_i. Combining (2) and (19), we may write the ratio $(\lambda_{i+1}/\lambda_i)$ in terms of energy of photon and the world-function

$$\frac{\lambda_{i+1}}{\lambda_i} = \frac{l_{i+1}}{l_i} = \frac{E_i}{E_{i+1}} = \frac{p_{\mu(i)}V^{\mu}_{(i)}}{p_{\mu(i+1)}V^{\mu}_{(i+1)}} = \frac{\Omega_{\mu(i)}V^{\mu}_{(i)}}{\Omega_{\mu(i+1)}V^{\mu}_{(i+1)}}, \tag{20}$$

where $\Omega_{\mu(i)} = (u_{Oi} - u_S)U_{\mu}$. Therefore, the infinitesimal `relative´ spectral shift δz_i between the observers O_{i+1} and O_i will be

$$\begin{aligned} \delta z_i = \frac{\delta\lambda_i}{\lambda_i} = \frac{\lambda_{i+1}-\lambda_i}{\lambda_i} = \frac{\delta l_i}{l_i} = \frac{l_{i+1}-l_i}{l_i} = \frac{p_{\mu(i)}V^{\mu}_{(i)}}{p_{\mu(i+1)}V^{\mu}_{(i+1)}} - 1 = \\ \frac{\Omega_{\mu(i)}V^{\mu}_{(i)}}{\Omega_{\mu(i+1)}V^{\mu}_{(i+1)}} - 1 = \frac{\tilde{\delta} z_i}{1+z_i} \equiv \frac{z_{i+1}-z_i}{1+z_i}. \end{aligned} \tag{21}$$

For definiteness, let consider case of $l_n > l_0$ (being red-shift, Fig. 1). In similar way, of course, we may treat a negative case of $l_n < l_0$ (being blue-shift), but it goes without saying that in this case a source is moving towards the observer. In first case, the observers at the points $O_{i(2)}$ $(i = 1, ..., n-1)$ should observe the monotonic increments of `relative´ spectral shifts $(\delta z_1, \delta z_2, \delta z_3, ..., \delta z_{n-1})$ when light ray passes across the infinitesimal distances $(O_{1(2)}, S_{(2)}), (O_{2(2)}, O_{1(2)}), ..., (O_{n(2)}, O_{(n-1)(2)})$. Thus, the wavelength of light emitted at $S_{(2)}$ is stretched out observed at the points $O_{i(2)}$. While weak, such effects considered cumulatively over a great number of successive increments of `relative´ spectral shifts could become significant. The resulting spectral shift is the accumulation of a series of infinitesimal shifts as the light ray passes from luminous source to adjacent observers along the path of light ray. This interpretation holds rigorously even for large spectral shifts of order one or more. If this view would prove to be true, then it would lead to the chain rule for the wavelengths:

$$\frac{\lambda_{O_{(n2)}}}{\lambda_0} \equiv \frac{\lambda_n}{\lambda_1} = \frac{\lambda_n}{\lambda_{n-1}} \cdot \frac{\lambda_{n-1}}{\lambda_{n-2}} \cdots \frac{\lambda_2}{\lambda_1} \cdot \frac{\lambda_1}{\lambda_0} = \prod_{i=1}^{n-1}(1 + \delta z_i), \tag{22}$$

where $\lambda_0 \equiv \lambda_{S_{(2)}}$, such that

$$1 + z = \frac{\lambda_n - \lambda_0}{\lambda_0} = \prod_{i=1}^{n-1}(1 + \delta z_i) = \prod_{i=1}^{n-1} \frac{p_{\mu(i)}V^{\mu}_{(i)}}{p_{\mu(i+1)}V^{\mu}_{(i+1)}} = \prod_{i=1}^{n-1} \frac{\Omega_{\mu(i)}V^{\mu}_{(i)}}{\Omega_{\mu(i+1)}V^{\mu}_{(i+1)}}. \tag{23}$$

With no loss of generality, we may of course apply (23) all the way to $n \to \infty$. Let us view the increment of the proper space scale factor, $l_i = l(u_i)$, over the affine parameters u_i $\quad (i = 1, 2, ..., n)$ as follows: $l_i = l_0 + i\varepsilon$, where ε can be made arbitrarily small by increasing n. In the limit $n \to \infty$, all the respective adjacent observers are arbitrarily close to each other, so that $\delta z_i = \delta l_i/l_i \simeq \varepsilon/l_0 \to 0$. This allows us to write the following relation for the infinitesimal `relative´ redshifts:

$$\begin{aligned} &(\delta z_{n-1} = \delta z_{n-2} = \cdots = \delta z_1 = \varepsilon/l_0)_{n\to\infty} = \lim_{n\to\infty} \delta z^{(a)}_{(n-1)} \equiv \\ &\lim_{n\to\infty}\left(\frac{1}{n-1}\sum_{i=1}^{n-1}\delta z_i\right), \end{aligned} \tag{24}$$

doi: https://doi.org/10.52526/25792776-2021.68.1-38

provided, $\delta z^{(a)}_{(n-1)}$ is the average infinitesimal increment of spectral shift. There does not seem to be any reason to doubt a validity of (24). Certainly, the identification adopted here can be readily proved as follows. The relation (23) then becomes

$$1+z=\lim_{n\to\infty}\prod_{i=1}^{n-1}(1+\delta z_i)=\lim_{n\to\infty}\left(1+\delta z^{(a)}_{(n-1)}\right)^{n-1}=\lim_{n\to\infty}\Big(1+ \frac{1}{n-1}\sum_{i=1}^{n-1}\frac{\delta l_i}{l_i}\Big)^{n-1}=\lim_{n\to\infty}\left(1+\frac{1}{n}\ln\frac{l_n}{l_0}\right)^{n}=\frac{l_n}{l_0}=\frac{p_{\mu(S)}V^{\mu}_{(S)}}{p_{\mu(O)}V^{\mu}_{(O)}}, \tag{25}$$

and hence

$$1+z=\frac{\triangle\tau_O}{\triangle\tau_S}=\frac{p_{\mu(S)}V^{\mu}_{(S)}}{p_{\mu(O)}V^{\mu}_{(O)}}=\frac{\Omega_{\mu(S)}V^{\mu}_{(S)}}{\Omega_{\mu(O)}V^{\mu}_{(O)}}= 1+\sum_{i=1}^{n-1}\tilde{\delta}z_i=\lim_{n\to\infty}\prod_{i=1}^{n-1}(1+\delta z_i)=\lim_{n\to\infty}\left(1+\delta z^{(a)}_{(n-1)}\right)^{n-1}, \tag{26}$$

where $\Omega_{\mu(O)}=(u_O-u_S)U_{\mu(O)}$ and $\Omega_{\mu(S)}=-(u_O-u_S)U_{\mu(S)}$. The first line of equation (26) is the overall spectral shift rule (12), which proved a validity of the relation (24).

It is worth emphasizing that the general equation (26) is the result of a series of infinitesimal stretching of the proper space scale factor in Riemannian space-time, whereas the path of a luminous source appears nowhere, thus this equation does not relate to the special choice of transport path. Therefore, to overcome the ambiguity of parallel transport of four-velocities in curved space-time, in what follows we advocate exclusively with this proposal. To obtain some feeling about this statement, below we give more detailed explanation. The infinitesimal increments of `relative´ spectral shifts $(\delta z_1,\delta z_2,\delta z_3,...,\delta z_{n-1})$, according to (15), can be derived from Doppler effect between adjacent emitter and absorber in relative motion measured in the respective tangent local inertial rest frames at infinitesimally separated space-time points. To obtain some feeling about this statement, below we give more detailed explanation. Imagine a family of adjacent observers $(O_{a_i}(u_i))$ situated at the points a_i $(i=1,...,n)$ on the world lines (o_i) at infinitesimal distances from the observers $(O_{i(2)})$, who measure the wavelength of radiation in relative motion which cause a series of infinitesimal stretching $(\delta l_0,...,\delta l_{n-1})$ of the proper space scale factor. Since each line segment l_{i-1} of proper space scale factor (at the affine parameter u_{i-1}) is identically mapped on the line segment $(l_i-\delta l_{i-1})$ (where δl_i denotes infinitesimal segment $a_iO_{i(2)}$) of proper space scale factor (at the affine parameter $u_i=u_{i-1}+\delta u_{i-1}$), the relative speed $v_{O_{i(2)}O_{a_i}}(u_i)$ of observer $(O_{i(2)}(u_i))$ to adjacent observer $(O_{a_i})(u_i)$ should be the same as it is relative to observer $(O_{(i-1)(2)}(u_{i-1}))$, that is $v_{O_{i(2)}O_{(i-1)}}(u_{i-1})\equiv v_{O_{i(2)}O_{a_i}}(u_i)$. Continuing along this line, we may commit ourselves in the series of `relative´ spectral shifts, equivalently, a certain substitution of increments of relative speeds. Taking into account that the infinitesimal speeds of source (S) relative to observers $(O_{i(2)})$ arise at a series of infinitesimal stretching of the proper space scale factor δl_i $(i=1,2,...,n)$ as it is seen from the Fig. 1, we may fill out the whole pattern of monotonic increments of `relative´ spectral shifts $(\delta z_1,\delta z_2,\delta z_3,...,\delta z_{n-1})$ by, equivalently, replacing the respective pairs $(O_{1(2)},S_{(2)}),(O_{2(2)},O_{1(2)}),...,(O_{n(2)},O_{(n-1)(2)})$ with new ones $(O_{1(2)},O_{a_1}),(O_{2(2)},O_{a_2}),...,(O_{n(2)},O_{a_n})$, which attribute to the successive increments of relative speeds $v_{O_{1(2)}S}(u_1),...,v_{O_{n(2)}O_{(n-1)(2)}}(u_n)$ of the source (S) away from an observer $(O_{n(2)})$ in the rest frame of $(O_{n(2)})$, viewed over all the values $(i=1,...,n)$. This framework furnishes justification for the concept of relative speed $c\beta_n\equiv v_{O_{n(2)}S_{(2)}}$, to be now referred to as the *kinetic* relative velocity, of the source (S) to observer $(O_{n(2)})$ along the line of sight. According to relation (24), at the limit $n\to\infty$, the relative infinitesimal speeds tends to zero, $v_{O_{i(2)}O_{a_i}}(u_i)=c\delta\beta_i=c\delta z_i=c\delta l_i/l_i\simeq c\varepsilon/l_0\to 0$, such that

$$\lim_{n\to\infty}\delta\beta_1=\lim_{n\to\infty}\delta\beta_2=\cdots=\lim_{n\to\infty}\delta\beta_{n-1}= \delta\beta^{(a)}\left(\equiv\lim_{n\to\infty}\frac{1}{n-1}\sum_{i=1}^{n-1}\delta\beta_i\right)=\lim_{n\to\infty}\frac{1}{n}\beta_n. \tag{27}$$

Remark: Although we are free to deal with any infinitesimal `relative´ spectral shift δz_i for the pair $(O_{i(2)})$ and (O_{a_i}), in local tangent inertial rest frame of an adjacent observer (O_{a_i}), where we may approximate away the curvature of space in the infinitesimally small neighborhood, nevertheless, the infinitesimal relative velocities arise in a generic pseudo-Riemannian space-time at a series of infinitesimal stretching of the proper space scale factor as alluded to above, so that the *SR law of composition*

doi: https://doi.org/10.52526/25792776-2021.68.1-38

of velocities cannot be implemented globally along non-null geodesic because these velocities are velocities at the different events, which should be in a different physical frames, and cannot be added together.

Facilitating further the calculations of recession velocity (β_n) in quest, therefore, we may address the pair of observers at points $O_{(n)2}$ and a_n. Suppose $V^\mu_{O_{n(2)}}$ and $V^\mu_{O_{a_n}}$ be the unit tangent four-velocity vectors of observers ($O_{n(2)}$) and (O_{a_n}) to the respective world-lines in a general Riemannian space-time, thus in their respective rest frame we have $V^0_{O_{n(2)}} = 1$ and $V^0_{O_{a_n}} = 1$, as the only nonzero components of velocity. For comparing the vectors $V^\mu_{O_{n(2)}}$ and $V^\mu_{O_{a_n}}$ at different events, it is necessary to seek a useful definition of the relative velocity by bringing both vectors to a common event by subjecting one of them to parallel transport. Since all the paths between infinitesimally separated space-time points $O_{(n)2}$ and a_n are coincident at $n \to \infty$, for comparing these velocities there is no need to worry about specific choice of the path of parallel transport of four-vector. Therefore, we are free to subject further the unit tangent four-velocity vector $V^\mu_{O_{n(2)}}$ to parallel transport along the null geodesic $\Gamma_{O_{n(2)a_n}}$ to the point a_n. Thereby, the ray passes an observer $O_{a_n}(u_n)(\equiv O_{(n-1)(2)}(u_{n-1}))$ with the proper space scale factor l_{n-1} who measures the wavelength to be λ_{n-1}. The ray passes next observer $O_{n(2)}(u_n)$ with the proper space scale factor $l_n = l_{n-1} + \delta l_{n-1}$. The ray's wavelength measured by observer $O_{n(2)}(u_n)$ is increased by $\delta\lambda_{n-1} = \lambda_n - \lambda_{n-1}$ leading to infinitesimal `relative´ spectral shift δz_{n-1}. A parallel transport yields at O_{a_n} the vector $\beta_{\mu(O_{a_n})} = \mathrm{g}_{\mu\nu'}(O_{a_n}, O_{(n)2})V^{\nu'}_{O_{(n)2}}$, where the two point tensor $\mathrm{g}_{\mu\nu'}(O_{a_n}, O_{(n)2})$ is the parallel propagator as before, which is now determined by the points $O_{(n)2}$ and O_{a_n}. At $O_{(n)2} \to O_{a_n}$, we have the coincidence limit $[\mathrm{g}_{\mu\nu}](O_{a_n}) = g_{\mu\nu}(O_{a_n})$. As we have at point O_{a_n} two velocities $V^\mu_{O_{a_n}}$ and $\beta^\mu_{(O_{a_n})} = g^{\mu\nu}\beta_{\nu(O_{a_n})}$, according to the equations (14) and (15), we may associate Doppler shift δz_{n-1} to four-velocity $\beta^\mu_{(O_{a_n})}$ of observer O_n observed by an observer O_{a_n} with four-velocity $V^\mu_{O_{a_n}}$ as measured by the latter. Then, according to (16), the infinitesimal Doppler shift can be written:

$$\delta z_{n-1} = \frac{\delta\lambda_{n-1}}{\lambda_{n-1}} = 1 - \frac{1}{(1+\beta^2_{(O_{a_n})})^{1/2} + \beta_{R(O_{a_n})}} = \frac{p_{\mu(O_{a_n})}\beta^\mu_{(O_{a_n})}}{p_{\mu(O_{a_n})}V^\mu_{(O_{a_n})}} - 1, \tag{28}$$

where the notation of (16) is used but applied now to point (O_{a_n}) (instead of (O_1)). Consequently, the three-velocity of an observer ($O_{n(2)}$) relative to observer at (O_{a_n}) is $v_{(\alpha)(O_{a_n})}$, the relative speed is $v_{(O_{a_n})}$, and $v_{R(O_{a_n})}$ is the speed of recession of (o_n). In the local inertial rest frame $\xi^\mu_{(\alpha)(O_{a_n})}$ of an observer (O_{a_n}), the velocity vector $\beta^\mu_{O_{a_n}}$ takes the form $(\gamma, \gamma\delta\beta_{(O_{a_n})}, 00)$, where an observer ($O_n(2)$) is moving away from the observer (O_{a_n}) with the relative infinitesimal three-velocity $\delta\beta_{(O_{a_n})}$ (in units of the speed of light) in a direction making an angel $\theta_{(O_{a_n})}$ with the outward direction of line of sight $\Gamma_{O_{n(2)O_{a_n}}}$ from $O_{(n)2}$ to O_{a_n}, and $\gamma = (1 - \delta\beta^2_{(O_{a_n})})^{-1/2}$. Hence, the equation (28) is reduced to

$$\begin{aligned} \delta z_{n-1} &= \frac{1+\delta\beta_{(O_{a_n})}\cos\theta_{(O_{a_n})}}{\sqrt{1-\delta\beta^2_{(O_{a_n})}}} - 1 = \beta_{R(O_{a_n})} - \beta^2_{R(O_{a_n})} + \frac{1}{2}\beta^2_{(O_{a_n})} + \cdots \simeq \beta_{R(O_{a_n})} = \\ &\frac{p_{(\alpha)(O_{a_n})}v^{(\alpha)}_{(O_{a_n})}}{E_{O_{a_n}}} = \delta\beta_{(O_{a_n})}\cos\theta_{(O_{a_n})}. \end{aligned} \tag{29}$$

Thus, at $n \to \infty$, the wavelength measured by the observer $O_{n(2)}$ is increased by the first-order Doppler shift caused unambiguously by the infinitesimal relative speed $\delta\beta^{(r)}_{n-1} \equiv \delta\beta_{(O_{a_n})}\cos\theta_{(O_{a_n})}$ along the line of sight with end-points $O_{(n)2}$ and O_{a_n}:

$$\delta z_{n-1} = \frac{\delta l_{n-1}}{l_{n-1}} = \delta\beta^{(r)}_{n-1}. \tag{30}$$

The SR law of composition of velocities along the line of sight can be implemented in the tangent inertial rest frame of an observer O_{a_n}:

$$\delta\beta^{(r)}_{n-1} = \frac{\beta_n - \beta_{n-1}}{1 - \beta_n\beta_{n-1}} \simeq \frac{\delta\beta_{n-1}}{1 - \beta^2_{n-1}}, \tag{31}$$

where $v_{n-1} = c\beta_{n-1}$ and $v_n = c\beta_n$ are, respectively, the three-velocities of observers O_{a_n} and O_n along the line of sight with end-points O_{a_n} and $O_{(n)2}$. According to (27), at $n \to \infty$, a resulting infinitesimal

doi: https://doi.org/10.52526/25792776-2021.68.1-38

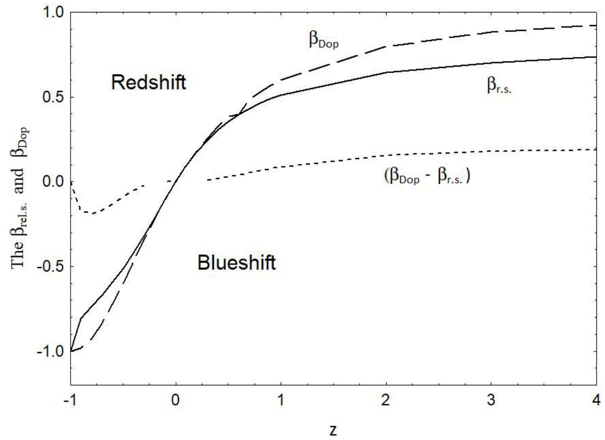

Figure 2. The relative velocity along the line of sight ($\beta_{r.s.}$) of luminous source (S) with $-1 \leq z \leq 4$ to observer (O), the global Doppler velocity (β_{Dop}), and their difference (in units of the speed of light).

increment δz_{n-1} of spectral shift reads

$$\lim_{n\to\infty} \delta z_{n-1} = \lim_{n\to\infty} \frac{\delta\beta_{n-1}}{1-\beta_{n-1}^2} = \lim_{n\to\infty} \frac{\beta_n}{n(1-\beta_n^2)}, \tag{32}$$

For our goal, the most straightforward guess at the convenient form of (26), by virtue of (24), is given by

$$1+z = \frac{p_{\mu S} V_S^\mu}{p_{\mu O} V_O^\mu} = \frac{\Omega_{\mu(S)} V_{(S)}^\mu}{\Omega_{\mu(O)} V_{(O)}^\mu} = \lim_{n\to\infty} (1+\delta z_{n-1})^n. \tag{33}$$

Certainly, it is more rewarding to go ahead with this relation, which incorporated with (32), yield a finite spectral shift

$$1+z = \frac{p_{\mu S} V_S^\mu}{p_{\mu O} V_O^\mu} = \frac{\Omega_{\mu(S)} V_{(S)}^\mu}{\Omega_{\mu(O)} V_{(O)}^\mu} = \lim_{n\to\infty} \left[1 + \frac{1}{n}\left(\frac{\beta_n}{(1-\beta_n^2)}\right)\right]^n. \tag{34}$$

This straightforwardly leads to the kinematic relationship of the overall spectral shift, z, and the speed $\beta_{r.s.}$ (in units of the speed of light) of source (S) relative to observer ($O \equiv O_n$) in its rest frame along the line of sight in a general Riemannian space-time:

$$1+z = \frac{p_{\mu S} V_S^\mu}{p_{\mu O} V_O^\mu} = \frac{\Omega_{\mu(S)} V_{(S)}^\mu}{\Omega_{\mu(O)} V_{(O)}^\mu} = \exp\left(\frac{\beta_{r.s.}}{1-\beta_{r.s.}^2}\right), \tag{35}$$

where, hereinafter, the relative speed $\beta_{r.s.} \equiv \lim_{n\to\infty} \beta_n$ in quest is marked with subscript $()_{r.s.}$. The relative speed of luminous source is plotted on the Fig. 2 for redshifts $-1 \leq z \leq 4$. Next we will study a particular case of establishing a global Doppler shift from a general solution (35).

2.1. A global Doppler shift along the null geodesic

Suppose the velocities of observers say $O_{i(2)}$ $(i = 1, ..., n-1)$, being in free fall, populated along the null geodesic $\Gamma_{S_{(2)}O_{(2)}}(v + \bigtriangleup v)$ of light ray (Fig. 1), vary smoothly along the line of sight with the infinitesimal increment of relative velocity $\delta\beta_i^r$. The (i)-th observer situated at the point $i(2)$ of intersection of the ray's trajectory $\Gamma_{S_{(2)}O_{(2)}}(v + \bigtriangleup v)$ with the world line (o_i) at affine parameter u_i, and measures the frequency of light ray as it goes by. According to the equivalence principle, we may approximate away the curvature of space in the infinitesimally small neighborhood of two adjacent observers. We should emphasize that if we approximate an infinitesimally small neighborhood of a curved space as flat, the resulting errors are of order $(\delta l_i/l_n)^2$ in the metric. If we regard such errors as negligible, then we can legitimately approximate space-time as flat. The infinitesimal increment of spectral shift δz_i is not approximated away in this limit because it is in that neighborhood of leading order $(\delta l_i/l_i)$. That is, approximating away the curvature of space in the infinitesimally small neighborhood does not mean approximating away the infinitesimal increment δz_i. Imagine a thin

doi: https://doi.org/10.52526/25792776-2021.68.1-38

world tube around the null geodesic $\Gamma_{S_{(2)}O_{(2)}}(v+\triangle v)$ within which the space is flat to arbitrary precision. Each observer has a local reference frame in which SR can be taken to apply, and the observers are close enough together that each one $O_{(i+1)(2)}$ lies within the local frame of his neighbor $O_{i(2)}$. This implies the vacuum value of a velocity of light to be universal maximum attainable velocity of a material body found in this space. Such statement is true for any thin neighborhood around a null geodesic. Only in this particular case, the relative velocity of observers can be calculated by the SR law of composition of velocities globally along the path of light ray. We may apply this law to relate the velocity β_{i+1} to the velocity β_i, measured in the i-th adjacent observer's rest frame. The end points of infinitesimal distance between the adjacent observers $O_{(i+1)(2)}$ and $O_{i(2)}$ will respectively be the points of intersection of the ray's trajectory with the world lines $o_{i+1}(u_{i+1})$ and $(o_i)(u_i)$. This causes a series of infinitesimal increment of the proper space scale factor from initial value $l_0 =\triangle\tau_S$ to the given value $l_i =\triangle\tau_{O_i}$, which in turn causes a series of infinitesimal increment of spectral shift $\delta z_i = \delta\lambda_i/\lambda_i = \delta l_i/l_i$. Within each local inertial frame, there are no gravitational effects, and hence the infinitesimal spectral shift from each observer to the next is a Doppler shift. Thus, at the limit $n\to\infty$, a resulting infinitesimal frequency shift δz_i, can be unambiguously equated to infinitesimal increment of a fractional SR Doppler shift $\delta\bar{z}_i$ from observer $O_{i(2)}$ to the next $O_{(i+1)(2)}$ caused by infinitesimal relative velocity $\delta\bar{\beta}^r_i$:

$$\left(\delta z_i = \frac{\delta l_i}{l_i}\right)_{n\to\infty} = \left(\delta\bar{z}_i = \delta\bar{\beta}^r_i = \frac{\bar{\beta}_{i+1}-\bar{\beta}_i}{1-\bar{\beta}_{i+1}\bar{\beta}_i} \simeq \frac{\delta\bar{\beta}_i}{1-\bar{\beta}^2_i}\right)_{n\to\infty}, \tag{36}$$

where by $\bar{()}$ we denote the null-geodesic value, as different choice of geodesics yields different results for the motion of distant test particles relative to a particular observer. The relation (36), incorporated with the identity (24), yield

$$\begin{aligned}(\delta z_{n-1} =)_{n\to\infty} = \left(\frac{\delta\beta_{n-1}}{1-\beta^2_n}\right)_{n\to\infty} = \Bigg(\delta\bar{z}^{(a)}_{(n-1)} = \delta\bar{\beta}^{r(a)}_{(n-1)} \equiv \\ \frac{1}{n-1}\sum_{i=1}^{n-1}\frac{\delta\bar{\beta}_i}{1-\bar{\beta}^2_i}\Bigg)_{n\to\infty},\end{aligned} \tag{37}$$

which, by virtue of (27), for sufficiently large but finite n gives

$$\frac{\beta_n}{1-\beta^2_n} = \sum_{i=1}^{n-1}\frac{\delta\bar{\beta}_i}{1-\bar{\beta}^2_i} = \int_0^{\bar{\beta}_n}\frac{d\bar{\beta}}{1-\bar{\beta}^2}, \tag{38}$$

or

$$\bar{\beta}_n = \frac{e^{\varrho_n}-1}{e^{\varrho_n}+1}, \quad \varrho_n \equiv \frac{2\beta_n}{1-\beta^2_n}. \tag{39}$$

Hence the general solution (35), by means of relation (38), is reduced to a global Doppler shift (14) along the null geodesic:

$$1+z = \exp\left(\frac{\beta_{r.s.}}{1-\beta^2_{r.s.}}\right) = \sqrt{\frac{1+\bar{\beta}_{r.s.}}{1-\bar{\beta}_{r.s.}}} = \frac{p_{\mu(O2)}V^{\mu}_{(S2)}}{p_{\mu(O2)}V^{\mu}_{(O2)}}, \tag{40}$$

where $\bar{\beta}_{rec} = \lim_{n\to\infty}\bar{\beta}_n$, $V^{\mu}_{(S2)}$ and $V^{\mu}_{(O2)}$ are the four-velocity vectors, respectively, of the source $S_{(2)}$ and observer $O_{(2)}$, $p_{\mu(S2)}$ and $p_{\mu(O2)}$ are the tangent vectors to the typical null geodesics $\Gamma_{S_{(2)}O_{(2)}}(v)$ at their respective end points. This procedure, in fact, is equivalent to performing parallel transport of the source four-velocity in a general Riemannian space-time along the null geodesic to the observer. Note that any null geodesic from a set of null geodesics mapped (s) on (o) can be treated in the similar way. In Minkowski space a parallel transport of vectors is trivial and mostly not mentioned at all. This allows us to apply globally the SR law of composition of velocities to relate the velocities $\bar{\beta}_{i+1}$ to the $\bar{\beta}_i$ of adjacent observers along the path of light ray, measured in the i-th adjacent observer's frame. Then, according to (36)-(40), a global Doppler shift of light ray emitted by luminous source as it appears to observer at rest in flat Minkowski space can be derived by summing up the infinitesimal Doppler shifts caused by infinitesimal relative velocities of adjacent observers.

2.2. The implications for the standard cosmological model

In the framework of standard cosmological model, one assumes that the universe is populated with comoving observers. In the homogeneous, isotropic universe comoving observers are in freefall, and

doi: https://doi.org/10.52526/25792776-2021.68.1-38

obey Wayl's postulate: their all worldlines form a 3-bundle of non-intersecting geodesics orthogonal to a series of spacelike hypersurfaces, called comoving hypersurfaces. In case of expansion, all worldlines are intersecting only at one singular point. The clocks of comoving observers, therefore, can be synchronized once and for all. Let the proper time, t, of comoving observers be the temporal measure. Suppose $R(t)$ is the scale factor in expanding homogenous and isotropic universe. One considers in, so-called, cosmological rest frame a light that travels from a galaxy to a distant observer, both of whom are at rest in comoving coordinates. As the universe expands, the wavelengths of light rays are stretched out in proportion to the distance $L(t)$ between co-moving points ($t > t_1$), which in turn increase proportionally to $R(t)$ (Harrison, 1993, 1995):

$$\frac{\lambda(t)}{\lambda(t_1)} = \frac{dt}{dt_1} = \frac{R(t)}{R(t_1)} = \frac{L(t)}{L(t_1)}. \tag{41}$$

Reviewing notations in this `cosmic wavelength stretching´ relation, $L_1 \equiv L(t_1)$ is the proper distance to the source at the time when it emits light, $L(t)$ is the same distance to the same source at light reception.

In what follows, the mathematical structure has much in common with those constructions used for deriving of (21)-(35). After making due allowances for (41), particularly, the infinitesimal `relative´ increment δz_j $(j = 1, ..., n-1)$ of redshift reads

$$\delta z_j = \frac{\delta\lambda_j}{\lambda_j} = \frac{\lambda_{j+1}-\lambda_j}{\lambda_j} = \frac{\delta L_j}{L_j} = \frac{L_{j+1}-L_j}{L_j} = \frac{\tilde{\delta} z_j}{1+z_j} \equiv \frac{z_{j+1}-z_j}{1+z_j}, \quad 1+z_j = \frac{\delta\lambda_j}{\lambda_1}, \tag{42}$$

where, the role of proper space scale factor l_i is now destined to the scale factor $R(t_i) \propto L(t_i)$. Consequently, the general relation (35) straightforwardly yields the particular solution as a corollary for the case of expanding RW space-time of standard cosmological model, i.e. the kinematic relationship of the overall cosmological redshift, z, and *kinetic* recession velocity ($\beta_{rec} \equiv \beta_{r.s.}$) (in units of the speed of light) of the comoving distant galaxy (A_1) of redshift z, which crossed past light cone at time t_1 away from comoving observer (O):

$$1 + z = \frac{R(t)}{R(t_1)} = \exp\left(\frac{\beta_{rec}}{1-\beta^2_{rec}}\right). \tag{43}$$

This interpretation so achieved has physical significance as it agrees with a view that the light waves will be stretched by travelling through the expanding universe, and in the same time the *kinetic* recession velocity of a distant astronomical object is always subluminal even for large redshifts of order one or more. It, therefore, does not violate the fundamental physical principle of *causality*. Moreover, the general solution is reduced to global Doppler shift (40) along the null geodesic, studied by Synge (1960) (see also Bunn & Hogg (2009), Narlikar (1994)).

If, and only if, for the distances at which the Hubble empirical linear `redshift-distance´ law ($cz = HL$) is valid, the relationship between the *physical* recession velocity, v_{rec}, and the expansion rate, $\dot{L}$ $(= HL)$, reads

$$\beta_{rec} = \frac{\sqrt{1+4\ln^2(1+\dot{L}/c)}-1}{2\ln(1+\dot{L}/c)}. \tag{44}$$

3. Concluding remarks

Let us briefly summarize the main results of this work. This report is about the much-discussed in literature question of interpretation of the spectral shift of radiation from a distant object in a curved spacetime. We aim to provide a unique definition for the *kinetic* relative velocity between a source and the observer as measured along the observer's line-of-sight. Extending those geometrical ideas of well-known kinematic spectral shift rule to infinitesimal domain, we try to catch this effect by building a series of infinitesimally displaced shifts and then sum over them in order to find the proper answer to the problem that we wish to address. Thereby, the general equation (26) is the result of a series of infinitesimal stretching of the proper space scale factor in Riemannian space-time, whereas the path of a luminous source appears nowhere, thus this equation does not relate to the

doi: https://doi.org/10.52526/25792776-2021.68.1-38

special choice of transport path. A resulting general relationship (35) between the spectral shift and the *kinetic* relative velocity is utterly distinct from a familiar global Doppler shift (14). We discuss the implications for a particular case when adjacent observers are being in free fall and populated along the null geodesic, so that the *kinetic* relative velocity of luminous source is reduced to global Doppler velocity (40) as studied by Synge. Moreover, the implications for the spatially homogeneous and isotropic RW space-time of standard cosmological model leads to cosmological consequences that resulting *kinetic* recession velocity of a distant astronomical object is always subluminal even for large redshifts of order one or more and, thus, it does not violate the fundamental physical principle of *causality*.

References

Bolós V. J., 2006, J. Geom. Phys., 56, 813

Bolós V. J., 2007, Commun. Math. Phys., 273, 217

Bolós V. J., Klein D., 2012, Gen Relativ Gravit., 44, 1361

Bolós V. J., Liern V., Olivert J., 2002, Int. J. Theor. Phys., 41, 1007

Bunn E. F., Hogg D. W., 2009, Am. J. Phys., 77, 6888

Chodorowski M. J., 2011, MNRAS, 413, 585

Davis T. M., Lineweaver C. H., 2004, PASAu, 21, 97

Ellis G. F. R. e. a., 1985, Phys. Rep., 124, 315

Emtsova E., Toporensky A., 2019, arXiv:[gr-qc], 1901.03602, 1

Gautreau R., 1984, Phys. Rev. D, 29, 198

Grøn Ø., Elgarøy Ø., 2007, Am. J. Phys., 75, 151

Harrison E. R., 1993, ApJ, 403, 28

Harrison E. R., 1995, ApJ, 446, 63

Harrison E. R., 1981 and 2000, Cosmology: the science of the universe, 1 and 2 edn. Cambridge U. Press, Cambridge

Kaya A., 2011, Am. J. Phys., 79, 1151

Klein D., Collas P., 2010, Phys. Rev. D, 81, 063518

Klein D., Randles E., 2011, Ann. Henri Poincaré, 12, 303

Manasse F. K., Misner C. W., 1963, J. Math. Phys., 4, 735

Massa E., 1974, Gen.Rel. and Grav., 5, 555, 573, 715

Misner C. W., Thorne K. S., Wheeler J. A., 1973, Gravitation. Freeman

Murdoch H. S., 1977, QJRAS, 18, 242

Narlikar J. V., 1994, Am. J. Phys., 62, 903

Peacock J. A., 1999, Cosmological Physics. Cambridge Univ. Press (Ninth printing with corrections 2010), address = Paris

Peacock J. A., 2008, arXiv:[astro-ph], 0809.4573, 1

Peebles P. J. E., 1993, Principles of Physical Cosmology. Princeton Univ.Press.

Peebles P. J. E., Schramm D., Turner E., Kron R., 1991, Nature, 352, 769

Silverman A. N., 1986, Am. J. Phys., 54, 1092

Synge J. L., 1960, Relativity: The General Theory. North-Hollaand, Amsterdam

Ter-Kazarian G., 2021, Communications of the Byurakan Astrophysical Observatory (Submitted)

Walker A. G., 1935, Proc. Lond. Math. Soc., 4, 170

Whiting A. B., 2004, The Observatory, 124, 174

doi: https://doi.org/10.52526/25792776-2021.68.1-38

Communications of BAO, Vol. 68, Issue 1, 2021, pp. 50-55

The Morphology of the Spiral Galaxies: Encoded Information on the Origin and Evolution Mechanisms

H.A.Harutyunian*

NAS RA V. Ambartsumian Byurakan Astrophysical Observatory (BAO), Armenia

Abstract

Consequences of the interaction between baryonic matter and dark energy carrier is considered for spinning objects. Some morphological features of spiral galaxies are used as fingerprints of formation processes to show that spiral arms of galaxies could be formed through mass ejection from the core of these objects. The Elmegreens' arm classification allows one to find some opportune features for this end. For the same purpose the ratio of vertical and radial sizes of some edge-on spiral galaxies found in deep fields and SDSS surveys are used.

Keywords: *dark energy – baryonic objects – interaction; spiral galaxies – edge-on spirals; spiral arms – formation; mass ejection – rotating objects*

1. Introduction

Often the formation and evolution features leave somehow their fingerprints on the cosmic objects. Not always are these fingerprints explicit, but one can find some of them having even very foggy ideas. For this purpose, one should use all the available information dealing with the objects' morphology and kinematical/dynamical properties also keeping in mind the laws and axioms of the modern physics.

Actually, researchers employ this approach all the time from the times immemorial. Indeed, all the scientific conclusions made by researchers, take into account the facts concerning the objects morphology. The more the classified morphological features, the richer the informational basis. Availability of various features excludes or decreases possibility of the wrong interpretations but at the same time undoubtedly increases the complexity.

On the other hand, any researcher usually has, at least, some general ideas concerning the cosmic objects formation processes and tries to fit the observational date to the adopted conception. The modern cosmogony from the very beginning adopted the Kant-Laplace hypothesis as the basic paradigm, which describes the formation of cosmic objects as a gravitational contraction of the rarified matter. The later modification of the initial hypothesis added the physical process responsible for the appearance of the rarified matter as if produced owing to the big bang.

There are some other paradigms, attempting to avoid the difficulties arising in the frame of the main paradigm. The adherents of the alternative conceptions are not as many as the ones working in the mainstream. In 50s of the last century, Viktor Ambartsumian put forward a new concept suggesting an opposite physical picture for the formation processes, namely, proposing origination of objects due to the decay of the protostellar superdense matter (Ambartsumian, 1947, 1958). Although this new approach allowed to prove the cosmogonic significance of stellar associations and to show the physical phenomenon of the galactic nuclei activity, finally the astronomical community rejected the principal idea. The rejection is based on the conclusion arrived at using the modern physics laws that the stable existence of large masses of nuclear density is not allowed.

Our recent studies showed clearly the possibility of evolutionary scenarios for the baryonic matter interacting with the dark energy or with its carrier. The reasonable conclusion arrived at owing to

*hhayk@bao.sci.am

doi: https://doi.org/10.52526/25792776-2021.68.1-50

studies states that such an interaction might change the mass of baryons, which inevitably leads to the conclusion that the cosmic objects and the Universe as a whole could be less massive, but having the same quantity of baryons. This hypothesis, based on the laws and axioms of the modern physics, allows one in solving some widely known paradoxes (Harutyunian, 2017, Harutyunian & Grigoryan, 2018).

Therefore, taking into account new opened perspectives in this issue, we believe that the scientific community rejected Ambartsumian's conception undeservedly and will try to show some observational facts which speak in favor of the mentioned approach.

2. Evolution of objects according to the Ambartsumian's conception

In the framework of Ambartsumian's conception, all the cosmic objects originate and evolve from a superdense bunch, which could maintain before they start evolving in special physical conditions, such as galactic nuclei or stellar deep interiors towards to the center. The evolution process suggests its decay and formation of smaller fragments of the initial bunch. The more massive the object, the bigger the difference of evolution status between the center and outermost layers. Undoubtedly, the course of this process depends highly also on to physical characteristics of the given bunch, namely, on the mass and angular momentum. Values of these to essential parameters as well as the angular momentum per a unit mass ultimately determine the evolutionary path and the morphological features of the object at any stage of its life.

Considering the merits and demerits of the general idea suggested by Ambartsumian,one might enumerate several. An essential merit is the naturalness of the involved process, which, on the other hand, agrees with the thermodynamics second law. Radioactive decay of the heavy atomic nuclei is the natural analogue of this physical process in the micro world and the expansion of the Universe is the same in the mega world. However, the weak issue concerning the instability of superdense large masses interrupted the further development of this paradigm.

After the discovery of dark energy, the physical picture of the baryonic world changed drastically. Nevertheless, we believe that the astronomical community managed to consider carefully not all consequences of this discovery. In particular, what we mention here, concerns the issues of interaction of baryonic matter with a carrier of dark energy. Although one of the widely accepted forms of dark energy is the constant energy density filling space homogeneously, researchers usually avoid using it on small scales, and especially when looking at microscopic processes.

The fact of the interaction between the ordinary baryonic matter and dark energy is beyond doubt. Otherwise, the galaxy recession would not accelerate and researchers would not discover dark energy in this way. That seems obvious. Then such interaction takes place constantly on all scales including the microcosm. Any interaction between different systems of objects involves exchange of energies of these systems according to the laws of thermodynamics, even if the density of dark energy is extremely low.

All the baryonic objects as well as the stationary systems consisted of these objects, starting with elementary particles and atomic nuclei and up to galaxies and clusters of galaxies have negative total energy, according to modern concepts. Dark energy, which expands the baryonic Universe and accelerates its expansion, is highly positive by definition. Therefore, due to the interaction between these two substances the baryonic side of interaction obtains some portion of energy. This follows from the second law of thermodynamics.

The virial theorem states that all objects and their systems are in a stationary state if the following equality is ensured:

$$2T + U = 0, \tag{1}$$

where and are the kinetic and potential energies. So, interacting with the carrier of dark energy, any baryonic object or system of object gains energy. For a spherical object of the mass and radius the potential energy is

$$U = -\frac{3}{5}G\frac{M^2}{R}. \tag{2}$$

doi: https://doi.org/10.52526/25792776-2021.68.1-50

If the process of interaction between dark energy and the given object increases the potential energy of later, one should observe decrease of the ratio. It can happen if decreases the mass of the object or grows its radius. In general, it is easy to see, that energy can grow if the mass of an object increases more slowly than the square root of its radius. Decrease of the mass can take place when in expense of accumulated additional energy an ejection of some portions of the initial mass or its decay into several parts occurs. Taking into account the uniformity of dark energy distribution and the stochastic behavior of mass ejection, one can arrive at a conclusion, that mass ejection process should happen by chance and in an isotropic way.

An object can possess of excessive energy at any stage of its evolution. It can happen, for instance, owing to energy accumulation during long time interactions or because of change its physical conditions, when the object loses energetic equilibrium with its environments. General physical laws state that in such situation a physical object triggers the necessary mechanisms to throw away the excessive energy to establish an equilibrium and bring the object to the lowest energetic level depending on the environmental conditions.

Dark energy on large scale simplements the process of radius growth for any spherical volume, which we perceive as an expansion of the Universe. The same should happen on any scale since dark energy is uniform across the space. Although on smaller scales, the forces generated by dark energy are very tiny but they act protractedly charging the baryonic objects and their systems. When the energy, accumulated by these objects and systems of systems (though any object is also a system composed of baryonic objects belonging to the lower hierarchical levels of the baryonic universe), become unstable and should release the additional energy.

The atomic nuclei and elementary particles belong to the lowest hierarchical level of objects reachable for studies by modern toolkits of research. Although this level differs from the ordinary macroworld, the knowledge available on their structure and physical features allows one to make some conclusions concerning their interaction with the dark energy carrier, if such interaction occurs in reality. One arrives at several conclusions, which may have far-reaching consequences, if one will finally prove their validity. In any case, one may use the technics of thought experiment and compare the results of it with observable data.

First, dark energy injected into atomic nuclei, if any, undoubtedly decreases the nuclear binding energy. Accordingly, simultaneously should increase the mass of atomic nuclei and baryons, making them more vulnerable against decay. Second, it does mean that in the past the nuclear binding energy could be incomparably large and masses of baryons in nuclei – very tiny. Third, in the far past of our baryonic universe could exist atomic nuclei consisted of huge number of baryons. Forth, in the deep bowels of very massive objects, baryonic matter can be in a state of the distant past – consisting of a huge number of baryons with negligible masses. As an observable manifestation of possible interaction of atomic nuclei with dark energy could serve the percentage of light element, since in this scenario the longer the evolutionary path, the lesser the heavy elements. In other words, evolution according this scenario decreases the metallicity of matter.

3. Energy release and the process of morphology formation.

Energy release is a common mechanism for all the baryonic objects belonging to all hierarchical levels of the Universe. Nuclear physicists call this process radioactivity. Planetary scientists call it seismology and volcanism. All stars and galactic nuclei emit electromagnetic radiation and eject mass with different rates. According to Ambartsumian's concept, galactic nuclei eject also huge clumps of baryonic matter, which form younger (and less massive) new galaxies eventually. All these processes combine their essential role in the much more comprehensive development course of object formation and evolution.

Any baryonic object survives thanks to the various forces of attractive behavior. In the microcosm, those are strong forces for baryons, their residuals for atomic nuclei, then molecular (electric) forces, and gravitational forces. The source of any force is the corresponding energetic field. Dark energy creates a force that tends to remove two baryonic points from each other. In this sense, this force acts against other forces and their balance governs all the dynamical and kinematical kinematic processes

doi: https://doi.org/10.52526/25792776-2021.68.1-50

in the baryonic world. How it happens and develops depends on each particular case.

The quantity of dark energy participating in the process of interaction with a baryonic object, most probably, should be proportional to the volume occupied by the object. This statement follows from the space uniformity of dark energy. Within the sphere of radius the amount of dark energy should be proportional to its volume

$$E_{de} = \frac{4\pi}{3} R^3 \rho_{de}, \tag{3}$$

where ρ_{de} is the dark energy spatial density. Denoting the matter density by ρ and comparing 3 with the expression 2, one finds that the ratio of gravitational and dark energies has the following form

$$k_E = \frac{E_{gr}}{E_{de}} = \frac{5}{3} G \frac{M}{R} \frac{\rho}{\rho_{de}} \sim \frac{\rho^2 R^2}{\rho_{de}}, \tag{4}$$

which can serve as a "measure of flexibility" of the object. It is obvious, that the bigger the ratio, the lesser the flexibility. In other words, object is more easily amendable to changes forced from the dark energy when the ratio is smaller.

Thus, this ratio depends on and changes with the object radius and mean density. It is not difficult to check the dependence of this factor on the mentioned values within the same hierarchical class of objects, for example, stars and planets or galaxies. If the density is constant, the "inflexibility" of an object increases proportionally toits radius square. It means that at the same density, large objects are more difficult to change when interacting with dark energy. In other cases, one should take into account also the change of the mean density.

The continuous accumulation of energy in a given baryonic object will eventually lead to the need to get rid of excess energy by ejecting portions of the matter. If the object is not rotating or slow rotating the ejection process will be isotropic. Otherwise, an additional centrifugal acceleration occurs in the equatorial region of the object, which essentially facilitates the ejection of matter from this region of the object. Moreover, since the equator is the most vulnerable part of a rotating object, if a piece of matter ejects, the ejection process has all chance to continue if the excessive energy is still huge for the object and hence the tension is not discharged completely yet. On the other hand, ejection from one side generates favorable conditions for another ejection in the diametrically opposite point, provided, that internal tension is sufficient.

One can implement this picture when interprets the morphological variety of galaxies. Indeed, if the object is non-rotational, ejected clumps of matter will have more or less isotropic distribution around the maternal object. This is the case of elliptical galaxies, which do not possess of disk substructure. Process of their formation resembles the physical picture of evaporation, when the clumps of matter take away the excessive energy in a moderate rate. Rotating objects of the same mass, as mentioned above, possesses of more ejection energy depending on the spinning rate. The higher the rotation rate for the given mass, the shorter the tension discharging time.

Let us consider now the spiral galaxies morphological classification scheme suggested by Elmegreen & Elmegreen (1982, 1987), based on the orderliness of spiral arms. Although this classification includes 12 (10 after revision) arm classes, authors divide all spiral galaxies into two larger groups, called floculent and grand design spiral arms. The grand design galaxies possess a morphology of classical two-arm symmetry with longer and prominent arms. The floculent galaxies, on the contrary, composed only of small pieces. Intermediate arm classes show characteristics of both the floculent and grand design types.One of the most essential correlations that found the authors is one that grand design galaxies are physically larger than floculent galaxies by a factor of -1.5. It does mean that symmetrical morphology requires more matter in average.

If one adhere to this scenario of galaxy formation, one inevitably arrives at a conclusion that the closer the location within the spiral arm to the center of galaxy, the younger the matter at the location in the sense of time passed after ejection the matter. On the other hand, the clumps of baryonic matter ejected from a massive object very recently evidently did not have a sufficient time for evolutionary change under the influence of dark energy.

The self-consistent consideration of the interaction mechanism between atomic nuclei and the dark energy carrier leads to very important evolutionary paths (Harutyunian & Grigoryan, 2018). First,

doi: https://doi.org/10.52526/25792776-2021.68.1-50

one can conclude that the interchange of energy resulted due to the interaction decreases the nuclear binding energy and destabilize the atomic nuclei. In its turn, it leads to the formation of lighter chemical elements. Therefore, the more massive galaxies possess a higher metallicity.So one arrives at the conclusion that the closer the part of spiral arm is located to the galaxy nucleus, the higher its metallicity. This regularity is well established and studied in detail by many researchers (see, for example, Ho et al., 2015, and ref. therein). The same conclusion applies to the case of elliptical galaxies, for which is also correct the statement the farther a star is from the galactic nucleus, the longer, on average, has elapsed since its ejection as a pre-stellar object.

4. Disk/plane ratio depending on the redshift.

It is obvious that Ambartsumian's concept on the galaxy formation suggests that in the course of evolution the size of the plane disk should grow. It follows from the main hypothesis that spiral arms originate due to the mass ejection from the central nucleus of the galaxy. The longer the mass ejection time, the farther the first ejected stars in the equatorial plane. Since the linear size of radius depends on various parameters characterizing the given galaxy, the ratio of the bulge height and disk radius can serve as a measure of disk growing, if it grows really. That is easy to do using a sample of edge-on spiral galaxies possessing different redshifts.

In the recent paper by Reshetnikov & Usachev (2021) the authors considered this issue using edge-on galaxies for rather wide interval of redshifts (up to z$\sim$1.2). The authors compare the ratio h_r/h_z (where h_r and h_z are the radial and vertical sizes of a galaxy) for the closer and farther galaxies. It is interesting that for galaxies from deep fields they find $h_r/h_z \leq 10$. For the galaxies chosen from the survey SDSS, this ratio is much wider. It does mean that evolution of galaxies leads to the diminution of the mentioned ratio. Authors mention that the result was expectable according to the CDM models of galaxy formation. It is evident that the same result is predicted also using the Ambartsumian's cosmogonic concept on the galaxy formation. The physical interpretation of the observed correlation is clear and transparent in the second case, since spiral arms represent a kind of matter jet, according to Ambartsumian's concept, which constantly grow their radial size.

Thus, according the observational data used by authors in the past the ratio h_r/h_z was lesser comparing with nowadays value. Of course, the height of bulge h_z could also change in the course of the galaxies evolution, but in our view, there is little chance that the observed grow of the considered ratio is a result of the h_z decrease. The bulge should also increase in size owing to the interaction with the dark energy carrier and accumulation of excessive energy amounts. Therefore, one can conclude that the thickness of the bulge grows slower than the radius of the disk. It seems to be natural, since the growing of bulge is a process resembling the vaporation mechanism, while in the process of spiral arms ejection the centrifugal force holds the main role.

5. Conclusion.

The role of dark energy may be decisive in the process of formation and evolution of baryonic cosmic objects, if the baryonic matter physically interacts with the carrier of dark energy at all scales. This approach allows one to revive Ambartsumian's cosmogonic ideas for the objects formation through the decay of the denser matter. However, for avoiding the objections against the initial concept, there is one significant difference in this version of interpretation. The point is that in the Ambartsumian's scheme the ejected baryonic matter assumed to have the same mass as it has in the core of a galaxy before ejection. The large masses needed for generation of spiral arms or new galaxies could not exist in the core even in the superdense state. The physical laws do not allow stationary or quasi-stationary existence of such clumps. In our scenario, we propose conservation of only the quantity of baryons, but not mass. Mass grows in expense of dark matter, when the matter is already out of the galactic core, where the physical conditions differ drastically from ones in the core.

The mass change occurs because of secular decrease of nuclear binding energy in atomic nuclei, which can accelerate abruptly when the clump of core-born matter ejected into open space. The process of matter adaptation to new conditions can occur very violently with release of huge quantities

doi: https://doi.org/10.52526/25792776-2021.68.1-50

of energy. We observe these processes in spiral arms, but not in bulge or halo. The reason, we believe, is the calm development of mass ejection processes in bulge and halo, where the aging of evaporated matter takes place gradually. Most probably, the slow evaporation process makes favorable conditions for long-lasting gradual aging of matter and makes the population of the halo metal-poor.

We are going to continue our research on the consequences of the interaction between baryonic matter and dark energy carrier to reveal more observational data fitting the results of though experiments.

References

Ambartsumian V. A., 1947, The evolution of stars and astrophysics

Ambartsumian V. A., 1958, in La structure et l'évolution de l'universe. pp 241–249

Elmegreen D. M., Elmegreen B. G., 1982, Mon. Not. R. Astron. Soc. , 201, 1021

Elmegreen D. M., Elmegreen B. G., 1987, Astrophys. J. , 314, 3

Harutyunian H. A., 2017, Astrophysics, 60, 572

Harutyunian H. A., Grigoryan A. M., 2018, Communications of the Byurakan Astrophysical Observatory, 65, 268

Ho I. T., Kudritzki R.-P., Kewley L. J., Zahid H. J., Dopita M. A., Bresolin F., Rupke D. S. N., 2015, Mon. Not. R. Astron. Soc. , 448, 2030

Reshetnikov V. P., Usachev P. A., 2021, Astrophysics, 64, 1

doi: https://doi.org/10.52526/25792776-2021.68.1-50

Communications of BAO, Vol. 68, Issue 1, 2021, pp. 56-74

Growth and merging phenomena of black holes: observational, computational and theoretical efforts

G.Ter-Kazarian*

Byurakan Astrophysical Observatory, 378433, Aragatsotn District, Armenia

Abstract

We briefly review the observable signature and computational efforts of growth and merging phenomena of astrophysical black holes. We examine the meaning, and assess the validity of such properties within theoretical framework of the long-standing phenomenological model of black holes (PMBHs), being a peculiar repercussion of general relativity. We provide a discussion of some key objectives with the analysis aimed at clarifying the current situation of the subject. It is argued that such exotic hypothetical behaviors seem nowhere near true if one applies the PMBH. Refining our conviction that a complete, *self-consistent* gravitation theory will smear out singularities at huge energies, and give the solution known deep within the BH, we employ the *microscopic theory of black hole* (MTBH), which has explored the most important novel aspects expected from considerable change of properties of space-time continuum at spontaneous breaking of gravitation gauge symmetry far above nuclear density. It may shed further light upon the growth and merging phenomena of astrophysical BHs.

Keywords: *galaxies: nuclei—black hole physics—accretion*

1. Introduction

One of the achievements of contemporary observational astrophysics is the development of a quite detailed study of the physical properties of growth and merging phenomena of astrophysical black holes, even at its earliest stages. But even thanks to the fruitful interplay between the astronomical observations, the theoretical and computational analysis, the scientific situation is, in fact, more inconsistent to day. Wheeler in 1967 coined a spacetime region, where the gravitational field is so strong that no information carrying objects and signals can escape it, by the term 'a black hole' (BH), although the possibility of the existence of such objects was discussed a long time before this. At the end of the eighteenth century Michell and Laplace independently came to the conclusion that if the mass of a star were large enough its gravity would not allow light to escape. Though this conclusion was based on the Newtonian theory the obtained result for the size of such 'dark stars' (the gravitational radius) coincides with the later prediction of Einstein's theory of gravity (see e.g. Barrow & Barrow, 1983, Israel, 1987). A principle feature that makes general relativity (GR) distinctively different from other field theories is the occurrence of curvature singularities in spacetime. The singularities lead to regions of the universe that cannot be observed. This causes an observer's inability to access the degrees of freedom that are hidden beyond the horizon which, in turn, leads to thermodynamical behavior of BHs. Notwithstanding, much remarkably efforts have been made in understanding of BH physics, many important issues still remain unresolved and, thus, a situation is unclear, than described so far. The astrophysical significance of the issue, and the importance of considering the gravitational collapse of a matter cloud within the framework of the GR theory, with reasonable physical properties for the matter included, stems from the fact that GR predicts that a star more massive than about five to eight times the mass of the Sun, cannot stabilize to a neutron star final state at the end of its life cycle. It must collapse continually under the force of its own gravity on exhausting its

*gago_50@yahoo.com

doi: https://doi.org/10.52526/25792776-2021.68.1-56

internal nuclear fuel, and there are no known forces of nature that would halt such a collapse. General relativity predicts that such a star must then terminate into a spacetime singularity where densities and spacetime curvatures blow up and the physical conditions are extreme. The estimates on the mass limit for a star in order to collapse, of course, are indefinitely vary depending on different models for the star's interior and equation of state for matter at very high densities. One of the most important open issues in the theory and astrophysical applications of modern day BH and gravitation physics is that of the Roger Penrose's Cosmic Censorship Conjecture (CCC) (Penrose, 1969). The CCC assumption that any physically realistic gravitational processes must not lead to the formation of a singularity which is not covered by an horizon, thus hiding it from external observers in the universe. This of course includes the complete gravitational collapse of a massive star which, if the CCC is true, must terminate generically into a BH final state only. Such a singularity is then crucial and is at the basis of much of the modern theory and astrophysical applications of BHs today. Despite the past four decades of serious efforts, we do not have as yet available any proof or even any mathematically precise formulation of the cosmic censorship hypothesis. The consideration of dynamical evolution of collapse is a crucial element of the CCC. Many solutions of Einstein field equations are known which present naked singularities (such as, for example, the super-spinning Kerr solutions), nevertheless almost none of these solutions can be obtained as the dynamically evolved final state of some initially regular matter configuration. For this reason, over the last decades a great deal of work has been done to test the CCC in the few dynamically evolving spacetimes we know. These are typically the scenarios that describe gravitational collapse in spherical symmetry, and some non-spherical collapse models have also been considered, for examples of critical collapse with angular momentum. In recent years, a wide variety of gravitational collapse models have been discovered where exact analytical calculations (e.g Giambo, 2004, Goswami & Joshi, 2002, Joshi & Malafarina, 2011, 2013, Villas da Rocha & Wang, 2000, and ref. therein) have meanwhile shown that mass concentrations collapsing under their own weight will no longer form BHs as collapse endstate, rather naked singularities, except for configurations of highest symmetry which are, however, of measure zero among all initial data. By this, even the theoretical existence of BHs is no longer justified. The first examples were restricted to some classes of inhomogeneous dust collapse, and they were extended to the case of collapse in the presence of only tangential pressures, and perfect fluids. The existence of classes of pressure perturbations is shown explicitly, which has the property such that an injection of a small positive (or negative) pressure in the Oppenheimer, Snyder and Datt (OSD) model (Datt, 1938, Oppenheimer & Snyder, 1939), or in a Tolman-Bondi-Lemaitre (TBL) (Bondi, 1947, Lemaìtre, 1933, Tolman, 1934) inhomogeneous dust collapse to a BH (simplest generalization of the OS model), leads the collapse to form a naked singularity, rather than a BH (Joshi & Malafarina, 2013). The classic OSD scenario is the basic paradigm for BH physics today, and the TBL models describe the most general family of dust, i.e. pressureless, collapse solutions. This result is therefore intriguing, because it shows that arbitrarily close to the dust BH model, we have collapse evolution with non-zero pressures that go to a naked singularity final state, thus proving a certain "instability" of the OSD BH formation picture against the introduction of small pressure perturbations. In such a case, the super-ultra-dense regions, or the spacetime singularity, that forms at the end of collapse would be visible to faraway observers in the universe, rather than being hidden in a BH. Thus, rigorous calculations have shown that the expectations of the 1970s have been hasty, that CCC assumption has been premature, because while the CCC states that the OSD collapse final fate is necessarily replicated for any realistic stellar collapse in nature, the result here shows that an arbitrarily small pressure perturbation of the OSD model can change the final outcome of collapse to a naked singularity and therefore the OSD BH may be considered 'unstable' in this sense.

In this respect, the first goal of this communication is to review briefly the necessary ideas behind the various specific constructions and suggestions on the conceptual problems of GR, the singularities and the thermodynamics of BHs in semiclassical and quantum physics. The second goal is to concentrate on the critical discussion of the past and present states, evaluating those strategies, approaches etc., that are explicitly and unambiguously given and applicable in any generic spacetime. This short review encompasses the many discoveries which unlocked the mysteries or exposed some of the illusions of the considered field. Without it we cannot show how the matters stand, we almost bound of

doi: https://doi.org/10.52526/25792776-2021.68.1-56

necessity to enter upon it, if we would write of them at all.

To innovate the solution to aforementioned problems, the third goal is to advocate with alternative proposal by utilizing the MTBH, which has explored a novel aspects expected from considerable change of properties of space-time continuum at spontaneous breaking of gravitation gauge symmetry far above nuclear density. It may shed further light upon the growth and merging phenomena of astrophysical BHs.

Although some key theoretical ideas were introduced with a satisfactory substantiation, we have also attempted to maintain a balance between being overly detailed and overly schematic. With this perspective in sight, we will proceed according to the following structure. To start with, in Section 2, we provide a brief discussion of the observable signature and computational efforts on understanding of growth and merging properties of BHs. Section 3 deals with the analysis aimed at clarifying the current situation of such properties within theoretical framework of PMBH. To fill the void which the standard PMBH presents and to innovate the solution to alluded problems, in Section 4 we recount some of the highlights behind of the MTBH, whereas the infra-structures will inevitably be accommodated inside the EH. The concluding remarks are given in Section 5.

2. The observable signature and computational efforts on understanding of growth and merging properties of BHs

With typical bolometric luminosity $\sim 10^{45-48}\mathrm{erg\,s^{-1}}$, the active galactic nuclei (AGNs) are amongst the most luminous emitters in the universe, particularly at high energies (gamma-rays) and radio wavelengths. From its historical development, up to current interests, the efforts in the AGN physics have evoked the study of a major unsolved problem of how efficiently such huge energies observed can be generated. This energy scale severely challenges conventional source models. The fact that accretion processes really take place in AGNs is already established and proven by many observations. The huge energy release from compact regions of AGN requires extremely high efficiency (typically ≥ 10 percent) of conversion of rest mass to other forms of energy. This serves for the majority of theoreticians as the main argument, without any physical justification, in favour of supermassive BHs (SMBHs), in the centers of, almost all, galaxies as central engines of massive AGNs. Within this scenario, a BH has been formed as an almost inevitable endpoint of the gravitational collapse of a large fraction of total mass of supermassive configuration occurring after entire burning of the whole amount of spared intrinsic energy. The BHs are fueled steadily from the thick accretion disks. Such evolutionary processes of accretion onto massive BHs as the prime energy sources have immense emissive power. The astrophysical BHs come in a wide range of masses, from $\geq 3\,M_\odot$ for stellar mass BHs (Orosz, 2003) to $\sim 10^{10}\,M_\odot$ for SMBHs (Lauer, 2007, Lynden-Bell, 2013). Demography of local galaxies suggests that most galaxies harbour quiescent SMBHs in their nuclei at the present time and that the mass of the hosted BH is correlated with properties of the host bulge. The visible universe should therefore be contained at least 100 billion supermassive BHs. A complex study of evolution of AGNs requires an answer to the key questions how the first black holes formed, how did massive BHs get to the galaxy centers, and how did they grow in accreting mass, namely an understanding of the important phenomenon of mass assembly history of accreting seeds of SMBHs. Given the current masses, most BH growth happens in the AGN phase. A significant fraction of the total BH growth, 60% (Treister, 2010), happens in the most luminous AGN, quasars. In an AGN phase, which lasts $\sim 10^8$ years, the central SMBH can gain up to $\sim 10^{7-8}M_\odot$, so even the most massive galaxies will have only a few of these events over their lifetime. The observations support the idea that BHs grow in tandem with their hosts throughout cosmic history, starting from the earliest times. These ideas gather support especially from a breakthrough made in recent observational, theoretical, and computational efforts on understanding of coevolution of BHs and their host galaxies, particularly through self-regulated growth and feedback from accretion-powered outflows (see e.g. Kelly (2010), Natarajan (2011), Shankar et al. (2009), Treister & Urry (2012), Volonteri & Natarajan (2009), Volonteri et al. (2010)). Whereas the multiwavelength methods are used to trace the growth of seed BHs, and the prospects for future observations are reviewed. The observations provide strong support for the existence of a correlation between SMBHs and their hosts out to the highest redshifts. Particularly, the observations of the

doi: https://doi.org/10.52526/25792776-2021.68.1-56

quasar luminosity function show that the most supermassive BHs get most of their mass at high redshift, while at low redshift only low mass BHs are still growing (Barger, 2005). This is observed both in optical (Croom, 2009) and hard X-ray luminosity functions (Barger, 2005), which indicates that this result is independent of obscuration. Natarajan (2011) has reported that the initial BH seeds form at extremely high redshifts from the direct collapse of pre-galactic gas discs. Populating dark matter halos with seeds formed in this fashion and using a Monte-Carlo merger tree approach, he has predicted the BH mass function at high redshifts and at the present time. The most aspects of the models that describe the growth and accretion history of supermassive BHs, and evolution of this scenario have been presented in detail by Volonteri & Natarajan (2009), Volonteri et al. (2010). In these models, at early times the properties of the assembling BH seeds are more tightly coupled to properties of the dark matter halo as their growth is driven by the merger history of halos. While a clear picture of the history of BH growth is emerging, significant uncertainties still remain (Treister & Urry, 2012), and in spite of recent advances (Natarajan, 2011, Treister, 2010), the origin of the seed BHs remains an unsolved problem at present.

While the exact mechanism for the formation of the first BHs is not currently known, there are several prevailing theories (Volonteri, 2010). A large number of representative models towards this are available in literature, (see e.g. Bromm & Loeb, 2003, Devecchi & Volonteri, 2009, Kelly, 2010, Natarajan, 2011, Natarajan & Treister, 2009, Shankar et al., 2009, Vestergaard, 2004, Volonteri, 2010, Volonteri & Natarajan, 2009, Volonteri et al., 2010, Willott, 2010), but all they are subject to many uncertainties. Each proposal towards formation and growth of initial seed BHs has its own advantage and limitations in proving the whole view of the issue. For example, most aspects of the models that describe the growth and accretion history of SMBHs, the evolution and assembly history of this scenario have been explored in detail in (Volonteri & Natarajan, 2009, Volonteri et al., 2010). In these models, at early times the properties of the assembling SMBH seeds are more tightly coupled to properties of the dark matter halo as their growth is driven by the merger history of halos. Specifically, the Hubble Space Telescope measurements of stellar kinematics highlight an evidence for the ubiquity of SMBHs.

However, the most important characteristics of the AGN powerhouse, the central masses and structures, and the BH formation and growth processes are not understood well. This issue is many-sided and fundamental, and can be settled fairly only by more investigations to be done for its better understanding. The scientific situation is, in fact, more inconsistent than described so far. Within respect to standard models, a hard look at the BH physics reveals following severe problems.

The observed time-scales for flux variations of some objects are inconsistent with contemporary BH accretion models. That is, on the basis of the diagram of the minimum variability time-scale versus the bolometric luminosity for 60 sources it has been shown that, in spite of auxiliary assumption of asymmetric emission geometry, a few BL Lac objects - B2 1308 + 72, 3C 66A, OJ 287, AO 0235 + 16 and Quasars - 3C 345, 3C 446, 3C 454.3, LB 9743 remained in forbidden zone (particularly the three of them) (Bassani et al., 2010), namely their observed sizes appeared to be less than the sizes of corresponding spheres of the event horizon.

The growth behavior of BHs widely based on the premises of runaway core collapse scenario. The latter has always been a matter of uncertainties because we do not have a thorough understanding of details of accretion physics, say, of the physical properties of invoked relativistic plasma flows outside a horizon, with compact coruscating bright spots due to beaming, or magnetohydrodynamic shocks and reconnection in the inner jet. Distinguishing these possibilities requires spatially resolved images much finer than the horizon size, which could be feasible in the near future. Then it is interesting to compare the accretion method with other methods such as radio timing or even the current research of BH imaging using Event Horizon Telescope. Although a thorough comparison is beyond the scope of the present communication, it will be an interesting topic for discussion elsewhere. Timing observations provide a useful means to study the properties of space–time around extreme gravity systems, such as BHs. That is, if external tracers lead to an estimated horizon radius, R_g, under a very generic assumption that the object is a BH, then it is possible that finer observations will reveal internal substructures smaller than R_g or flaring events quicker than the time-scale R_g/c. Pulsar timing, therefore, has been identified as a space–time probe because of the high precision achievable in the

doi: https://doi.org/10.52526/25792776-2021.68.1-56

timing measurements. It is also because of the unique nature of pulsars – highly compact and thus uneasily disrupted, narrow mass range, and for millisecond pulsars, high stability in the rotation rate (a stable, reliable clock). Saxton (2016) proposed that pulsar timing observations will be able to distinguish between systems with a centrally dense dark matter sphere and conventional galactic nuclei that harbour a SMBH. The lack of a perfect horizon means that the effective strong-lensing silhouette of the central structure may differ significantly from SMBH predictions. Besides, there are some theoretical expectations for swarming of pulsars (and other compact stars) to concentrate in galaxy nuclei (Freitag et al., 2006, Miralda-Escudé & Gould, 2000, Pfahl & Loeb, 2005). So far, one magnetar is known near Sgr A*, and there is debate about how many pulsars might also be discoverable (e.g. Macquart & Kanekar (2015)). In particular, our Galactic Center (Sgr A*) deviates from containing a SMBH for at least 15 reasons (Kundt, 2012), the 15th being the happy survival, so far, of cloudlet G2 during its ongoing approach of Sgr A*.

What kind of observational signature the BHs bear, if any, and whether such phenomena can possibly be observed? Wouldn't they hide forever, on grounds of their expected dimness, their not being able to radiate? Such questions were first asked seriously between theorists and observers, with a distinct emphasis on candidates of stellar mass. A first, promising suggestion was the X-ray emitting stellar binary system Cyg X-1, the brightest stellar X-ray source in the Cygnus region, whose optically invisible component had to be more massive than a neutron star. And how to blow the jets seen to spring forth from the dark component of the Cyg X-1-system? Binary neutron stars are observed to blow jets, whereas BHs cannot do that because they lack an inclined, co-rotating magnetosphere, for generating the jets' pair plasma (Kundt, 2011). In Fischer and Kundt could not find a single BH in the whole class of (stellar-mass) BH-candidates (Kundt & Fischer, 1989).

Most impressive evidence against a BH at our Galactic center presented by Su et al. (2010, 2011). The FERMI Bubbles (or plumes), at photon energies $\lesssim 10^2$GeV, probably emitted by buoyantly rising relativistic pair plasma from the near vicinity of Sgr A*, throughout the Milky-Way halo, to heights well above 20 kpc. These same halo structures had already been detected and mapped decades earlier by Sofue (2000), from radio and X-ray data.

Galactic centers are often observed to be quite luminous, stormy, jet-blowing, and pluming (at $\lesssim 10^2$ GeV), from their center all the way out into their halo. How is this central activity powered? Kundt (1996) assumed that it caused by nuclear burning of the central disk, combined with magnetic reconnections in its (very) fast and deferentially rotating corona. A burning disk avails of abundant rotational, infall, and nuclear energy, for both non-thermal and thermal ejections: of radiation, jets, winds, and plumes. A SMBH would suppress all this.

3. Assessment of Growth and Merging Properties of Black Holes With in Phenomenological Models

With aforementioned observational advances, a tacit assumption of theoretical interpretation of astrophysical scenarios is a general belief reinforced by statements in textbooks, that the PBHM is capable to describe the growth and merging behavior of accreting BHs. Altogether, the question then arises: What procedure is in fact employed by the astronomers in the course of reaching the conclusion while estimating a growth of energy-mass of astrophysical BH? The following stepwise properties are commonly attributed to above procedure:

- From observations of surroundings of the BH, at first, the astronomers by simulation estimated a total amount of the outside mass that potentially can be swallowed driven by an accretion onto BH.
- Secondly, this quantity of mass, without any substantiation, is simply accepted as a real *physical* measure of growth of energy-mass of the astrophysical BH.

Although arguably all these reasoning seemed appealing and attractive, nevertheless there is no convincing reason to rely on a validity of such procedure and, therefore, we do not share this view. It is rather surprising that the PBHM is routinely used to explore the growth and merging phenomena of

doi: https://doi.org/10.52526/25792776-2021.68.1-56

astrophysical BHs. Such beliefs are suspect and should be critically re-examined. In the framework of PMBHs there is no provision for growth and merging behavior of BHs because of the nasty inherent appearance of BH *singularities*, and that if the *infinite collapse to the singularity* inside the BH is accepted as a legitimate feature of Nature. Certainly, during a super-increasing of total mass of configuration one undoubtedly will arrive (irrelevant to gravitational theory in use) to a critical turning point of relativistic collapse, beyond which the gravitational forces of compression prevail over all the other forces. Than it is enough to add from the outside a small amount of energy near-by the critical point in order to begin a process of irresistible infinite catastrophic compression of configuration under the pressure of grand forces. The improbability of such an inference has been greatly enhanced by the breaking down of the theory inside the event horizon which is causally disconnected from the exterior world. Either the Kruskal continuation of the Schwarzschild metric, or the Kerr metric, shows that the static observers fail to exist inside the horizon. The PMBH then presents a major challenge that renders time reversibility impossible. Objects thrown into the BH can never be retrieved, because it will get into infinite collapse to the central singularity inside the BH. Any timelike worldline must strike the central singularity which wholly absorbs the infalling matter. Therefore, the ultimate fate of collapsing matter once it has crossed the BH surface is unknown. This certainly inhibits one to answer quantitatively such purely academic question, say, what is a further evolution of the decrease of the energy and entropy carried by the accreting mass that was swallowed by the BH; or what is further evolution of the coalescence and merger of binary BHs at grazing collision of members, when triggered by the emission of gravitational waves their orbits will tighten by spiraling inwards. At this, immediately the question arises whether or not yet observable four laws of the mechanics for a stationary, asymptotically flat, black BH in four will be valid as well for not stationary processes of BH formation and growth.

3.1. Some Conceptual Problems Plagued GR

A general relativity has stood the test of time and can claim remarkable success, although there are serious problems of the energy-momentum conservation laws of gravitational interacting fields, the localization of energy of gravitation waves, the role of singularities of BHs, and also severe problems involved in quantum gravity. This state of affairs has not much changed up to present and proposed abundant models are not conductive to provide non-artificial and unique recipe for resolving these controversial problems. Eventually, experimental gravitation is a major component of the field, characterized by continuing efforts to test the GR's predictions. GR certainly can claim remarkable success at the post-Newtonian level where the experiments have reached high precision, including the light deflection, the Shapiro time delay, the perihelion advance of Mercury, the Nordtvedt effect in lunar motion, and frame-dragging (Will, 2014). Thereby gravitational wave damping has been detected in an amount that agrees with general relativity to better than half a percent using the Hulse-Taylor binary pulsar system (Hulse & Taylor, 1975), also see subsequent observations of its energy loss (Taylor & Weisberg, 1982). A growing family of binary pulsar systems is currently yielding new tests focusing on strong gravity and gravitational waves. These experiments will search for new physics beyond GR at many different scales: the large distance scales of the astrophysical, galactic, and cosmological realms; scales of very short distances or high energy; and scales related to strong or dynamical gravity.

The geometrical interpretation of gravitation, having arisen from the dual character of the metrical tensor in its metrical and gravitational aspects, is a noteworthy result of GR. Although this has the advantage in solving the problems of cosmology, nevertheless such a distinction of the gravitational field among the fields yields the difficulties in the unified theories of all interactions of elementary particles, and in quantization of gravitation. Moreover, there are problems of energy-momentum conservation laws of gravitational interacting fields, the localization of energy of gravitation waves, the singularities or BHs, and also severe problems involved in quantum gravity. The well defined local energy-momentum density for the gravitational field may set the conceptual basis for the understanding of energy loss by gravitational radiation.

The difficulty for this is rooted in the weak principle of equivalence (WPE), i.e. the *universality of free fall*. The gravitational action only depends on the gravitational field, since any further background structure would be precluded by diffeomorphism invariance. Since the WPE can be used to get rid

doi: https://doi.org/10.52526/25792776-2021.68.1-56

of the gravitational field on a given point of spacetime, a crucial conceptual and practical caveats are involved in the association of energy and angular momentum with the gravitational field. That is, Riemannian geometry in general does not admit a group of isometries, therefore, it is impossible to define energy-momentum as Noether local currents related to exact symmetries. This has challenged validity of the concepts of energy and angular momentum, when one attempts to perform their straightforward extension to the gravitational field.

Such an approach rapidly meets important conceptual difficulties. Namely, the formulation of meaningful global or quasi-local mass and angular momentum notions in GR and in the particular context of BH spacetimes always needs the introduction of some additional structure in the form of quasi-local quantities and quasi-symmetries that restricts the study to an appropriate subset of the solution space of GR. Although a remarkable surge of activity of investigations in this field has arisen recently, but the theory of quasi-local observables in general relativity is far from being complete. It is surprising that one has not only no ultimate, generally accepted expression for the energy-momentum and especially for the angular momentum, but there is no consensus in the relativity community even on general questions, for example, *what should one mean by energy-momentum?*

In the literature there are various, more or less *ad hoc*, lists of criteria of reasonableness of the quasi-local quantities (e.g. Christodoulou & Yau (Christodoulou & Yau)). However, finding an appropriate quasi-local notion of energy-momentum has proven to be surprisingly difficult (for the comprehensive review see Szabados (2004)). The situation is much less clear in the case of extended but finite spacetime domains, otherwise there are still controversies and open issues. For example, the Bartnik mass (Bartnik, Bartnik, 1989), which is a natural quasi-localization of the ADM mass, overestimates the physical quasi-local mass; or, the Hawking energy (Hawking, 1968) and its slightly modified version, the Geroch energy (Geroch, 1973), which are a well defined 2-surface observable, have not been linked to any systematic (Lagrangian or Hamiltonian) scenario. Similar situation holds for, e.g., the Penrose mass (Penrose, 1982, Penrose & Rindler, 1986), Dougan-Mason energy-momenta (Dougan & Mason, 1991), Brown-York-type expressions (Brown & York, 1993), etc, (for details see (Szabados, 2005)).

The emphasis in modern gravitational research is on the fundamental questions at the intersection between particle physics and cosmology, including quantum gravity and the very early universe. The GR as a geometrized theory of gravitation clashes from the very outset with basic principles of field theory. In accord to above said, this rather stems from the fact that Poincaré transformations no longer act as isometries, which posed severe problems in a Riemannian space interacting quantum field theory. The major unsolved problem is the non-uniqueness of the physical vacuum and the associated Fock space. A peculiar shortcoming is in the following two key questions to be addressed yet: (i) the absence of the definitive concept of space-like separated points, particularly, in the canonical approach, and the *light-cone* structure at each spacetime point; (ii) the separation of positive- and negative-frequencies for completeness of the Hilbert-space description. Due to it, a definition of positive frequency modes cannot, in general, be unambiguously fixed in the past and future, which leads to $|in> \neq |out>$, because the state $|in>$ is unstable against decay into many particle $|out>$ states due to interaction processes allowed by lack of Poincaré invariance. A non-trivial Bogolubov transformation between past and future positive frequency modes implies that particles are created from the vacuum and this is one of the reasons for $|in> \neq |out>$. This state of affairs has not much changed up to present and proposed abundant models are not conductive to provide non-artificial and unique recipe for resolving such controversies.

3.2. Curvature Singularities

In the framework of GR, the PBHM implies the most general Kerr-Newman BH model, with the only independent observable integral parameters of total mass (M), angular momentum (J) and charge (Q). Note that, even in the vacuum, asymptotically flat, four dimensional case relatively little is known about stability of the solutions to Einstein's equations beyond the linear level. In particular, the Kerr solution has not been proved to be stable, although both linearized analytic calculations and numerical calculations indicate that it is (e.g. Krivan et al. (1997)). Even though being among the most significant advances in astrophysics, it is rather surprising that PBHM is routinely used to explore the BH growth and merging phenomena as though it cannot be accepted as convincing model

doi: https://doi.org/10.52526/25792776-2021.68.1-56

for addressing this problem. Certainly, in this framework the very source of gravitational field of the BH is a kind of meaningless curvature singularity at the central point of the stationary nonrotating ($J = 0$, $Q = 0$) Schwarzschild BH, or a ring singularity at the center of the rotating axisymmetric Kerr BH, which are hidden behind the event horizon. The theory breaks down inside the event horizon which is causally disconnected from the exterior world. The Kruskal manifold is the maximal analytic extension of the Schwarzschild and Kerr solutions inside event horizon, so no more regions can be found by analytic continuation. But, the Kruskal continuation shows that the static observers fail to exist inside the horizon. This interior solution is not physically meaningful and essentially irrelevant.

Black holes then present a major challenge that they render time reversibility impossible. Objects thrown into a BH can never be retrieved, because any timelike worldline must strike the central singularity which wholly absorbs the infalling matter. Any object that collapses to form a BH will go on to infinite collapse to a singularity inside the BH. This feature is interpreted either as BHs connect our world to other universe via wormholes (Coleman, 1988, Hawking, 1988), or as an information thrown into a BH can not be retrieved anymore. There is also an opposite view point that any object thrown into a BH actually does leave some signals behind in own world (Dray & 't Hooft, 1985a,b). Whatever it will be, in both cases the PBHM ultimately precludes any accumulation of matter inside event horizon and, thus, neither the growth of BHs nor the increase of their mass-energy density could occur at accretion of outside matter, or by means of merger processes.

Admitting an *infinite collapse to the singularity* inside the BH as a physical law of Nature, it is impossible to answer, for example, what is further evolution of the coalescence and merger of binary BHs at grazing collision of members when, triggered by the emission of gravitational waves, their orbits will tighten by spiraling inwards? The nasty inherent appearance of BH singularities, in fact, inhibit one to answer such purely academic questions. It is why an excising the BH interior, for example, is currently considered as an approximate solution to avoid singularities in dynamical simulations (e.g. Baumgarte & Shapiro (2003)).

3.3. Black Hole Thermodynamics in Semiclassical Physics

A current theoretical understanding of growth and merging behavior of BHs is based on the Hawking's theorem of surface area of a BH (Carter, 1979, Hawking, 1968). Namely, in any interaction between matter or radiation with the BH, the time dependent horizon area is never allowed to decrease with time. This is the meaning of the irreducible mass of the horizon, i.e. in a possible collision of several BHs, the surface area of the resulting merged black hole always exceeds the sum of the separate progenitor BHs. Say, if a BH was being off the ordinary mass shell and carried no entropy, it would be possible to violate the law of energy conservation and 2^{nd} law of thermodynamics, because the energy and entropy in the exterior spacetime could be decreased by throwing matter into a BH. In the framework of incomplete theory, therefore, the only way to maintain these laws there is nothing left but to admit stepwise, without any substantiation, that (i) the BH resides on the *ordinary mass shell* ($E_{BH} = M_{BH}\, c^2$) and (ii) it has entropy (S_{BH}). Then the increase of these quantities may compensate the decrease of the energy and entropy carried by the mass that was swallowed. This is the meaning of the first and 2^{nd} laws of BH dynamics (Bardeen et al., 1973). The law of increase of area looks like the 2^{nd} law of thermodynamics for the increase of entropy, if one assigns an entropy to BH that is proportional to its surface, and that the surface gravity stands for a temperature (Bekenstein, 1973). At first sight, this choice seems quite natural, but at closer inspection one finds that these intriguing ideas have encountered to severe objection: *the entropy of a thermodynamic system is a measure of the large number of the real physical microstates* that an observer would not be aware of when measuring macroscopic parameters, and so-called *no hair* theorems allow BH, in best case, to have only a single microstate.

Classically, BHs are perfect absorbers but do not emit anything; their physical temperature is absolute zero. However, the spacetime associated to gravitational collapse to a BH cannot be everywhere stationary. Therefore, in semiclassical geometric optics approximation, a particle creation determined by details of the collapse is allowed in non-stationary curved spacetime. This is a transient phenomenon because exterior spacetime is stationary at late times of existence of horizon independent of the details of the collapse. The infinite time dilation at the horizon of Schwarzschild BH suggests

doi: https://doi.org/10.52526/25792776-2021.68.1-56

a possible flux of such particles, which is the meaning of the Hawking radiation - the radiation seen by an observer in the space-time background of a Schwarzschild BH when gravity will pull one of the members of pair into the BH permanently, while the other assumed to be escaped from the BH. Due to this radiation, a BH that forms from gravitational collapse will eventually evaporate, after which the spacetime has no event horizon. The equation for Hawking's black body radiation temperature, $T_H = c^3\hbar(8k_B G_N M)^{-1}$, clearly shows that the more mass is radiated away from the BH, the hotter this becomes. What then is the endpoint of BH evaporation? Moreover, the thermal properties of thermodynamic systems reflect the statistical mechanics of underlying microstates. Entropy is normally a measure of the degeneracy of microstates, Σ, in some underlying microscopic description of a physical system, determined by Boltzmann's formula $S = k_B log\Sigma$. Since the Bekenstein-Hawking entropy of generalized second law (GSL) of BH thermodynamics, $S_H k_B^{-1} = 4G_N M^2(c\hbar)^{-1} = A_H(2l_{Pl})^{-2}$ of a BH, where A_H is the area of the horizon and l_{Pl} is the Planck length $l_{Pl} = \sqrt{G_N\hbar/c^3} \approx 10^{33}$ cm, is naturally a huge number, how can one exhibit such a wealth of microstates? Within string theory, there is a class of BHs where these problems can be conveniently addressed, the so-called extremal BHs, for which the mass is tuned, so that the tendency to gravitational collapse is precisely balanced by the electrostatic repulsion. Consequently, the temperature vanishes and the BH behaves somehow in this limiting case as if it were an elementary particle. These results, however, rely heavily on supersymmetry and serious difficulties are met in attempts to extend them to non-supersymmetric BHs (see below).

Continuation of the Schwarzschild metric to the *Euclidean Schwarzschild metric* implies that the non-singularity of the Euclidean metric is required for equilibrium. The quantum field theory (QFT) can be in equilibrium with a BH only at the Hawking temperature, which is inversely proportional to the mass of BH. Thereby the thermal equilibrium of a BH with an infinite reservoir of radiation at Hawking temperature is unstable since if the BH absorbs radiation its mass increases and its temperature decreases.

Similarly, the two features violet Hawking's area theorem: (i) in pair creation effectively a spacelike energy flux is involved - in contrast to the one of the essential postulates of the area theorem which requires that the energy-momentum tensor $T_{\mu\nu}$ should satisfy the dominant energy condition. This held if for all future-directed timelike vector fields v, the vector field $j(v) \equiv -v^\mu T_\mu{}^\nu \partial_\nu$ is future-directed non-spacelike, or zero, i.e. no spacelike energy fluxes are allowed; (ii) the mass of BH decreases during evaporation by energy conservation, as well as inevitably do the surface area and entropy.

Hawking radiation allows an interpretation of the laws of BH mechanics as physically corresponding to the ordinary laws of thermodynamics. Having associated the entropy $S_{BH} := [kc^3/(4G\hbar)] \times Area(S)$ to the (spacelike cross Section 5 of the) event horizon, the area theorem was replaced by a generalized 2^{nd} law (GSL) of thermodynamics, which includes the sum of the entropies of all BHs plus the entropy of matter in exterior spacetime (Bekenstein, 1974). The GSL provides means for the quantity S_{BH} to be the physical entropy of a BH. Notwithstanding it is possible to construct thought experiments (e.g. the so-called Geroch process) in which the GSL is violated, unless a universal upper bound $S_m/E \leq (2\pi k/\hbar c)R$ for the entropy-to-energy ratio for bounded systems exists, where E and S_m are, respectively, the total energy and entropy of the system, and R is the radius of the sphere that encloses the system (Bekenstein, 1981, 1982).

A semi-classical method of modeling Hawking radiation as a tunneling of particles through a gravitational barrier has been developed in the framework of QFT on a curved gravitational background (e.g. Birrell & Davies (1982), Kerner & Mann (2008) and references therein). Certain gravitational backgrounds gave rise to thermal radiation from the vacuum. This provides an alternate conceptual means for understanding the physics of cosmological pair production at a wide variety of cosmological event horizons in exotic spacetimes. However, all these processes for certain do not give physical insight regarding the nature of the *microstates of a BH* and nor does it offer a substantiated reason for the *BH entropy* S_{BH}. Moreover, in semi-classical analysis of the Hawking evaporation process, if the correlations between the inside and outside of the BH are not restored during the evaporation process, then by the time that the BH has evaporated completely, an initial pure state will have evolved to a mixed state, i.e., *information* will have been lost in the process of BH formation and evaporation - the *black hole information paradox* (e.g. Will (2014)). If information is lost into the BH, which is

doi: https://doi.org/10.52526/25792776-2021.68.1-56

ascribable to the propagation of the quantum correlations into the singularity within the BH, this put QFT in curved spacetime in conflict with a basic principle of quantum mechanics (Townsend, 1997), because of incompatibility with the unitary time evolution of a state vector in a Hilbert space. This violates the causality and energy-momentum conservation laws.

Some authors claim that the resolution requires an understanding of the Planck scale physics. Putting together the basic laws of physics, i.e. Heisenberg's uncertainty principle $\triangle p \triangle x \sim \hbar$, the existence of gravitating mass $E = mc^2$ and Schwarzschild radius $R_g = 2Gm/c^2$ in Einstein's theory of gravity, these unambiguously assert the Planck's length $L_P := \sqrt{\hbar G/c^3} = 1.6 \cdot 10^{-33}$ cm to be a lower limit on the possible accuracy of position measurements (e.g. Fredenhagen (1995)). The universe at the Planck scale is strong gravity where the Riemannian curvature of spacetime is comparable to the inverse square of a favorite Planck length scale. Another possible scale for strong gravity is the TeV scale associated with many models for unification of the forces, or models with extra spacetime dimensions.

3.4. Black Hole Thermodynamics in Quantum Physics

Stemming primarily from classical and semiclassical analyses, the discovery of the thermodynamic behavior of BHs has given rise to quantum physics occurring in strong gravitational fields. At the purely classical level, BHs with in GR, of course, has nothing to do with the Planck scale quantum physics, because just outside the event horizon of an astrophysical black hole is weak gravity. Moreover, if pure states evolve to mixed states in a fully quantum treatment of the gravitational field, then at least the aspect of the classical singularity as a place where *information can get lost* must continue to remain present in quantum gravity. Nevertheless, the efforts to understand the mysterious statistical mechanical properties of BHs has led to many speculations about their quantum gravity origin. This in part is also due to the fact that the QFT in curved spacetime predicts an infinitely increase of a local temperature on the horizon of a BH. This should not be believed when kT reaches the Planck energy $(\sim \hbar c/G)^{1/2}c^2$ because quantum gravity effects cannot then be ignored and this temperature is then of the order maximum temperature in string theory. The latter appeals to GR as the low energy effective theory. Certainly, the quantum gravity is not needed to derive the BH entropy, since it can be derived even from the general principles of a conformal field theory (CFT) on the horizon of the BHs Carlip (e.g. 2002), Park (e.g. 2002).

However, BHs are localized objects, thus one must be able to describe their properties and dynamics even at the quasi-local level. The Schwarzschild BH, fixing its temperature at infinity, has negative heat capacity. Similarly, in an asymptotically anti-de-Sitter spacetime fixing the BH temperature via the normalization of the timelike Killing vector at infinity is not justified because there is no such physically distinguished Killing field (Brown et al., 1994). These difficulties lead to the need of a quasi-local formulation of BH thermodynamics. While the laws of BH thermodynamics refer to the event horizon, which is a global concept in the spacetime, the subject of the recent quasi-local formulations is to describe the properties and the evolution of the so-called *trapping horizon*, which is a quasi-locally defined notion (e.g. Hayward (1998)).

The area scaling character of the entropy perhaps implies a *holographic principle* (Susskind, 1995, 't Hooft, 1993), formulated in the (spacelike) holographic entropy bound. This suggests that, at the fundamental (quantum) level, one should be able to characterize the state of any physical system located in a compact spatial domain by degrees of freedom on the surface of the domain too. This relation holds whenever holography dual of the QFT exists. In accord, the number of physical degrees of freedom in the domain is bounded from above by the area of the boundary of the domain instead of its volume, and the number of physical degrees of freedom on the 2D surface is not greater one-fourth of the area of the surface measured in Planck area units L_P^2. If Σ be a compact spacelike hypersurface with boundary S, then the entropy $S(\Sigma)$ of the system in Σ should satisfy $S(\Sigma) \leq kArea(S)/(4L_P^2)$. Formally, this bound can be obtained from the Bekenstein bound with the assumption that $2E \leq Rc^4/G$, i.e. that R is not less than the Schwarzschild radius of E. Also, as with the Bekenstein bounds, this inequality can be violated in specific situations (Bousso, 2002, Wald, 2004). The origin of the holographic principle must lie in the number of fundamental degrees of freedom involved in a unified description of spacetime and matter (Bousso, 1999, 2002). This covariant entropy bound

doi: https://doi.org/10.52526/25792776-2021.68.1-56

is much more quasi-local than the previous formulations, and is based on spacelike 2D surfaces and the null hypersurfaces determined by the 2D surfaces in the spacetime. Its classical version has been proved by Flanagan et al. (2000).

Another quasi-local formulation of the holographic principle is suggested by Szabados (2005). Though not yet fully understood in general, the holographic principle is the key issue to the correspondence of anti-de Sitter spaces/conformal field theories (AdS/CFT) (Aharony, 2000, Maldacena, 1998). The AdS/CFT argues that the quantum gravity on (d + 2)-dimensional anti-de Sitter spacetime (AdS_{d+2}) is equivalent to a certain conformal field theory in d + 1 dimensions (CFT_{d+1}). By appealing to a duality between gravitational systems and conformal field theories, consequently the string theory seems to be able to count the described above microstates explicitly (e.g. Gubser et al. (1996)). In fact, the microstates are those due to entanglement of the vacuum of the BH (Israel, 1976). Indeed, one can always define the entanglement entropy in any quantum mechanical system. This is the entropy for an observer in the d-dimensional space-like submanifold A, in a given (d + 1)-dimensional QFT, who is not accessible to B, which is a complement of A, as the information is lost by the smearing out in region B.

This origin of entropy looks analogous to the BH entropy. That is, the microstates of the BH are due to the entangled nature of the BH vacuum, and are a result of an observer's inability to access the degrees of freedom that are hidden beyond the horizon. The subsystem B is analogous to the inside of a BH horizon for an observer sitting in A, i.e., outside of the horizon. Indeed, this was the historical motivation of considering the entanglement entropy in QFT (Aharony, 2000, 't Hooft, 1985). Brustein et al. (2006) argue that the entanglement mechanism is not specific to BHs but to any spacetime with a bifurcating Killing horizon.

For a comprehensive review of recent progresses on the holographic understandings of the entanglement entropy in the AdS/CFT correspondence, BH entropy and covariant formulation of holography, see (Nishioka et al., 2009). As notably pointed out by these authors, even after quite intense efforts in AdS/CFT for recent years, fundamental mechanism of the AdS/CFT correspondence still remains a mystery. In particular, one cannot answer which region of AdS is responsible to particular information in the dual CFT. There is also an essential discrepancy between the entanglement entropy and the BH entropy, that the entanglement entropy is proportional to the number of matter fields, while the BH entropy is not. The former includes ultraviolet divergences as opposed to the latter. Thus, due to the existing discrepancies and the lack of clear predictions verified by observations, there is no compelling reason to rely on string theory as it stands.

3.5. Where Our Analysis is Leading to

Many important issues still remain unresolved. Primary among these are the *BH information paradox* and issues related to the *degrees of freedom responsible for the BH thermodynamics*.

Yet about 47 years after its conjecturing, solid physical information regarding the physical origin of BH entropy is still lacking, which arises several puzzling questions. For example, since there is no unique rigid notion of *time translations* in a classical GR-dynamics, the BH entropy at least appears to be *incompatible* with any notion of *ergodicity*. Up to date no one was able to make a convincing calculation of BH entropy based on statistical mechanics, which associates entropy with a large number of microstates being compatible with a concept of *ergodicity*. In this regard, proving the GSL is generally valid would require using quantum-statistical mechanics, but this discipline does not exist. This then ruptures the familiar BH entropy illusion which has insufficient dimensions.

Although no results on BH thermodynamics have been subject to any experimental or observational tests, the attempts of theoretical interpretation of the BH thermodynamics provide a basis for further research and speculation on the nature of its quantum gravitational origin. In the entanglement entropy and thermal atmosphere approaches, the relevant degrees of freedom are those associated with the ordinary degrees of freedom of quantum fields outside of the BH.

The string theory implies weak coupling states, so it is not clear what the degrees of freedom of these weak coupling states would correspond to in a low energy limit where these states may admit a BH interpretation. There is no indication in the calculations that these degrees of freedom responsible for BH entropy should be viewed as being localized near the BH horizon. As pointed out by Will

doi: https://doi.org/10.52526/25792776-2021.68.1-56

(2014), it is far from clear as to whether one should think of these degrees of freedom as residing outside of the BH (e.g., in the thermal atmosphere), on the horizon (e.g., in Chern-Simons states), or inside the BH (e.g., in degrees of freedom associated with what classically corresponds to the singularity).

At first sight described above choice for the definition of the laws of gravitation, and thereof for that of thermodynamics and entropy of BHs, seems quite natural, however, we do not share this view. It seems that the holographic principle, even at quantum level, indeed could not ultimately restore the *complete information* on the real physical state, but rather the *elusive* one, of any system located in a compact spatial domain by the degrees of freedom on the surface of the domain. Moreover, since there is no unique rigid notion of *time translations* in a classical general relativistic dynamics, the BH entropy at least appears to be *incompatible* with any notion of *ergodicity*. This then ruptures the BH entropy illusion which has insufficient dimensions. Only the complete *internal solution* was able to give a *reliable information* on the thermodynamic behavior and entropy of black hole, if and only if it is known deep within the BH. Thus, it is premature to draw conclusions and only time will tell whether any of described above intriguing arguments is correct and actually realized in Nature.

Our misgiving about the views above also comes in part from a leading principle, that *an appearance of singularities indicates only to the actual limits of validity of the theory, beyond which the laws of physics are violated*. This we might expect to be reinforced by a robust intuition founded on past experience of simple physics. From this perspective, the aforementioned predictions on the BH physics are then suspected to be only *artifacts of incomplete* theory. Consequently, a new conceptual framework will be required in order to have a proper understanding of the BH physics.

Thus we conclude that PBHM, at least at its current state of development, is quite incapable of making predictions on growth and merging properties of the astrophysical BHs. One should therefore deliberately forebear from presumption of such behaviors, which seem nowhere near true if one applies the phenomenological model. That in this framework there is no provision for growth behavior of BHs, is because one assigns only an insufficient attributes to this. The PBHM is a rather restricted model.

Yet, it is still thought provoking how one can be sure that some hitherto unknown source of internal pressure does not become important above such extreme densities and halt the collapse? The failure of the PMBH does not necessarily imply a failure of the BH concept in general. In spite of a thorough search no reason could be found to introduce the required huge energy scale in BH physics but considerable change of properties of space-time continuum in density range far above nuclear density. We believe that a complete, *self-consistent* gravitation theory will smear out singularities at huge energies, and give the solution known deep within the BH. Only such a true solution was able to give a reliable information on the thermodynamic behavior and entropy of BH. This may shed further light upon the growth and merging phenomena of astrophysical BHs.

4. The MTBH

To fill the void which the standard PBHM presents, one plausible idea to innovate the solution to mentioned above key problems would appear to be MTBH (Ter-Kazarian, 2010, 2014, 2015, 2016a,b, Ter-Kazarian & Shidani, 2017, 2019) and references therein. Being suitable for applications in ultra-high energy astrophysics, the MTBH is a bold assumption in its own right. Needless to say that we will refrain here from providing lengthy details of MTBH. Wherever new results follow from earlier work, we restricted ourself only by a simple reference to earlier papers.

The MTBH is an extension of PBHM and rather completes it by exploring the most important processes of spontaneous breaking of gravitation gauge symmetry at huge energies, and thereof for that of rearrangement of vacuum state. Whereas a significant change of properties of space-time continuum, so-called inner distortion (ID), arises simultaneously with the strong gravity. This manifests its virtues below the ID-threshold length (0.4fm), yielding the transformations of Poincaré generators of translations, see e.g. (Ter-Kazarian & Shidani, 2019). Accordingly, a matter found in ID-region of spacetime continuum is undergone phase transition of II-type, i.e., each particle goes off from the mass shell. Hence, a shift of mass and energy-momentum spectra occurs upwards along the energy scale. The thermodynamics of a resulting matter, so-called *proto-matter*, is drastically differed from the

doi: https://doi.org/10.52526/25792776-2021.68.1-56

thermodynamics of strongly compressed ordinary matter. The energy density and internal pressure have sharply increased in the central region of configuration, proportional to gravitational forces of compression up to $\sim 10^{25}$ order of magnitudes with respect to corresponding central values of neutron star. In the resulting so-called proto-matter, the pressure becomes dominant over gravitational force at very short distances when matter falls into central singularity as the collapse proceeds and, thus, it halts the infinite collapse. This supplies a powerful pathway to form a the equilibrium superdense *proto-matter* core (SPC), subject to certain rules. The stable equilibrium holds for outward layers too. This counteracts the collapse and equilibrium condition remains valid even for the masses up to $\sim 10^{10}M_{\odot}$. As a corollary, this theory has smeared out the central singularities of BH at very strong gravitational fields. One of the most remarkable drawback of MTBH is the fact that instead of *infinite collapse* and *central singularity*, an inevitable end product of the evolution of massive object is the stable SPC, where static observers exist. It will ultimately circumvent a principle problem of an observer's inability to access the degrees of freedom that are hidden beyond the horizon, and a necessity to assign the *elusive entropy to BH*. This in somehow or other implies that a physical entropy is assigned to SPC as a measure of the large number of thermodynamical real microstates of proto-matter, which is compatible with a concept of *ergodicity*. This may shed further light upon the growth and merging phenomena of astrophysical BHs, that are in evidence throughout the universe.

The ID mechanism accommodates the highest energy scale in central SPC. Encapsulated in an entire set of equations of equilibrium configuration, the SPC is a robust structure that has stood the tests of the most rigorous theoretical scrutinies of a stability (Ter-Kazarian et al., 2007). It also helps to reassure us that the stable equilibrium holds in outward layers too. In this way, an accumulation of matter is allowed about SPC. Moreover, above nuclear density, the SPC always resides inside the event horizon, therefore it could be observed only in presence of accreting matter. The external physics of accretion onto the SPC in first half of its lifetime is identical to the processes in phenomenological BH models. In other words, there is no observable difference between the gravitational field of SPC and Schwarzschild BH, so that the observable signature of BHs available in literature is of direct relevance for the SPC-configurations too. But MTBH manifests its virtue when one looks for the internal physics, accounting for growth and merging behavior of BHs.

To clarify the distinction between the PBHM and the MTBH, it should help a few noteworthy points of Figure 1 which schematically plotted non-rotating BH in phenomenological and microscopic frameworks.

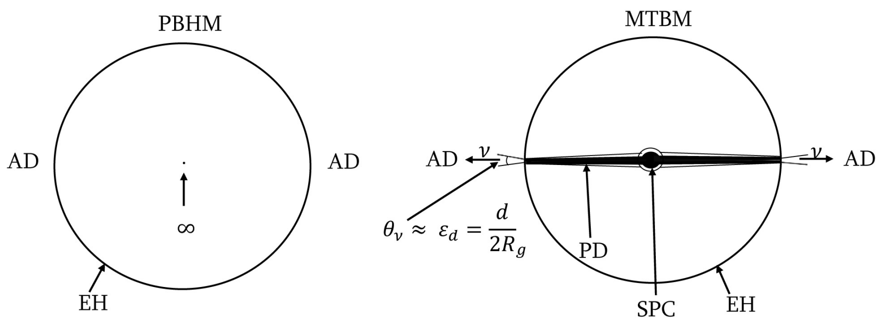

Figure 1. *Left panel*: Phenomenological model of non-spinning BH. The meaningless singularity occurs at the center inside the BH. *Right panel*: Microscopic model of non-spinning BH, with the central stable SPC. An infalling matter with the time forms PD around the SPC. In final stage of growth, a PD has reached out the edge of the event horizon. Whereas a metric singularity inevitably disappears and UHE neutrinos may escape from event horizon to outside world through vista - a thin belt area $S = 2\pi R_g d$ - with opening angle θ_ν. *Accepted notations:* EH=Event Horizon, AD=Accretion Disk, SPC=Superdense Proto-matter Core, PD=Proto-matter Disk.

A crucial point of the MTBH is that a central singularity cannot occur, which is now replaced by SPC, where the static observers are existed. The seed BH might grow up driven by the accretion of outside matter when it was getting most of its mass.

Some evidence for a rotating BH in phenomenological and microscopic frameworks is highlighted

doi: https://doi.org/10.52526/25792776-2021.68.1-56

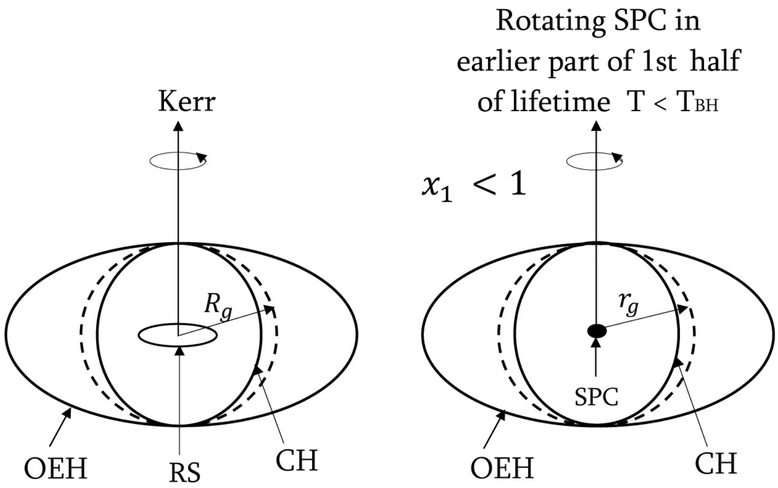

Figure 2. *Left panel*: Kerr model of spinning BH. The meaningless ring singularity occurs at the center inside the BH. *Right panel*: Microscopic model of rotating SPC in earlier part of first half of its lifetime $T < T_{BH}$. The picture is not to scale. *Abbreviated notations*: OEH :=Oblate Event Horizon, SPC :=Superdense Proto-matter Core, RS :=Ring Singularity, PCH := Prolate Cauchy Horizon.

in Figure 2. In the first half of its lifetime, the external physics outside of outer oblate event horizon of accretion onto the rotating SPC is very closely analogous to the processes in Kerr's model. But a difference between Kerr and microscopic models is the interior solutions. The interior solution of MTBH is physically meaningful, because it has smeared out a central ring singularity of the Kerr BH replacing it by the equilibrium SPC inside event horizon. The Figure 3 emphasizes an apparent distinction between Kerr model and rotating SPC in second half of its lifetime. That is, a thin co-spinning proto-matter disk with time has reached out the edge of the outer oblate event horizon, where a metric singularity inevitably disappears. Then, similar to previous non-rotating case, the ZeV-neutrinos produced in deep layers of SPC and proto-matter disk may escape from event horizon to outside world. These neutrinos are collimated in very small opening angle.

Without loss of generality, the typical features of SPC-configurations are summarised in the Figure 4 and Figure 5, to guide the eye. The radial profiles of the pressure, the density, the dimensionless gravitational (x_0)- and ID (x)- potentials are plotted in Figure 2, for example, for the given SPC of the mass $\sim 6.31 \times 10^3\, M_\odot$ (that of the Sun, $M_\odot$), and the state equation is presented in Figure 3. The special units in use denote $P_{OV} = 6.469 \times 10^{36}\,\mathrm{erg\,cm^{-3}}$, $\rho_{OV} = 7.195 \times 10^{15}\,\mathrm{g\,cm^{-3}}$ and $r_{OV} = 13.68\,\mathrm{km}$.

The available solar system observational verifications, at weak gravitational fields, offer many opportunities to improve tests of relativistic gravity. As it is seen from Figure 2 and Figure 3, the agreement is satisfactory between the proposed theory of gravity, underlying MTBH, and mentioned observational verifications. Thereby the free adjustable parameter ε in metric component, in case of static spherically symmetrical system, $g_{00} \simeq 1 - \frac{R_g}{\tilde{r}} + \varepsilon\frac{R_g^2}{\tilde{r}^2}$, can be written in terms of Eddington-Robertson expansion parameters β and γ, as $\varepsilon = 2(\beta - \gamma)$. The best fit for satisfactory agreement between the proposed theory of gravity and observation is reached at $\varepsilon = (2.95 \pm 3.24) \times 10^{-5}$. Moreover, it is consistent with GR up to the limit of neutron stars. However, this theory manifests its virtues applied to the physics at huge energies.

For preceding developments of MTBH, and its implications for ultra-high energy (UHE) astrophysics, the interested reader is invited to consult the original papers.

We have undertaken a large series of numerical simulations with the goal to trace an evolution of the mass assembly history of plausible accreting supermassive BH seeds in 377 AGNs to the present time, and examine the observable signatures today (Ter-Kazarian, 2014, 2015). The MTBH explains the origin of ZeV-neutrinos, which are of vital interest for the source of UHE-particles. We compute the ZeV-neutrino fluxes from plausible accreting supermassive BHs, closely linked with the 377 AGNs.

We reconcile the observed unusual high luminosity of NuSTAR X-ray pulsations from M82X-2 with

doi: https://doi.org/10.52526/25792776-2021.68.1-56

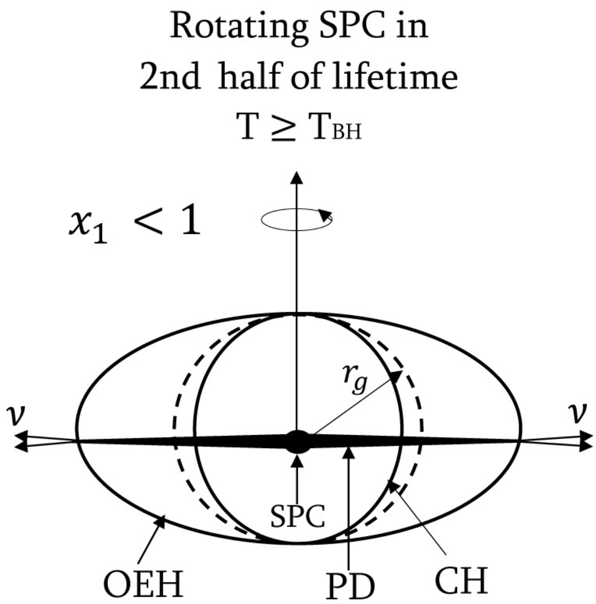

Figure 3. Microscopic model of rotating SPC in second half of its lifetime. An infalling matter already formed a thin co-spinning proto-matter disk which has reached out the edge of the outer oblate event horizon. A singularity inevitably disappears and the neutrinos escape to outside world through the vista. *Abbreviated notations*: OEH :=Oblate Event Horizon, SPC :=Superdense Proto-matter Core, PCH := Prolate Cauchy Horizon, PD :=Proto-matter Disk.

the most extreme violation of the Eddington limit (Ter-Kazarian, 2016a,b, Ter-Kazarian & Shidani, 2017).

We construct microscopic models of accreting intermediate mass BHs (IMBHs). The mass estimates collected from the literature of all the observational evidence for 137 IMBH-candidates, allow us to calculate all their essential physical characteristics (Ter-Kazarian & Shidani, 2019).

5. Concluding Remarks

Below we briefly reflect upon a few relevant points. There are deep conceptual and technical problems involved, and these provide scope for the arguments discussed. Despite the past four decades of serious efforts, we do not have as yet available any proof or even any mathematically precise formulation of the cosmic censorship hypothesis. We present examples of rigorous calculations, which have shown that the expectations of the 1970s have been hasty, that CCC assumption has been premature. We review briefly the observable signature and computational efforts of growth and merging phenomena of astrophysical BHs We collect and briefly discuss the necessary ideas behind the various specific constructions and suggestions on the conceptual problems of GR, the singularities and the thermodynamics of BHs in semiclassical and quantum physics. We concentrate on the critical discussion of the past and present states, evaluating those strategies, approaches etc., that are explicitly and unambiguously given and applicable in any generic spacetime. It was far from being complete, and our claim here is not to discuss the problems considered in detail, but rather to give a collection of problems that are effectively or potentially related to interpretation of the growth and merging properties of BHs with in the phenomenological model.

We argue that PBHM, at least at its current state of development, is quite incapable of making predictions on growth and merging properties of the astrophysical BHs. To innovate the solution to aforementioned problems, we outline the key points of MTBH, which has explored a novel aspects expected from considerable change of properties of space-time continuum at spontaneous breaking of gravitation gauge symmetry far above nuclear density. It may shed further light upon the growth and merging phenomena of astrophysical BHs. Of course, much remains to be done before one can

doi: https://doi.org/10.52526/25792776-2021.68.1-56

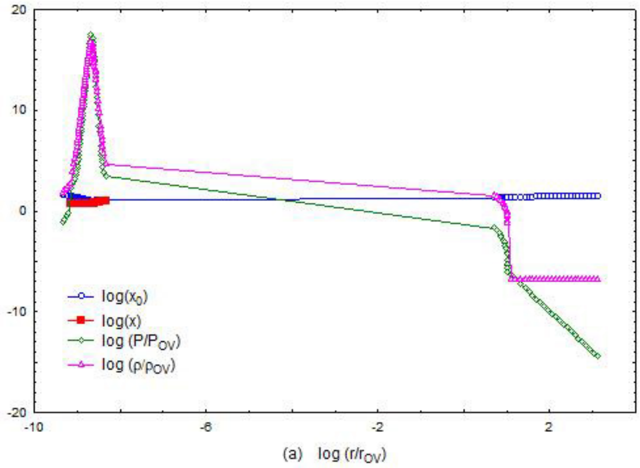

Figure 4. The radial profiles of the pressure, the density, the dimensionless gravitational (x_0)- and ID (x)- potentials of the SPC of mass $\sim 6.31 \times 10^3\, M_\odot$.

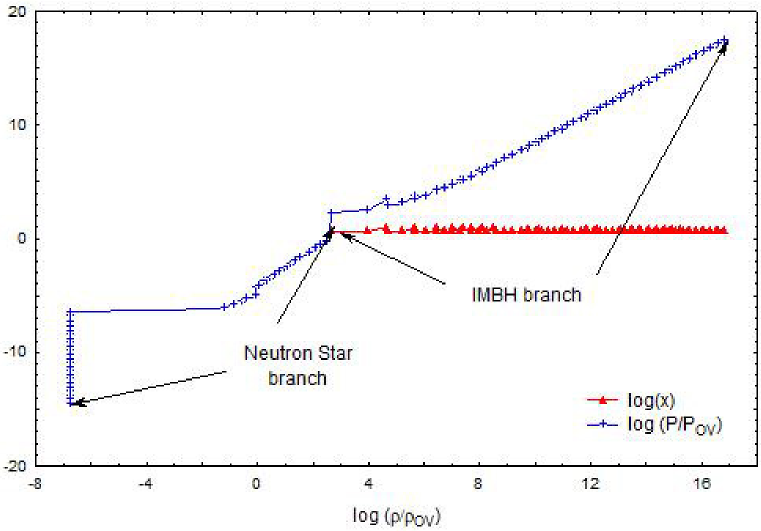

Figure 5. The state equation of the SPC of mass $\sim 6.31 \times 10^3\, M_\odot$.

determine whether this approach can ever contribute to the larger goal of gaining new insight into the growth and merging phenomena of astrophysical BHs.

doi: https://doi.org/10.52526/25792776-2021.68.1-56

References

Aharony O. e. a., 2000, Phys. Rept., 323, 183

Bardeen J. M., Carter B., Hawking S. W., 1973, Communications in Mathematical Physics, 31, 161

Barger A. J. e. a., 2005, Astrophys. J., 129, 578

Barrow J. D., Barrow J. S., 1983, The Left Hand of Creation. Basic Books, New York

Bartnik R., , in Marcel Grossmann Meeting on recent developments in theoretical and experimental general relativity, gravitation and relativistic field theories.

Bartnik R., 1989, Phys. Rev. Lett., 62, 2346

Bassani L., Dean A. I., Sembey S., 2010, Astron. Astrophys., 125, 52

Baumgarte T. W., Shapiro S. L., 2003, Astrophys. J., 585, 921

Bekenstein J. D., 1973, Phys. Rev. D, 7, 2333

Bekenstein J. D., 1974, Phys. Rev. D, 9, 3292

Bekenstein J. D., 1981, Phys. Rev. D, 23, 287

Bekenstein J. D., 1982, Phys. Rev. D, 14, 355

Birrell N. D., Davies P. C. W., 1982, Quantum Fields in Curved Space. Cambridge Un. Press, Cambridge

Bondi H., 1947, Mon. Not. Astron. Soc., 107, 343

Bousso R., 1999, J. High Energy Phys., JHEP07(1999), 003

Bousso R., 2002, Rev. Mod. Phys., 74, 825

Bromm V., Loeb A., 2003, Astrophys. J., 596, 34

Brown J. D., York J. M., 1993, Phys. Rev. D, 47, 1420

Brown J. D., Creighton J. D. E., Mann R., 1994, Phys. Rev. D, 50, 6394

Brustein R., Einhorn M. B., Yarom A., 2006, J. of High Energy Phys., Issue 01, id. 098

Carlip S., 2002, Phys. Rev. Lett., 88, 241301

Carter B., 1979, An Einstein Centenary Survay. Cambridge Univ. press, Cambridge

Christodoulou D., Yau S.-T., , in Proc. of the AMS-IMS-SIAM Joint Summer Research Conference.

Coleman S., 1988, Nucl. Phys., B, 307, 867

Croom S. M. e. a., 2009, MNRAS, 399, 1755

Datt S., 1938, Zs. f. Phys., 108, 314

Devecchi B., Volonteri M., 2009, Astrophys. J., 694, 302

Dougan A. J., Mason L. J., 1991, Phys Rev Lett., 67, 2119

Dray T., 't Hooft G., 1985a, Commun. Math. Phys., 99, 613

Dray T., 't Hooft G., 1985b, Nucl. Phys. B, 253, 173

Flanagan E. E., Marolf D., Wald R. M., 2000, Phys. Rev. D, 62, id.084035

Fredenhagen K., 1995, Rev. in Math. Phys., 7, 559

Freitag M., Amaro-Seoane P., Kalogera V., 2006, Astrophys. J., 649, 91

Geroch R., 1973, Ann. N.Y. Acad. Sci., 224, 108

Giambo R. e. a., 2004, Gen. Relativ. Grav., 36, 1279

Goswami R., Joshi P. S., 2002, Class. Quantum Grav., 19, 5229

Gubser S. S., Klebanov I. R., Peet A. W., 1996, Phys. Rev. D, 54, 3915

Hawking S. W., 1968, J. Math. Phys., 9, 598

Hawking S. W., 1988, Phys. Rev. D, 37, 904

doi: https://doi.org/10.52526/25792776-2021.68.1-56

Hayward S. A., 1998, Class. Quantum Grav., 15, 3147

Hulse R. A., Taylor J. H., 1975, Astrophys. J., 195, L51

Israel W., 1976, Phys. Lett. A, 57, 107

Israel W., 1987, in Three hundred years of gravitation. Cambridge Univ. Press, Cambridge, p. 199

Joshi P. S., Malafarina D., 2011, Int. J. Mod. Phys. D, 20, 2641

Joshi P. S., Malafarina D., 2013, Gen. Rel. Grav., 45, 305

Kelly B. C. e. a., 2010, Astrophys. J., 719, 191

Kerner R., Mann R. B., 2008, Class. Quant. Grav., 25, Issue 9, id. 095014

Krivan W., Laguna P., Papadopoulos P., Andersson N., 1997, Phys. Rev. D, 56, 3395

Kundt W., 1996, Lecture Notes in Physics, 471, 265

Kundt W., 2011, in XIVth Brazilian School of Cosmology and Gravitation. Cambridge Sci. Pub, Cambridge, p. 109

Kundt W., 2012, Acta Politechnica, 53 (2013): Supplement

Kundt W., Fischer D., 1989, J. Astrophys. Astron., 10, 119

Lauer T. R. e. a., 2007, Astrophys. J., 662, 808

Lemaìtre G., 1933, Ann. Soc. Sci. Bruxelles I, A, 53, 51

Lynden-Bell D., 2013, Nature, 223, 690

Macquart J.-P., Kanekar N., 2015, Astrophys. J., 805, 172

Maldacena J. M., 1998, Adv. Theor. Math. Phys., 2, 231

Miralda-Escudé J., Gould A., 2000, Astrophys. J., 545, 847

Natarajan P., 2011, in Fluid Flows to Black Holes: A Tribute to S Chandrasekhar on his Birth Centenary. World Scientific Publishing Co. Pte. Ltd., p. 191

Natarajan P., Treister E., 2009, MNRAS, 393, 838

Nishioka T., Ryu S., Takayanagi T., 2009, J. of Phys. A: Math. and Theor., 42, 35

Oppenheimer J. R., Snyder H., 1939, Phys. Rev., 56, 455

Orosz J. A., 2003, in Proceedings of IAU Symposium, vol. 212. Edited by van der Hucht, K and Herrero, A and Esteban, C

Park M. I., 2002, Nucl. Phys. B, 634, 339

Penrose R., 1969, Riv. Nuovo Cimento, 1, 252

Penrose R., 1982, Proc. R. Soc. London, Ser. A, 381, 53

Penrose R., Rindler W., 1986, Spinors and space-time. Cambridge University Press, Cambridge

Pfahl E., Loeb A., 2005, Astrophys. J., 615, 253

Saxton C. J., 2016, MNRAS, 461, 4295

Shankar F., Weinberg D. H., Miralda-Escude J., 2009, Astrophys. J., 690, 20

Sofue Y., 2000, Astrophys. J., 540, 224

Su M., Slatyer T. R., Finkbeiner D. P., 2010, Astrophys. J., 724, 1044

Su M., Slatyer T. R., Finkbeiner D. P., 2011, AAS, 43

Susskind L., 1995, J. Math. Phys., 36, 6377

Szabados L. B., 2004, Liv. Rev. Relat., 7, 140

Szabados L. B., 2005, Class. Quantum Grav., 22, 855

Taylor J. H., Weisberg J. M., 1982, Astrophys. J., 253, 908

Ter-Kazarian G. T., 2010, Ap&SS, 327, 91

Ter-Kazarian G. T., 2014, Ap&SS, 349, 919

doi: https://doi.org/10.52526/25792776-2021.68.1-56

Ter-Kazarian G. T., 2015, J. of Astrophysics, 2015, 1

Ter-Kazarian G. T., 2016a, Advances in Astrophys., 1, 21

Ter-Kazarian G. T., 2016b, Ap&SS, 361, 20

Ter-Kazarian G. T., Shidani S., 2017, Advances in Astrophys., 2, 162

Ter-Kazarian G. T., Shidani S., 2019, Ap&SS, 364, 23

Ter-Kazarian G. T., Shidani S., Sargsyan L., 2007, Ap&SS, 310, 93

Tolman R. C., 1934, Proc. Natl. Acad. Sci. USA, 20, 410

Townsend P. K., 1997, arXiv e-prints, pp gr–qc/9707012

Treister E. e. a., 2010, Science, 328, 600

Treister E., Urry C. M., 2012, Advances in Astronomy, 2012, ID 516193

Vestergaard M., 2004, Astrophys. J., 601, 676

Villas da Rocha J. F., Wang A., 2000, Class. Quantum Grav., 17, 2589

Volonteri M., 2010, A&ARv, 18, 279

Volonteri M., Natarajan P., 2009, MNRAS, 400, 1911

Volonteri M., Lodato G., Natarajan P., 2010, MNRAS, 383, 1079

Wald R. M., 2004, Living Rev. Relat., 4 lrr-2001-6

Will C. M., 2014, Living Rev. Relativity, 17, 4

Willott C. J. e. a., 2010, Astrophys. J., 140, 546

't Hooft G., 1985, Nucl. Phys. B, 256, 727

't Hooft G., 1993, arxiv:9310026[gr-qc]

doi: https://doi.org/10.52526/25792776-2021.68.1-56

Communications of BAO, Vol. 68, Issue 1, 2021, pp. 75-89

Tables of physical and morphological properties of nearby extended radio galaxies

R.R.Andreasyan*and H.V.Abrahamyan†

NAS RA Byurakan Astrophysical Observatory (BAO), Byurakan 0213, Aragatzotn Province, Armenia

Abstract

It is brought the physical and morphological data of 267 nearby radio galaxies identified with elliptical galaxies brighter than 18th magnitude (sample 1) and for 280 extragalactic radio sources with known position angles between the integrated intrinsic radio polarization and radio axes (sample 2).

Keywords: *radio galaxies, extragalactic radio sources, Fanaroff-Riley classes, FRI, FRII*

1. Introduction

One of the well-known manifestations of activity of galaxies is the radiation in radio wavelength. Galaxies with more powerful radio radiation are named radio galaxies. In many cases the radio images of these extragalactic radio sources have sizes larger than optical images. They can have dimensions of hundreds kiloparsecs and sometimes of megaparsecs. These radio sources are named extended extragalactic radio sources. The main mechanism of radiation in these galaxies is the synchrotron mechanism of radiation of relativistic particles (mainly electrons) in magnetic fields of parent galaxies. Usually there are no concretization of the large-scale configuration of magnetic field, and there is no attention on the role of field configuration in the observing morphology of extragalactic radio sources. The first classification of extragalactic radio sources is the Fanaroff & Riley (1974) (FR) classification. It was done using the morphological features, the edge darkened-FRI, and edge brightened, relatively more luminous FRII types. There are found many other morphological and physical differences between the different FR classes of extragalactic radio sources: in the total luminosity, in radio core powers, in ratio of core to lobe radio power, in the relationships between emission-line luminosity and radio power (Zirbel & Baum (1995); Gopal & Wiita (2000); Gendre et al. (2011) etc.). In (Andreasyan (1984)) we have suggested a mechanism of the formation and evolution of extragalactic radio sources in framework of the cosmological conception of V.Ambartsumian (Ambartsumian (1966)). It was done a main suggestion about the magnetic field configuration of host supergiant elliptical galaxy. We conclude that the magnetic field of the host galaxy or AGN has a dipole configuration, with dipole axes parallel to the rotation axes of host galaxy. Extragalactic radio sources are formed from relativistic plasma clouds, ejected from the central part of the optical galaxy and moving in its large-scale, dipole magnetic field. It was also done a classification of extragalactic radio sources by their elongation parameters (K), where K is the ratio of the largest dimension of radio image to the perpendicular dimension. In the frame of suggested mechanism, the well-known Fanaroff-Riley Dichotomy and many other morphological fetchers finds a very simple physical explanation.

In our early works we studied correlation between different morphological and physical properties of extragalactic radio sources classified by Fanaroff-Riley and by our elongation parameters K. We find: The correlation of radio axis with the optical axis in nearby radio galaxies (Andreasyan & Sol (1999)); The ellipticity of elliptical galaxies identified with the different types of extragalactic radio

*randrasy@bao.sci.am, Corresponding author

†abrahamyanhayk@gmail.com

doi: https://doi.org/10.52526/25792776-2021.68.1-75

sources (Andreasyan & Sol (2000)); The correlation of the radio polarization angle with the radio axes of extragalactic radio sources (Andreasyan et al. (2002)); The relation between FR classes and elongation K parameters (Andreasyan (2019)), et. all. Here we bring the tables of all data used in above mentioned studies.

2. Observational data

For the statistical analyses in our studies we have used data for more than 500 extragalactic radio sources. These are 267 nearby radio galaxies identified with elliptical galaxies brighter than 18th magnitude (sample1) (Andreasyan & Sol (1999)), and 280 extragalactic radio sources with known position angles between the integrated intrinsic radio polarization and radio axes (sample 2) (Andreasyan et al. (2002)). A little part of sources from sample 2 are also objects from sample 1.

In mentioned papers we has brought some data from samples 1 and 2, bat all observational data of these samples are not published, and here we bring the full samples 1 and 2.

In these samples we bring also classification of radio galaxies with their elongation parameter K using the published radio maps. In samples 1 and 2 we have 289 extragalactic radio sources with known both, FR classification and K parameters used in (Andreasyan & Sol (2000)) and (Andreasyan (2019)).

3. Tables of extragalactic radio sources from samples 1 and 2.

3.1. *Sample 1.*

Data for 267 nearby radio galaxies identified with elliptical galaxies brighter than 18th magnitude. For nearby radio sources, we have data on: radio source name (Col.1); the position angle of the major axis of optical elliptical galaxy oPA found mainly from the Palomar maps (Col.2); the position angles of radio axes (rPA) obtained from the published radio maps (Col.3); the relative position angle between optical and radio axis dPA (Col.4); the ellipticity E of the optical galaxy identified with radio sources (Col.5); the classes by elongation parameter K: K>2.5 or K<2.5 (Col.6); Fanaroff-Riley classes FR taken from the literature (Col.7); the optical magnitude M of parent galaxy (Col.8); the radio spectral index SI (Col.9); The redshift z (Col.10); the radio luminosity logP (Col.11); The parameter K (Col.12); references for radio maps and FR classes (Col.13).
The references from Column 13 we give in Appendix.

Table 1: Sample 1.

1 **Object**	2 **oPA**	3 **rPA**	4 **dPA**	5 **E**	6 **K**	7 **FR**	8 **M**	9 **SI**	10 **z**	11 **logP (WHz)**	12 **K**	13 **ref**
0005−199	5	81	76	2.8	>2.5		16.5	0.7			4.2	26
0007+124	2	21	19		>2.5	II	17.7	0.78	0.157		2.6	20 5
0013−316	39	110	71	1	>2.5		16.5	0.92			3.5	26
0018−194	17	111	86	4	<2.5	II	17	0.69	0.095		1.4	21
0023−33	34	70	36	1.7	<2.5		16.7	0.5	0.05		1.6	26
0034+254	163	83	80	2	>2.5	I	14.8	0.66	0.032	24.07	2.8	15 15
0039+211	82	0	82	2	>2.5			0.9	0.102	24.89	2.6	56
0040−06	58	165	73		<2.5		17				1.5	21
0043+201	69	172	77	2	>2.5		15.7	0.75	0.106	25.06	4	57
0043−424	159	136	23	2	<2.5	II	16	0.87	0.053	27.23	2.4	25 7
0053+261	171	146	25		<2.5	I	17.5	1.06	0.195	27.15	1.4	18 2
0055+265	152	109	43		>2.5	I	13	0.84	0.047	25.67	2.6	15 15
0055+300	42	129	87	3.1	<2.5	I	12.2	1.04	0.017	24.52	2.4	15 15
0104+321	135	147	12		<2.5	I	12.1	0.57	0.017	25.07	2	27 2
0106+130	131	20	69	1	>2.5	II	15.1	0.76	0.06		3.4	17 2
0108−142	53	100	47	1	>2.5	I	15.8		0.052	24.96	3.2	85 7
0109+492	101	13	88	1	>2.5	II	15.6	0.77	0.067	26.21	4.3	18 2
0110+152	105	170	65		>2.5		15.5	1.2	0.048	24.34	2.6	61

doi: https://doi.org/10.52526/25792776-2021.68.1-75

0114−476	17	157	40		<2.5	II	16.5	0.6	0.146	26.86	2.2	21 3
0116+319	50	115	65		<2.5		14.5	0.42	0.059	25.1	1.6	75
0120+33	70	120	50		<2.5		13	1.4	0.016	23.35	2	15
0123−016	52	178	54		>2.5	I	12.2	0.66	0.018	25.27	2.6	29 15
0124+189	76	13	63	1	>2.5		15.5	0.56	0.043		2.8	85
0131−367	164	89	75	3.2	>2.5	II	14.2	0.51	0.03	25.76	2.6	20 7
0149+35	30	87	57		>2.5	I	14.5	0.6	0.016	23	5	15 15
0153+053	73	84	11	2	<2.5		13.2	0.5			2.2	63
0206+355	137	132	5		<2.5	I	13	0.66	0.037	25.44	1.5	16 15
0214−480	100	175	75	1	>2.5	I	14.5	1	0.064	26	3.3	54 7
0220+427	33	50	17		<2.5	I	12.5	0.5	0.022	24.69	2	17 2
0222+369	80	48	32		<2.5		15	0.24	0.033	23.7	1.6	70
0229−208	174	110	64	1.6	>2.5	II	16	0.62	0.09	25.46	4	26
0239−85	113	95	18	3.1	<2.5						2	65
0247−207	45	40	5	0.2	>2.5	I	15.4	0.97	0.087	25.35	5.5	26 7
0255+133	87	159	72	4	>2.5	II	16.8		0.075	24.07	2.6	57
0257−398	115	60	55	2	<2.5		15.3	0.64			1.5	26
0258+350	70	126	56		<2.5		13.5	0.54	0.016	24.63	2.2	22
0258+435	231	289	58	2	>2.5			0.67	0.065		2.7	86
0300+162	134	110	24	2	<2.5	I	14.5	0.77	0.032	25.45	1.8	17 2
0305+039	144	56	88	2	<2.5	I	13	0.43	0.029	25.68	1.2	20 7
0307−305	78	93	15	3.4	<2.5	II	16.5	0.54	0.068	25.15	2.4	26 7
0312−343	132	114	18	1.2	<2.5		15.6	0.62			2	26
0314+412	57	32	25	3	>2.5	I					2.6	58 7
0314+416	171	96	75	3	>2.5	I	12.5	0.62	0.026	25.43	4	45 2
0320−374	60	126	66	3.8	>2.5	I	8.9	0.52	0.005	25.46	2.6	26 7
0325+023	153	63	90	3	>2.5	II	13.5	0.52	0.03	25.58	2.6	20 7
0326+396	128	82	46	1	<2.5	II	14.9	0.6	0.024	24.68	2.4	15
0331+391	101	180	79	1	>2.5		15	0.52	0.02	24.48	2.6	15
0332−39	25	140	65	1.7	>2.5		15.3	1.05			3.5	26
0336−355	112	51	61	1.2	<2.5	I	10.9	0.8	0.005	23.52	2.4	26 7
0344−345	103	104	1	1.8	<2.5	I	17	0.73	0.054	25.4	2	25 7
0349−279	72	53	19		>2.5	II	17	0.72	0.066	26.48	2.6	20 7
0349+212	126	17	71		>2.5		16	0.7	0.133		3.5	87
0356+102	72	25	47	2	>2.5	II	14.2	0.78	0.031	26.02	3.5	18 2
0427−539		80	5		<2.5	I	13.2	0.7	0.038	25.55	2.4	54 7
0429−51	8	1	7	2.6	<2.5		12.7				2.3	63
0434−225	149	109	40	0.6	<2.5	I	14.6	0.74	0.069	25.2	2.4	26 7
0446−208	174	18	24	0.6	<2.5		16.4	1			2.2	26
0449−175	0	145	35	1.7	<2.5	I	13.7	1.1	0.031	24.34	2.4	26 7
0452−190	140	82	58	3.1	>2.5		14.5	0.54			3.3	26
0453−206	172	112	60	0.4	<2.5	I	14	0.73	0.035	25.22	1.6	26 7
0511−305	85	33	52	1.3	>2.5	II	17	0.84	0.058	25.39	2.7	20 3
0518−458	96	102	6	3	<2.5	II	15.7	1.07	0.035	26.86	2	21 7
0521−365	75	123	48	2.6	<2.5	I	15.3	0.43	0.061	26.64	1.4	26 16
0523−327	156	157	1	1.7	>2.5	II	15.4	0.94	0.076	25.3	3.5	26 7
0546−329	175	8	13	1.8	<2.5	I	14.5	0.97	0.037	24.73	2.2	26 7
0548−317	4	72	68	2.4	>2.5	II	14.5	0.66	0.033	24.53	2.7	26 7
0632+263	16	115	81	0.1	>2.5		15		0.04		3.8	14
0634−205	178	177	1	1.6	>2.5	I	16.8	0.8	0.056	26.48	3.7	21 7
0651+542	129	102	27		>2.5	II	19	0.87	0.238	27.39	2.7	31 2
0652+426	124	50	74	2	<2.5						2	13
0712−349	106	133	27	1.8	<2.5		15.9	0.55			2	26
0712+534	120	114	6	1	<2.5	I	15	0.6	0.064	24.83	2.2	13 15
0714+286	73	133	60	3	>2.5		16		0.083		2.6	13
0718−340	56	63	7	0.9	>2.5	II	16.5	0.5	0.03	24.71	2.9	26 7
0734+806	49	150	79		>2.5	II	17	0.68	0.118	26.68	3.1	17 2
0744+559	70	63	7	2	<2.5	II	15.2	0.77	0.035	25.82	2.2	76 2
0745+521	37	92	55	1	>2.5	II		0.68	0.063		3	83
0755+379	144	107	37		<2.5	I	13.2	0.59	0.041	25.63	2.2	13
0800+248	53	70	17		<2.5	I	15.7	0.68	0.043	24.41	2.3	15 7
0802+243	13	118	75	0.1	>2.5	II	15.2	0.79	0.06	26.24	3	18 2
0810+66		85	60		<2.5		15.7				1.5	57

doi: https://doi.org/10.52526/25792776-2021.68.1-75

0818+472	103	4	81	1	>2.5	II	16.5	0.69	0.13		2.6	45 4
0819−30	44	119	75		>2.5	II	18	0.68	0.086		3.1	20
0819+061	98	38	60		>2.5	II	18	0.69	0.082	26.23	2.7	20 7
0836+299	59	30	29	2	<2.5	I	15.7	0.78	0.065	25.68	1.8	15 15
0843+316	42	45	3		>2.5		16.5	0.85	0.068	25.86	2.8	59
0844+540	45	113	68	1	>2.5		15		0.045		2.9	85
0844+319	123	170	47	1	<2.5	I	13.5	0.78	0.068	25.86	2.4	15
0908+376	80	5	75		>2.5	II	15.6	0.56	0.105	25.73	2.6	62
0913+385	30	42	12		<2.5		15.7	0.82	0.071	26.24	1.5	59
0915+320	46	31	15	1	<2.5	I	15.5	0.48	0.062	24.88	1.8	15 7
0915−119	130	24	74		>2.5	I			0.065		2.6	64 7
0916+342	30	110	80		>2.5		13	0.87	0.017	23.6	3.2	15
0922+366	130	170	40		<2.5	I	15.5	0.98	0.112	25.99	2	16
0923+330			5		<2.5		16	1.12	0.14		1.9	16
0924+302	49	55	6	1	<2.5		14.5	1.04	0.027	24.72	2	72
0936+361	118	164	46		>2.5	II	16.8	0.74	0.137		6	18 2
0938+399	45	14	31	3	>2.5	II	16.2	0.56	0.108	26.31	4	16 4
0940−304	90	21	69	5	<2.5		14.5	0.58			1.5	26
1000+201	112	7	75		>2.5	I	16.5	0.8	0.168	26.56	2.6	85 7
1002−320	52	29	23	1.9	>2.5		17.4	0.93			2.8	26
1003+351	45	123	78	3	>2.5	II	15.5	0.51	0.099	26.62	3.5	73 2
1005+007	38	71	33	1	<2.5		15.4				2.4	38
1005+282	5	150	45	2	>2.5	II	16.4	1.15	0.148	25.36	2.6	59
1014+398	115	130	15		>2.5	II	15.5	1.1	0.106		5	16
1015+491	95	10	85		>2.5	I	14.8	0.57	0.08		3.2	62
1033+003	131	8	57	2	<2.5		15.2				1.8	85
1040+317		50	21		<2.5	I	15.5	0.62	0.036	24.97	2	15 7
1053−282	48	26	22	3.3	>2.5	II	15.5	0.61	0.061	25.3	2.7	26 7
1102+304	147	70	77	2	>2.5	II	15.7	0.72	0.072	25.32	3.8	15
1107−372	30	78	48	2.3	<2.5		12.4	0.7		22.8	1.8	26
1108+272		80	5		<2.5	I	14.6	0.48	0.033	23.01	2.3	15 7
1113+295	138	71	67	2	>2.5	II	14.2	0.64	0.049	25.7	2.8	15 7
1116+281	40	113	73		>2.5		14.3	0.65	0.067	25.3	2.7	59
1122+390	35	118	83	2.1	>2.5	I	11.6	0.57	0.007	23.98	2.9	28 7
1123−351	174	120	54	1.8	<2.5		16	0.7	0.033		2.2	26
1127+012	100	12	88	3	>2.5		16.7				2.7	85
1137+123	139	12	53	2	<2.5		16.5				1.6	85
1141+374	130	52	78		>2.5	II	15.9	0.94	0.115	26.46	¿5	23
1141+466	147	40	73		>2.5	II	15.8	1.1	0.162		2.6	23
1142−341	31	150	61	2.1	>2.5		15.6	0.92			2.8	26
1146−11	79	104	25		<2.5	II	18	0.96	0.117		1.3	21
1154−038	45	109	64	2	>2.5		14.3				3.3	85
1155+266	55	130	75		>2.5						2.7	56
1204+241		166	5		<2.5		15.2	0.76	0.077	24.83	1.5	59
1209+746	60	155	85		>2.5		16.5		0.061		3.5	61
1216+061	150	83	67	3	>2.5	II	11	0.51	0.007	24.8	3	20 7
1218+296	40	152	68	0.7	<2.5		11.2	0.24	0.002	21.6	1.8	65
1222+131	116	167	51	1	<2.5	I	10	0.6	0.003	23.8	1.9	17 2
1225+265	50	70	20		<2.5	II	16.1	0.79	0.064		2.4	59
1227+83	160	70	90	1.8	<2.5		12.8				1.5	66
1228−335	164	83	81	2	<2.5		15.4	0.6			2.4	26
1228+127	157	101	56	1.4	<2.5	I	8.7	0.79	0.004	25.65	2	17 2
1240+029	166	33	47	1.9	>2.5		12.9				2.6	63
1249+035	27	146	61	2	>2.5						2.6	85
1250−102	65	162	83	1	>2.5		12	1.2	0.014	23.27	4	37
1251+278	30	169	41	0.1	<2.5	I	15.5	0.58	0.086	26.27	1.5	19 15
1254+277	51	11	40	3	<2.5	I	12.3	0.86	0.025	22.63	1.8	15 7
1256+281	171	275	76	2	>2.5	I	14.9	1.04	0.024	24.5	2.6	74 15
1257−253	37	150	67	2.4	>2.5		16	0.7			3.5	26
1257+282	17	39	22		<2.5	I	14	0.75	0.023	23.05	2.2	67
1258−321	167	125	42	3.2	<2.5		12.8	0.59			1.8	26
1313+072	40	71	31		<2.5		15.5		0.051	24.75	2	20
1316+299	67	97	30		<2.5		15	0.71	0.073	25.85	1.5	13

doi: https://doi.org/10.52526/25792776-2021.68.1-75

1317+258	75	54	21	2	>2.5						2.6	86
1318−434	100	24	76	2	>2.5	I	14.5	0.96	0.011	25.01	3.9	21 7
1319+428	130	79	51		>2.5	II	16	0.95	0.079	26.15	3	17 2
1321+318	69	111	42		>2.5	I	13.9	0.65	0.016	24.6	3	67 15
1322−428		40	10	2	<2.5	I	7	0.79	0.002	23.8	2.4	54 8
1322+366	75	7	68	3	>2.5	II	14	0.46	0.018	24.35	3.5	13
1323−271	154	68	86	3.9	>2.5	II	12.9	0.67	0.043	24.99	4	26
1323+370	87	154	67	2	>2.5	II	15	0.7	0.08		2.7	62
1331−099	55	107	52		>2.5	II	17.5	0.9	0.081	26 26	2.8	21 16
1333−337	47	125	78	0.9	>2.5	II	11.9	0.79	0.013	25.06	3.3	26 17
1344−241	149	155	6	3.9	<2.5		14.4	1.05			2	26
1346+268	18	20	2		<2.5	I	13.8	0.92	0.063	25.73	2	13 7
1350+316	62	100	38		<2.5	I	15.6	0.7	0.045	25.4	1.5	19 2
1354−251	147	155	8	3.9	<2.5		15.4	0.64			1.5	26
1357+287	100	15	85		>2.5	II	14,8	0.8	0.063	25.06	2.6	59
1358−113	41	125	84	2	>2.5	II	15	0.7	0.037	24.89	3	29
1400−337	90	4	86	2.1	<2.5		12.4	1.28	0.014		1.4	26
1401+35	70	0	70		<2.5		12.8	0.92	0.013	23.6	1.5	62
1401−05			15		<2.5		17				1.9	21
1407+177	6	73	67	2	<2.5	I	13.4		0.016	23.68	1.8	21 15
1411+094	84	178	86		>2.5		18.3		0.162		2.8	85
1413−36	43	35	8	2.6	>2.5		17.5	0.74			3	26
1414+110	146	85	61	1	<2.5	I	13.3	0.67	0.024	25.36	1.6	20 2
1420+198	95	135	40		>2.5	II	18	0.78	0.27	27.58	3	45 2
1422+268	118	96	22	2	<2.5	I	15.6	0.74	0.037	25.07	2.4	15 7
1427+07	54	157	77		>2.5		15.6				2.6	20
1433+553	110	143	33	1	<2.5		17	0.8	0.14	25.05	2.3	87
1441+262	150	68	82		>2.5	II	14.3	0.79	0.062	25.03	3.1	59
1441+522		125	25		<2.5	II	17	0.76	0.141	26.76	2.2	19 2
1449−129	135	89	46		<2.5	I	18		0.07	25.26	2.2	20 7
1452+165	161	59	78	3	<2.5	II	14.9	0.71	0.046		1.5	21
1457+29	130	169	39		<2.5		17.2				1.3	59
1458+21A			0		<2.5						2.2	56
1459+21E			20		<2.5						2.3	56
1502+262		150	12		>2.5	I	15.2	0.92	0.054	26.46	3.3	13 2
1509+059	26	145	61	3.3	>2.5						2.7	63
1512+30	110	31	79		>2.5	II	15.4	0.75	0.093	24.99	2.8	59
1514+004	53	132	79	3	>2.5	II	16.5	0.4	0.052		3.1	20
1514+072	21	16	5	3	<2.5	I	16	1.02	0.035	26.1	1.4	29 4
1519+078			90		>2.5		15	1.93	0.046	25.09	2.6	57
1525+291	8	14	6		<2.5	I	15.4	0.73	0.065	24.89	1.5	15 7
1527+308	175	130	45		>2.5		15	0.98	0.114	25.39	2.7	59
1547+309	136	120	16		>2.5		16.5	0.96	0.111		3.2	37
1549+202	119	80	39		>2.5	II	18.5	0.88	0.09	26.5	3.8	18 2
1553+245	19	129	70	3	>2.5	I	14.4	0.28	0.043	23.36	3.5	13 7
1555+308	120	122	2		>2.5		16.1	0.58	0.075		3.2	59
1556+274	109	291	2	2	<2.5						2.4	74
1559+021	138	100	38	3	>2.5	II	15.5	0.61	0.104	27	2.9	20 4
1601+173	64	180	64	2	<2.5		13.5		0.034		1.8	91
1602+178	117	171	54	1	<2.5	I	14.6	0.15	0.032		2	85 7
1602+34			37		<2.5		15.4	0.82	0.032	23.4	2.4	15
1604+183	89	176	87	2	>2.5		15				2.8	90
1610+296	1	66	65	3	<2.5	I	14.8	0.72	0.031	24.13	1.5	15 7
1610−607	127	86	41	2	>2.5	II	12.8	1.15	0.017		3.4	54
1615+325	28	17	11		>2.5	II	16	0.61	0.152	26.69	3	19 7
1615+351	252	323	71	1	>2.5	II	14.9	0.76	0.03	25.31	3.5	60 7
1621+380	175	70	75	5	>2.5	I	14.1	0.56	0.031	24.58	2.8	60 7
1626+397	34	82	48		<2.5	I	12	1.19	0.03	25.87	2	17 2
1636+379		75	5	1	<2.5	I	16.4	0.8	0.179		2.3	56
1637−771	89	165	76	4	>2.5	II	16	0.5	0.043		2.6	25 8
1640+826	27	124	83	2	>2.5	I	14				3	76
1643+274	120	35	85		>2.5	II	15.8	0.92	0.102	25.1	2.7	59
1648+050	127	100	27		<2.5	I	19	1	0.154	28.26	2.2	20 7

doi: https://doi.org/10.52526/25792776-2021.68.1-75

1652+39	170	135	35		<2.5		13.7	0.18	0.034	24.35	1.8	81
1655+32A			50		<2.5						2.1	56
1657+325		10	5		<2.5		16.8	0.75	0.063	25.32	1.5	56
1658+302		70	10		<2.5	I	14.7	0.66	0.035	24.91	1.5	16 15
1658+326	24	10	14	2	<2.5		16.1	0.85	0.102	25.42	1.7	56
1658+32B			68		>2.5						2.6	56
1710+156	5	169	16	4	<2.5		16.7				1.5	85
1712+641	208	150	58	1	>2.5		17.3	0.74	0.081		2.8	57
1717−009	35	89	54		>2.5	II	16.8	0.71	0.03	26.7	2.6	20 4
1726+318	78	110	32		>2.5	II	15.5	0.57	0.166	26.85	2.9	16 11
1741+390		90	75		>2.5		15		0.042		2.6	16
1744+557	10	77	67	2	>2.5		13.2		0.03		2.8	13
1747+303	70	150	80		>2.5		16.7	1.17	0.13	23.96	2.9	59
1752+325	110	41	69		>2.5		14.3	0.91	0.045	24.44	2.6	59
1759+211	60	50	10	2	<2.5		17.5				2.3	89
1820+689	133	177	44	2	<2.5		15	0.7	0.131		1.5	88
1826+743	147	161	14		>2.5	II	18	0.68	0.256		2.8	17 11
1833+326	73	48	25	2	>2.5	II	14.5	0.59	0.058	26.3	2.7	17 2
1833+653	97	19	78		>2.5		17		0.161		2.6	85
1834+197	22	142	60	1	>2.5		14	0.79	0.016		2.7	13
1842+455	51	68	17		>2.5	II	15	0.7	0.091	25.73	3.2	19 2
1845+797	60	145	85		>2.5	II	14.4	0.75	0.056	26.56	5	17 2
1855+379	55	4	51		<2.5	I	14.9	0.84	0.055	25.02	1.1	15 7
1928−340	138	9	51	1.3	>2.5	II	17	0.7	0.098	26.21	3	26 16
1929−397	130	124	6	1.2	<2.5		16	0.7	0.075		2.4	26
1939+606	8	26	18		<2.5	II	18	0.71	0.201	27.4	1.9	19 2
1940+504	34	28	6	1	<2.5	I	14	0.56	0.024	25.23	1.5	17 11
1949+023	163	92	71		>2.5	II	15	0.45	0.059	26.33	2.6	20 4
1957+405	152	109	43		>2.5	II	15	0.74	0.057	25.76	2.9	17 4
2013−308	123	64	59	1.9	>2.5	I	15.4	0.86	0.089	25.33	2.8	26 7
2014−558	11	157	34		<2.5		15.5	0.7	0.061		2.2	21
2031−359	146	170	24	1.1	<2.5		15.5	0.78			1.5	26
2040−267	68	158	90	0.1	>2.5	II	13.5	0.73	0.038	24.98	3.4	20 7
2053−201	11	52	41		<2.5	I	17.8		0.156	26.29	2.4	92 7
2058−135	29	101	72	1	<2.5	II	15.5	0.81	0.046	24.89	2	21
2058−282	55	135	80	0.8	>2.5	I	14.8	0.74	0.038	25.67	3	20 7
2059−311	24	106	82	3.7	>2.5		14.5	0.5			3.5	26
2103+124	59	138	79	2	>2.5		17.3	0.56			3	85
2104−256	138	22	64		>2.5	II	16.8	0.89	0.039	25.3	3.2	26 8
2116+262	65	22	43	5	<2.5	I	14		0.016	23.57	1.8	15 7
2117+605	106	35	71	2	>2.5	II	15	0.72	0.054		2.8	19 4
2121+248		4	85		<2.5	I	15.5	0.75	0.102	27.09	2	18 2
2128−388	106	49	57	1.3	>2.5		14.4	0.64			2.7	26
2141+279	35	173	42		>2.5	II	18.5	0.86	0.215	27.31	2.9	17 2
2152−699	130	14	64		>2.5	I	13.8	0.71	0.027	26.38	2.8	54 7
2158−380	97	50	47	2.7	>2.5		14.6	0.71			2.8	26
2225−308	145	141	4	0.3	>2.5	I	15.8	0.74	0.055	24.9	4.5	26 7
2229+391	7	9	2	2	<2.5	I	13	0.58	0.017	24.93	2.2	18 2
2236−176	94	53	41	1.3	>2.5	I	15.3	0.81	0.075	25.38	3.5	26 7
2236−364	49	132	83	4.6	<2.5		15.2	0.57			1.8	26
2236+350	5	46	41		<2.5	I	15	0.58	0.028	24.4	2.4	15 15
2244+366	131	34	83		<2.5	II	16	0.8	0.082		2.2	16
2247+113	48	31	17	1	<2.5	I	14.4	0.75	0.023	25.21	2	21 2
2318+079	2	30	28	1.7	>2.5	I	12.8		0.011	23.17	2.6	67 15
2333−327	88	132	44	1.9	<2.5		14.6	0.61			1.5	26
2335+267	60	140	80		>2.5	I	13.2	0.75	0.029	25.88	4	17 2
2350−374	25	56	31	2.4	>2.5		16	0.55			3	26
2353−184	153	140	13	0.9	<2.5		16	0.78			1.3	26
2353+56	135	115	20	4	>2.5						6	63
2354−351	162	150	12	2.4	>2.5		14.4	1.2	0.049		3	26
2354+471	52	64	12	1	<2.5	I	15	0.72	0.046	24.63	2.3	28 15
2356−611	3	134	49	2	>2.5	II	16	1.36	0.096	27.79	3	54 3

doi: https://doi.org/10.52526/25792776-2021.68.1-75

3.2. *Sample 2.*

280 extragalactic radio sources with known position angles between the integrated intrinsic radio polarization and radio axes: In (Col.1 and 2) we bring Radio Source Name; (Col.3) dPA is a relative position angle between radio axis and integrated polarization; (Col.4) Ref. for the data of dPA; (Col.5) K is the ratio of major to minor axis of radio image; (Col.6) Ref. for the radio maps; (Col.7) FR the Fanaroff Riley classes; (Col.8): Ref. for the FR classes.

Table 2: Sample 2. (*In Col.4: Cl - Clarke et al., 1980, MNRAS,190,205; Ha - Haves,1975, MNRAS,173,553; Da - Davis et al., 1983, MNRAS,205,1267; PB - Birch, 1982, Nature, 298,451; Mi - Mitton, 1972, MNRAS,155,373*)

1 **Source**	2 **Name**	3 **dPA**	4 **Ref**	5 **K**	6 **Ref**	7 **FR**	8 **ref**
0002+12		73	Cl	3.5	20		
0003−00	3c2	39	Ha	2.2	30		
0007+12	4c12.03	83	Cl	2.6	20	II	5
0013+79	3c6.1	64	PB	3.5	19	II	2
0017+15	3c9	71	Cl	2.2	24	II	2
0020−25		79	Cl	1.7	20		
0031+39	3c13	69	Cl	5	27	II	2
0033+18	3c14	89	Cl	3	27	II	2
0034−01	3c15	85	Cl	2.6	27	II	1
0035+38	4c38.03	84	PB	3.6	28		
0038+32	3c19	88	Cl	2.8	27	II	2
0040+51	3c20	44	Cl	4	19	II	2
0043−42		0	PB	2.4	25	II	7
0048+50	3c22	79	Cl	5	27	II	2
0052+68	3c27	53	Cl	3.5	50	II	50
0104+32	3c31	51	Cl	2	27	I	2
0105+72	3c33.1	87	Cl	3.8	17	II	2
0106+13	3c33	73	Cl	3.4	17	II	2
0107+31	3c34	74	Cl	3.9	27	II	2
0114−47		32	Cl	2.2	21	II	3
0115+02	3c37	70	Ha	3	32		
0123+32	3c41	74	Cl	3.5	55	II	2
0125+28	3c42	60	PB	4	18	II	2
0128+25	4c25.07	22	PB	1.4	46		
0128+06	3c44	89	Cl	2.7	18		
0131−36		15	Ha	2.6	20	II	7
0132+37	3c46	87	Cl	5	17	II	2
0133+20	3c47	6	Cl	2.2	17	II	2
0134+32	3c48	43	Mi	1.5	33		
0145+53	3c52	50	Cl	2.1	17		
0152+43	3c54	43	Cl	4.5	55		
0154+28	3c55	83	Cl	3.7	24	II	2
0159−11	3c57	65	Ha	1.6	32		
0210+86	3c61.1	38	PB	4.5	17	II	2
0211+34	4c34.06	58	PB	3.5	22		
0213−13	3c62	20	Cl	2.7	80	II	7
0214−48		84	Cl	3.3	54	I	7
0219+08	3c64	73	Cl	2.4	20		
0220+39	3c65	69	Cl	3.5	55	II	2
0221+27	3c67	64	Cl	5	33	II	2
0222−00	4c-00.12	59	Cl	3.7	30		
0229+34	3c68.1	88	Cl	2.7	18	II	2
0229+35		79	PB	3	16		
0232−02	4c-02.12	58	Cl	4	30		

doi: https://doi.org/10.52526/25792776-2021.68.1-75

0234+58	3c69	88	Cl	4.5	19		
0241−51		72	Cl	2.8	21		
0241+29	4c29.08	64	PB	2.5	22		
0300+16	3c76.1	3	Cl	1.8	17	I	2
0307+16	3c79	78	Cl	4.5	29	II	2
0313+34	4c34.13	80	Cl	2.8	47		
0323+55	3c86	55	Cl	5	17		
0325+02	3c88	16	Cl	2.6	20	I	7
0336−35		76	Cl	2.4	26		
0344−34		56	Cl	2	25	I	7
0349−27	OE-283	77	PB	2.6	20	II	7
0349+26	4c26.12	77	Cl	4	22		
0356+10	3c98	19	Cl	3.5	18	II	2
0403−13	OF-105	85	Ha	2.3	48		
0404+03	3c105	80	Cl	3.5	20	II	1
0404+42	3c103	86	Cl	3.2	17		
0410+11	3c109	83	Cl	3	19	II	2
0415+37	3c111	81	PB	4	18	II	1
0427−53		84	Cl	2.9	54		
0431−133		82	PB	2.8	25		
0433+29	3c123	58	Cl	2	18	II	2
0453+22	3c132	66	Cl	1.9	18	II	2
0459+25	3c133	33	Cl	2.4	18	II	2
0501+38	3c134	87	Cl	3.4	17		
0511−48		14	Cl	1.4	21		
0511−30		46	Cl	2.7	20	II	3
0511+00	3c135	1	Cl	1.5	21	II	1
0515+50	3c137	84	Cl	5	53		
0518−45	PikA	9	Cl	2	21	II	8
0518+16	3c138	80	Ha	2.2	33		
0521+28	3c139.2	65	Cl	3.5	44		
0528+06	3c142.1	72	Cl	4.2	79		
0538+49	3c147	50	Mi	1.7	33		
0605+48	3c153	20	Cl	1.7	24	II	2
0610+26	3c154	86	Cl	5	45		
0618−37		18	Cl	2	26		
0634−20		82	PB	3.7	21	II	14
0640+23	3c165	55	Cl	4.5	20		
0651+54	3c171	16	Cl	2.7	31	II	2
0656−24		81	Cl	1.1	20		
0659+25	3c172	79	Cl	3.5	18	II	2
0702+74	3c173.1	32	Cl	2.2	17	II	2
0710+11	3c175	43	Cl	3.5	50	II	2
0711+14	3c175.1	68	Cl	2.4	27	II	2
0715−36		59	Cl	1.7	21		
0723+67	3c179	81	Cl	4	40	II	12
0724−01	3c180	18	Cl	2.1	20		
0725+14	3c181	49	Cl	2	34	II	2
0733+70	3c184	64	Cl	5	24	II	2
0734+80	3c184.1	88	Cl	3.1	17	II	2
0736−06	01-161	69	Cl	3	21		
0742+02	3c187	76	Cl	2.6	20		
0755+37	4c37.21	2	Cl	2.2	13	I	
0800−09		19	Cl	2	21		
0802+10	3c191	34	Ha	2.3	34	II	2
0802+24	3c192	49	Cl	3	18	II	2
0809+48	3c196	47	Cl	1.5	24	II	2
0814+22	4c22.20	19	Cl	2	45		
0818+47	3c197.1	22	Cl	2.6	45	II	6
0819−30		55	PB	3.1	20	II	
0819+06	3c198	57	Cl	2.7	20	II	6
0824+29	3c200	57	Cl	3.5	27	II	2
0833+65	3c204	15	PB	1.7	18	II	2

doi: https://doi.org/10.52526/25792776-2021.68.1-75

0835+58	3c205	59	Cl	2.2	18	II	2
0836+19	4c19.31	76	Cl	3	27		
0838+13	3c207	80	Cl	2.4	31	II	2
0840+29	4c29.31	48	PB	4	22		
0843−33		15	Ha	1.7	20		
0850+14	3c208	63	PB	3.5	24	II	2
0854+34	4c34.30	62	PB	1.5	22		
0855+14	3c212	85	Cl	3	18	II	2
0903+16	3c215	58	Cl	2	18	II	2
0905+38	3c217	89	Cl	2.8	27	II	2
0917+45	3c219	60	Cl	3.5	17	II	2
0927+36	3c220.2	25	Cl	2.4	27		
0931+39	4c39.26	87	PB	1.5	22		
0936+36	3c223	85	Cl	5	18	II	2
0938+39	3c223.1	30	Cl	4	16	II	4
0939+14	3c225	57	Cl	5	17	II	2
0941+10	3c226	77	Cl	4.5	18	II	2
0945+07	3c227	76	Cl	3.1	20	II	1
0947+14	3c228	81	Cl	4	18	II	2
0951+69	3c231	50	Mi	1.7	17	I	2
0958+29	3c234	68	Cl	3	17	II	2
1030+58	3c244.1	49	Cl	2.2	17	II	2
1040+12	3c245	78	Cl	3.5	27	II	2
1048−09	3c246	72	Cl	2	20		
1056+43	3c247	57	Cl	1.4	18	II	2
1059−01	3c249	81	Cl	4.5	77		
1100+77	3c249.1	88	Cl	3.5	31	II	2
1106+25	3c250	78	Cl	5	27	II	2
1107+37	4c37.29	88	PB	3.5	22	II	7
1108+35	3c252	5	Cl	1.8	17	II	2
1111+40	3c254	17	Mi	1.3	18	II	2
1136−67		76	Cl	3	21		
1136−13	OM-161	69	Cl	2.9	36		
1137+66	3c263	70	Cl	2.7	17	II	2
1140+22	3c263.1	34	Cl	2.2	24	II	2
1142+19	3c264	71	Cl	2	20	I	2
1142+31	3c265	64	Cl	3.6	50	II	2
1143−31		86	Cl	2	21		
1147+13	3c267	73	Cl	3.5	50	II	2
1157+73	3c268.1	55	Cl	4.3	19	II	2
1158+31	3c268.2	64	Cl	2.7	17	II	11
1203+64	3c268.3	83	Cl	3.2	33	II	2
1206+43	3c268.4	2	Cl	2.2	24	II	2
1211−41		6	PB	2.2	25		
1216−10		52	Cl	2.2	20		
1216+06	3c270	8	Cl	3	20	I	17,7
1218+33	3c270.1	69	Cl	2.3	27	II	2
1222+13	3c272.1	36	Cl	1.9	17	I	7
1222+21	4c21.35	43	Cl	2.8	32		
1222+42	3c272	88	Cl	4	27	II	2
1226+02	3c273	69	Cl	3	41		
1228+12	3c274	89	Cl	2	17	I	2
1232+21	3c274.1	81	Cl	2.8	17	II	2
1233+16		72	Cl	4.5	20		
1241+16	3c275.1	43	Cl	2.4	27	II	2
1249+09		82	Cl	3	51		
1251+15	3c277.2	62	PB	4	27	II	2
1251+27	3c277.3	21	Cl	1.5	19	I	15
1251−12	3c278	57	Cl	1.3	20	I	8
1253+37	4c37.35	78	PB	5	23		
1254+47	3c280	58	Cl	1.2	18	II	2
1257+38	4c38.34	77	PB	3	22		
1258+40	3c280.1	86	Cl	3.1	24	II	2

doi: https://doi.org/10.52526/25792776-2021.68.1-75

1301+38	4c38.35	68	PB	2.8	16	II	16
1308+27	3c284	80	Cl	3	17	II	2
1313+07		7	Cl	2	20		
1317−00	4c00.50	89	Cl	2.3	21		
1318+11	4c11.45	44	Cl	1.3	27		
1319+42	3c285	4	Cl	2.2	28	II	2
1328+30	3c286	37	Mi	2	38		
1330+02	3c287.1	52	Cl	1.8	20	II	7
1335−06	4c-06.35	85	Ha	2.6	32		
1343+50	3c289	78	Cl	3	27	II	2
1350+31	3c293	53	Cl	1.5	19	I	2
1352+165	3c293.1	68	Cl	2.3	21		
1354−17	op-190.4	6	Cl	2.7	21		
1354+19	4c19.44	84	Cl	3.5	35	II	12
1358−11		4	Cl	5	29	II	
1409+52	3c295	5	PB	2	31	II	2
1413−36		57	PB	3	26		
1414+11	3c296	1	Cl	1.6	20	I	2
1420+19	3c300	36	Cl	3	45	II	2
1422+20	4c20.33	65	Cl	3.4	37		
1423+24	4c24.31	75	Cl	5	32		
1425−01	3c300.1	37	Cl	2.1	21		
1441+52	3c303	61	Cl	2.2	19	II	2
1449−12		87	Cl	2.2	20		
1458+71	3c309.1	45	Ha	2	33		
1502+26	3c310	54	Cl	3.3	13	I	2
1508+08	3c313	55	Cl	2.6	17	II	7
1511+26	3c315	72	Cl	1.4	18	I	2
1512+37	4c37.43	79	Cl	3.5	49		
1514+00	4c00.56	28	Cl	3.1	20	II	
1522+54	3c319	45	Cl	3.5	14	II	2
1529+24	3c321	64	Cl	3.2	44	II	2
1529+35	3c320	46	PB	1.5	18	II	7
1545+21	3c323.1	72	Cl	3.4	19	II	11
1547+21	3c324	80	Cl	5	39	II	2
1549+62	3c325	44	Cl	1.4	18	II	2
1549+20	3c326	88	Cl	5	18	II	2
1553+20	3c326.1	56	PB	1.5	27		
1556−21		15	Cl	1.7	21		
1559+02	3c327	70	Cl	2.9	20	II	4
1602−63		8	Cl	1.9	21		
1602−09		90	Cl	2.8	20		
1609+66	3c330	69	Cl	2.7	17	II	2
1610−608		22	PB	3.4	54	II	
1615+32	3c332	75	Cl	3	19	II	7
1618+17	3c334	81	Cl	3	27	II	2
1622+23	3c336	80	Cl	2.2	18	II	2
1626+27	3c341	86	Cl	3.7	17	II	2
1626+39	3c338	85	PB	3.2	82	I	2
1627+23	3c340	87	Cl	4	27	II	2
1627+44	3c337	36	Cl	1.8	17	II	2
1634+26	3c342	78	Cl	3	22		
1637−77		41	PB	2.6	25	II	8
1641+17	3c346	79	Cl	2	31	II	7
1641+39	3c345	76	Ha	2.2	43	II	13
1648+05	3c248,HerA	78	Ha	2.2	20		
1658+47	3c349	74	Cl	3	17	II	2
1704+61	3c351	19	PB	2.3	18	II	2
1709+46	3c352	77	Cl	2.8	27	II	2
1717−00	3c353	5	Cl	2.6	20	I	7
1723+51	3c356	30	Cl	3.5	50	II	2
1726+31	3c357	61	PB	2.9	16	II	11
1730−13		26	Cl	1.5	41		

doi: https://doi.org/10.52526/25792776-2021.68.1-75

1733−56		83	PB	5	80	II	7
1737−60		85	PB	2.6	25		
1826+74	3c379.1	50	Cl	2.8	17	II	11
1832+47	3c381	67	Cl	3.3	19	II	2
1836+17	3c386	13	Cl	1.5	18	I	2
1842+45	3c388	63	PB	3.2	19	II	2
1845+79	3c390.3	53	Cl	5	17	II	2
1938−155	OV-164	74	Da	1.8	80		
1939+60	3c401	38	PB	1.9	19	II	2
1949+02	3c403	37	Cl	2.6	20	II	4
2014−55		47	Cl	2.2	21		
2018+29	3c410	51	Cl	1.5	44		
2019+09	3c411	60	Cl	2.6	31		
2040−26		2	Cl	3.4	20	II	7
2058−28		68	Cl	3	20		
2104−25	OX-208	39	Cl	3.2	26	I	7
2104+76	3c427.1	89	Cl	3.4	19	II	2
2106+49	3c428	83	Cl	5	50		
2117+60	3c430	55	Cl	2.8	19	II	4
2121+24	3c433	21	Cl	2	18	I	2
2130−53		53	Cl	1.1	21	I	7
2135−14	OX-158	77	Cl	1.7	20	II	8
2141+27	3c436	3	Cl	2.9	17	II	2
2145+15	3c437	69	Cl	3.5	18	II	2
2153−69		67	PB	1.5	21		
2153+37	3c438	47	PB	2.3	19	I	7
2203+29	3c441	32	Cl	2	18	II	2
2211−17	3c444	12	Cl	2.2	20	II	7
2212+13	3c442	83	Cl	3	18		
2221−02	3c445	67	Cl	2.7	21	II	1
2229+39	3c449	73	Cl	2.2	18	I	2
2239+33		74	PB	2.8	16		
2243+39	3c452	77	Cl	5	17	II	2
2247+11		24	Cl	2	21	I	2
2251+15	3c454.3	72	Ha	2.8	43		
2252+12	3c455	80	Cl	3	38	II	2
2310+05	3c458	23	Cl	2.4	20		
2314+038	3c459	85	Da	3.3	52	II	7
2317−27		85	PB	2.7	25	II	7
2318+23	3c460	65	Cl	4.5	24	II	2
2335+26	3c465	78	Cl	4	17	I	2
2345+18	3c467	45	Cl	3	31		
2352+79	3c469.1	87	Cl	3.2	17	II	2
2354−11		62	Cl	2.4	21		
2356−61		66	Cl	3	54	II	3
2356+27	4c27.54	78	PB	4	22		
2356+43	3c470	86	Cl	5	45	II	2

References

Ambartsumian V. A., 1966, Transactions of the IAU, 12B, Academic Press, London-New York, 672

Andreasyan R. R., 1984, Ap., 19, 245

Andreasyan R. R., 2019, Communications of the Byurakan Astrophysical Observatory (ComBAO), 66, 8

Andreasyan R. R., Sol H., 1999, Ap., 42, 275

Andreasyan R. R., Sol H., 2000, Ap., 43, 413

Andreasyan R. R., Appl S., Sol H., 2002, Ap., 45, 198

Fanaroff B. L., Riley J. M., 1974, MNRAS, 167, 31

Gendre M., Wall J. V., Best P. N., 2011, AAS, 21831702G

Gopal K., Wiita P. J., 2000, A&A, 507, 363

Zirbel E. S., Baum S. A., 1995, ApJ, 52, 448

doi: https://doi.org/10.52526/25792776-2021.68.1-75

Appendices

LITERATURE for radio-maps and FR classes.

1) Hardcastle, M.J., Alexander,P., Pooley, G.G., Riley,J.M.,1998, MNRAS, 296, 445
2) Laing, R.A., Riley, J.M., Longair, M.S., 1983, MNRAS, 204, 151
3) Subrahmanyan, R., Saripalli, L., Hunstead, W., 1996, MNRAS, 279, 257
4) Leahy, J.P., Black,A.R.S., Dennet-Thorpe,J., et al., 1997, MNRAS, 291, 20
5) Hardcastle, M.J., Alexander,R., Pooley,G.G., Riley,J.M., 1997, MNRAS, 288, 859
6) Black, A.R.S., Baum,S.A., Leahy,J.P., et al., 1992, MNRAS, 256, 186
7) Zirbel, L.E. Baum, S.A., 1995, ApJ, 448, 521
8) Morganti, R., Killeen,N.E.B., Tadheunter,C.N., 1993, MNRAS, 263, 1023
9) Pearson,T.J., Readhead,A.C.S., 1988, ApJ, 328, 114
10) Nilsson, K. 1998, A&AS, 132, 31
11) Fanaroff, B.L. & Riley, J.M., 1974, MNRAS, 167, 31p
12) Peacock,J.A., Wall,J.V., 1981, MNRAS, 194, 331
13) Bridle,A.H., Fomalont,E.B., 1978, AJ, 83, 704
14) Fomalont,E.B, Bridle,A.H., 1978, AJ, 83, 725
15) Fanti,C., Fanti,R., Gioia,J.H., et al, 1977, A&AS.,29,279
16) Rudnick,L., Adams,M.T., 1979, AJ, 84, 437
17) Macdonald,G.H., Kenderdine,S., Neville,A.C. 1968, MNRAS, 138, 259
18) Mackay,C.D., 1969, MNRAS, 145, 31
19) Branson,N.J.B.A., Elsmore,B., Pooley,G.G., Ryle,M., 1972, MNRAS, 156, 377
20) Fomalont,E.B., 1971, AJ, 76, 513
21) Schilizzi,R.T., McAdam,W.B., 1975, Mem. R. Astron. Soc., 79, 15
22) Conway,R.G., Burn,B.J., Vallee,J.P., 1977, A&AS., 27, 155
23) Machalski,J., Maslowski,J., Condon,J.J., Marlene,A., 1982, AJ, 87, 1150
24) Laing,R.A., 1981, MNRAS, 195, 261
25) Ekers,R.D., 1969, Aust. J. Phys. Astrophys. Suppl., 6, 3
26) Ekers,R.D., Wall,J.V., Shaver,P.A., et al, 1989, MNRAS, 236, 737
27) Jenkins,C.J., Pooley,G.G. Riley,J.M., 1977, Mem.R. Astron. Soc., 84, 61
28) Vigotti,M., Grueff,G., Perley,R., et al, 1989, AJ, 98, 419
29) Antonucci,R.R.J., 1985, ApJS., 59, 499
30) Dunlop,J.S., Peacock,J.A., Savage,A., et al, 1989, MNRAS, 238, 1171
31) Pooly,G.G., Henbest,S.H., 1974, MNRAS, 169, 477
32) Hintzen,P., Ulvestad,J., Owen,F., 1983, AJ, 88, 709
33) Van Breugel,W., Miley,G., Heckman,T., 1994, AJ, 89, 5
34) Barthel,P.D., Miley,G.K., Schilizzi,R.T., Lonsdale,C.J., 1988, A&AS, 73, 515
35) Saikia,D.J., Shastri,P., Sinha,R.P., et al, 1984, JA&A, 5, 429
36) Saikia,D.J., Shastri,P., Cornwel,T.J., et al, 1989, JA&A, 10, 203
37) Saikia,D.J., Kulkarni,I.V.K. & Porcas,R.W., 1986, MNRAS, 219, 719
38) Spencer,R.E., McDowel,J.C. & Charlesworth,M., 1989, MNRAS, 240, 657

doi: https://doi.org/10.52526/25792776-2021.68.1-75

39) Fernini,I., Burns,J.O., Bridle,A.H. & Perley,R.A., 1993, AJ, 105, 1690

40) Owen,F.N. & Puschel,J.J., 1984, AJ, 89, 932

41) Perley,R.A., Fomalont,E.B. & Jonston,K.J. 1980, AJ, 85, 649

42) Perley,R.A., Fomalont,E.B. & Jonston,K.J., 1982, ApJ, 255, L93

43) Browne,I.W.A., Orr,M.J.L., Davis,R.J., et al, 1982, MNRAS, 198, 673

44) Hogbom,J.A. & Carlsson,I., 1974, A&A, 34, 341

45) Riley,J.M. & Pooley,G.G., 1975, Mem. R. Astron. Soc., 80, 105

46) Grueff,G. Kotanyi,C., Schiavo-Campo,P., et al, 1981, A&AS, 44, 241

47) Gerhardt,M.R., 1977, Nat, 266, 819

48) Wardle,J.F.C., Moore,R.L. & Angel,J.R.P., 1984, ApJ, 279, 93

49) Potash,R.I. & Wardle,J.F.C., 1979, AJ, 84, 707

50) Leahy,J.P. Muxlow,T.W.B. & Stephens,P.W., 1989, MNRAS, 239, 401

51) Ulvestad,J., Johnston,K., Perley,R.& Fomalont,E., 1981, AJ, 86, 1010

52) Ulvestad,J.S., 1985, ApJ, 288, 514

53) Poley,G.G., Leahy,J.P., Shakeshaft,J.R. & Riley,J.M., 1987, MNRAS, 224, 847

54) Christiansen,W.N., Frater,R.H., Watkinson,A., et al, 1977, MNRAS, 181, 183

55) Longair, M.S., 1975, MNRAS, 173, 309

56) Riley, J.M., 1975, MNRAS, 170, 53

57) Slingo, A., 1974, MNRAS, 168, 307

58) Miley, G.K., Perola, G.C., Van der Kruit, P.C., Van der Laan, H., 1972, Nat, 237, 269

59) Fanti, R., Gioia, J., Lary, C., & Ulrich, M.-H., 1978, A&AS, 34, 341

60) Ekers, R.D., Fanti, R., Lary, C., & Ulrich, M.-H., 1978, A&A, 69, 253

61) Fanti, C., Fanti, R., Feretti, L., et al, 1983, A&AS, 51, 179

62) Machalsky, J., & Condon, J.J., 1983, AJ, 88, 143

63) Birkinshaw, M., & Davies, R.L., 1985, ApJ, 291,32

64) Ekers, R.D. & Simkin, S.M., 1983, ApJ, 265, 85

65) Jones, D.L., Wrobel, J.M., & Shaffer, D.B., 1984, ApJ, 276, 480

66) Ekers, R.D., Kotanyi, C.G., 1978, A&A, 67, 47

67) Jenkins, C.R., 1982, MNRAS, 200, 705

68) Parma,P., de Ruiter,H.R., Fanti,c., Fanti,R., 1986, A&AS, 64, 135

69) de Ruiter,H.R., Parma,P., Fanti,c., Fanti,R., 1986, A&AS, 65, 111

70) Fanti,C., Fanti,R., de Ruiter,H.R., Parma,P., 1986, A&AS, 65, 145

71) Fanti,R., Fanti,C., de Ruiter,H.R., Parma,P., 1987, A&AS, 69, 57

72) Ekers,R.D., Fanti,R., Lari,C., Parma,P., 1981, A&A, 101, 194

73) Barthel,P.D., Scilizzi,R.T., Miley,G.K., et al., 1985, A&A, 148, 243

74) O'Dea,P. & Owen, F.N., 1985, AJ, 90, 927

75) Wrobel, J.M., Simon, R.S., 1986, ApJ., 309, 593

76) Mack,K.-H., Klein,U., O'Dea,C.P., Willis,A.G., 1997, A&AS, 123, 423

77) Rhene,G., Marvel,K., Wilson,T., et al., 1996, ApJS, 107, 175

78) Law-Green,J.D., Leahy,J.P., Alexander,P., et al., 1995, MNRAS, 274, 939

doi: https://doi.org/10.52526/25792776-2021.68.1-75

79) Bogers,W.J., Hes,R., Barthel,P.D., Zensus,J.A., 1994, A&AS, 105, 91

80) Colina,L., De Juan, 1995, ApJ, 448, 548

81) Van Breugel,W., Schilizzi,R., 1986, ApJ, 301, 834

82) Capetti,A., Morganti,R., Parma,P., Fanti,R., 1993, A&AS, 99, 407

83) Rudnik,L., & Owen,F.N., 1977, AJ, 82, 1

84) Pacholczyk, A.G., 1978, A handbook of radio sources

85) Fomalont,E.B., Palimaka,J.J., Bridle,A.H., 1980, AJ, 85, 981

86) Burns,J.O., & Owen,F.N., 1979,AJ, 84, 1478

87) Owen,F.N., White,R.A., Burns,J.O., 1992, ApJS, 80, 501

88) Owen,F.N., White,R.A., Ge JingPing, 1993, ApJS, 87, 135

89) Saikia,D.J., Wiita,P.J., Cornwell,T.J., 1987, MNRAS, 224, 53

90) Perola, G.C. & Valentijn, E.A., 1979, A&A, 73, 54

91) Valentijn, E.A. & Perola, G.C., 1978, A&A, 63, 29

92) Hazard, C., 1972, Astrophys. Letters, 11, 139

93) Allington-Smith, J.R.A., Ellis, R.S., Zirbel, E.L., 1993, ApJ, 404, 521.

doi: https://doi.org/10.52526/25792776-2021.68.1-75

Communications of BAO, Vol. 68, Issue 1, 2021, pp. 90-96

Condensations Expelled from the Stars, and Pairs of Stars, Connected with Bright Filaments

A.L. Gyulbudaghian*[1] and R.A. Mendezz†[2]

[1]Byurakan Astrophysical Observatory, Armenia,
[2]Departamento de Astronomia, Universidad de Chile, Chile

Abstract

During several surveys of high-quality film-copies of the ESO B, R, ESO/SRC J, and EJ plates, except other young unstable objects (HH objects, star-forming regions, cometary nebulae) were found also two types of other unstable objects. 1. Bright condensations, connected with stars by bright filaments. 2. Pairs of stars, connected with each other by bright filaments. The objects of first type are mostly seen in infrared, on 2MASS K images. Due to their infrared colours, two of condensations and half of all stars can have thick dust discs.

Keywords: *stars: star-forming regions, expelled condensations, pairs of stars*

1. Introduction

During several surveys of Southern Hemisphere many types of interesting young nebular objects were found. These types are as follows. 1. Herbig-Haro objects. 2. Cometary nebulae. 3. Star-forming regions. 4. Tight trapezium-type systems, consisting of young stars (Gyulbudaghian et al., 2004). 5. Radial systems of dark globules (Gyulbudaghian & Mendez, 2015). 6. Saw-type ionized shock fronts (Gyulbudaghian, 2019a).We have done a systematic inspection of high-quality film-copies of the ESO B, R, ESO/SRC J, and EJ plates. We looked at all the Southern plate prints, but the final detailed search we concentrated mainly on places, where dark clouds could be easily identified on the prints.

In this paper we present the results of discovering (during the surveys) also of two other types of interesting objects. 1. Bright condensations, connected with stars by bright filaments (jets?). 2. Pairs of stars, connected by bright filaments. These two types of objects are very interesting and their further investigation will be very useful.

2. Condensations, Expelled from the Stars

1. Object CLN 70 (Gyulbudaghian, 2011). This object on DSS2 R image is a pair of stars, connected with a filament (see Figure 1). Each star is connected with a condensation by a filament. The data on condensations are summarized in Table 1 (N1 and N2) and on stars in Table 2 (N1 and N2). We can see in Table 1, that condensation N1 has only R colour, hence it can be an HH object.

2. The star SAO 235903 (HD 70584, B8/9V). On DSS2 R image it is a bright nebular star (N3 in Table 2), on 2MASS K image it is a star with two condensations (N3 and N4 in Table 1) on one straight filament (the condensations are seen also on DSS2 R image).These images are presented in Figure 2.

3. Star-forming region SFR 2 (Gyulbudaghian, 2019a). This object is well seen on 2MASS K image. With the star (N4 in Table 2) two condensations (N5 and N6 in Table 1) are connected with bright filaments (see Figure 3).

*agyulb@bao.sci.am, Corresponding author
†rmendez@u.uchile.cl

doi: https://doi.org/10.52526/25792776-2021.68.1-90

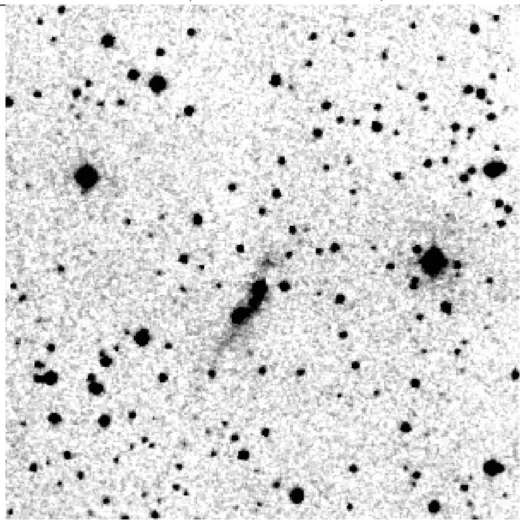

Figure 1. DSS2 R image of CLN70. The sizes of this and other images are 6´ x 6´. For this and other images N is to the top, E is to the left.

Table 1. Data on condensations, connected with stars by filaments

NN	α(2000)	δ(2000)	B	B-V	R	J	J-H	H-K	Q
1	06^h 00^m 04.72^s	32° 06´ 44¨	-	-	18.200	-	-	-	-
2	06 00 07.76	32 05 26	19.75	2.25	17.870	15.215	0.616	0.254	0.184
3	08 20 35.90	-50 18 59	-	-	-	13.836	0.757	0.311	0.228
4	08 20 36.54	-50 19 05	-	-	12.820	14.151	0.895	0.275	0.427
5	08 58 37.72	-42 32 11	20.84	-	-	16.077	1.048	0.462	0.263
6	08 58 37.72	-42 32 16	-	-	-	16.390	1.233	0.744	-0.032
7	10 35 25.35	-59 14 48	-	-	-	13.583	0.853	0.384	0.200
8	10 35 25.64	-59 14 52	-	-	-	14.842	1.051	0.487	0.223
9	10 38 36.62	-58 02 38	-	-	-	13.657	0.456	0.227	0.070
10	10 38 36.85	-58 02 43	-	V=16.690	-	15.221	0.613	0.499	-0.228
11	15 03 25.36	-63 23 20	-	-	19.670	14.353	1.582	0.889	0.071
12	17 58 33.86	-26 07 24	-	-	-	17.399	3.207	2.086	-0.339

4. Object vdBH 40b (van den Bergh & Herbst, 1975). The star (N5 in Table 2, B2II) on DSS2 R image has a bright reflection nebula. On 2MASS K image there are two condensations (N7 and N8 in Table 1), connected with the star by a straight filament (see Figure 4).

5. The star SAO 238289 (HD 92383, B0.5 Vn, object N6 in Table 2) on DSS2 R image has a bright reflection nebula. On 2MASS K image two condensations (N9 and N10 in Table 1) are on the straight filament,connected with the star. This filament is seen also on DSS2 R image (see Figure 5).

6. The star DG Cir. The star (N7 in Table 2) on DSS2 R image is a single star, on 2MASS K image has a filament, with a condensation (object N11 in Table 1) at the end (see Figure 6).

7. Star-forming region HHL 59 (Gyulbudaghian & Mendez, 2014). On the DSS2 R image there are two stars with a bright nebulosity, on the 2MASS K image there is a compact bright nebula (with embedded IR stars) with filaments and condensations at the ends of filaments. The star N8 (see Table 2) has a condensation N12 (see Table 1), connected with a filament (see Figure 7).

In Table 1 are summarized the data on condensations. In column 1 is presented the number of condensations, in columns 2 and 3 – their coordinates, in columns 4 – 9 – the colours of stars, in column 10 — reddening free quantity Q = (J-H) – 1.70(H-K). Values of Q < -0.10 are indicative of an IR excess consistent with a dust disc (Comerón et al., 2005). It is possible to see from Table 1, that there are only two objects with Q < -0.10: objects N10 and N12.

doi: https://doi.org/10.52526/25792776-2021.68.1-90

Table 2. Data on condensations, connected with stars by filaments

NN	α(2000)	δ(2000)	B	B-V	R	J	J-H	H-K	Q
1	$06^h00^m05.15^s$	32° 06´ 26¨	15.030	0.450	13.60	13.235	0.941	2.143	-2.702
2	06 00 06.35	32 06 06	16.240	2.250	14.42	13.17	0.677	0.215	0.311
3	08 20 34.83	-50 18 50	9.354	0.298	9.05	8.276	0.047	0.275	-0.217
4	08 52 39.51	-42 31 59	-	-	20.53	13.919	1.477	0.635	0.397
5	10 35 26.17	-59 14 59	10.624	0.356	10.04	9.11	0.079	0.17	-0.21
6	10 38 36.37	-58 02 29	9.356	0.039	9.30	9.092	0.059	0.057	-0.038
7	15 03 23.80	-63 22 59	13.630	0.500	12.42	9.75	1.004	0.924	-0.587
8	17 58 34.09	-26 06 56	19.650	2.470	15.20	10.048	2.265	1.817	-0.823

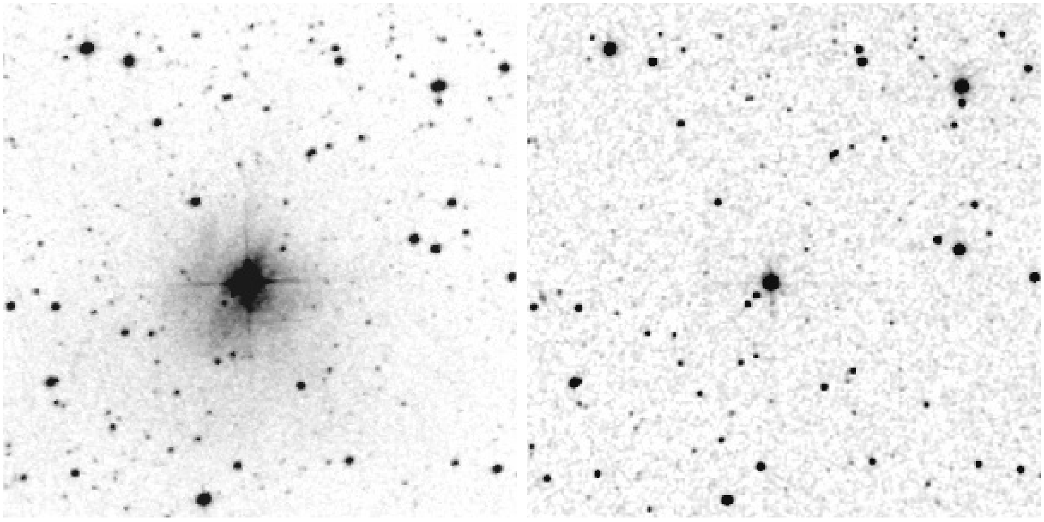

Figure 2. *Left panel:* DSS2 R image of the nebular star SAO 235903. Right panel: 2MASS K image of the nebular star SAO 235903.

3. Stars, connected with bright filaments

In Table 2 the data on stars, connected with condensations, are given. In column 1 is the number of stars, in columns 2 and 3 — their coordinates, in columns 4 – 9 – the colours of stars, in column 10 — the reddening free quantity Q. From Table 2 it is possible to see, that there are 5 objects with Q < -0.10. Hence, more than half of stars in the table can have dust discs.

1.Star-forming region CLN 70 (Gyulbudaghian, 2011). As is already mentioned above, on DSS2 R image there are two stars, connected with a bright filament (see Figure 1). Star N1 has a large negative value of Q, hence it has a thick dust disc, but star N2 has a positive value of Q, it has no dust disc (see Table 3).

2.Star-forming region SFR 3 (Gyulbudaghian, 2019a). On the DSS2 R image there is a pair of stars (N5 and N6 in Table 3, see Figure 8, left panel), connected with a pair of filaments. Both stars have large negative values of Q, hence they have thick dust discs. On the 2MASS J image there is again a pair of stars (N3 and N4 in Table3), connected with a pair of filaments (see Figure 8, right panel). Both stars have positive values of Q, they have no dust disc.

3.Two stars (N7 and N8 in Table 3), connected with a bright filament on the DSS2 B image (see Figure 9), in other colours the filament is absent. Both stars have positive values of Q – they have no dust disc.

4.Star-forming region HHL 59 (Gyulbudaghian & Mendez, 2014). Two stars (N9 and N10 in Table 3), connected with a pair of filaments (better seen on the image, obtained with SII filter, see Figure 3, left panel in Gyulbudaghian & Mendez (2014)). Both stars have large negative values of Q, hence they have thick dust discs.

In Table 3 the data on stars in pairs are given. In column 1 the number of stars is given, in columns 2 and 3 — their coordinates, in columns 4 – 9 - the colours of stars, and in column 10 — the reddening

doi: https://doi.org/10.52526/25792776-2021.68.1-90

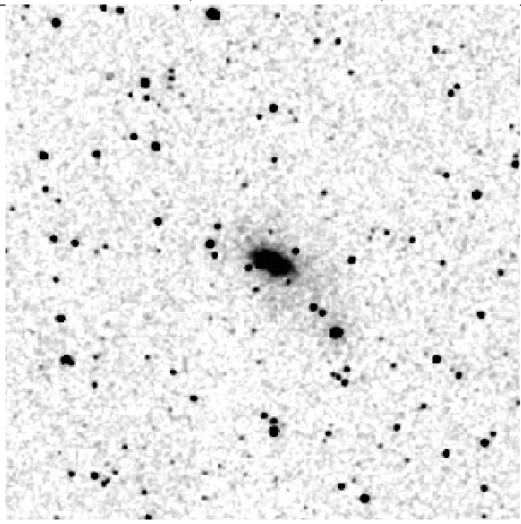

Figure 3. 2MASS K image of the star-forming region SFR 2.

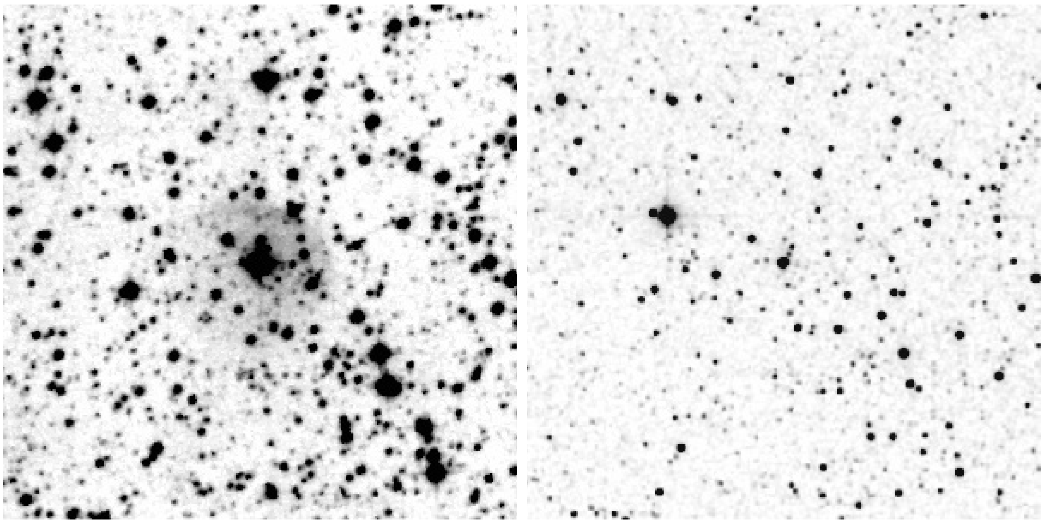

Figure 4. *Left panel:* DSS2 R image of vdBH 40b. Right panel: 2MASS K image of vdBH 40b.

free quantity Q. We can see, that there are 5 objects with $Q < -0.10$, hence half of the stars in the table can have dust discs.

4. Conclusion

As a result of searches on the high-quality film-copies of the plates of the Southern Hemisphere, except of several types of unstable objects, two other types of objects were also found. 1. Stars, connected with the condensation by a bright filament. Eight such objects were found, in four of them the stars are connected with two condensations, in others with one condensation. There is an opportunity, that the condensations were expelled from the stars. Almost all the condensations of these objects are seen only on the 2MASS K images. Two condensations and half of stars have infrared colours, typical for stars with thick discs. Three stars have spectral class B. 2. The pairs of stars, connected with each other by bright filaments. There are arch-shaped and also straight filaments. One of the filaments is seen only on DSS2 B image. Half of the stars have infrared colours, typical for stars with thick dust discs.

doi: https://doi.org/10.52526/25792776-2021.68.1-90

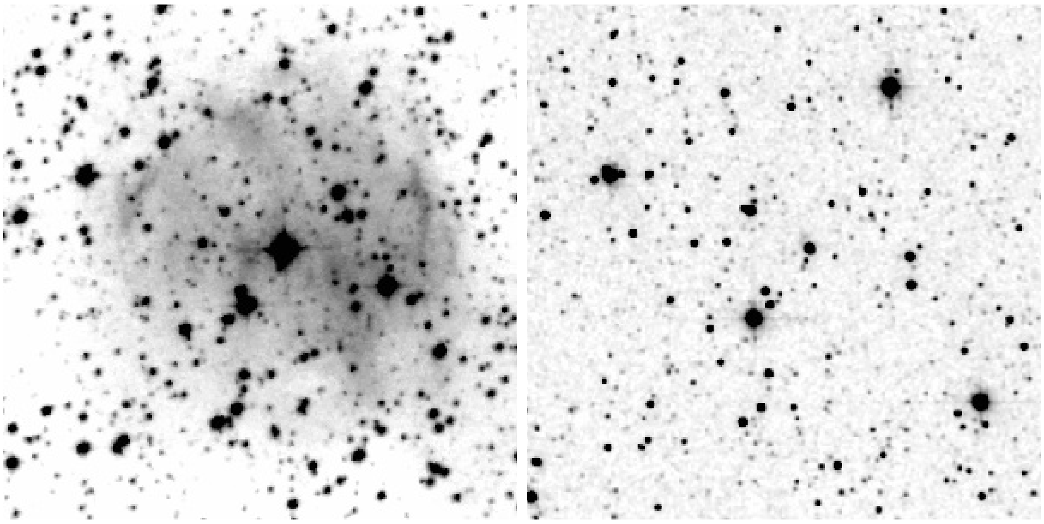

Figure 5. *Left panel:* DSS2 R image of the nebular star SAO 238289. Right panel: 2MASS K of the nebular star SAO 238289.

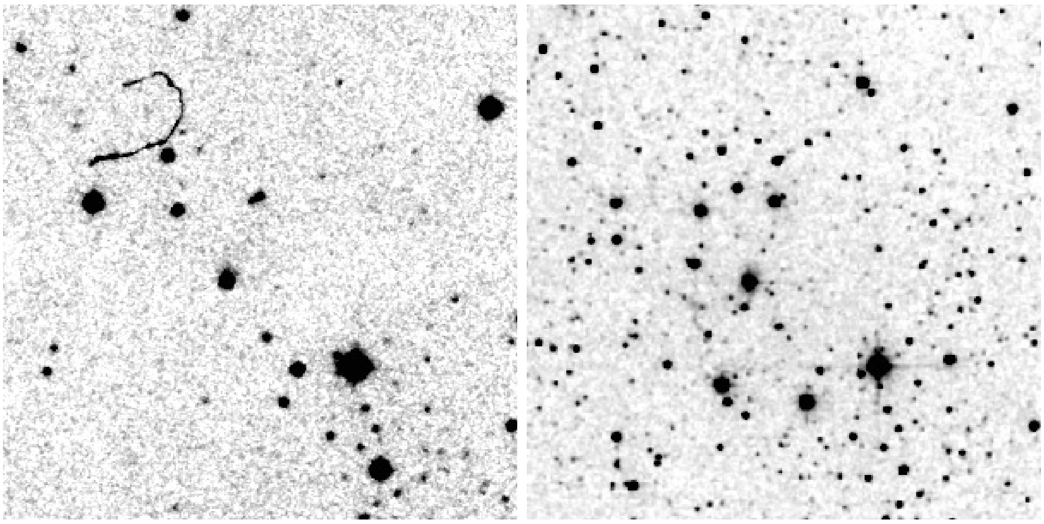

Figure 6. *Left panel:* DSS2 R image of the star DG Cir. Right panel: 2MASS K of the star DG Cir.

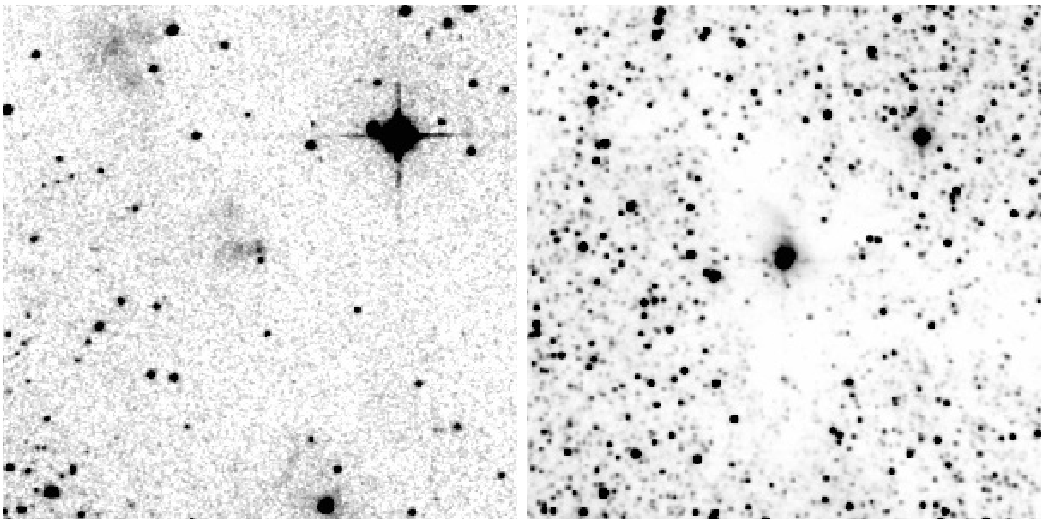

Figure 7. *Left panel:* DSS2 R image of the star-forming region HH L59. Right panel: 2MASS K of the star-forming region HH L59.

doi: https://doi.org/10.52526/25792776-2021.68.1-90

Table 3. Data on the components of pairs of stars, in which the components are connected with each other by bright filaments

NN	α(2000)	δ(2000)	B	B-V	R	J	J-H	H-K	Q
1	06^h00^m 05.15^s	32° 06´ 26¨	15.03	0.45	13.6	13.235	0.941	2.143	-2.702
2	06 00 06.35	32 06 06	16.24	2.25	14.42	13.17	0.677	0.215	0.311
3	08 22 51.67	-42 07 49	-	-	-	14.576	1.955	1.516	-0.622
4	08 22 51.91	-42 08 03	-	-	-	14.342	0.893	1.591	-1.812
5	08 22 52.84	-42 07 30	16.28	-0.8	14.72	13.17	0.857	0.496	0.014
6	08 22 52.84	-42 07 46	16.64	0.32	15.08	14.939	1.449	-0.369	2.076
7	08 27 37.36	-51 09 50	19.83	-	17.13	13.48	1.02	0.435	0.28
8	08 27 39.51	-51 06 45	16.01	1.12	14.27	13.063	0.474	0.149	0.221
9	17 58 34.09	-26 06 56	19.65	2.47	15.2	10.042	2.265	1.817	-0.823
10	17 58 34.23	-26 06 51	16.37	-0.54	12.48	11.476	1.942	1.439	-0.504

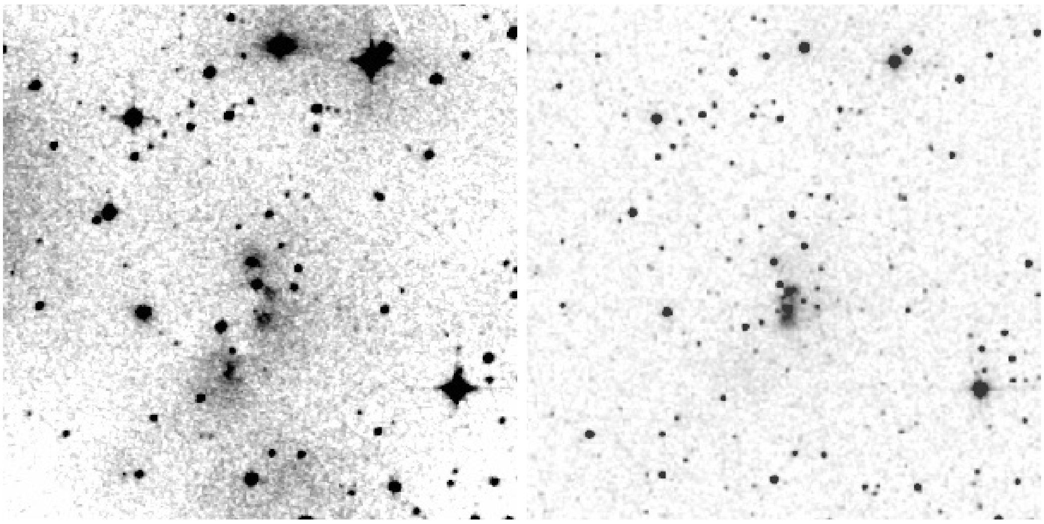

Figure 8. *Left panel:* DSS2 R image of the star-forming region SFR 3. Right panel: 2MASS K of the star-forming region SFR 3.

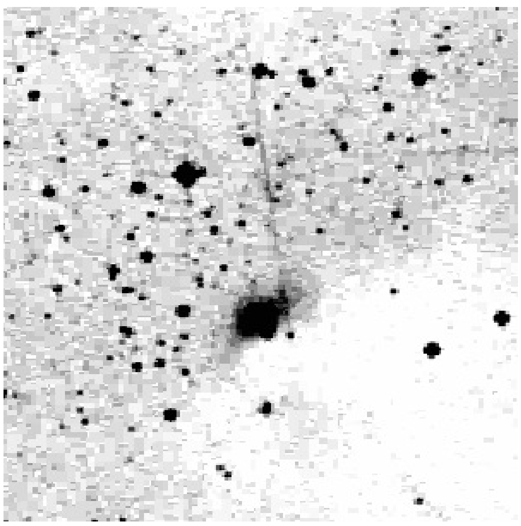

Figure 9. DSS2 B image of two stars, connected with a filament.

doi: https://doi.org/10.52526/25792776-2021.68.1-90

References

Comerón F., Schneider N., Russeil D., 2005, Astron. Astrophys. , 433, 955

Gyulbudaghian A. L., 2011, Astrophysics, 54, 476

Gyulbudaghian A. L., 2019a, Astrophysics, 62, 360

Gyulbudaghian A. L., 2019b, Communications of the Byurakan Astrophysical Observatory, 66, 20

Gyulbudaghian A. L., Mendez R. A., 2013, Astrophysics, 56, 531

Gyulbudaghian A. L., Mendez R. A., 2014, Astrophysics, 57, 520

Gyulbudaghian A. L., Mendez R. A., 2015, Rev. Mex. Astron. Astrofis. , 51, 183

Gyulbudaghian A. L., May J., González L., Méndez R. A., 2004, Rev. Mex. Astron. Astrofis. , 40, 137

van den Bergh S., Herbst W., 1975, Astron. J. , 80, 208

doi: https://doi.org/10.52526/25792776-2021.68.1-90

Communications of BAO, Vol. 68, Issue 1, 2021, pp. 97-104

BAO Plate Archive Project: Recent Results

G. A. Mikayelyan*, G. M. Paronyan, N. M. Azatyan, G. R. Kostandyan, A. L. Samsonyan, H. R. Andreasyan, H. V. Abrahamyan, D. H. Andreasyan, A. G. Suqiasyan, and A. M. Mickaelian

NAS RA V. Ambartsumian Byurakan Astrophysical Observatory (BAO)

Abstract

We present the recent results of the Byurakan Astrophysical Observatory (BAO) Plate Archive Project that is aimed at digitization, extraction and analysis of archival data and building an electronic database and interactive sky map. BAO Plate Archive consists of some 37,000 photographic plates and films, obtained with 2.6m telescope, 1m and 0.5m Schmidt telescopes and other smaller ones during 1947-1991 and then by digital methods since 1996. Its most important part, the famous Markarian Survey (or the First Byurakan Survey, FBS) 1874 plates were digitized in 2002-2007 and the Digitized FBS (DFBS, www.aras.am/Dfbs/dfbs.html) was created. New science projects have been conducted based on this low-dispersion spectroscopic material. Several other smaller digitization projects have been carried out as well, such as part of the Second Byurakan Survey (SBS) plates, photographic chain plates in Coma, where the blazar ON 231 is located and 2.6m film spectra of FBS Blue Stellar Objects. However, most of the plates and films were not digitized. In 2015, we have started a project on the whole BAO Plate Archive digitization, creation of electronic database and its scientific usage. Armenian Virtual Observatory (ArVO, www.aras.am/Arvo/arvo.htm) database will accommodate all new data. The project lasted 4 years in 2015-2018. Later on, the project was renovated for 2020-2021. The final result will be an Electronic Database and online Interactive Sky map to be used for further research projects.

Keywords: *photographic plates – photographic films – digitization – astrometry – photometry – spectroscopy – astronomical archives – databases – virtual observatories*

1. Introduction

The astronomical plate archives created on the basis of numerous observations at many observatories are the most important part of the astronomical observational heritage. The necessity of digitization of astronomical plates was emphasized and current progress in various national and international projects was given at Astroplate workshops (e. g. Hudec 2014, Kazantseva 2014, Nesci et al. 2014, Osborn 2014, Stupka & Benesova 2014).

Byurakan Astrophysical Observatory (BAO) Plate Archive is one of the largest astronomical archives in the world and is considered to be BAO main observational treasure. It is the results of decades' hard work of Armenian astronomers and the work of BAO telescopes and other expensive equipment, as well as the results of their activities. Today BAO archive holds some 37,000 astronomical plates, films or other carriers of observational data. However, previous observational and informational registration methods currently do not make it available to wide range of scientists, and especially its usage for solution of new research problems. Digitization of BAO plates is a significant contribution to the Wide-Field Plate Data Base (WFPDB) developed in Sofia, Bulgaria (Tsvetkov & Tsvetkova, 2012).

A project on Digitization of BAO Plate Archive and creation of BAO Interactive Astronomical Database (shortly BAO Plate Archive project, BAO PAP) has started in February 2015. It was aimed at preservation of BAO valuable observational material accumulated during 1947-1991, creation

*gormick@mail.ru

doi: https://doi.org/10.52526/25792776-2021.68.1-97

of full Database of all BAO observations, creation of BAO Interactive Sky Map with visualization of all observations and quick access to the data, development and accomplishment of new research projects based on the existing observational material, and integration of BAO observations into the international databases. A number of BAO young astronomers were involved in this project and it lasted 4 years. Later on, the project was renovated for 2020-2021 to complete the full tasks. Project objectives are the preservation of BAO observational archive, preservation of scientific information contained in photographic plates and other careers, creation of opportunity of dissemination and wide usage of observational data, putting in correspondence of observational material to modern standards and usage methods, proposing new science projects and creation of possibility of their further accomplishment, and making BAO activities visible.

A short description of BAO Plate Archive was given by Mickaelian (2014) and more detailed papers are given in Mickaelian et al. (2016, 2017, 2020).

2. BAO telescopes and observing programs

BAO observers worked with a number of BAO telescopes during 1947-1991 and obtained several dozens of thousands of plates, films and other products. The table gives general understanding on observations of 10 BAO telescopes that worked on photographic photometry, electrophotometry, slit and objective prism spectroscopy, and polarimetry of many thousands astronomical objects.

Table 1. Overview of BAO telescopes and produced observational material.

Telescopes	**Sizes** (cm)	**Years**	**Observing methods**	**Plates**
5” double–astrograph	13/	1947–1950	photometry	3000
6” telescope	15/	1947–1950	photometry	3000
8” Schmidt	20/20/31	1949–1968	photometry	4500
20” Cassegrain (AZT-14)	51/400	1955–1991	electropolarimetry	n/a
10” telescope–spectrograph	25/	1953–19??	spectroscopy	n/a
Nebular spectrograph (ASI-1)	n/a	1953–19??	spectroscopy	n/a
16” Cassegrain	41/800	1952–1991	electrophotometry	n/a
21” Schmidt (AZT-1)	53/53/183	1955–1991	photometry	12000
40” Schmidt (AZT–10)	102/132/213	1960–1991	photometry, spectroscopy	7500
ZTA–2.6	264/1016	1975–1991	photometry, spectroscopy	7000
BAO all telescopes		**1947–1991**		**37000**

We give in Table 1 an overview of BAO telescopes and produced observational material. Telescope “Sizes” are given for the mirror and focal length for classical telescopes and for the correcting lens, mirror and focal length for Schmidt type telescopes. Here we list the main observational projects accomplished on the three most important BAO telescopes (2.6m classical reflector, 1m Schmidt and 0.5m Schmidt; Figure 1).

21” (0.5m) Schmidt telescope:

- Polarization of cometary nebula NGC 2261
- Nuclei of nearby Sa and Sb galaxies
- Nuclei of nearby Sc galaxies
- Search for flare stars in Pleiades
- Search for flare stars in Orion
- Search for flare stars in NGC 7000 (Cygnus)
- Search for flare stars in Praesepe

doi: https://doi.org/10.52526/25792776-2021.68.1-97

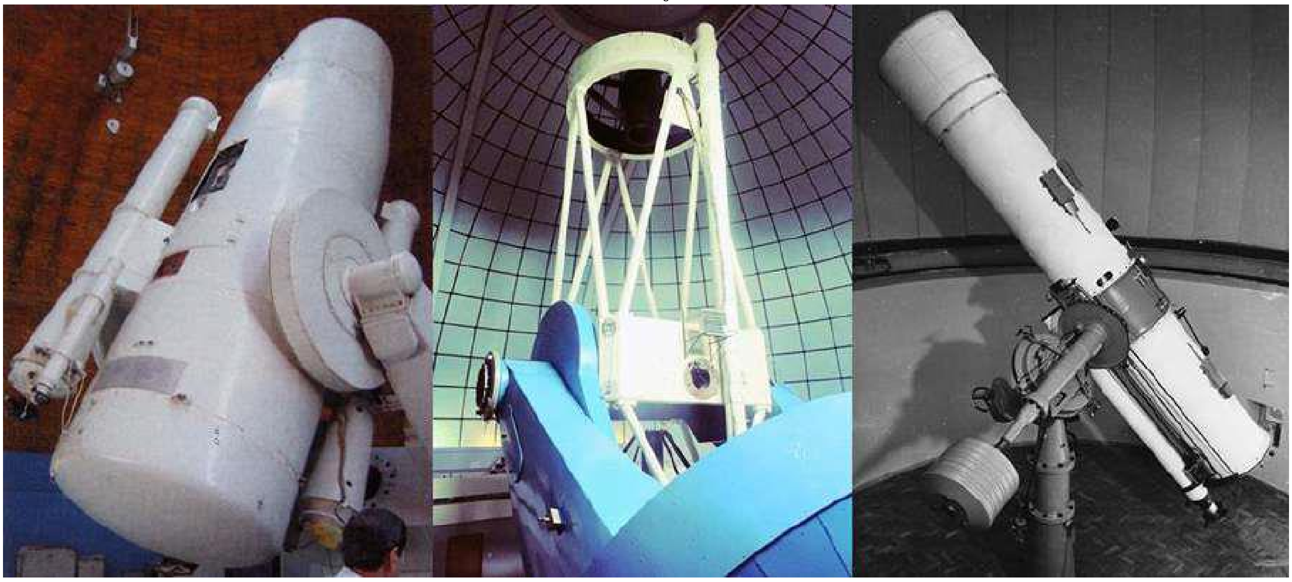

Figure 1. BAO most important telescopes (from left to right): 1m Schmidt, 2.6m classical reflector and 0.5m Schmidt.

- Search for flare stars in Taurus Dark Clouds (TDC)
- Variability of Markarian galaxies
- Monitoring of extragalactic supernovae in certain areas

40" (1m) Schmidt telescope:

- Detailed colorimetry of bright galaxies
- First Byurakan Survey (FBS, Markarian survey; Markarian et al. 1989)
- Search for flare stars in Pleiades
- Search for flare stars in Orion
- Search for flare stars in NGC 7000 (Cygnus)
- Search for flare stars in Praesepe
- Search for flare stars in Taurus Dark Clouds (TDC)
- Second Byurakan Survey (SBS; Stepanian 2005)
- Extension of the FBS in the Galactic Plane

ZTA-2.6m telescope:

- Morphological study of Markarian galaxies
- Investigation of star clusters
- Investigation of groups and clusters of galaxies
- Spectroscopy FBS blue stellar objects
- Spectroscopy FBS late–type stars
- Spectroscopy SBS galaxies and stellar objects (BAO/SAO)

doi: https://doi.org/10.52526/25792776-2021.68.1-97

- Direct images of the central regions of Markarian galaxies
- Spectroscopy of T Tauri and flare stars
- Spectroscopy of Byurakan-IRAS Galaxies (BIG objects)
- Spectroscopy of ROSAT AGN candidates (BAO/HS/OHP/INAOE)

Summarizing, the main observational projects run on these telescopes were:

21" (0.5m) Schmidt: Polarization of cometary nebula NGC 2261, Nuclei of nearby Sa and Sb galaxies, Nuclei of nearby Sc galaxies, Search for are stars in Pleiades, Orion, NGC 7000 (Cygnus), Praesepe and Taurus Dark Clouds (TDC), Variability of Markarian galaxies, Monitoring of extragalactic supernovae in certain areas, etc.;

40" (1m) Schmidt: the First Byurakan Survey (FBS, Markarian survey; Markarian et al. 1989), the Second Byurakan Survey (SBS; Stepanian 2005), Extension of the FBS in the Galactic Plane, Detailed colorimetry of bright galaxies, Search for are stars in Pleiades, Orion, NGC 7000 (Cygnus), Praesepe and Taurus Dark Clouds (TDC), etc.;

ZTA-2.6m telescope: Morphological study of Markarian galaxies, Investigation of star clusters, Investigation of groups and clusters of galaxies, Spectroscopy of FBS blue stellar objects, FBS late-type stars, SBS galaxies and stellar objects (BAO/SAO), T Tauri and are stars, Byurakan-IRAS Galaxies (BIG objects) and ROSAT AGN candidates (BAO/HS/OHP/INAOE), and Direct images of the central regions of Markarian galaxies.

Especially efficient were Byurakan spectroscopic surveys accomplished by Markarian and colleagues with 1m Schmidt telescope: FBS and SBS.

3. BAO Plate Archive Project

The digitization of astronomical plates and films pursues not only the maintenance task, but also it will serve as a source for new scientific research and discoveries, if only the digitized material runs according to modern standards and, due to its accessibility, it will become an active archive. The project is aimed at compilation, accounting, digitization of BAO observational archive photographic plates and films, as well as their incorporation in databases with modern standards and methods, providing access for all observational material and development of new scientific programs based on this material.

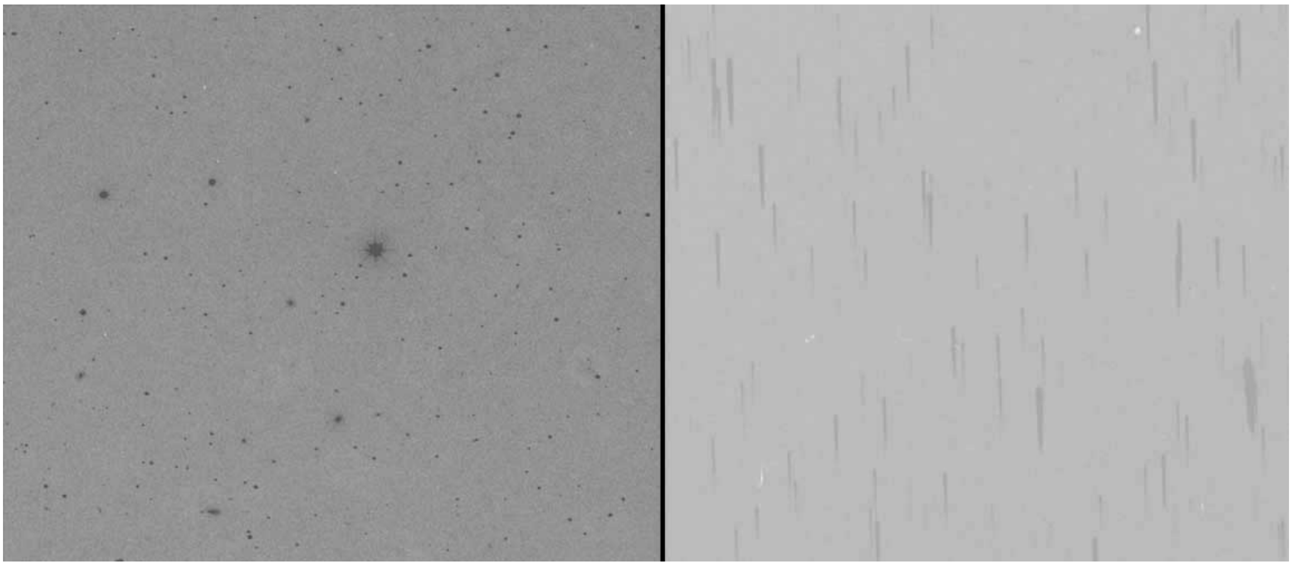

Figure 2. Example of photometric and spectroscopic plates.

Scientific Programs Board (SPB) was created to evaluate the existing observational material, to select sets of priorities to be scanned first and to propose new research projects. It consists of

doi: https://doi.org/10.52526/25792776-2021.68.1-97

BAO most experienced observers, as well as researchers from NAS RA Institute of Informatics and Automation Problems (IIAP) are involved for their experience in computer science related to databases and computational methods.

Project Executing Team (PET) consists of more than 10 members led by the Head of BAO Astroinformatics Department Gor Mikayelyan, and the members are involved in scanning and reduction of data.

The project has started in February 2015 and it lasted 4 years. In August 2020 the project was renovated and now the digitization of the plates is finished. Altogether 30121 photographic plates and films were digitized. About half of them are photometric plates of different sizes and the other ones are spectroscopic plates, photometric chains, spectroscopic chains, etc. In Figures 2, 3 and 4 we give the examples of digitized plates.

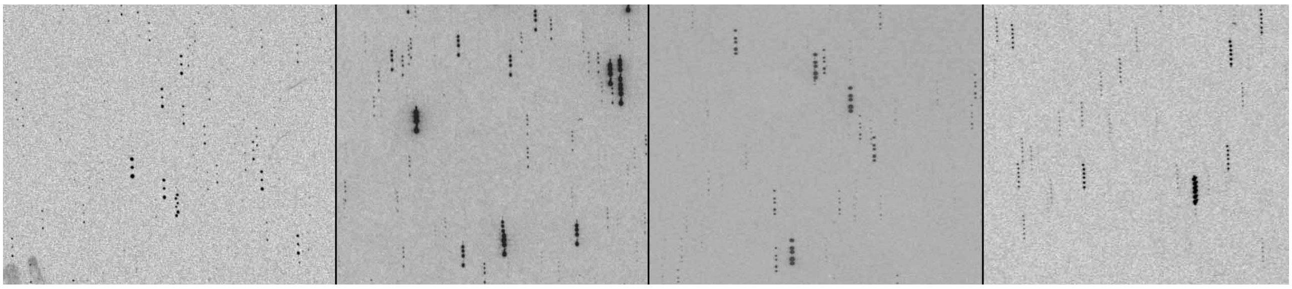

Figure 3. Example of photometric chains.

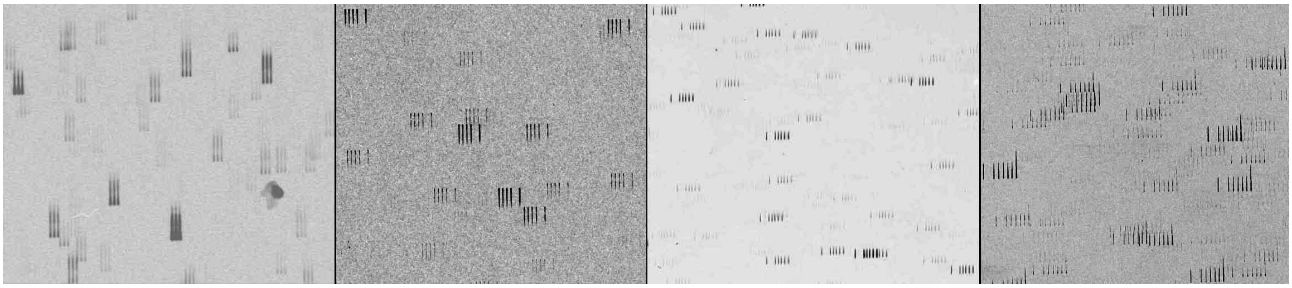

Figure 4. Example of spectroscopic chains.

In May 2021 we have started the works of astrometric calibration and now about 5000 plates already have an astrometric solution. We use https://astrometry.net webpage for astrometric calibration of the plates. We plan to finish the astrometric calibration of all plates in December 2021.

4. Digitized First Byurakan Survey

A number of digitization projects have been accomplished at BAO, including the most important one, **Digitized First Byurakan Survey (DFBS;** http://www.aras.am/Dfbs/dfbs.html; Massaro et al. 2008, Mickaelian et al. 2007) based on the digitization of the famous Markarian Survey (Markarian et al., 1989). Its main scanning and resulting features are given in Table 2.

We give in Figure 5 (left panel) a piece of visualized DFBS field together with its corresponding DSS2 area. Some 40,000,000 DFBS low-dispersion spectra have been extracted from 1874 plates, measured and analyzed by means of the dedicated software bSpec (Figure 5, right panel), written by Giuseppe Cirimele. The spectra extraction and analysis software is described in Mickaelian et al. (2010) and Knyazyan et al. (2011). DFBS plate database is available in Vizier, Strasbourg (Mickaelian et al., 2005).

doi: https://doi.org/10.52526/25792776-2021.68.1-97

Table 2. Main scanning and resulting characteristics of the DFBS

Items	**Description**
Teams	Byurakan Astrophys. Obs., Univ. Roma "La Sapienza", Cornell Univ.
Years	2002-2005
Instrument	Epson Expression 1680 Pro scanner
Scanning options	1600 dpi (15.875μ pix size), 16 bit, transparency mode, "scanfits"
Plate size	9601×9601 pix, 176 MB file
Spectra	107 × 5 pix (1700μ in length)
Dispersion	33 Å/pix average (22-60 Å/pix), 28.5 at H_γ
Spectral resolution	50Å (average)
Astrometric solution	1" rms accuracy
Scale	1.542" /pix
Photometry	0.3^m accuracy
Data volume	1874 plates, ∼400 GB
Number of objects	∼20,000,000 (∼40,000,000 spectra)

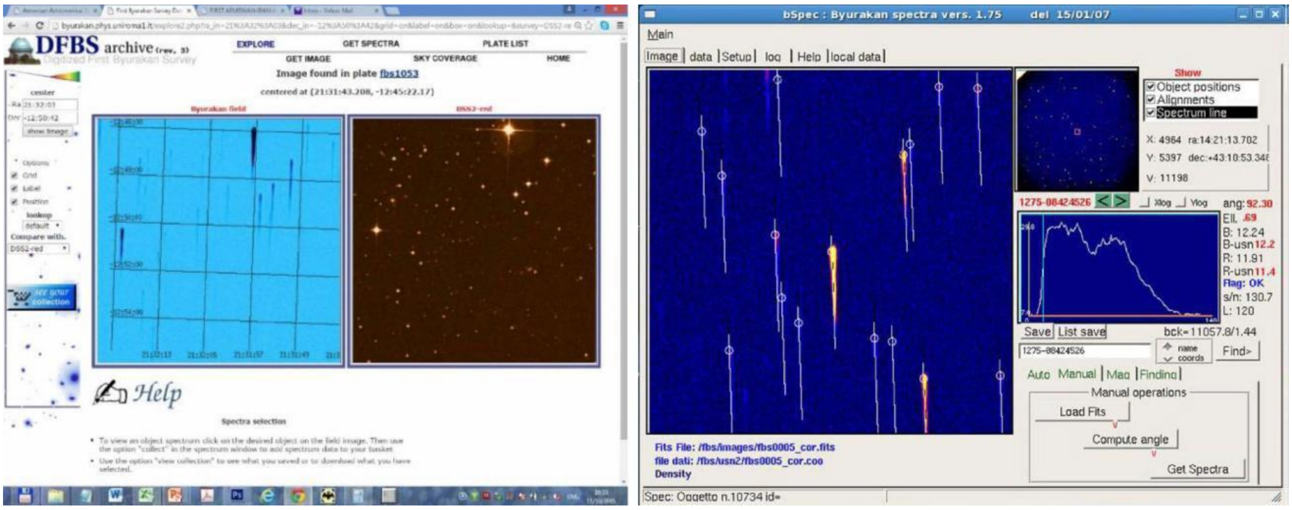

Figure 5. Left: DFBS data visualization with comparison of similar DSS2 field. Right: DFBS spectra extraction and analysis software bSpec.

5. Summary

BAO Plate Archive is one of the most important astronomical databases. At present the main part of the project has been accomplished, the scanning of the plates has produced more than 30,000 digital images of roughly 200 MB files (each image). All they have been stored and double copies are available.

BAO Plate Archive Project will lead to preservation of BAO valuable observational material obtained during 1947-1991. However, our goal is not only to create a passive archive of scanned plates and films, but also to make use of especially those fields, where more studies are possible. Proper motion and variability studies are most important, as time domain material is contained in historical plates. Such possibilities based on DFBS were shown by Mickaelian et al. (2006a); DFBS as a unique database for proper motion, variability studies, and object classification. New variable stars discovered on digitized plates of Moscow collection was reported by Sokolovsky et al. (2014).

There are a number of further **possible research projects** that will be conducted having the plates digitized:

- Correction of ephemerides of known asteroids and search for new asteroids (ex. Berthier et al. 2009, Mickaelian et al. 2019, Thuillot et al. 2007)
- Discovery and study of variable stars (ex. Mickaelian et al. 2011, Nesci et al. 2009)

doi: https://doi.org/10.52526/25792776-2021.68.1-97

- Revealing high proper motion stars (ex. Mickaelian & Sinamyan 2010)
- Study of variability of known blazars and discovery of new blazars
- Revealing Novae and Supernovae progenitors (Nesci et al. 2009)
- Discovery of new QSOs
- Discovery of new white dwarfs (ex. Sinamyan & Mickaelian 2011)
- Discovery of new late-type stars (ex. Gigoyan et al. 2010, 2019)
- Discovery of optical sources of gamma-ray bursts
- Optical identifications of X-ray, IR and radio sources (ex. Hovhannisyan et al. 2009, Mickaelian & Gigoyan 2006, Mickaelian & Sargsyan 2004, Mickaelian et al. 2006b).

Acknowledgements

BAO Plate Archive Project team would like to thank BAO Administration for supporting the project. We also would like to thank the astrometry.net team because the astrometric calibration of the plates became possible thanks to https://astrometry.net webpage.

References

Berthier J., Sarkissian A., Mickaelian A. M., Thuillot W., 2009, "European Planetary Science Congress 2009, held 14-18 September in Potsdam, Germany, p. 526

Gigoyan K. S., Sinamyan P. K., Engels D., Mickaelian A. M., 2010, Astrophysics, 53, 123

Gigoyan K. S., Kostandyan G. R., Gigoyan K. K., Zamkotsian F., Sarkissian A., 2019, Astrophysics, 62, 573

Hovhannisyan L. R., Mickaelian A. M., Weedman D., et al. 2009, AJ, 251, 138

Hudec R., 2014, in Proc. Astroplate-2014 Conf., Eds. L. Mišková & S. Vítek. Prague, p. 1

Kazantseva L., 2014, in Proc. Astroplate-2014 Conf., Eds. L. Mišková & S. Vítek. Prague, p. 13

Knyazyan A., Mickaelian A. M., Astsatryan H., 2011, Int. J. "Inform. Theories and Appl.", 18, 243

Markarian B. E., Lipovetsky V. A., Stepanian J. A., et al. 1989, Comm. SAO, 62, 5

Massaro E., Mickaelian A. M., Nesci R., Weedman D., (Eds.) 2008, The Digitized First Byurakan Survey, ARACNE Editrice, Rome, 78p.

Mickaelian A. M., 2014, in Proc. Astroplate-2014 Conf., Eds. L. Mišková & S. Vítek. Prague, p. 109

Mickaelian A. M., Gigoyan K. S., 2006, A&A, 455, 765

Mickaelian A. M., Sargsyan L. A., 2004, Astrophysics, 47, 213

Mickaelian A. M., Sinamyan P. K., 2010, MNRAS, 407, 681

Mickaelian A. M., Hagen H.-J., Sargsyan L. A., Mikayelyan G. A., 2005, Catalog No. VI/116 at CDS, Strasbourg

Mickaelian A. M., Gigoyan K. S., Nesci R., Rossi C., 2006a, Mem.S.A.It., 77, 1159

Mickaelian A. M., Hovhannisyan L. R., Engels D., et al. 2006b, A&A, 449, 425

Mickaelian A. M., Nesci R., Rossi C., et al. 2007, A&A, 464, 1177

Mickaelian A. M., Sargsyan L. A., Nesci R., et al. 2010, ASP Conf. Series, Vol. 434: Astronomical Data Analysis Software and Systems XIX, p. 325

Mickaelian A. M., Mikayelyan G. A., Sinamyan P. K., 2011, MNRAS, 415, 1061

Mickaelian A. M., Abrahamyan H. V., Andreasyan H. R., et al. 2016, in Astronomical Surveys and Big Data. Eds. A. M. Mickaelian, A. Lawrence & T. Yu. Magakian. ASP Conf. Ser., V. 505, p. 262

Mickaelian A. M., Gigoyan K. S., Gyulzadyan M. V., et al. 2017, ComBAO, 64, 102

Mickaelian A. M., Sarkissian A., Berthier J., Meftah M., Thuillot W., Vachier F., 2019, Icarus, 330, 5

doi: https://doi.org/10.52526/25792776-2021.68.1-97

Mickaelian A. M., Gigoyan K. S., Mikayelyan G. A., et al. 2020, ComBAO, 67 2, 293

Nesci R., Mickaelian A. M., Rossi C., 2009, ATel, 2338, 1

Nesci R., Bagaglia M., Nucciarelli G., 2014, in Proc. Astroplate-2014 Conf., Eds. L. Mišková & S. Vítek. Prague, p. 75

Osborn W., 2014, in Proc. Astroplate-2014 Conf., Eds. L. Mišková & S. Vítek. Prague, p. 15

Sinamyan P. K., Mickaelian A. M., 2011, Astrophysics, 54, 403

Sokolovsky K. V., Antipin S. V., Zubareva A. M., et al. 2014, ARep, 58, 319

Stepanian J. A., 2005, RMxAA, 41, 155

Stupka J., Benesova E., 2014, in Proc. Astroplate-2014 Conf., Eds. L. Mišková & S. Vítek. Prague, p. 31

Thuillot W., Berthier J., Sarkissian A., et al. 2007, Highlights of Astronomy, 14, 616

Tsvetkov M., Tsvetkova K., 2012, in Proc. IAU S285: New Horizons in Time-Domain Astronomy. Cambridge Univ. Press, p. 417

doi: https://doi.org/10.52526/25792776-2021.68.1-97

Communications of BAO, Vol. 68, Issue 1, 2021, pp. 105-113

An Astronomical Attempt to Determine the Temporal Origin of an Episode of the Armenian Epic "Sasnay Tsrer"

G. Broutian

NAS RA V. Ambartsumian Byurakan Astrophysical Observatory (BAO), Armenia

Abstract

An attempt was made to estimate the time period of the Armenian epic "Sasnay Tsrer" by astronomical means. An episode in which Tsovinar mentions a bright star as night guide for sending her sons from Mesopotamia to Armenia has been examined from the point of view of astronomy. On basis of the "khachapasht" (cross worshipers) self-proclamation of representatives of the House of Sasun and wearing the sign of the cross on their right hand, this guiding star is identified with the constellation Cygnus (ancient Armenian Angkh - Vulture), which depicts the outline of a cross in the northern sky. Subsequently, we calculated when Cygnus' main star, Deneb, was closest to the North Pole. The calculations show that this event took place 17,500 years ago. This time frame was taken as the time of the creation of the above-mentioned episode of the Sasnay Tsrer Epic.

Keywords: *Epic Sasnay Tsrer: Astronomical dating: Angegh - Vulture - Cygnus constellation*

1. Introduction

The temporal origin of creation of the Armenian Epic Sasnay Tsrer has been debated by various authors based on identifications of the heroes of the Epic and other historical individuals. For example, it is argued that real historical persons - Theodoros Rshtouni, lord of Taron and Sassoun Davit Bagratouni (Bagarat's son), lord of Sassoun Tornik Mamikonian, Yovnan form Khout and so on served as historical prototypes for characters of the Epic - K'eri Toros (Uncle Toros), David of Sassoun and Dzenov Ohan.[1] According to these "identifications", Sasnay Tsrer dates back to the period of Arab invasions.[2]

At the same time, there are references to Sanasar and his brother Baghdasar (in some versions under different names), one of the heroes of the first branch of the Epic, in the works of Movses Khorenatsi (V century) and Tovma Artsrouni (IX-X century).[3] These facts date the time of the Epic to at least V century (in the time of Moses Khorenatsi).

However, these are not the only demarcations for the time of Sasnay Tsrer Epic. The two heroic brothers of the first branch of the Epic are clearly parallel in their activities and names to the sons of Sennacherib of Assyria (705-680 BC), Adrammelech and Sarasar (4 Kings, 19, 37). This connects time of the Epic to the era of the kingdom of Van. Of course, there is also temporal disagreement as according to the Epic, Sanasar and Baghdasar are contemporaries of the Caliph of Baghdad, whose character should be associated with the Arab invasions and the subsequent time periods. As such, there are clear timeline disagreements that are compounded by other factors forming bases to suggest

[1] Manouk Abeghian, Complete works, v. 1, Publ. of Academy of Sciences of RA, Yerevan, 1966 pp. 354 380, v. 8, 1985, pp. 12 65 (in Armenian).

[2] It was on this basis that the 1000th anniversary of the Sasnay Tsrer Epic was celebrated in Soviet Armenia in 1939. See Armenian Soviet Encyclopedia, v. 10, pp. 195 - 199, Yerevan, 1984 (in Armenian).

[3] Movses Khorenatsi, History of Armenia, I, 23, p. 70-71, II, 07, p. 111, with diligence of Manouk Abeghian, Tbilisi, 1913 (in Armenian), Tovma Artsrouni, and Anonym, The history of the House of Artsrouni, Yerevan University publ., Yerevan, 1978, p. 78 (in Armenian).

doi: https://doi.org/10.52526/25792776-2021.68.1-105

older time periods for the origins of this Epic. These examples demonstrate that the time periods obtained by identi

cation of various epic characters with a known historical individual can vary greatly. Identification and combination of characters with coincidence of names or certain actions of historical figures known to us cannot be relied upon. Therefore, it is not accurate, to determine the time of the Sasnay Tsrer Epic or some of its episodes by identifying the names of the heroes. As such, it is necessary to search for other means to determine the time of the whole Epic or some of its episodes.

1.1. The problem

It is known that the most reliable way to determine time of different historical events is to connect the events with an astronomical phenomena (e.g., solar and lunar eclipses, nova and supernova airs, appearance of some comets, etc.) and approximate date of the event through this approach. The same approach can be used for literary and folklore compositions, if it is possible to find references to various astronomical phenomena in the narrative. Now we will explore the possibility to determine origins of Sasnay Tsrer by astronomical means. Fortunately, narratives that have come down to us in this Epic have preserved a number of fragments that, when properly interpreted astronomically, can serve as evidence for timing of the formation of those fragments. Ignoring enumeration of the examples, we will focus on discussion of one of them. In Sasnay Tsrer Epic, from the beginning of the first branch, definition of the Armenian nation as a "khachapasht" (worshiper of the cross) is repeated several times in different narratives.[4] In addition, all the main heroes of the House of Sasoun carry on their right arm a special sign given from the Heaven - the Cross.[5] This is mentioned in different narratives as "Khach Patrastin (Cross Ready)", "Paterazmin (Cross of War)", "Pataragin (Cross of Liturgy)", "Khach (Meat Cross)" etc. Moreover, the first bearer of this miraculous cross - Sanasar, receives it from Heaven after bathing in the milky spring, and getting stronger and fully armed.

"Angels put the Cross of War
On the right arm,
So that no beats could harm Sanasar".[6]

This is noteworthy as there is a large constellation in the northern hemisphere, that forms a huge brilliant cross with its 5-6 main bright stars in northern sky. This concerns to the Swan (Cygnus) constellation, that forms the heavenly cross with the stars: α Cygni (Deneb), β Cygni (Albireo), γ Cygni (Sadr), δ Cygni (Fawaris), ε Cygni (Aljanah), and η Cygni. On modern heavenly charts the Swan constellation is located between the northern constellations of Draco, Lyra, Vulpecula, Pegasus, Cepheus and Lacerta (see Figure 1).

We also know that according to ancient Armenian division of the starry sky this constellation was called Ang l (or Ank l), that means "Vulture". There is an image of a vulture instead of a swan on an Armenian heavenly chart printed by Ghoukas Vanandetsi in 1695 in Amsterdam (Figure 2). Near the tail of the bird we have a legend *"Ankh"* which means "Vulture". Besides, names of constellations (and individual stars) stated in Armenian medieval manuscript sources do not contain the name "Swan", however, there is mention of the name "Kerkez", which means "vulture".[7]

It is known that the bird vulture was the heavenly character of the ancient god Nergal.[8] Nergal was the main god of Hayasa - one of the oldest Armenian states (BC XIV - XIII c).[9] Thus, the entitlement

[4]See for example, Sasountsi Davit, Publ. of Academy of Sciences of RA, Yerevan, 1961, pp. 4, 5, 23, 48. (in Armenian).

[5]Ibid. pp. 40, 41.

[6]Ibid

[7]See, for example, Grigor Broutian, Armenian Calendar, Mother See of Holy Etchmiadzin, 1997, page 490 (in Armenian). Not all of the names of stars and constellations listed here have been identified with modern-day celestial realities, but some may have been identified as reliable. For Kerkez, Acharian gives: There is a Persian word karkas (kerkes) "Vulture" (Hr. Acharian, Armenian Etymological Dictionary, vol. 4, Yerevan University Press, Yerevan, 1979, p. 574).

[8]Armen Davtian, Armenian stellar mythology, Yerevan, 2004, pp. 207-222 (in Armenian).

[9]Gr. Khapancian, Historical-linguistic studies, Publ. of Academy of Sciences of Arm. SSR, Yerevan, 1956, pp. 88-89 (in Russian).

doi: https://doi.org/10.52526/25792776-2021.68.1-105

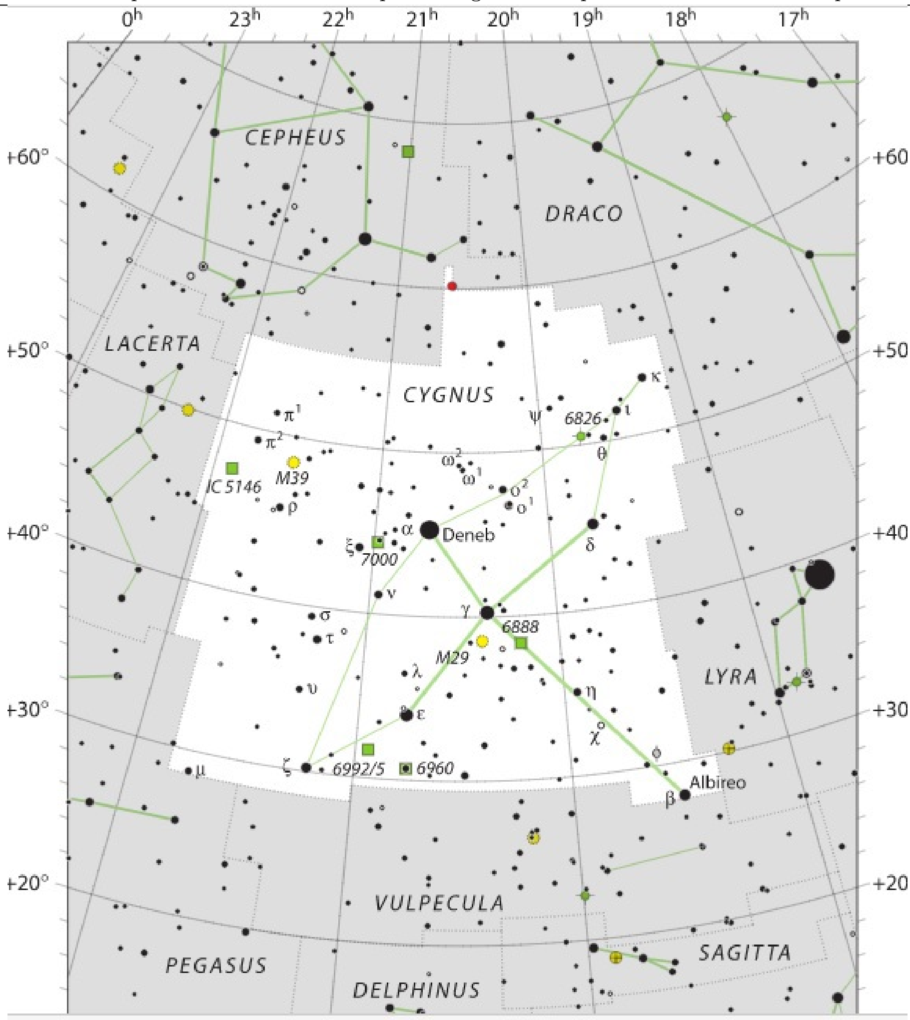

Figure 1. The Armenian Ang l - Vulture (modern Swan - Cygnus) constellation and its heavenly neighborhood on modern sky chart

"khachapasht" (worshiper of the cross) means a person who worships the god Angl - Nergal.[10] On the other hand, we know that worshiping any god is essentially the same as worshiping that celestial image of that god. Taking into account the fact that Hayasa was only one of the ancient Armenian states, we get that "khachapasht" = worshiper of Vulture - Nergal = resident of Hayasa = Armenian. In other words, we got exactly what is directly written in the Epic.

Now let's look at how it is possible to use this identification (Armenian = worshiper of cross = worshiper of Nergal = worshiper of the Swan-Vulture star) to determine the origin of the Epic Sasnay Tsrer.

Of course, the above-mentioned relationship alone is not sufficient to determine the origin of the Epic. We need additional information to help us estimate the correct time of the relationship. Details in the following episode of the Epic can provide the additional information needed. After Tsovinar learns that the Caliph has promised to sacrifice her sons to his Great Idol, she orders them to flee to Armenia to their grandfather to the north.

"Run away, go to the city of the Armenian king.

[10]This is also shown by the carrying of a special (bestowed from heaven) cross on the right arm of the heroes of the House of Sasoun. They receive the cross after special (ritual) actions (to pray, to bathe in a special spring). In other words, it turns out that they receive the sign of this cross after a special offering ritual. This is reminiscent of becoming a mahtesi (a person who had gone as a pilgrim to Jerusalem) highly valued in Christianity (especially among Armenian Christians), which was traditionally associated with making a covenant in Jerusalem (Christ's tomb) and then having a special (including a special cross) tattoo on the arm. In fact, the cross on the arm of the heroes of the House of Sasoun, is the expression of the celestial symbol of the god worshiped by the cross worshiping nation on their own body.

doi: https://doi.org/10.52526/25792776-2021.68.1-105

Figure 2. The Armenian Ang l (modern Swan - Cygnus) constellation and the neighboring constellations on the heavenly chart printed in 1695 in Amsterdam by Ghoukas Vanandetsi

Catch the bright star at night as a target."[11]

In other words, as a night guide to the journey, she points to a bright star in the sky and orders the sons to go in the direction of that star, confident that it will take them to Armenia.

Here we have a combination of several realities!

1) Tsovinar is instructing her cross worshiper children to always follow the same star.

2) That star is bright.

3) She assures that guided by that star, her sons will reach their homeland, Armenia.

4) To be guided by a star implies following the deity whose heavenly mythical image is that star, to worship that god and to do the will of that god.

5) In order to reach Armenia from the territory of Baghdad (i.e., from central Mesopotamia) guided by a star, it is necessary for that star to be in the northern part of the sky, as Armenia is located north of Mesopotamia.

6) As a result of the Earth's daily rotation, all the stars in the sky revolve around the pole once a day and no star has a stable position in the sky. During the night, the stars move in the sky from east to west with a speed of one rotation in 24 hours. Therefore, the same star at different times of the night has different positions in the sky. The position of the star in the night sky can change from the eastern horizon to the western horizon. Therefore, it is impossible to point out any star the direction of which will always lead to a specific destination including Armenia. Due to its position, the only star in the sky that can be used as a guide at night, is the polar

[11] Sasountsi Davit, p. 21.

doi: https://doi.org/10.52526/25792776-2021.68.1-105

star. That is, only the star at the north pole of the sky, or very close to the pole, can serve as a guide.[12] Since focus of events is in the northern hemisphere of the Earth, the star near the north pole (or at the very pole) can play that role in the sky. In other words, we conclude that *the only star that can serve as a guide in Earth's northern hemisphere is the star at or near the North Pole.*

Meanwhile, there is an inconvenience here. In the epic it is clearly mentioned that the star, which is the guide of the night, is **"bright"**.The instruction given to the sons has a certain mention: *"Catch the bright star as a target."* Today the star in the night sky, which is very close to the North Pole, called "Polaris", is not so bright. This star is known as the F7Ib class yellow supergiant star, located at a distance of 433 light-years from us, with an average magnitude of $1^m.98$.[13] That is, it is approximately **a second magnitude star**. In order to be designated "bright", the star had to be at least of 1.0^m - 1.5^m magnitude or brighter. According to modern data, the Polar Star is the 48th in the list of the brightest stars (excluding the Sun). That is, there are 47 stars in the night sky brighter than Polaris. Along with this, let us remember that as a result of the Earth's precession, the direction of the Earth's polar axis changes over the millennia, and thus the appearance of the night sky. This recurring phenomena was discovered in the 2nd century BC by Hipparchus. According to current adjusted data, its periodicity is 25,776 years. At this rate, the axis of daily rotation of the Earth[14] forms a cone around the axis of the ecliptic at an angle of about 47 degrees. Naturally, during that time the real pole can "appear" near different stars. Naturally, during that time the real pole can "appear" near different stars. At present, the north pole of the sky (the pole of the world) is right next to the star called the Polaris (the angular distance is $00°44'09''$ and in different historical eras it has been close with different stars. For example, 6,000 years ago, the north pole was near the star α Draconis (Tuban), 12,500 years ago it was near the star α Lyrae (Vega), which is the brightest star in the northern hemisphere.

Modern calculations show that during these long-term "wandering" of the pole, about 18,000 years ago, the north pole of the sky was near the star currently known as α Cygni (Deneb). In the central part of the Figure 3 there is the pole of ecliptic in the constellation of the Dragon. The position of the north pole of the world in different eras is presented as a circle around it. The current +2,000 year is at the top. To the right of it (clockwise) are the past dates up to 10,000 BC, and to the left (counterclockwise) are given the dates of the future, up to +14,000. The figure clearly shows that about 18,000 years ago, the North Pole was right next to the main star of the constellation Cygnus (Swan, formerly - Vulture). We also know that Deneb star is a variable star of class A2Ia with an average visible stellar magnitude of 1m.25 and is approximately a first magnitude blue-white star. A simple calculation shows that Deneb is about twice as bright as the Polaris (exactly 1.9589 times) and in the list of the brightest stars in the sky, Deneb is in the 20th place (versus of the 48th place for Polaris).

Let's add another important fact to our discussion. We know that the Swan (Vulture) constellation has played an important role in ancient Armenia, as witnessed by the ancient megalithic monument known as "Zorats K'arer" in Syunik region of Armenia near the town Sisian. This megalithic structure is remarkable in several respects. First is the arrangement of megaliths that quite accurately replicate the arrangement of the bright stars of the Swan (Vulture) constellation in the sky. Second is that according to latest research, arrangement of the megaliths of this monument best correspond to arrangement of stars of the constellation Swan, which existed 32,000 years ago (Malkhasyan, 2020). In other words, at least a certain part of the Zorats Karer monument must have been erected 32,000 years before us and there must have been the cult of the Vulture in Armenia which appears in the form of a celestial cross, the expression of which is the modern Swan constellation.

[12]What is said here refers to the territory of the northern hemisphere of the Earth. For the area of the southern hemisphere, the star at or near the south pole plays the same role.

[13]Stellar magnitude is a quantitative measure of the luminosity of stars. It was first used by Hipparchus in the 2nd century BC, dividing the observed brightness scale of the stars into 6 groups. According to Hipparchus, the brightest stars were considered to be of the first magnitude, and the faintest stars were of the sixth magnitude.

[14]In professional astronomical literature, this is also called the "axis of the world", and the points of intersection of this axis with the celestial sphere are called "poles of the world" (north and south, respectively).

doi: https://doi.org/10.52526/25792776-2021.68.1-105

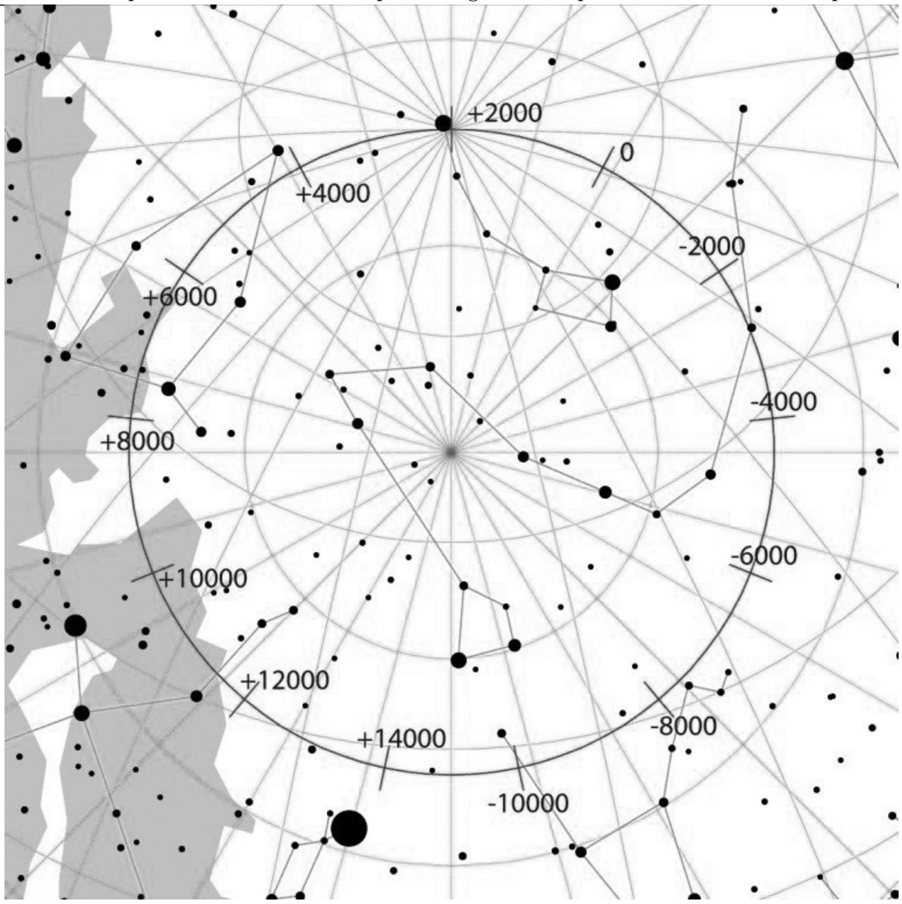

Figure 3. The change in the position of the north pole of the sky during one period of precession (the pole of the ecliptic is in the center). Above is the picture of the star Polaris in the constellation Ursa Minor (Little Bear, old Armenia - The Other Chart), and below the bright star is the Lyrae star - Vega. On the left side is the constellation Swan with the stars Deneb, Sadr, Favaris and Albireo.

In this regard, we can also mention the T-shaped pillar with the image of a vulture found in the ancient site of Portasar (Göbekly tepe in Turkish), not far from the city of Edessa (Urfa) in the southern part of historical Armenia. The vulture depicted on this pillar also corresponds to the arrangement of the stones of the megalithic part of the Zorats K'arer and the arrangement of the stars of the constellation Swan (Cygnus).[15]

Now, let's aggregate everything that relates to the "cross worshipper" nature of Armenians.

a. Armenians considered themselves "cross worshipper"

b. Stars forming the image of a cross comprise the constellation Vulture = Swan - Cygnus

c. The god Angl = Nergal was also the main deity of Hayasa, one of the oldest Armenian state formations

d. Main heroes of the House of Sasoun wore on their right arm a special sign of cross bestowed from Heaven, that is, the image of the Vulture-Swan constellation

e. For those traveling north from Mesopotamia to Armenia, only the star at the North Pole or one very close to the pole could be a guide in the night sky.

Taking all this into account, we conclude that Tsovinar should have instructed her sons to follow as a guiding star in the night sky, the main star of the constellation Vulture-Swan, which is twice as bright as the relatively weak star called Polaris. Hence, the episode describing the departure of Sanasar and Baghdasar from Mesopotamia to Armenia must have been created when the main star of the Vulture-Swan was as close as possible to the north pole of the sky.

This is how we get an alternative way to determine the creation period of the episode of Sasnay

[15] Vachagan Vahradian, Marine Vahradian, On the name of the monument K'arahounj, "Bazmavep", 2010, 1-2, pp.161-177. (In Armenian). In particular see Figure 5, p. 176.

doi: https://doi.org/10.52526/25792776-2021.68.1-105

Tsrer. In other words, it turns out that at least a certain part of the Sasnay Tsrer Epic must have been created at the time when the north pole of the sky was near the main star of the Vulture-Swan constellation Deneb. Thus, in order to find the time of the creation of this episode in the Sasnay Tsrer Epic, it is necessary to find out in what era the north pole of the sky was near the star Deneb.

The diagram in Figure 3 clearly shows that the north pole near Deneb was about 16,000 years before birth of Christ, which means 18,000 years ago. Of course, determining the time on this diagram visually can contain a large level of error. On the graph, both the position of the stars and the path of the North Pole are given approximately. In order to have the most reliable result, it is necessary to perform the calculations using the formulas of spherical trigonometry.

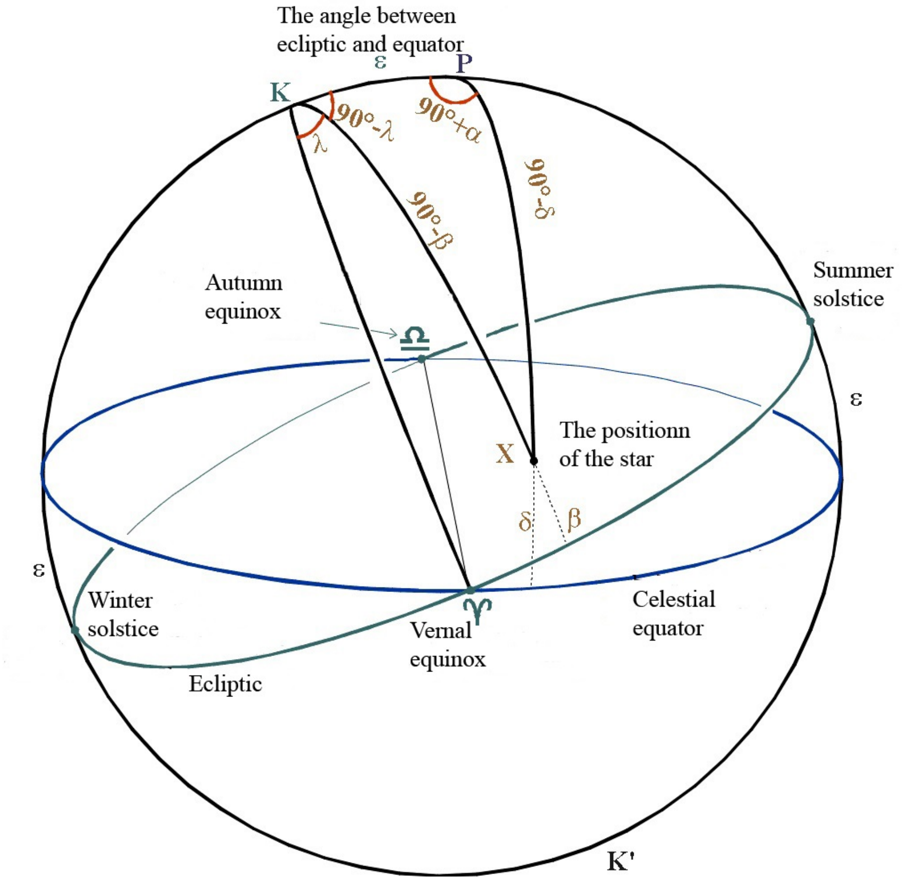

Figure 4. The relation of ecliptic and equatorial coordinates. P denotes the north pole of the world, K denotes the north pole of the ecliptic, and X denotes the position of the star in the sky. α and δ are the equatorial coordinates of the star (right ascension and declination), and β and λ are the equatorial coordinates (latitude and longitude).

2. The Calculations

As the north pole of sky (pole of the world), as a result of the centuries-old precession of the Earth's polar axis, revolves around the north pole of the ecliptic with a period of 25,776 years, the star that we are interested in will be in the position closest to the north pole of the sky when the north pole of the ecliptic, the north pole of the sky and the star are arranged on a line. Specifically, on the same arc of the great circle of the celestial sphere (Figure 4). To solve our problem, let us consider the spherical triangle KPX on the celestial sphere. The diagram in Figure 4 shows that the condition, when the ecliptic pole, the north pole of the sky and the star we are interested in are arranged on a line is equivalent to the condition that angle K in the triangle KPX (angle XKP) is equal to 0. That is the change in the position of the north pole of the sky during one period of precession (the pole of the ecliptic is in the center). Above is the picture of the star Polaris in the constellation Ursa Minor

doi: https://doi.org/10.52526/25792776-2021.68.1-105

(Little Bear, old Armenia - The Other Chart), and below the bright star is the α Lyrae star - Vega. On the left side is the constellation Swan with the stars Deneb, Sadr, Favaris and Albireo.

$$90^\circ - \lambda = 0$$

From above:

$$\lambda = 90^\circ$$

Using formulas from the spherical trigonometry, we move from equatorial and coordinates of the star to its ecliptic coordinates β and γ.

$$\tan\lambda = \frac{\sin\alpha\cos\varepsilon + \tan\delta\sin\varepsilon}{\cos\alpha} \tag{1}$$

$$\sin\beta = \cos\varepsilon\sin\delta - \sin\varepsilon\cos\delta\sin\alpha \tag{2}$$

Here is the angle between the ecliptic and the equator. From here we get for γ and β.

$$\lambda = \begin{cases} \arctan\frac{\sin\alpha\cos\varepsilon+\tan\delta\sin\varepsilon}{\cos\alpha}, & \cos\alpha > 0,\ \sin\alpha\cos\varepsilon + \tan\delta\sin\delta\sin\varepsilon \geq 0; \\ \arctan\frac{\sin\alpha\cos\varepsilon+\tan\delta\sin\varepsilon}{\cos\alpha} + 360^\circ, & \cos\alpha > 0,\ \sin\alpha\cos\varepsilon + \tan\delta\sin\varepsilon < 0; \\ \arctan\frac{\sin\alpha\cos\varepsilon+\tan\delta\sin\varepsilon}{\cos\alpha} + 180^\circ, & \cos\alpha > 0. \end{cases} \tag{3}$$

$$\beta = \arcsin\left(\cos\varepsilon\sin\delta - \sin\varepsilon\cos\delta\sin\alpha\right) \tag{4}$$

By inserting into the equation 3 the values of equatorial coordinates α and δ of Deneb (α_{2000} = $20^h41^m25.9^s$ = 310.3579166°; and $\delta_{2000} = 45°16'49''$ = 45.2802777°) and the adjusted value of ϵ (23°26.21 = 23.4391666°), we get its ecliptic coordinates β and λ.

In our case $cos\alpha > 0$, and sinαcosϵ + tgδsin$\epsilon < 0$, then the second of the conditions of equation 3 occurs, so we add 360° to the value obtained for λ.

For the ecliptic longitude of Deneb we obtain λ = 335.3315°. If we denote the ecliptic longitude λ of Deneb at the position closest to the North Pole by λ_0, then we can write the above condition as follows: λ_0 = 90°. Hence: λ - λ_0 = 335.3315° - 90° = 245.3315°.

The ecliptic latitude is not dependent on time, and from equation 4 we get β = 59.90676344° or $\beta = 59°54'24.35''$

The rest is simple arithmetic. Assuming that the Earth's polar axis rotates at a constant speed[16], we calculate how many years it will take the rotation of this axis at an angle of 245.3315° if the complete rotation takes 25,776 years. That is equal to:

$$\frac{245.3315 \cdot 25776}{360} = 17565.7654.$$

It turns out that the star Deneb was in the closest position to the north pole of the sky 17,565.7684 years ago[17]. The fractional part of this number is not significant in the case of our problem as the magnitude of the error for determining the time period is significantly greater than the impact of the fractional value. To evaluate the possible error in determining time with this method, consider that Deneb can be considered at the North Pole when looking at the sky with the naked eye, it is "forward" or "back" from its nearest position by no more than its angular distance from the pole. From the above β = 59.90676344° we get that Deneb was at the closest position to the pole at a distance of 90° - 59.90676344° - 23.440833° = 6.65240356°. This is equivalent to an angle of $6°39'8.7''$. This value is less than the angular distance between Deneb and Sadr. It is of this order that the error in the observational determination of the position of the North Pole should be. This type of displacement of the pole takes place in about 500 years (exactly 476 years). As such, the error of the determination of the time period is 500 years with the fluctuation interval on the order of 1000 years.

[16] The latest data show that we can consider the speed of this precession to be constant.

[17] It is noteworthy that at that time the north pole almost coincided with the stars o1 Cygni and o2 Cygni representing the celestial vulture's beak.

doi: https://doi.org/10.52526/25792776-2021.68.1-105

Summarizing the calculation results, we determine that the episode in Sasnay Tsrer Epic about Tsovinar sending his two twin sons from Baghdad to Armenia could have been created about 17,500 years ago (with 1000 years of uncertainty). Of course, this finding does not suggest that the whole Epic was created at that time. The result obtained refers only to the specific subject matter that the episode discussed from Sasnay Tsrer was created 17,500 years ago.

In order to determine creation time of the whole Epic, it is necessary to examine other episodes that contain astronomical relationships. In this manner, it can be possible to determine time period of the creation of different episodes and different parts of this Epic. Without a doubt, this will be very beneficial for the complete and correct understanding of Sasnay Tsrer.

References

Malkhasyan H. A., 2020, Communications of the Byurakan Astrophysical Observatory, 67, 27

doi: https://doi.org/10.52526/25792776-2021.68.1-105

On the simultaneous generation of radio and soft X-ray emission by AXP 4U 0142+61

Z. N. Osmanov *

School of Physics, Free University of Tbilisi, 0183, Tbilisi, Georgia

E. Kharadze Georgian National Astrophysical Observatory, Abastumani, 0301, Georgia

Abstract

In the present paper we study the possibility of a simultaneous generation of radio waves and soft X-rays by means of the quasi-linear diffusion (QLD) in the anomalous pulsar AXP 4U 0142+61. Considering the magnetosphere composed of the so-called beam component and the plasma component respectively, we argue that the frozen-in condition will inevitably lead to the generation of the unstable cyclotron waves. These waves, via the QLD, will in turn influence the particle distribution function, leading to certain values of the pitch angles, thus to an efficient synchrotron mechanism, producing soft X-ray photons. We show that for physically reasonable parameters of magnetospheric plasma, the QLD can provide generation of radio waves in the following interval 40 MHz-111 MHz connected to soft X-rays for the domain 0.3 keV-1.4 keV.

Keywords: *pulsars: individual: AXP 4U 0142+61 – stars: magnetars – radiation mechanisms: non-thermal – plasmas.*

1. Introduction

Anomalous X-ray pulsars (AXPs) (young isolated neutron stars) since their discovery (Fahlman & Gregory, 1981, e.g. Mazets et al., 1971) deserve a great attention despite a few number of known AXPs (Kaspi, 2007). These objects are intensively studied last several years, but their nature still remains unknown. One of the interesting features of AXPs is their long period of rotation, which in turn leads to very strong magnetic fields exceeding the so-called Schwinger limit, $B_{cr} \approx 4.41 \times 10^{13}$ G. Therefore, they are called magnetars. AXPs exhibit strong X-ray fluxes and a corresponding luminosity exceeds the spin-down luminosity by many orders of magnitude. On the other hand, despite some predictions, that magnetars must be dark in the radio band (e.g. Baring & Harding, 1998), Camilo et al. (2006) and Malofeev et al. (2010) reported the detection of radio pulsations from magnetar-type neutron stars. In particular, Camilo et al. (2006) observed the position of the anomalous pulsar XTE J1810 - 197 at frequencies from $\nu = 1.4$GHz to $\nu = 49$GHz. It was shown that XTE J1810 - 197 emits bright, narrow, highly linearly polarized radio pulses. Malofeev et al. (2010), based on two high-sensitivity radio telescopes of the Pushchino Radio Astronomy Observatory - the Large Phased Array and the DKR-1000, have reported the detection of weak radio pulsed emission from the X-ray pulsar AXP 4U 0142 + 61 at two low frequencies, 40 MHz and 111 MHz. It is worth noting that this pulsar was monitored by the Westerbork Synthesis Radio Telescope at a frequency 1380 MHz. The observations did not detect a source of radio emission (with 1380 MHz) at the location of AXP 4U 0142+61.

In the present paper we focus on the anomalous X-ray pulsar 4U 0142+61, which exhibits radiation from the soft- to hard- X-rays, (e.g. den Hartog et al., 2006, Enoto et al., 2011, Góhler et al., 2005). The aim of this work is to study the possibility of a simultaneous generation of soft X-rays and radio waves stimulated by the quasi-linear diffusion (QLD). For explaining the radiation in the soft X-rays, we account for the synchrotron emission process. But, since in the magnetospheres of magnetars.

*z.osmanov@freeuni.eduge, Corresponding author

doi: https://doi.org/10.52526/25792776-2021.68.1-114

magnetic fields are very strong, the corresponding energy loses are efficient and for studying the synchrotron radiation one has to take into account a certain mechanism balancing the dissipative factors. This in turn leads to the one dimensional distribution function of particles and as a result the synchrotron mechanism completely vanishes. In this paper we rely on the pulsar emission model developed by Lominadze et al. (1979), Machabeli & Usov (1979). According to this approach, in the pulsar magnetospheres the cyclotron instability appears (Kazbegi et al., 1992), which during the quasi-linear stage, causes a diffusion of particles along and across the magnetic field lines, leading to the required balance.

This mechanism was applied to magnetars, pulsars and active galactic nuclei in a series of papers: (Chkheidze et al., 2010, Gogaberishvili et al., 2021, Machabeli & Osmanov, 2009, 2010, Malov & Machbeli, 2001, Osmanov, 2014, Osmanov & Machabeli, 2010, Osmanov, 2010a,b). One of the interesting consequences of the QLD is the fact that it provides a simultaneous generation of waves in two different emission bands: relatively low energy- and high energy- domains. In particular, the high energy radiation appears by means of the feedback of the cyclotron waves on relativistic particles due to the diffusion, and as a result, the pitch angles are arranged according to the aforementioned balance. Therefore, during the QLD, the physical system will be characterized by two radiation regimes: (a) the high energy synchrotron mechanism and (b) a low energy emission process provided by the cyclotron waves. In this context the recent observations performed by the MAGIC Cherenkov telescope deserve a great interest. In particular, Aliu et al. (2008) reported about the discovery of the very high energy (VHE) pulsed emission (>25 GeV) from the Crab pulsar and it has been shown that the VHE signals are coincident with optical signals in a phase. For explaining the origin of the coincidence, Machabeli & Osmanov (2009) have considered the mechanism of the QLD applying it to the plasma in the magnetosphere of the Crab pulsar on the light cylinder (a hypothetical area where the linear velocity of rigid rotation exactly equals the speed of light) lengthscales. We have found that the QLD provides the simultaneous generation of emission in different frequency bands. In the later studies (Chkheidze et al., 2010, Machabeli & Osmanov, 2010) the same problem was examined in more detail.

In the present paper we consider the anomalous pulsar 4U 0142+61 to investigate the role of the QLD in generation of the detected soft X-rays and radio waves respectively. The paper is organized as follows: In Section 2 we introduce the mechanism of the QLD, in Section 3 we apply the method to AXP 4U $0142+61$ and obtain results, and in Section 4 we summarize them.

2. Main consideration

We assume that the pulsar's magnetosphere is composed of the so-called primary beam with the Lorentz factor, γ_b and the bulk component with the Lorentz factor, γ_p (Chkheidze et al., 2010, Machabeli & Osmanov, 2009, 2010). By Kazbegi et al. (1992) it was shown that in the pulsar magnetospheric plasmas, which satisfy the frozen-in condition, the anomalous Doppler effect induces resonance unstable cyclotron waves

$$\omega - k_{\parallel} c - k_x u_x - \frac{\omega_B}{\gamma_b} = 0 \tag{1}$$

with the corresponding frequency (Malov & Machbeli, 2001)

$$\nu \approx \frac{\omega_B}{2\pi\delta\gamma_b}, \qquad \delta = \frac{\omega_p^2}{4\omega_B^2\gamma_p^3}, \tag{2}$$

where $k_{\parallel}$ is the longitudinal (along the magnetic field lines) component of the wave vector, $u_x \approx c^2\gamma_b/(\rho\omega_B)$ is the so-called curvature drift velocity, c is the speed of light, ρ is the magnetic fields' curvature radius, k_x is the wave vector's component along the drift, $\omega_B \equiv eB/mc$ is the cyclotron frequency, $B \approx 2.35 \times 10^{14} R_{st}^3/R^3$G is the magnetic induction close to the star's surface, $R_{st} \approx 10^6$cm is the pulsar's radius, R is the distance from the pulsar's center, e and m are the electron's charge and the rest mass respectively, $\omega_p \equiv \sqrt{4\pi n_p e^2/m}$ is the plasma frequency and n_p is the plasma number density.

For studying the development of the QLD, one should note that two major forces control dissipation. When particles emit in the synchrotron regime, they undergo the radiative reaction force $\mathbf{F}$,

doi: https://doi.org/10.52526/25792776-2021.68.1-114

having the following components (Landau & Lifshitz, 1971):

$$F_{\perp} = -\alpha_s \frac{p_{\perp}}{p_{\parallel}} \left(1 + \frac{p_{\perp}^2}{m^2 c^2}\right), F_{\parallel} = -\frac{\alpha_s}{m^2 c^2} p_{\perp}^2, \tag{3}$$

where $\alpha_s = 2e^2 \omega_B^2 / 3c^2$ and $p_{\perp}$ and $p_{\parallel}$ are the transversal (perpendicular to the magnetic field lines) and longitudinal (along the magnetic field lines) components of the momentum respectively.

In nonuniform magnetic field, electrons also experience a force $\mathbf{G}$, that is responsible for conservation of the adiabatic invariant, $I = 3cp_{\perp}^2/2eB$. The corresponding components of $\mathbf{G}$ are given by (Landau & Lifshitz, 1971):

$$G_{\perp} = -\frac{cp_{\perp}}{\rho}, \qquad G_{\parallel} = \frac{cp_{\perp}^2}{\rho p_{\parallel}}. \tag{4}$$

The wave excitation leads to a redistribution process of the particles via the QLD, which is described by the following kinetic equation (Machabeli & Usov, 1979, Malov & Machabeli, 2002)

$$\begin{aligned} \frac{\partial f}{\partial t} + \frac{1}{p_{\perp}} \frac{\partial}{\partial p_{\perp}} \left(p_{\perp} \left[F_{\perp} + G_{\perp}\right] f\right) = \\ = \frac{1}{p_{\perp}} \frac{\partial}{\partial p_{\perp}} \left(p_{\perp} D_{\perp,\perp} \frac{\partial f}{\partial p_{\perp}}\right), \end{aligned} \tag{5}$$

where f is the distribution function of the zeroth order, $D_{\perp,\perp} = D\delta|E_k|^2$, is the diffusion coefficient, $|E_k|^2$, is the energy density per unit of wavelength and $D = e^2/8c$ (Chkheidze et al., 2010). For estimating $|E_k|^2$, it is natural to assume that half of the plasma energy density, $mc^2 n_b \gamma_b/2$ converts to the energy density of the waves $|E_k|^2 k$, then for $|E_k|^2$ we obtain

$$|E_k|^2 = \frac{mc^3 n_b \gamma_b}{4\pi\nu}, \tag{6}$$

where

$$n_b = \frac{B}{Pce}, \tag{7}$$

is the number density of the beam and $P \approx 8.7\,$s is the rotation period of the pulsar.

By taking into account the relations $\psi \equiv p_{\perp}/p_{\parallel}$, $p_{\parallel} = mc\gamma_b$, one can show from Eqs. (3, 4) that

$$\frac{F_{\perp}}{G_{\perp}} \approx 2.7 \times 10^{-6} \times \left(\frac{B}{10^3 G}\right)^2 \times \left(\frac{\gamma_b}{10^7}\right) \times \left(\frac{\psi}{10^{-5} rad}\right)^2, \tag{8}$$

where B is normalized to the value of the magnetic field in the magnetosphere on the lengthscales, $\sim 10^{10}$cm. We see from this ratio that for physically reasonable parameters, one can neglect the transversal component of the radiation reaction force. Therefore, Eq. (5) reduces to

$$\begin{aligned} \frac{\partial f}{\partial t} + \frac{1}{p_{\perp}} \frac{\partial}{\partial p_{\perp}} \left(p_{\perp} G_{\perp} f\right) = \\ = \frac{1}{p_{\perp}} \frac{\partial}{\partial p_{\perp}} \left(p_{\perp} D_{\perp,\perp} \frac{\partial f}{\partial p_{\perp}}\right). \end{aligned} \tag{9}$$

As it is clear from Eq. (9), two major factors compete in this "game". On the one hand, the force responsible for conservation of the adiabatic invariant attempts to decrease the transversal momentum (thus the pitch angle), whereas the diffusion process, by means of the feedback of the cyclotron waves, attempts to increase the transversal momentum. Dynamically this process saturates when the aforementioned factors balance each other. Therefore, it is natural to study the stationary regime, $\partial f/\partial t = 0$ and examine a saturated state of the distribution function. After imposing the condition $\partial f/\partial t = 0$ on Eq. (9) one can straightforwardly solve it

$$f(p_{\perp}) = Cexp\left(\int \frac{G_{\perp}}{D_{\perp,\perp}} dp_{\perp}\right) = Ce^{-\left(\frac{p_{\perp}}{p_{\perp 0}}\right)^2}, \tag{10}$$

doi: https://doi.org/10.52526/25792776-2021.68.1-114

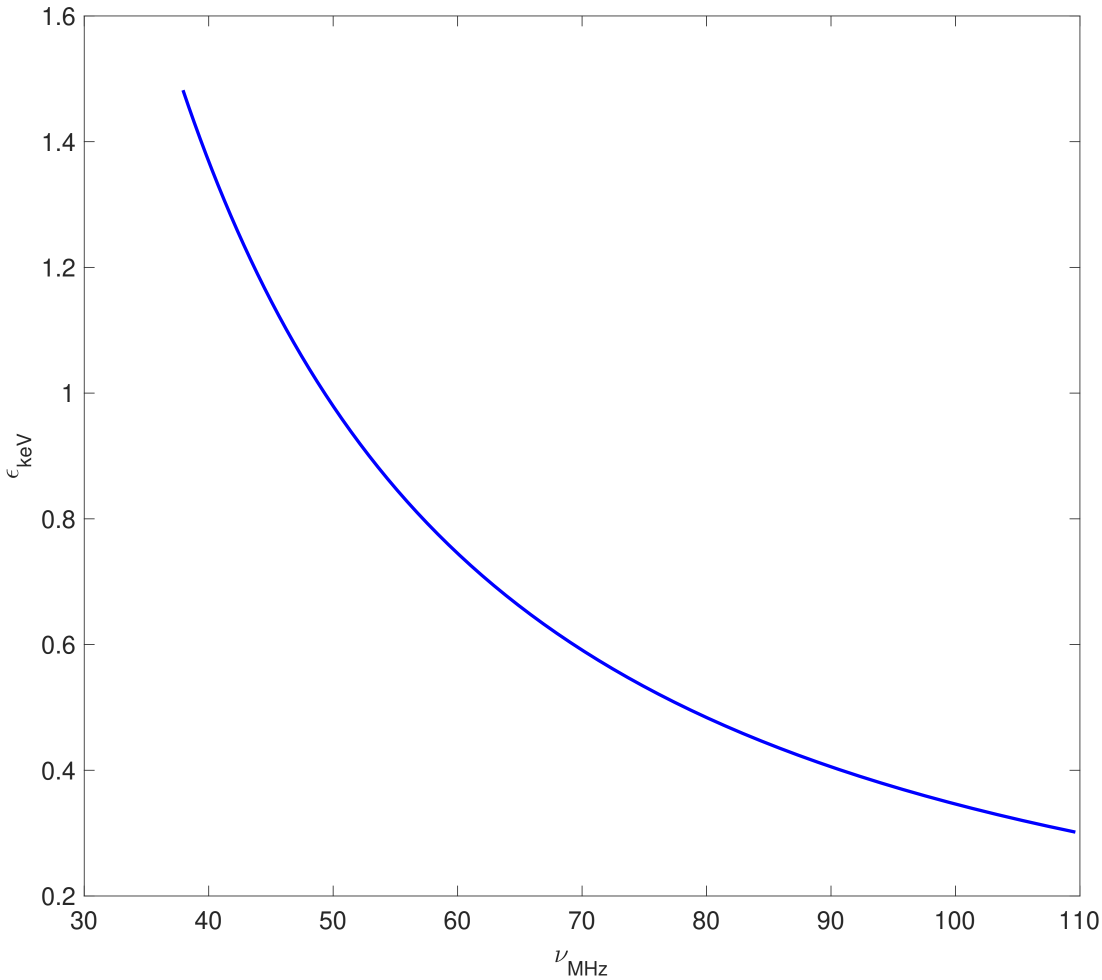

Figure 1. Behaviour of ϵ_{keV} with respect to ν_{MHz}. The set of parameters is: $P \approx 8.7$, $\gamma_p = 2.77$, $B_{st} \approx 1.3 \times 10^{14}$ G, $R_{st} \approx 10^6$ cm, $R = 4.8 \times 10^9$ cm.

where $C = const$ and

$$p_{\perp 0} \equiv \left(\frac{2\rho D_{\perp,\perp}}{c}\right)^{1/2}. \tag{11}$$

Since f is a continuous function of the transversal momentum, it is natural to examine an average value of it and estimate the corresponding mean value of the pitch angle, $\bar{\psi} \equiv \bar{p}_{\perp 0}/p_{\|}$,

$$\bar{\psi} = \frac{1}{p_{\|}} \frac{\int_0^{\infty} p_{\perp} f(p_{\perp}) dp_{\perp}}{\int_0^{\infty} f(p_{\perp}) dp_{\perp}} \approx \frac{1}{\sqrt{\pi}} \frac{p_{\perp 0}}{p_{\|}}. \tag{12}$$

As the investigation shows, the QLD leads to a certain distribution of particles with the pitch angles, which will inevitably result in the synchrotron radiation mechanism with the following energy of emitted photons (e.g. Rybicki & Lightman, 1979)

$$\epsilon_{eV} \approx 1.2 \times 10^{-8} B \gamma_b^2 \sin\bar{\psi}. \tag{13}$$

3. Results

In this section we will apply the mechanism of the quasi-linear diffusion to the anomalous pulsar 4U 0142+61 for studying the possibility of simultaneous generation of radio waves and soft X-rays. In the

doi: https://doi.org/10.52526/25792776-2021.68.1-114

framework of the proposed model, the QLD is provided by the feedback of the cyclotron waves. Let us consider mildly relativistic particles of the plasma component with $\gamma_p = 3$ and the beam component with $\gamma_b = 10^7$. Then, by taking into account that the energy is uniformly distributed, $n_b\gamma_b \approx n_p\gamma_p$, one can reduce Eq. (2)

$$\nu \approx 1.9 \times \left(\frac{\gamma_p}{3}\right)^4 \times \left(\frac{\gamma_b}{10^7}\right)^{-2} \times \left(\frac{R}{10^{10}cm}\right)^{-6} MHz. \tag{14}$$

As we see from this expression, the cyclotron frequency is very sensitive to a location in the magnetosphere. One can straightforwardly show that considering the following interval of the beam Lorentz factors $(1-2)\times 10^7$ the best fit to observations (40 MeV, 111 MeV) is achieved by the parameters, $\gamma_p \sim 2.77$, $R \sim 4.8\times 10^9$cm. Despite the mentioned fact that these are resonance cyclotron waves, we see that the corresponding frequency interval is relatively wide. The reason is following: the resonance happens for given values of the Lorentz factors - thus for a certain value of it, there is a certain value of the radiation frequency. But relativistic particles are distributed by their kinetic energy, which lies in a broad interval. Therefore, in exciting waves all resonance particles (with broad energy spectra) participate and the resulting frequencies will have a relatively broad interval as well.

As a next step we would like to estimate how efficient is the mentioned instability. Kazbegi et al. (1992) have shown that for $\gamma_b/(2\rho\omega_B) \ll \delta$ (which is the case) the increment characterizing amplification of the cyclotron waves is given by

$$\Gamma = \frac{\omega_b^2}{2\nu\gamma_p}, \tag{15}$$

where $\omega_b \equiv \sqrt{4\pi n_b e^2/m}$ is the plasma frequency corresponding to the beam component. One can show that for the aforementioned parameters, the value of the growth rate lies in the following interval $\sim 10^3 - 10^4\text{s}^{-1}$. Therefore, the corresponding timescale, $\tau \sim 1/\Gamma$, is of the order of $\sim 10^{-4} - 10^{-3}$s. On the other hand, we have seen that the best fit to observations is achieved for the waves excited in the location, $R \sim 5.9\times 10^9$cm. This means that plasma stay inside the magnetosphere for relatively long time. In particular, the escape timescale, $t_{esc} \sim (R_{lc}-R)/c$ ($R_{lc} = cP/(2\pi)$ is the light cylinder radius) is of the order of ~ 1s. As we see, the instability timescale is by many orders of magnitude less than the escape timescale, which means that the process is extremely efficient and physically feasible.

We have already explained that the cyclotron waves will influence the particle distribution via diffusion (feedback mechanism) leading to certain pitch angles (see Eqs. (12, 13)). In Figure 1 we show the dependence of synchrotron photon energy on the radio frequency. The set of parameters is: $P \approx 8.7$ s, $\gamma_p = 2.77$, $B_{st} \approx 1.3\times 10^{14}$ G, $R_{st} \approx 10^6$cm, $R = 4.8\times 10^9$cm. It is clear from the plot that ϵ_{keV} is a continuously decreasing function of radio frequencies. This is direct consequence of Eqs. (2, 6, 11, 12, 13). In particular, according to Eq. (13) the photon energy behaves as to be $\epsilon_{eV} \sim \gamma_b\overline{\psi}$, on the other hand, by taking into account the relation $D_{\perp,\perp} = D\delta|E_k|^2$, one can see from Eqs. (6, 11, 12) that $\overline{\psi} \sim \gamma_b$, which by combining with Eq. (13) leads to the following dependence $\epsilon_{eV} \sim \gamma_b^3$. Therefore, more energetic particles produce more energetic synchrotron photons, but since the cyclotron frequency is a decreasing function of γ_b (see Eq. (14)), lower radio frequencies correspond to higher X-ray photon energies.

As it is clear from the plot, the relativistic electrons with Lorentz factors $(1-1.7)\times 10^7$, can lead to a simultaneous generation of radio waves (from 40 MHz to 111 MHz) and soft X-rays (from $0.3-1.4$ keV) respectively. According to the proposed model, emission mechanisms are produced by plasmas inside the magnetosphere of the anomalous pulsar 4U 0142+61, relatively far as from the neutron star's surface, as from the light cylinder area, $R \sim 4.8\times 10^9$cm.

4. Summary

The main aspects of the present work can be summarized as follows:

1) In this paper we examined the role of the quasi-linear diffusion in producing soft X-rays and radio emission in the magnetosphere of the anomalous pulsar 4U 0142 + 61.

doi: https://doi.org/10.52526/25792776-2021.68.1-114

2) Considering the anomalous Doppler effect, which leads to the unstable cyclotron waves, we have studied the feedback of these waves on a distribution of relativistic particles. Solving the equation governing the QLD, the corresponding expression of the average value of the pitch angle is derived and analyzed for physically reasonable parameters. It has been found that the higher the the synchrotron photon energy, the lower the radio frequency.

3) We have shown that the quasi-linear diffusion might provide a simultaneous generation of radio emission (40 MHz-111 MHz) and soft X-rays (0.3 keV-1.4 keV) in plasmas located on the distance 4.8×10^9cm from the pulsar's center for appropriate parameters $\gamma_p = 2.77$, $\gamma_b = (1 - 1.7) \times 10^7$.

The present investigation shows that the QLD is a mechanism that can explain a simultaneous generation of the observationally evident radio waves (Malofeev et al., 2010) and soft X-rays (Góhler et al., 2005). The aim of the present paper was to examine only one part of the problem, although a complete study requires to investigate the spectral pattern of emission as well. In the standard theory of the synchrotron emission it is assumed that due to the chaotic character of the magnetic field lines (Bekefi & Barrett, 1977, Ginzburg, 1981), the pitch angles lie in a broad interval (from 0 to $\pi/2$). In our model the distribution function of particles is strongly influenced by the process of the QLD and as a result the pitch angles are restricted by the balance of dissipative and diffusive factors. This will inevitably lead to a spectral pattern, different from that of Bekefi & Barrett (1977), Ginzburg (1981). Therefore, we will investigate this problem in future studies.

References

Aliu E. et al., 2008, ApJ, 674, 1037A

Baring, M. G. & Harding, A. K., 1998, ApJ, 507, L55

Bekefi, G., & Barrett, A. H. 1977, Electromagnetic vibrations, waves and radiation, The MIT Press, Cambridge, Massachusetts and London, England

Camilo, F., Ransom, S., Halpern, J. et al., 1981, Nature, 442, 892

Chkheidze, N., Machabeli, G. & Osmanov, Z., 2010, ApJ, 721, 318

den Hartog, P. R., Kuiper, L., Hermsen, W., Rea, N., Durant, M., Stappers, B., Kaspi, V. M., Dib, R., 2006, Ap&SS, 308, 647

Enoto, T., Makishima, k., Nakazawa, K., Kokubun, M., Kawaharada, M., Kotoku, J. & Shibazaki, N., 2011, Publ. Astron. Soc. Jpn. (accepted)

Fahlman, G. G. & Gregory, P. C., 1981, Nature, 293, 202

Ginzburg V.L., 1981, "Teor. Fizika i Astrofizika", Nauka M. 1981

Gogaberishvili, G., Osmanov, Z. N., & Mahajan, S. M. 2021, MNRAS, 503, 3592

Góhler, E., Wilms, J & Staubert, R., 2005, A&A, 433, 1079

Landau L.D. & Lifshitz E.M., 1971, Classical Theory of Fields (London: Pergamon)

Malofeev, V. M., Teplykh, D. A. & Malov, O. I., 2010, Astron. Rep., 54, 995

Kaspi, V., 2007, Ap&SS, 308, 1

Kazbegi, A.Z., Machabeli, G.Z & Melikidze, G.I., 1992, in Proc. IAU Collog. 128, The Magnetospheric Structure and Emission Mechanisms of Radio Pulsars, ed. T.H. Hankins, J:M: Rankin & J:A: Gil (Zielona Gora: Pedagogical Univ. Press), 232

Lominadze, J.G., Machabeli, G.Z. & Mikhailovsky, A.B., 1979, J. Phys. Colloq., 40, No. C-7, 713

doi: https://doi.org/10.52526/25792776-2021.68.1-114

Machabeli G. & Osmanov Z., 2009, ApJL, 700, 114

Machabeli G. & Osmanov Z., 2010, ApJ, 709, 547

Machabeli G.Z. & Usov V.V., 1979, Pis'ma Astron. Zh., 5, 445

Malov, I.F. & Machabeli, G.Z., 2001, ApJ, 554, 587

Malov I.F. & Machabeli G.Z., 2002, Astronomy Repports, Vol. 46, Issue8, p.684

Mazets, E. P., Golenetskii, S. V., Ilinskii, V. N., Aptekar, R. L., Guryan, Iu. A., 1979, Nature, 282, 587

Osmanov, Z., 2014, MNRAS, 444, 2494

Osmanov, Z. & Machabeli, G., 2010, A&A, 516, A12

Osmanov, Z., 2010a, ApJ, 721, 318

Osmanov, Z., 2010b, MNRAS, 411, 973

Rybicki G.B. & Lightman A. P., 1979, Radiative Processes in Astrophysics. Wiley, New York

doi: https://doi.org/10.52526/25792776-2021.68.1-114

Coupling and recoupling of binaries in chaotic three body systems

T. S. Sachin Venkatesh*

Delhi Technological University, New Delhi, India

Abstract

Three body systems where one of the bodies is ejected without escaping the binary system have previously been studied in various restricted forms. However, none of these studies dwells on the problem in a general setting. Thus, to study this phenomenon qualitatively, we try to expand this problem's scope to unequal mass systems and generalize them by considering various configurations of fixed initial points with precisely calculated initial velocities, some zero velocity models, and some optimized models. We will see the use of terminology similar to the previous studies done in this domain, but incorporate different analytical and evaluation methods.

Keywords: *Celestial mechanics, Three-body problem, Gravitational interaction, Chaos, Orbits, Astronomical simulations*

1. Introduction

The three-body problem is one of the long-standing fundamental problems of dynamical systems. Until 1975, there were not many models of three-body systems and the ones that existed were too restrictive and specific about the parameters of the model. In 1890, Poincaré proved the non-existence of the uniform first integral of a three-body problem in general, and also highlighted the sensitive dependence to initial conditions of its trajectories, a brief account of the same is given in Chenciner (2012). Three-body systems without mass hierarchy are never thought to be stable for very long. They can indeed exist for some time, but they are not found to be stable long term. In these systems, each body orbits the center of mass of the system. Mostly, two of the bodies form a close binary system, and the third body orbits this binary at a distance much larger than that of their orbit. This arrangement is called hierarchical. The reason for this behavior is that if the inner and outer orbits are comparable in size, the system may become dynamically unstable, leading to a body being ejected from the system. Hut & Bahcall (1983) had done a qualitative study on such ejecting systems. However, their model was restricted to an equal mass system in 2 dimensions specifically modeled according to resonance scattering. They also stated that generalizing that specific problem to 3 dimensions would not provide new insights as they would qualitatively be the same.

2. Methods

We focus this work on chaotic systems, where the three body system finally reduces to a binary and an *escaper*. We then compare them to a benchmark, a stable unequal mass three body system on the basis of their phase space, the total energy of the system and the evolution of different binaries in the systems. The stable system used as a benchmark has a mass ratio of 1:1:2 and a cyclic phase space, demonstrating that the system is stable over a large number of iterations. Due to its computationally expensive nature, the system was simulated for only 500 iterations. The test systems simulated were constructed using the dataset provided by Boekholt & Portegies Zwart (2015) for

*tssachin.venkatesh@gmail.com

doi: https://doi.org/10.52526/25792776-2021.68.1-121

different configurations of Plummer models and an extensive list of initial positions. All simulated systems initially exist in a temporarily bound triple mass system.

We notice the use of Euler-Cromer method to account for the accumulation of errors in the total energy of the model, keeping in mind the instability in the system. To minimize error propagation in position and velocity space, the Levenberg-Marquardt method was used to account for minuscule and extreme values as artificial values creep in over longer iterations in the previous method which cannot be tolerated in the case of these values.

With the kinetic energy of the system, E_{kin} given by

$$E_{kin} = \frac{1}{2}\sum_{i=1}^{3} M_i \frac{\mathrm{d}R_i}{\mathrm{d}t}.\frac{\mathrm{d}R_i}{\mathrm{d}t}$$

and the potential energy, E_{pot} given by

$$E_{pot} = -\frac{G}{2}\sum_{i=1}^{3}\sum_{j=1}^{3}\frac{M_i M_j}{r_{ij}},$$

we have total energy $E_{tot} = E_{kin} + E_{pot}$

The simulations were stopped when the systems dissolved into a binary and an *escaper*. We will categorize a body as an *escaper* along the same lines as Boekholt & Portegies Zwart (2015). The conditions are :

- The *escaper* has a positive energy, $E_{esc} > \mathbf{0}$
- The *escaper* is moving away from the centre of mass, $\mathbf{r}.\mathbf{v} > \mathbf{0}$

The barycentric frame of the bodies were considered when calculating the energy of the *escaper*. We do not differentiate between hard binaries and soft binaries as it has been stated by Hills (1989) that these metrics do not do justice and do not provide enough information in the case of unequal mass triple systems. An upper limit of 500 iterations is set, to not exceed the benchmark and a lower limit of 200 iterations. Models that dissolved into a binary and an *escaper* before 200 iterations were not included in the sample space.

3. Observations and discussion

Of all the systems simulated, some displayed a peculiar behaviour where a body is ejected without escaping from the binary. After a long solitary path, such bodies turn around and engage the binary system once again to form a temporarily bound triple system. This mechanism will be called as *quasi-ejection* henceforth. Based on the evolution of the system, if it dissolves into a binary and an *escaper* after being in a temporarily bound triple system for *iterations* > *lower limit*, we categorise them accordingly :

- If the end binary of a system is the same as the binary formed after the first *quasi-ejection*, we call it a ***flyby***
- If the end binary of a system is not the same as the binary formed after the first *quasi-ejection*, we call it an ***exchange***

The ratio of *flybys* to *exchanges* was practically equal across all system configurations, with some bias towards *flybys*. However, the result of importance here is that the *escaper* turned out to be the lowest mass body in most cases and the end binary constituted the more massive bodies. If $E_{tot} > 0$, the system must split and if $E_{tot} < 0$, the system may lead to an *escaper* or form a stable three body system. But the combined constraints of E_{tot} of the system and the dynamic exchange of E_{tot} between each body point towards the lowest mass body being the *escaper* in most cases. This is complimented by the result deduced from E_{esc}.

doi: https://doi.org/10.52526/25792776-2021.68.1-121

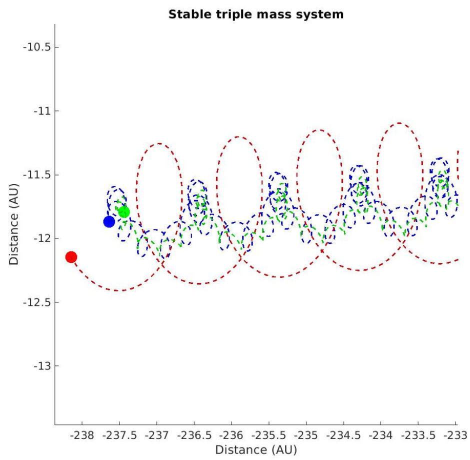

Stable three body system, the benchmark for this study. The mass ratio of the bodies are 1:1:2 (Blue:Red:Green).

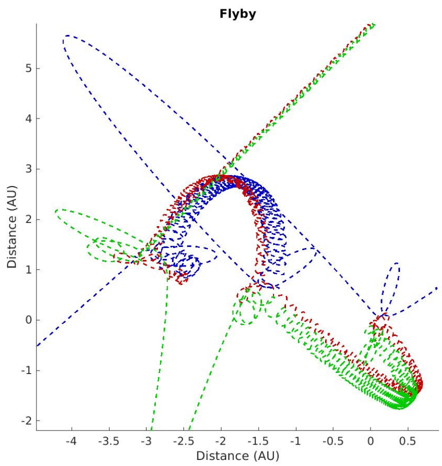

The initial binary is formed by the red and green bodies while the blue body traverses a returning trajectory. Splitting and recoupling continue until the system permanently splits into the initial binary and an *escaper*.

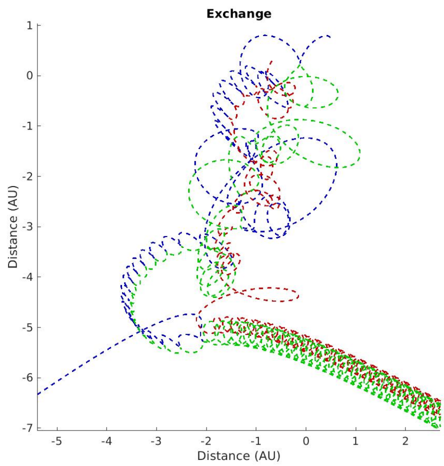

The initial binary is formed by the red and blue bodies, which is cut short by the body in green. Splitting and recoupling continue until the system permanently splits into the non initial binary and an *escaper*.

Figure 1. The code written by Sheen (2016) forms the basis for all the simulations. We added total energy calculation for both the system and the bodies and a phase diagram to this program. This helps predict the successive motion of the bodies and thus, the stability of the systems designed using data from Boekholt & Portegies Zwart (2015).

doi: https://doi.org/10.52526/25792776-2021.68.1-121

We suspect the mass hierarchy of the bodies to be the primary governing factor in this problem of coupling and recoupling of binaries, not the initial conditions as one may believe. In *Exchanges* where the initial binary constituted of the lowest and highest mass bodies and the *escaper* was the highest mass body were extremely low, especially in disproportionate mass systems. This can be attributed to the Hill sphere (Astakhov et al., 2003) mechanism, thus destabilizing the binary. Nevertheless, in almost all cases, the new binary is formed by the massive bodies which attain stability, and the lowest mass body ends up being the *escaper*. Given the wide scope for further studies in this sub-domain and the large impact it can have on qualitative analysis of similar systems in the future, and therefore is likely to increase our understanding of the mechanisms and methods at play, preliminary results have been presented here. To go beyond these results requires a more detailed analysis and robust computations, which are postponed to a future article.

Acknowledgements

Special thanks to Suyog Garg and Shobhit Ranjan for their insights on the article and for providing useful comments.

References

Astakhov S. A., Burbanks A. D., Wiggins S., Farrelly D., 2003, Nature. , 423, 264

Boekholt T., Portegies Zwart S., 2015, Computational Astrophysics and Cosmology, 2, 2

Chenciner A., 2012, Poincaré and the Three-Body Problem. Seminaire Poincare XVI, http://www.bourbaphy.fr/chenciner.pdf

Hills J. G., 1989, in Bulletin of the American Astronomical Society. p. 796

Hut P., Bahcall J. N., 1983, Astrophys. J. , 268, 319

Sheen M., 2016, Simulation files - 3 Body Problem, https://github.com/mws262/MAE5730_examples/tree/master/3BodySolutions

doi: https://doi.org/10.52526/25792776-2021.68.1-121

Whereas an observer has nothing to do with it!

Emir E. Ashursky*

Institute for Scientific Prognosys, Kiev, Ukraine

Abstract

In this article, the author, as possible, subjects to a comprehensive (though mostly, it's true, critical) analysis the one-sided attempts of a number of current Western astrophysicists to somehow substantiate the well-known Fermi paradox. Is it a joke to say: in own perverted designs, some of them even go so far as to unceremoniously rearrange the cause with the effect! However, so to speak, "for greater pluralism of views", we'll along the way quote many other, much clearer and sapider opinions on this topic — right from the lips of alternatively thinking scholars (and besides — I note – with a world name!). Wherein some of them frankly assess the today stalemate uncertainty as a kind of creative stagnation; second are inclined towards the version of consumerity-driven global theoretical shift; while third directly declare that it is time for representatives of the exact sciences, obviously, to prepare for the change of the old starry paradigm to cardinally updated one. But still, without waiting for the weather by the sea (as well as just for spite the arrogant purse-proud Yankees, who, alas, do not seriously recognize our current potential capabilities, or even past truly grandiose achievements), here we will try independently to resolve some of the most controversial issues.

Keywords: *proscopy - many-phase evolution - Drake equation - anthropic principle - pulsating Universe - informons - pranophytes - ontological memory -theosophical doctrine - hegemony of robots*

1. Introduction

The freshest widely publicized successes of overseas theorists who have by guess "studied" the first seconds after the Big Bang through orbiting telescopes and nuclear colliders, along with pride in modern world science, cannot but evoke in you and me a bit of sound skepticism about their activities. For such a zero retropolation often, alas, contradicts many accepted logical postulates. In particular, if long-term forecasts are anyway built usually thanks to the sufficient availability of 100% proven archived facts, then it is still not entirely clear, what speculative "peeping" into pre-human history can be based on. And from here - you, as it were, shouldn't be extra surprised by the abundance of all kinds of false moves and other semantic absurdities (from the model of the Cold Big Bang - to the ever-memorable torsion fields) by the spontaneous witnesses of which most of us had a chance to become.

In this regard, I will give a couple of illustrative examples. In 2017, Nikolai Kardashev, director of the FIAN Astrospace Center (Moscow), said that, in his opinion, all highly developed civilizations had long since left our Universe, having moved to other areas of the Multiversum that are more suitable for them. True, it is not so difficult to guess the oblique cause for such a rather strange unscientific statement for an academician. The fact is that at the very beginning of his research career, Nikolai Semyonovich often assured his colleagues in all seriousness that in the near future he had real plans to meet, and perhaps even personally make contacts with someone of the intelligent alien inhabitants. However, as soon as his this-worldly path began gradually but steadily to approach its eternal implacable finale, the gray-haired metropolitan "ex-dreamer" was already forced nolens-volens to look for any options of more or less decorous tactical retreat.

*e.ashursky@gmail.com

doi: https://doi.org/10.52526/25792776-2021.68.1-125

Although in this sense, his faithful deputy at the institute Igor Novikov, who was carried away back in the mid-1980s, frankly, with a very, very dubious idea of creating a time machine, turned out to be by no means more far-sighted than his boss. Much has already been said about the apparent delusionality of such baseless fantasies, which contradict all recognized natural science canons (especially with regard to chrono-voyages into the past). However, the author is going to share own interesting views and thoughts on this matter with the readers of ComBAO in more detail already in the next (autumn) issue of the magazine. But nevertheless, Igor Dmitrievich himself is still to no avail toiling with his inflamed "idée fixe" to this day...

So in general, presumably, it was not in vain that the ancient Latins used to say: ≪*Errare humanum est, stultum est in errore perseverare*≫. For in the end, a similar fate has not passed the greatest genius of Soviet astronomy V.A. Ambartsumyan either. Particularly, in 1958, at the traditional Brussels conference "Solvay" in physics, he read one of his most famous reports, publicly declaring for the first time that "*enormous explosions take place in galactic nuclei and as a result a huge amount of mass is expelled. In addition, they (galactic nuclei) must contain bodies of unknown nature*". Thus, he gave, in essence, a creative impetus to a new science – the theory of galactic evolution. And everything would be fine, but only in his subsequent works, Viktor Amazaspovich, having apparently succumbed to all kinds of fashionable then illusory-deceptive hypotheses, presented own position in a slightly different way. To wit: supposedly such smoked-bluish jets are nothing more than spontaneous intrusions of matter from parallel cosmic reality. Although in fact it is now generally accepted that this is most likely due to the interaction of the magnetic field with the accretion disk around the black hole (well or, as a quite valid option, the very massive neutron star).

By the by, it was no coincidence that we took the liberty of making here this brief (but, I hope, useful) excursion into the times of the formation of the newest progressive knowledge about space. For in this article, the author, as possible, subjects to a comprehensive (though mostly, it's true, critical) analysis the one-sided attempts of a number of current Western astrophysicists to somehow substantiate the well-known Fermi paradox. Is it a joke to say: in their perverted designs, some of them even go so far as to unceremoniously rearrange the cause with the effect!

However along the way, so to speak, "for greater pluralism of views", we will quote many other, much clearer and sapider opinions on this topic – right from the lips of alternatively thinking scholars (and besides – I'll note - with a world name!). Wherein some of them frankly assess the today stalemate uncertainty as a kind of creative stagnation; second are inclined towards the version of consumerity-driven global theoretical shift; while third directly declare that it is time for representatives of the exact sciences, obviously, to prepare for the change of the old starry paradigm to cardinally updated one. But still, without waiting for the weather by the sea (and also *just* for spite the arrogant purse-proud Yankees, who, alas, do not seriously recognize our current potential capabilities, or even past truly grandiose achievements), here we will try independently to resolve some of the most controversial issues.

2. Whereas an observer is surely far-fetched here by ears.

It's no secret that the amateurish naivety of the so-called anthropic principle is now being criticized by many competent and widely known in the world specialists. Although, in fact, in the model of the "pulsating Universe" (as well as in L. Smolin's very just relevant today evolutionary hypothesis), the choice of the initial free parameters is obviously not accidental. First, it can be assumed that they – as inviolable reference samples – are entirely passed from generation to generation. Secondly, even if they are formed anew at each next Bang, it is due to having some kind of "through" ontological memory. But even with the culling away both of these facultative guesses, as a decisive unshakable argument against the imaginary anthropophilicity of our existence is what in absolutely any Universe there must present subtle demigods & angels (pranophytes) as well as, apparently, the smallest fragments of the mind (informons). This, of course, also applies to those cases when the self-assembly of heavy elements or molecules (and hence, the habitual life for us) would turn out to be too energy-intensive and de-facto unpromising from the astrophysical point of view.

By the way, actually one can imagine in theory 3 principled dynamic schemes of universe:

doi: https://doi.org/10.52526/25792776-2021.68.1-125

a) a kind of swing "from energy (Will) $\Longrightarrow$ to information (Reason) and back";

b) continuous experiments or even improvisations of Will itself (let's note that the old theosophical teaching about the previously existed 5 discarnate races also fits into here);

c) and finally, as if independently of them, a fashionable freshly-baked hypothesis about our being as a computer simulation of the physical world can be considered either (moreover, in this case, bits and bytes well familiar to IT-specialists become already the main source of interaction of all real-virtual objects).

In the first paragraph, predicting events (proscopy) is possible due to a clear step-by-step repeatability of history; and in the second – through the management of the events relevant for the Will. As for the semi-fantastic idea of parallel worlds (or, say, multidimensional space), it doesn't, apparently, jump beyond this framework, and only brings some own colorful variety to the overall picture.

By the way, the seeming polarity of interests of Reason and Will is actually sometimes felt, perhaps, except that in the socio-historical plane. At the rest they are everywhere going side by side, as if complementing each other, and moreover under the general supremacy (for now, at least) of Reason. That's why we can oppose them each other on the scale of the Universe (and even then — as one of several permissible options) only in terms of time parameters: from the energy of saturated but structureless chaos - to an extremely structured but cold lifeless Cosmos. And just at this finishing segment, due to the critical shortage of energetic resources, the transition from the current living civilization to the hegemony of robots seems to be quite real.

3. And what is proposed by the author instead?

So, what are the logical conclusions from this? Well, first of all, the fact that the "strong anthropic principle" on the version of J. A. Wheeler ("*Observers are necessary to bring the Universe into being*"), despite even its wit and ostentatious elegance, is actually a rather trivial, i.e. doesn't give researchers any practical benefit. As for the "weak" (a little earlier proposed by our countryman G. M. Idlis in such formulation: "*We are observing a deliberately not an arbitrary region of the Universe, but the one whose special structure made it suitable for the emergence and development of life*") then here, alas, things are much worse. Not only is it, already inherently imbued with sophistry (having unceremoniously reshuffled cause and effect) but also does not correspond at all to the reality around us. Because for any corpuscular parameters, the probability of the emergence of intelligent life (and along with it – of an observer himself) remains all the same high enough! Well, perhaps only, however, not in vacuum space; and of course, not right there away – as if by a fleeting whim of a goldfish but at least after a few billion years...

Nevertheless some are trying to appeal here to the notorious Drake equation:

$$N = R \cdot f_p \cdot n_e \cdot f_l \cdot f_i \cdot f_c \cdot L$$

They say, if even by the most moderate standards, in our galaxy should be 10 highly developed extraterrestrial cultures but there is not a single one of them so far - then, in their opinion, it means that the uniqueness of a formal observer is something for granted. While in reality, the last circumstance can, perhaps, testify only to the fact trite Laplace-Cartesian explanation here, alas, does not work. That is, more specifically, this indicates the etiological complexity of the origin of civilizations associated with the nonlinearity of the paths "from inanimate to living" (which, as it were, is confirmed by the spread version about the 5 races that preceded us).

In general, comparing H. P. Blavatsky's theory of the root races with modern biologists' evolutionary tree, one involuntarily comes to the conclusion that the former quite might serve as a kind of well-adapted soil for the normal "growth" of the latter. In other words, at first for a pretty long time the primary bricks of organized matter (in the form of stable atoms and complex polymer molecules) took shape painstakingly from the ether, the astral, the mental body as well as proton substrate, and then everything already continued according to the familiar school scenario.

doi: https://doi.org/10.52526/25792776-2021.68.1-125

But, incidentally, only a rough simplified picture of earthly evolution was still given here. Since, in fact, both of these processes went on almost simultaneously with each other; however at the preparatory stage, the laws of theosophy (or, if you like, astrophysics) "ruled" in it, though hereinafter they have already become predominantly of biological nature. In this regard, the emergence of a habitual phenomenon of life can be somehow discussed, perhaps, from the moment of a successful mutually beneficial synthesis of the mental sheath (responsible, as known, for ancestral memory) with the immanent sensitivity of organic rings.

***

Thus, here we – in contrast to the obviously far-fetched anthropic – come to the formulation of another principle, much more important for science. Its essence is that the Universe at this stage is being ordered in a qualitative aspect, disordering simultaneously in a quantitative (thermal) one. Moreover, this fundamental property should, apparently, apply to all laws of thermodynamics (and in particular, the second). Although the same concerns to synergetics either – contrary to what I. Prigogine imagined (supposedly, individual fluctuations arise against the background of a general increase in entropy, but all this is only in some limited space).

So, most likely, disordering goes along the energetic vector, and self-regulation along the informational one. But this dependence, however, is not linear, since a developed intellect creates new algorithmic products much easier and faster – without high energy consumptions (when compared with that was at the dawn of Universe's formation). And hence, the dilemma about "what namely (elementary micro-regulating or machine-human macro-intelligence) the current algorithms are spawned by" is no longer almost meaningful, since any modern intelligence, in turn, is a product of the streamlining. That is, the vast majority of today laws of physics, chemistry and biology (and especially the firsts of them) are the result of the action of self-organizing processes, for they all, in one way or another, are associated with orderly movement!

4. Well, and what do world luminaries think about that?

And finally, as promised, we will cite some of the brightest and original (though sometimes, it is true, quite sharp) opinions of popular writers and recognized luminaries of academic science, including even last year's Nobel laureates.

So, the anthropic principle, as we found out, inherently presupposes not only suitable primary conditions, but a precise and adequate adjustment of a number of necessary parameters. Although at the same time, according to the famous British physicist sir Roger Penrose, it could hardly serve as the main driving force behind externally directed evolution: after all, consciousness is, in general, only a kind of handy tool for natural selection.

And according to the editor-in-chief of "Skeptic" magazine Michael Shermer, rejecting the belief in a single carbon form of life, one can conclude that in reality it is we who are perfectly and accurately tuned to the Universe, and not vice versa. And even if it is difficult for us to fully understand how exactly physical phenomena correlate with the earth mind, it still "supposes" about this quite differently!

For his part, the legendary Polish science fiction writer Stanislaw Lem emphasizes that where per definition is empty, there are no corresponding reason to talk about some personality with own worldview. And, besides, the Universe cannot be accused of deliberate intent, which means that the very existence of an abstract observer is not obligate too. In other words, it develops the way it wants – and no special higher sense can stand behind that.

And here it should also be borne in mind that we are usually tend to find correlations wherever, as seems to us, it could not do without a prior conscious adjustment or "garbling the cards". One such case is the conditional analogy with the firing squad (on the illustrative example of the Canadian philosopher John Leslie) – when a prisoner, who was about to expect death, suddenly remains unharmed, constantly being puzzled after that by persistent obsession: didn't this company of riflemen deliberately missed?

doi: https://doi.org/10.52526/25792776-2021.68.1-125

In turn, the European authority №1 on neural networks Jürgen Schmidhuber points out that the anthropic principle does not allow to predict anything truly useful and important for us or to answer at least some topical questions of being.

So, taking into account all these characteristics, it can even be equated to the main working tool of psychologists. Well and if someone is still not quite in the know, let me remind you: with no matter how severe personal grief this or that client turns to such "mental savers", a real professional psychologist will first of all try to assure him, supposedly all that has happened is in fact the greatest attainable good and almost heavenly happiness. Because in any alternative scenario, the new psychologically calculated situation would certainly be a hundred times worse!

Let's now turn to the "weak anthropic principle". From its definition directly, in particular, it follows, that somewhere around us there may well be other material universes (but already with different settings). And in them, moreover, intelligent life is practically no longer capable of originating. But if one talks about the multidimensional quantum mechanical interpretation, then (according to an emeritus professor of humanities John Earman) we do not yet have any even vague guesses about the very mechanism of splitting of that hypothetical proto-Universe. And, of course, there is no information about where, when and for what reason such could have happened at all. That's why at this stage of our planetary development, we have no right to assert competently about the plurality of worlds.

And finally, it should be added that some deeply religious scholars (for example, member of the Royal Society rev. John Polkinghorne) use the anthropic principle as another convincing proof of God-presence. I.e. that supposedly it was the Lord who created such a subtle cosmic setting which allowed an intelligent earthly observer to exist. No wonder that, as the famous Christian apologist and neoplatonist William Craig notes, in the midst of heated discussions on the anthropic principle, the boundaries between physics and philosophy are becoming already rather blurred.

However, the argument about man as the crown of divine creation is intuitive one: so it cannot yet, by and large, be confirmed or refuted. After all, de-facto you and I are only a small insignificant piece of the Universe, the sudden disappearance of which it will not even notice; and the notorious anthropic principle is just a mistake of the player, who clearly, alas, overestimated his role.

References

1. В. А. Амбарцумян: «Философские вопросы науки о вселенной» - Ереван, 1973 г.
2. W. Ambartsumian: "Philosophische Probleme der modernen Kosmologie."– Berlin, 1965.
3. Hynek J. Allen & Vallee Jacques: "The Edge of Reality". - Chicago: Henry Regnery. 1975.
4. К. И.Чурюмов, А.Ф.Пугач: «Небо без чудес» – Киев, «Политиздат Украины», 1987г.
5. Станислав Лем: «Одиноки ли мы в космосе?» - М., журнал «Знание — сила» № 7, 1977 г.
6. Э. Э. Ашшурский: «Сквозь призму философского анализа» //Киев, изд. «Пам'ятки України», 1998 г.
7. Э. Э. Ашшурский: «Опыт философского осмысления противоречий современной науки» // Киев, изд. «Эсперанца», 1994 г.
8. И. Р. Пригожин, И. Стенгерс – «Порядок из хаоса: Новый диалог человека с Природой». – М.: Прогресс, 1986. – 431 с.
9. Г. В. Чефранов: «Бог. Вселенная. Человек» //Таганрог, изд. ТРТИ, 1992 г.
10. Наталия Лескова: «То, что мы делаем, — это впервые» (интервью с Н.С.Кардашевым) // журнал «Наука и жизнь». — № 11 за 2017.г., с. 14—19.
11.Э. Э. Ашшурский: «Философия в поисках и находках» //Киев, изд. «Эсперанца», 1997 г.

doi: https://doi.org/10.52526/25792776-2021.68.1-125

Communications of BAO, Vol. 68, Issue 1, 2021, pp. 130-138

Study of the radio and optical properties of Active Galactic Nuclei

H. V. Abrahamyan *

NAS RA Byurakan Astrophysical Observatory (BAO), Byurakan 0213, Aragatzotn Province, Armenia

Abstract

The investigation of the physical properties of active galactic nuclei is one of the most important tasks of astronomy. Until now, the properties of AGN have not been fully studied. Therefore, we have studied a number of important properties of AGN. For example, one of the main properties of AGN is the variability. We have studied samples of AGN derived by different methods. For these sources, we have identified some properties of activity for the radio and optical ranges. These properties give us some insight into the active galaxies.

Keywords: *active galactic nuclei, QSO, radio spectral index, cross-correlation*

1. Introduction

During the first half of the 20th century, photographic observations of nearby galaxies detected some characteristic signatures of AGN emission, although there was not yet a physical understanding of the nature of the AGN phenomenon. Some early observations included the first spectroscopic detection of emission lines from the nuclei of NGC 1068 and Messier 81 by Edward Fath (published in 1909), and the discovery of the jet in Messier 87 by Heber Curtis (published in 1918). Further spectroscopic studies by astronomers including Vesto Slipher, Milton Humason, and Nicholas Mayall noted the presence of unusual emission lines in some galaxy nuclei. In 1943, Carl Seyfert published a paper in which he described observations of nearby galaxies having bright nuclei that were sources of unusually broad emission lines. Galaxies observed as part of this study included NGC 1068, NGC 4151, NGC 3516, and NGC 7469. Active galaxies such as these are known as Seyfert galaxies in honor of Seyfert's pioneering work.

The development of radio astronomy was a major catalyst to understanding AGN. Some of the earliest detected radio sources are nearby active elliptical galaxies such as Messier 87 and Centaurus A. Another radio source, Cygnus A, was identified by Walter Baade and Rudolph Minkowski as a tidally distorted galaxy with an unusual emission-line spectrum, having a recessional velocity of 16,700 kilometers per second. The 3C radio survey led to further progress in discovery of new radio sources as well as identifying the visible-light sources associated with the radio emission. In photographic images, some of these objects were nearly point-like or quasi-stellar in appearance, and were classified as quasi-stellar radio sources (later abbreviated as "quasars").

Soviet Armenian astrophysicist Viktor Ambartsumian introduced Active Galactic Nuclei in the early 1950s. At the Solvay Conference on Physics in 1958, Ambartsumian presented a report arguing that *"explosions in galactic nuclei cause large amounts of mass to be expelled. For these explosions to occur, galactic nuclei must contain bodies of huge mass and unknown nature. From this point forward Active Galactic Nuclei (AGN) became a key component in theories of galactic evolution."* His idea was initially accepted skeptically.

A major breakthrough was the measurement of the redshift of the quasar 3C 273 by Maarten Schmidt, published in 1963. Schmidt noted that if this object was extragalactic (outside the Milky

*abrahamyanhayk@gmail.com

doi: https://doi.org/10.52526/25792776-2021.68.1-130

Way, at a cosmological distance) then its large redshift of 0.158 implied that it was the nuclear region of a galaxy about 100 times more powerful than other radio galaxies that had been identified. Shortly afterward, optical spectra were used to measure the redshifts of a growing number of quasars including 3C 48, even more distant at redshift 0.37.

The enormous luminosity of these quasars as well as their unusual spectral properties indicated that their power source could not be ordinary stars. Accretion of gas onto a supermassive black hole was suggested as the source of quasars' power in papers by Edwin Salpeter and Yakov Zeldovich in 1964. In 1969 Donald Lynden-Bell proposed that nearby galaxies contain supermassive black holes at their centers as relics of "dead" quasars, and that black hole accretion was the power source for the non-stellar emission in nearby Seyfert galaxies. In the 1960s and 1970s, early X-ray astronomy observations demonstrated that Seyfert galaxies and quasars are powerful sources of X-ray emission, which originates from the inner regions of black hole accretion disks.

Today, AGN are a major topic of astrophysical research, both observational and theoretical. AGN research encompasses observational surveys to find AGN over broad ranges of luminosity and redshift, examination of the cosmic evolution and growth of black holes, studies of the physics of black hole accretion and the emission of electromagnetic radiation from AGN, examination of the properties of jets and outflows of matter from AGN, and the impact of black hole accretion and quasar activity on galaxy evolution.

Many active galaxies, especially active galactic nuclei (AGN), are strong in radio wavelengths (e.g. many objects in Véron-Cetty & Véron (2010) have strong radio; the catalogue of Blazars by Massaro et al., 2015 is complied exclusively from objects having radio detection); hence studying radio emission from galaxies may be a key to identify the active ones among them. Radio galaxies, quasars, blazars, megamasers and other classes of objects are strong radio emitters. Radio galaxies and their relatives, radioloud quasars and blazars, are types of AGN that are very luminous at radio wavelengths, with luminosity up to 10^{39} W in the range of 10 MHz to 100 GHz. This radio emission is due to the synchrotron process; the observed radio structure is determined by the interaction between two opposite jets and the external medium, affected by relativistic beaming. The host galaxies are almost exclusively giant elliptical galaxies and radio galaxies can be detected at large distances, making them valuable tools for observational cosmology. Recently, much work was done related to the effects of these objects on the intergalactic medium as well, particularly in galaxy groups and clusters.

2. Creation of Cross-Correlation program: The IRAS PSC/FSC Combined Catalogue

To study the IR point sources we took IRAS PSC and FSC catalogues. They were created in 1986 (IRAS PSC) and 1989 (IRAS FSC), and provide information of fluxes at wavelengths 12, 25, 60 and 100 μm. IRAS PSC contains 245,889 sources and IRAS FSC contains 173,044 sources at galactic latitude $|b| > 10^0$. Each source in these catalogues has coordinate errors. We did a cross-correlation between IRAS PSC and FSC and considered errors for each source; we took those identifications having positional errors between the sources not exceeding 3σ (which corresponds to 99.73% probability). For that, in frame of the Armenian Virtual Observatory (ArVO), we created a software through which we made cross-correlations. To obtain information about fluxes in other IR bands we did cross-correlation using the same method with AKARI-IRC All-Sky Survey Point Source Catalogue, AKARI-FIS All-Sky Survey Bright Source Catalogue and used VizieR for WISE catalogue having very accurate positions.

In catalogues IRAS-PSC and IRAS-FSC, for each source we have positional errors given as Minor and Major axes, which relate to the orientation of the satellite during the observations. For crosscorrelations, we used Major and average axes positional errors for each object. We created a software through which we made cross-correlations. This software allows considering positional errors for each source individually and we have taken identifications having coordinate differences between counterparts not exceeding 3σ (calculated using both sigmas from PSC and FSC). As a result, we obtained 73,770 identifications when using the Major axes and 72,777 when using the average errors.

doi: https://doi.org/10.52526/25792776-2021.68.1-130

To avoid losing identifications, finally we build our Catalogue using identification with Major axes (Abrahamyan et al. (2015)). Some sources have two or more associations. For these sources we take associations using the following criteria:

- the first (nearest by distance) association is taken, if the second one (and others) is 3 times farther than the first one (these are the best identifications and we call them Category 1). We have 58,296 (79%) such associations.
- in case of positional ambiguity (when the genuine association is not clear as in Category 1), we take those associations having close fluxes (coincidence within 20%) and quality flags indicating the same nature of objects. We call them Category 2 associations and we have 10,488 (14%) such cases.
- the first (nearest by distance) association is taken, if the second one (and others) is 2 times farther than the first one (weaker criterion giving worst identifications). We call them Category 3 associations and we have 4901 (7%) such cases.

We are left with 85 worse associations, which also may be regarded as genuine ones with weaker criteria. We have built a distribution of the number of objects from distances of their identifications. Figure 1 shows that the majority of identified objects have limited distance and we have derived by interpolation with polynomial fit that 73.4 arcsec should be taken as the radius of reliable associations.

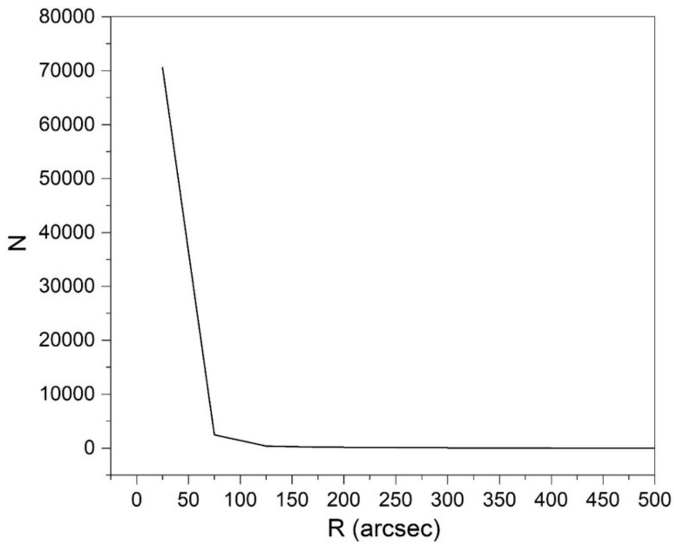

Figure 1. Distribution of the number of sources by distances of their identifications (IRAS-PSC and IRAS-FSC)

.

For cross-correlations with IRAS catalogues most astronomers use search radius $60''$. However, as we see from the comparison and analysis of these identification tools, if we take $60''$ for cross-correlations, then we lose many genuine associations.

For our IRAS PSC/FSC Combined Catalogue we give the probability of classification for each source into "star" or "galaxy". For this purpose we used fluxes and quality flags from IRAS and other catalogues. If IRAS source is confidently identified with AKARI-IRC and there is no match in AKARI-FIS, then in all probabilities the object is a star, and if an IRAS source is detected in AKARI-FIS without a record in AKARI-IRC, then in all probabilities the object is a galaxy. For brighter sources, when all records are available, we use the IR colours, i.e. we follow the change of the flux from shorter to longer wavelengths; in case of a decrease it is a high probability star and in case of an increase it is a high probability galaxy. We can in fact estimate the type of all sources based on IRAS flux and quality flag data, as well as on AKARI and WISE/2MASS measurements. If all data show the same type of object, then we give it as a genuine one, and if there is a ambiguity, we give the most probable

doi: https://doi.org/10.52526/25792776-2021.68.1-130

type with a flag. In Figure 2, for a possible star and a galaxy we built spectral energy distributions (SED) based on our collected data from NIR 2MASS JHK to FIR IRAS and AKARI. The star is IRAS 00012+7614 = IRAS F00012+7614 and the galaxy is IRAS F00041-3446. These sources were chosen as examples because they are very typical for stars and galaxies. The star is TYC 4492-1689-1 (V = 10.43) and the source chosen as a galaxy is also the radiosource NVSS J000639-342943.

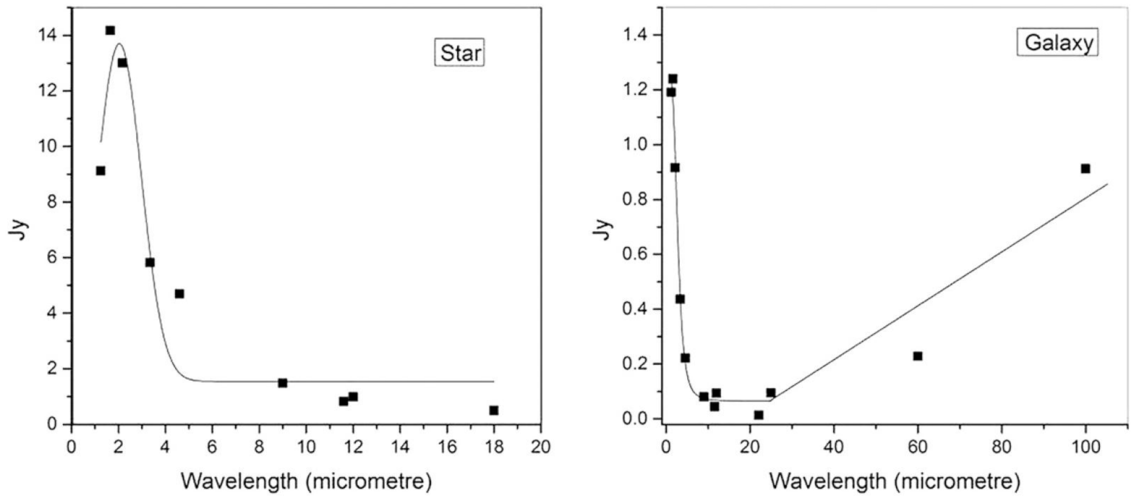

Figure 2. “Star” (IRAS 00012+7614 = IRAS F00012+7614) and “Galaxy” (IRAS F00041-3446) SEDs based on 2MASS, WISE, AKARI and IRAS photometric data.

We have created a software through which we made cross-correlations with search radius for each source individually based on its positional error, taking only those associations having positional distance between sources not exceeding 3σ. We have created the IRAS PSC/FSC Combined Catalogue to show the efficiency of the software and to have a joint IRAS catalogue for further statistical studies and investigations of individual sources. IRAS PSC/FSC contains 345,163 sources, including 73,770 common ones from both catalogues (IRAS-PSC and IRAS-FSC). We calculated the improved coordinates for these 73,770 sources, as well as individual positional errors based on shifts of IRAS-PSC and IRAS-FSC positions. We also have calculated improved Minor and Major axes coordinates errors.

3. Radio variable sources at 1400 MHz and their optical variability

NVSS and FIRST radio catalogues have been cross-matched. Our principle is to take into account positional errors for individual sources, and we have applied similar to our previous research method (Abrahamyan et al. (2015)). In the FIRST catalogue there is no information on positional errors for each source, that is why 5 arcsecond as errors for all sources is adopted. In NVSS catalogue, each source is given with its individual positional error. We have created a software through which cross-correlations are done. This software allows considering positional errors for each source individually and we have taken associations having coordinate differences between counterparts not exceeding 3σ (calculated using both σ-s from NVSS and FIRST). As a result, we have obtained 556,282 associations between NVSS and FIRST (Abrahamyan et al. (2018)).

Our main task is the revelation of the variability of radio sources in radio wavelengths. For variability criteria, we will take into account those radio sources which have associations within less than 3σ of the positional errors and for which the second association is 2 times farther than the first one. The systematic shift (SS) between fluxes of NVSS and FIRST catalogues was considered. We counted SS between these catalogues to get rid of systematic errors that could appear due to different flux calibration. As FIRST accuracy is higher, we have shifted NVSS using SS. The first step that was accomplished is computing systematic shift (SS) for fluxes between NVSS and FIRST (SS = -0.765 mJy).

doi: https://doi.org/10.52526/25792776-2021.68.1-130

$$\Delta F = |F_{FIRST} - (F_{NVSS} - SS)| - 3\sigma \tag{1}$$

where σ is the combined flux error:

$$\sigma = \sqrt{(Error^2_{FIRST} + Error^2_{NVSS})} \tag{2}$$

We have carried out a cross-correlation of NVSS and FIRST catalogues to distinguish sources which have large differences of fluxes at 1400 MHz. We have selected 6301 radio sources with flux difference at least 15 mJy. Further investigation of these radio sources led to a new sample of radio sources, which have high optical variability.

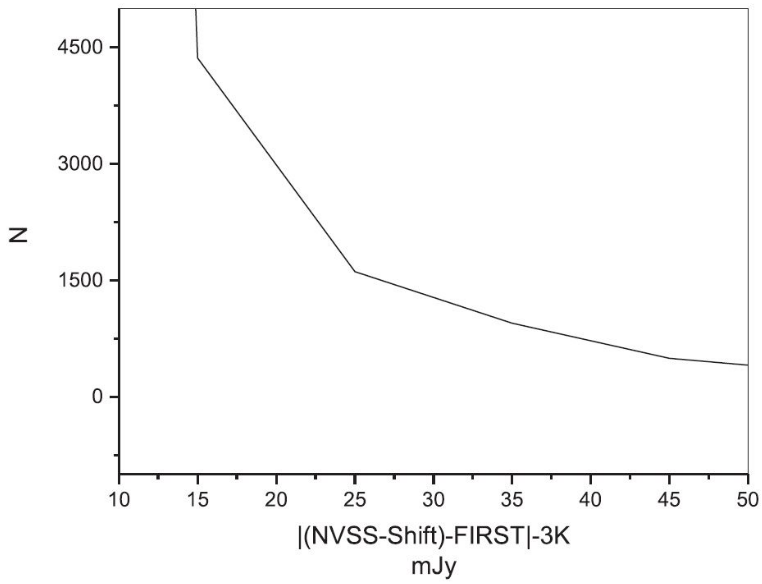

Figure 3. ΔF distribution showing breaks at 15, 25 and 45 mJy.

.

Activity types of 6301 radio sources having radio variability.

N0.	Activity type	Numbers
1	Blazar (BZB, BZG, BZQ, BZU)	308
2	QSO	639
3	Sy 1.0 / Sy 1	19
4	Sy 1.2	2
5	Sy 1.5	6
6	Sy 1.9	2
7	Sy 2.0 / Sy 2	9
8	AGN	97
9	Starburst	1
10	FSS (Flat-Spectrum radio source)	87
11	USS (Ultra-Steep-Spectrum radio source)	36
	Known (total)	**1206 (19%)**
	Unknown	**5095 (81%)**
	Total	**6301 (100%)**

Activity types of 2425 radio sources having both radio and optical variability.

N0.	Activity type	Numbers
1	Blazar (BZB, BZG, BZQ, BZU)	176
2	QSO	333
3	Sy 1.0 / Sy 1	9
4	Sy 1.5	6
5	Sy 2.0 / Sy 2	5
6	AGN	45
7	FSS (Flat-Spectrum radio source)	41
8	USS (Ultra-Steep-Spectrum radio source)	4
	Known (total)	**619 (25.5%)**
	Unknown	**1806 (74.5%)**
	Total	**2425 (100%)**

Figure 4. 6301 radio sources

.

4. Optical variability of blazars

To understand some properties of blazars, we used Roma Multifrequency Catalog of Blazars (BZCAT) 5th version. Altogether, 3,561 objects are given as BZB, BZQ, BZG, or BZU corresponding to BLL, FSR quasars, galaxies, and blazars of uncertain/transitional type (Abrahamyan et al. (2019)). Having 3,561 blazars that have radio variability, we try to check how many of these sources are optically variable. We cross-correlated these radio sources with POSS1-based and POSS2-based optical

doi: https://doi.org/10.52526/25792776-2021.68.1-130

catalogs: APM, USNO A2.0, USNO B1.0, and GSC 2.3.2. In Figure 5, we give graphs of the absolute magnitude versus redshift. Basically, three separated areas (BZB, BZG, and BZQ) are observed. Three types of blazars (BZB, BZG, and BZQ) are mostly separated, but there is overlap with each other to some extent.

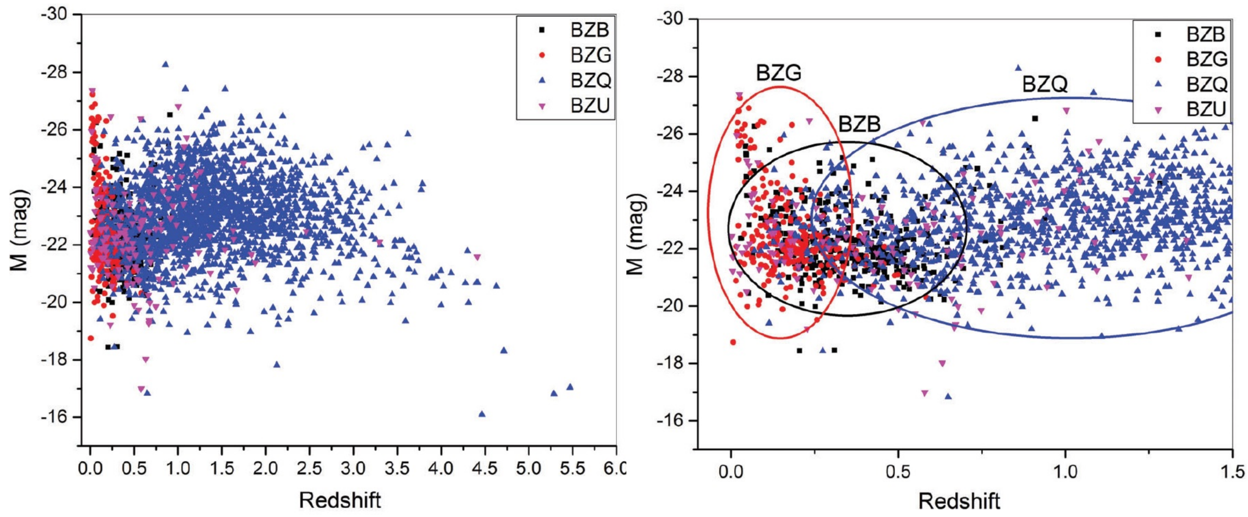

Figure 5. Absolute magnitude vs. redshift

.

Thus, we have 2,121 radio sources that have optical variability. For each source,we have four means for understanding their variability and for each source, based on this, we give variability category flags from 0 to 3 For a detailed picture of variability of these sources, we counted 4 category flags together.

Summarizing number for four category flags (all possible configurations of the flags)	Number of variable sources	Total	Comments
3333	23	51	Extreme variability
3332	10		
3322, 3331	18		
3330, 3321, 3222	23	126	High variability
3221, 3311, 2222	42		
3310, 3220, 3211	61		
3300, 3210, 3111, 2220	122	483	Medium variability
3200, 3110, 2210, 2111	118		
2200, 2110, 1111	243		
3000, 2100, 1110	299	1,461	Low variability
2000, 1100	670		
1000	492		
Total	2,121		

Figure 6. Number of optically variable radio sources based on their variability categories and flags (0—have not variability, 1—low variability, 2—medium variability, and 3—high variability)

.

We have obtained 2,121 blazars that have optical variability using POSS1 and POSS2 epoch measurements. We have compared our work with the one reported by Hovatta et al. (2014). In the work, the authors investigated optical data from the PTF and the CRTS to study the variability of γ -ray-detected and non detected objects in a large population of AGN selected from the Candidate Gamma-Ray Blazar Survey and Fermi Gamma-Ray Space Telescope catalogs. Their samples include 714 sources with PTF data and 1,244 sources with CRTS data. We compared our list with the list by Hovatta et al. (2014). As a result, we obtained 704 identified sources.

doi: https://doi.org/10.52526/25792776-2021.68.1-130

5. The nature of active galaxies based on their radio properties

We use data from Véron-Cetty & Véron (2010) catalog (VCV-13). This catalog includes 133,336 quasars, 1,374 BL Lac objects, and 34,231 active galaxies (including 16,517 Seyfert 1.0). We have considered 34,231 active galaxies for our research (Abrahamyan (2020) and Abrahamyan et al. (2020)).

For investigation, galaxies with magnitudes in the range of 12^m-19^m have been taken. In the next step, we have cross-correlated (Abrahamyan et al. (2015)) these objects with radio catalogs: FIRST, NVSS, 87GB, GB6, 3C, 4C, 7C, 8C, 9C, 10C, SUMSS, WISH, WENSS, Molonglo Reference Catalogue of Radio Sources, Texas Survey of radio sources at 365 MHz, Miyun 232 MHz survey, CLASS survey of radio sources, 74 MHz VLA Low-frequency Sky Survey Redux, and the GMRT 150 MHz all-sky radio survey. As a result, we have 4,437 objects that have been radio-identified. 4,437 objects have 1–10 radio fluxes at different wavelengths. In this work, radio catalogs that cover the 38MHz to 15.7 GHz frequency range have been used. For our investigation, we have taken objects that have six or more radio fluxes at different wavelengths. With six and more radio fluxes, there is an opportunity to better understand some physical properties in radio. So, we have 198 objects with six or more radio fluxes.

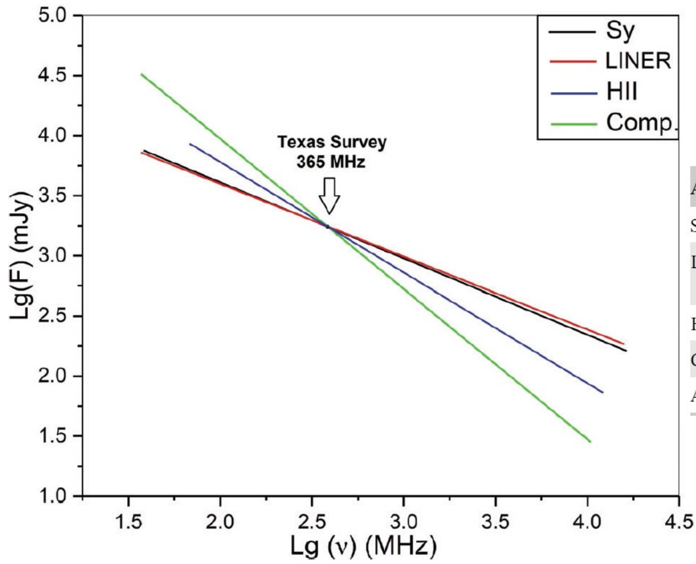

Average radio spectral indices for different types of active galaxies

Activity type	Average radio spectral index
Seyfert	−0.6013 ± 0.027
Low-ionization narrow emission-line region	−0.5955 ± 0.025
HII	−0.6672 ± 0.039
Composite	−0.7128 ± 0.043
All	−0.6089 ± 0.056

Figure 7. Average radio spectra for our object

.

Active galaxies are very interesting objects in the Universe. In order to understand some physical properties, we must identify which properties our objects have in radio range. We have 198 active galaxies with six or more radio fluxes at different wavelengths. A very important radio property for radio objects is the radio spectral index. It shows steep radio spectra. Using six or more frequencies, we have developed a graph for all 198 galaxies (lg[flux] vs. lg[frequencies]). Using an lg[flux] versus lg[frequencies] graph for each source, we have made linear fitting. The software "Origin" gives the formula for each linear fit, and using that, we have measured the radio spectral index for each source. The plot shows steep radio spectra for each line, and that is considered radio spectral index. As examples, we give average radio spectra for our objects in Figure 7.

Using redshift information, we have estimated physical sizes for our objects. We have eight objects that have HII activity. For these sources, we have also estimated physical sizes, and for one of them, we have obtained very big physical size (832.2 kpc) compared to the other HII objects, which are up to 116.35 kpc. With the purpose of calculating the average size and drawing other comparisons, we have excluded this object. Therefore, using physical sizes, we have developed the dependence of radio spectral index on physical size (Figure 8).

doi: https://doi.org/10.52526/25792776-2021.68.1-130

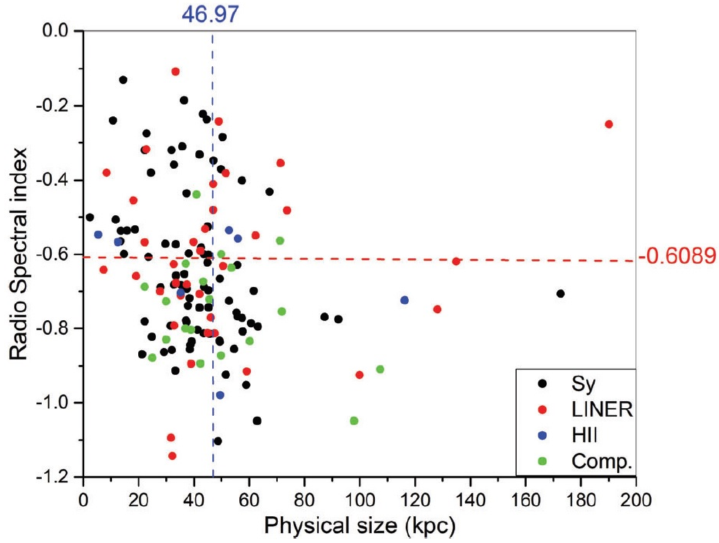

Physical sizes of active galaxies

Activity type	Range of sizes (kpc)	Average size (kpc)	RMS (kpc)
Seyfert	2.39 ÷ 305.46	44.88	35.62
Low-ionization narrow emission-line region	7.36 ÷ 190.19	50.15	36.14
HII	5.4 ÷ 116.35	46.81	33.81
Comp.	22.27 ÷ 107.51	50.23	22.46
All	2.39 ÷ 305.46	46.97	32.26

Figure 8. Radio spectral index versus physical size

.

6. Result and conclusion

Optical identifications of a few thousands of IRAS sources showed that IRAS Point Source and IRAS Faint Source catalogues contain many quasars and active galactic nuclei, late-type stars, planetary nebulae, variables, etc. To increase the efficiency of using IRAS PSC and FSC, which contain a lot of common sources, one needs a joint catalogue of all IRAS point sources with improved data based on both catalogues. However, cross-correlation of the catalogues is not so easy, as the association of many sources is relative, and not always it is obvious, which source from one catalogue corresponds to the other one in the second catalogue. This problem exists in case of using standard cross-correlation tools like VizieR. Therefore, we have created a tool for cross-matching astronomical catalogues and we have applied it to IRAS PSC and FSC. Using this tool we have carried out identifications with a search radius corresponding to 3σ of errors for each source individually rather than a standard radius for all sources. As a result, we obtained 73,770 associations. We showed that in case of cross-correlation of these catalogues by VizieR, we had to take 161.95 arcseconds radius not to lose any association; however, in this case a lot of false associations appear for many sources. In addition, we have made cross-correlations with AKARI-IRC, AKARI-FIS and WISE catalogues. As a result we created a catalogue with high positional accuracy and with 17 photometric measurements from 1.25 to 160 μm range, providing a detailed catalogue for IRAS point sources (Abrahamyan et al. (2015)).

In the next work we have cross-correlated NVSS and FIRST radio catalogues having radio flux measurements at the same 1.4 GHz frequency. This way we benefit from repeated observations from both catalogues, as they give more accurate positions and fluxes and more important, reveal large differences between the two measured fluxes, thus allowing to establish radio variability. As a result, 79,382 radio variables have been revealed, including 6301 with flux differences at 1.4 GHz larger than 15 mJy, 1917 with flux differences > 45 mJy and 260 with flux differences > 200 mJy. By using a special technique, 2425 optically variable objects out of 6301 radio sources have been revealed. 2425 radio sources with both high radio and optical variability into four categories have been divided. 1206 (19%) out of 6301 radio sources have activity types from available catalogues and 619 (25.5%) out of 2425 radio sources with at the same time radio and optical variability have activity types from available catalogues. In addition, 279 radio sources out of 2425 have high variability in optical range. We have established their activity types when available. The IR fluxes and colours for the 6301 variable radio sources have been studied. Colour–colour diagrams show that most of the "unknown" sources are galaxies. The activity types for 110 (42%) out of 260 extremely high variable radio sources also have been retrieved (Abrahamyan et al. (2018)).

doi: https://doi.org/10.52526/25792776-2021.68.1-130

The analysis of blazars' parameters from BZCAT leads to a conclusion that they do not have the same properties. The preliminary criterion to include an object in the catalog was the strong radio emission; however, two type of radio sources were selected: BL Lacertae (BLL) objects and Flat Spectrum Radio Quasars (FSRQ). As a number of properties are typical of blazars (strong radio emission, optical variability, continuum optical spectra without lines, polarization, high luminosity, etc.), using the optical data, we investigate them to clarify which property plays the most significant role in their classification as blazars. We found that 60% of blazars have optical variability. We use a technique developed based on POSS1 and POSS2 photometry and group the variability into extreme, strong, medium, and low classes. In the optical range, 51 blazars have powerful variability (extreme variables), and 126 are high variables. In addition, 63% of blazars have detected radiation in X-ray and 28% have detected radiation in gamma rays. We give the average statistical characteristics of blazars based on our analysis and calculations Abrahamyan et al. (2019).

In the next work we investigate radio properties of active galaxies taken from Véron-Cetty & Véron (2010) catalogue. The galaxies are limited to magnitudes in the range of 12^m - 19^m. We have cross-correlated the list with radio catalogues and selected those galaxies, which have data on 6 or more radio fluxes at different wavelengths. As a result, we have 198 galaxies, which satisfying these conditions. Using SDSS DR15, we have obtained 96 spectroscopic identifications out of the 198 objects. After the classification, 85% of 96 objects have changed their types. Available data on the classification of these objects and our classification showed that 56.7% of them are Seyfert galaxies. For all the objects we have built radio spectra and estimated radio spectral indices. As a result, we obtain $\overline{\alpha} = -0.6089 \pm 0.056$ ($\overline{\alpha}_{Seyfert} = -0.6013 \pm 0.027$, $\overline{\alpha}_{LINER} = -0.5955 \pm 0.025$, $\overline{\alpha}_{HII} = -0.6672 \pm 0.039$, $\overline{\alpha}_{Comp.} = -0.7128 \pm 0.043$). We discuss the radio properties of active galaxies based on their radio spectral indices. Using the spectra from the SDSS catalog, 96 objects were studied and detailed types of activity were given for them. For more confident classification we used three diagnostic diagrams and direct study of the spectra. As a result, we have changed classification for 85% of these objects (Abrahamyan (2020) and Abrahamyan et al. (2020)).

Acknowledgements

I would like to thank my esteemed supervisor – Dr. Areg Mickaelian for his invaluable supervision, support and tutelage during the course of my PhD degree.

This work was partially supported by the RA MES State Committee of Science, in the frames of the research project No. 15T-1C257. This work was made possible in part by a research grant from the Armenian National Science and Education Fund (ANSEF) based in New York, USA (grants astroex-4193 and astroex-4195).

References

Abrahamyan H. V., 2020, Astronomische Nachrichten, 341, 6-7, 703

Abrahamyan H. V., Mickaelian A. M., Knyazyan A. V., 2015, Astronomy and Computing, 10, 99

Abrahamyan H. V., Mickaelian A. M., Paronyan G. M., Mikayelyan G. A., Gyulzadyan M. V., 2018, Astronomy and Computing, 25, 176

Abrahamyan H. V., Mickaelian A. M., Paronyan G. M., Mikayelyan 2019, Astronomische Nachrichten, 340, 5, 437

Abrahamyan H. V., Mickaelian A. M., Paronyan G. M., Mikayelyan 2020, Astrophysics, 63, 3, 322

Hovatta T., et al., 2014, Mon. Not. R. Astron. Soc. , 439, 690

Véron-Cetty M. P., Véron P., 2010, Astron. Astrophys. , 518, A10

doi: https://doi.org/10.52526/25792776-2021.68.1-130